UCRL-16398

University of California

Ernest O. Lawrence Radiation Laboratory

ANALYTICAL METHODS IN BACTERIAL KINETICS

TWO-WEEK LOAN COPY

This is a Library Circulating Copy
which may be borrowed for two weeks.
For a personal retention copy, call
Tech. Info. Division, Ext. 5545

Berkeley, California

DISCLAIMER

This document was prepared as an account of work sponsored by the United States Government. While this document is believed to contain correct information, neither the United States Government nor any agency thereof, nor the Regents of the University of California, nor any of their employees, makes any warranty, express or implied, or assumes any legal responsibility for the accuracy, completeness, or usefulness of any information, apparatus, product, or process disclosed, or represents that its use would not infringe privately owned rights. Reference herein to any specific commercial product, process, or service by its trade name, trademark, manufacturer, or otherwise, does not necessarily constitute or imply its endorsement, recommendation, or favoring by the United States Government or any agency thereof, or the Regents of the University of California. The views and opinions of authors expressed herein do not necessarily state or reflect those of the United States Government or any agency thereof or the Regents of the University of California.

Research and Development

UCRL-16398

UNIVERSITY OF CALIFORNIA

Lawrence Radiation Laboratory
Berkeley, California

AEC Contract No. W-7405-eng-48

ANALYTICAL METHODS IN BACTERIAL KINETICS

Victor Henry Edwards and Charles R. Wilke

January 27, 1967

ANALYTICAL METHODS IN BACTERIAL KINETICS

Contents

Abstract vii

General Introduction ix

Part I: Modeling and Analysis of Bacterial Kinetic Data 1

I. Summary 1

II. Problems in Analysis of Bacterial Kinetics 2

III. Classification Schemes in Bacterial Kinetics 6

IV. Proposed Models 13

A. Reviews 13

B. Monod-Hinshelwood Period 13

1. General Remarks 13

2. Substrate-limited Models 14

3. Product-limited Models 17

4. Models in which both Product and Substrate Control Rates 19

C. More Elaborate Approaches 21

1. Remarks 21

2. Culture Age 21

3. Statistics of Cell Division 22

4. Segregated Models of Culture Kinetics 25

5. Structured Models of Microbial Populations 26

V. Data Analysis 29

A. Introduction 29

B. Properties of the Model 30

C. Computer Program 34

D. Tests of Curve-fitting Program 37

1. Test #1 37

2. Test #2 37

3. Test #3 45

4. Test #4 53

5. Test #5 53

6. Test #6 58

7. Test # 7 61
8. Conclusions 66
9. Recommendations for the Use of the Curve fitting Computer Program 66
Appendices 70
I. Extimation of Coefficients in the Generalized Logistic Equation 70
II. Description of Curve-fitting Computer Program 72
References 95
Part II: Sulfate Reduction by Bacteria 99
I. Summary 99
II. Introduction 100
III. Methods 103
A. Organism 103
B. Batch Culture Methods 105
C. Continuous Culture Methods 106
1. Early Continuous Culture Apparatus 106
2. Improved Continuous Culture Apparatus 108
D. Data Analysis 113
IV. Results 115
A. Development of Medium M 115
1. Effect of Potassium Phosphate, Ammonium Chloride and Ferrous Sulfate 117
2. Effect of Magnesium Sulfate and Calcium Chloride 118
3. Effect of Sodium Sulfate 120
4. Effect of Lactic Acid 123
5. Effect of Yeast Extract 128
6. Effect of pH 135
7. Medium M 145
B. Effects of Mode of Cultivation 152
1. Effect of Sulfide Concentration, Mixing and pH Control 152

2. Materials of Construction 154
C. Continuous Culture Experiments 166
1. Maximum Growth Rate Experiment 166
2. Steady-state Continuous Culture 173
3. Effect of Wall Growth 179
D. Kinetic Analysis 182
Nomenclature 201
Appendices 202
I. Classification of the Sulfate-reducing Bacteria 202
II. Methods 203
III. Tables of Supplementary Data 211
IV. Derivation of Wall Growth Equations 225
References 227
Part III: Electronic Sizing and Counting of Bacteria 229
I. Introduction 229
II. Literature Review 231
A. Theory of Electronic Sizing and Counting of Particles 231
1. Response to Particle Size 231
2. Coincidence Effects 233
a. Primary Effects 233
b. Secondary Effects 234
3. New Developments in Technique 235
B. Sizing and Counting of Bacteria 238
III. Determination of the Size Distribution of Polystyrene Bead Volume Standards 240
A. Methods 240
1. Sample Preparation 240
2. Photography and Diameter Measurement 242
B. Results 247
1. Astigmatism 247
2. Computer Program 249
C. Discussion 252

D. Conclusions 260
IV. System Calibration 261
A. Characteristics of the Aperture 261
1. Physical Characteristics 261
B. Characteristics of Electronics 270
C. Linearity of Response to Particle Sizes 274
D. Effect of Pulse-Shaping on Resolution 281
E. Effects of Other Variables on Counting System Results 286
1. Effect of Particle Conductivity 286
2. Reproducibility 289
3. Effect of Aperture Voltage 291
V. Measurements of Bacterial Cells 294
A. Methods 294
1. Organism and Cultivation 294
2. Measurement of Cell Concentration 295
3. Data Analysis 295
B. Electronic Counting of Bacteria 300
C. Electronic Sizing of Bacteria 327
1. Model for the Electrical Conductivity of the Bacterial Cell 327
2. Experimental Results 329
3. A Modified Model of the Bacterial Cell 352
VI. Summary 354
Appendices 355
I. Preparation of Carbon Supports for Electron Microscopy . . 355
II. Test of the Reproducibility of the Traveling Microscope 356
III. Estimation of Astigmatism in Photographs 358
IV. Computer Program PDDANL and Selected Results 364
V. Computer Programs BUGSIZE and NOISE 376
General Summary 393
Acknowledgments 396
References 397

ANALYTICAL METHODS IN BACTERIAL KINETICS

Victor Henry Edwards and Charles R. Wilke
Lawrence Radiation Laboratory
University of California
Berkeley, California

January 27, 1967

ABSTRACT

This three part report is mainly concerned with the development of methods useful in the study of the kinetics of bacterial growth and metabolism. In the first part of this work, a comprehensive review of the literature of mathematical models for bacterial growth is given. A computerized method for the analysis of batch culture kinetic data is presented that fits a generalized logistic equation to the data. The fitted equations are useful for interpolation, integration, differentiation, and other manipulations of the data.

In the second part of this work, experimental data obtained with a salt tolerant strain of sulfate-reducing bacteria grown in both batch and continuous culture is presented and a novel continuous culture apparatus is described. The data, which were taken for use in evaluation of the feasibility of projects using these bacteria, are analyzed using the computer program developed in the first part of this work. The results are correlated and discussed in relation to some of the proposed models discussed in the first part of this work.

In the third part of this work, a sophisticated apparatus for measuring bacterial cell size-concentration distributions is described. The technique, based on a resistance principle, is shown to differentiate between normal cells and heat-killed cells, a result that should be of

considerable use in the study of bacterial sterilization kinetics. The apparatus is calibrated and used in obtaining information on the cell size under a variety of experimental conditions. A computer program for the analysis of the computer-coupled output is presented. The system described will provide a powerful tool in the study of microbial kinetics.

GENERAL INTRODUCTION

Living organisms consume, produce, and modify a very large number of chemical compounds. Microorganisms in general and bacteria in particular tend to have much more rapid metabolic rates than macroorganisms because of their high surface-to-volume ratio. Because of their high conversion rates at ambient conditions, their rapid growth rates, their wide range of chemical activities, and the rapid progress in biological research, bacteria are becoming progressively more important to man as an alternative to conventional chemical processes in chemical conversions. The three areas of greatest potential for commercial microbial activities are food production, production of complex chemicals such as the antibiotics, and the purification of polluted water. For the engineer to take fullest advantage of bacterial conversions, he must know the bacterial metabolic rates and how they are affected by the environment and history or physiological state of the culture. These kinetic studies are important to the design and operation of processes for the production of microorganisms or their products. Kinetic studies can also lead to a better understanding of the mechanism of the process under consideration. Such fundamental information may then suggest techniques to the engineer for controlling the process to increase the yield of the desired product(s). A final advantage of modeling the kinetics of a given system is that the model may be used to predict the kinetics over a broad range of variables into regions where no data has been taken. Optimal conditions of operation of the process can be predicted with the model and verified by experiment.

In the first part of this three part dissertation, our purpose is to review the equations and models proposed to describe the rates of growth and metabolic activity by bacteria. It is also our purpose to present a computerized technique for the analysis of batch culture kinetic data that fits equations to the data. The fitted equation can then be used for interpolation, extrapolation, integration, differentiation, and other manipulations of the data.

In the second part of this work, experimental data obtained with a salt tolerant strain of sulfate-reducing bacteria grown in both batch and continuous cultures is presented and a novel continuous culture apparatus is described. The data, which were taken for use in evaluation of the feasibility of projects using these bacteria, are analyzed using the computer program developed in the first part of this work. The results are discussed in relation to some of the proposed models discussed in the first part of this work.

In the third part, a sophisticated apparatus for measuring bacterial cell size-concentration distributions is described. Calibration of the instrument and the meaning of the results obtained with the system are discussed. A computer program for analysis of the computer-coupled output is presented. The system described will provide a powerful tool in studies of microbial kinetics.

PART I: MODELING AND ANALYSIS OF BACTERIAL KINETIC DATA

I. SUMMARY

For engineers to design equipment for the production of bacteria and their products, they need models that relate the rate of production to the important variables of the system. Modeling is difficult because there are many potentially important variables in a culture, and it is necessary to select a few crucial variables to make the model mathematically tractable.

To assist in the development of a conceptual view of a bacterial cell culture, various schemes for the classification of fermentation processes are presented.

The development of the modeling of bacterial kinetics is outlined with a literature survey of mathematical models of bacterial kinetics.

A generalized version of the logistic equation is proposed for use in the measurement of rates of growth and metabolism in batch culture, and a computer program to fit the equation to the data is presented. The program is shown to successfully fit both synthetic and real batch kinetic data, including correct prediction of the derivatives of the fitted dependent variables.

II. PROBLEMS IN ANALYSIS OF BACTERIAL KINETICS

Kinetic analysis of bacterial growth and metabolism is difficult because of the complexity of the chemical and physical processes that constitute life. A typical bacterial cell contains approximately 1000 enzyme molecules, 1000 ribosomes, between one and several chromosomes, and many smaller molecules. An idealized bacterial cell, shown in Fig. 1, is surrounded by a polysaccharide-protein-lipid cell wall, comprising about 20% of the dry weight of the cell. Between the cell wall and the cytoplasm is a double layered protein-lipid membrane that acts as a semipermeable barrier to many of the molecules and ions important to the survival of the cell. The membrane is capable of selectively absorbing some nutrients in the cell to a point where they are at a much higher concentration inside the cell than outside. This means of absorbing nutrients from the environment is referred to as active transport or aided transport. It requires energy to function. Normal diffusion also ocurrs with some compounds and is referred to as passive transport. There is also evidence indicating that the membrane plays an active part in the oxidative metabolism of the cell. Molecules and ions passing through the membrane arrive at the cytoplasm inside the cell. The nuclear region, containing the blueprints of the cell, is located in the cytoplasm although there is now considerable evidence that the nuclear material may be also associated with the cell membrane. Protein is synthesized by a complex mechanism involving amino acid building blocks connected to transfer-RNA(ribonucleic acid) molecules that work with the ribosomes, messenger RNA, and an enzyme to form new protein. In some of its metabolic pathways, the cell prevents over-production of products of a given pathway by either stopping production of one or more enzymes or by direct inhibition of one of the enzymes in the pathway. These control mechanisms increase the difficulty of modeling bacterial kinetics.

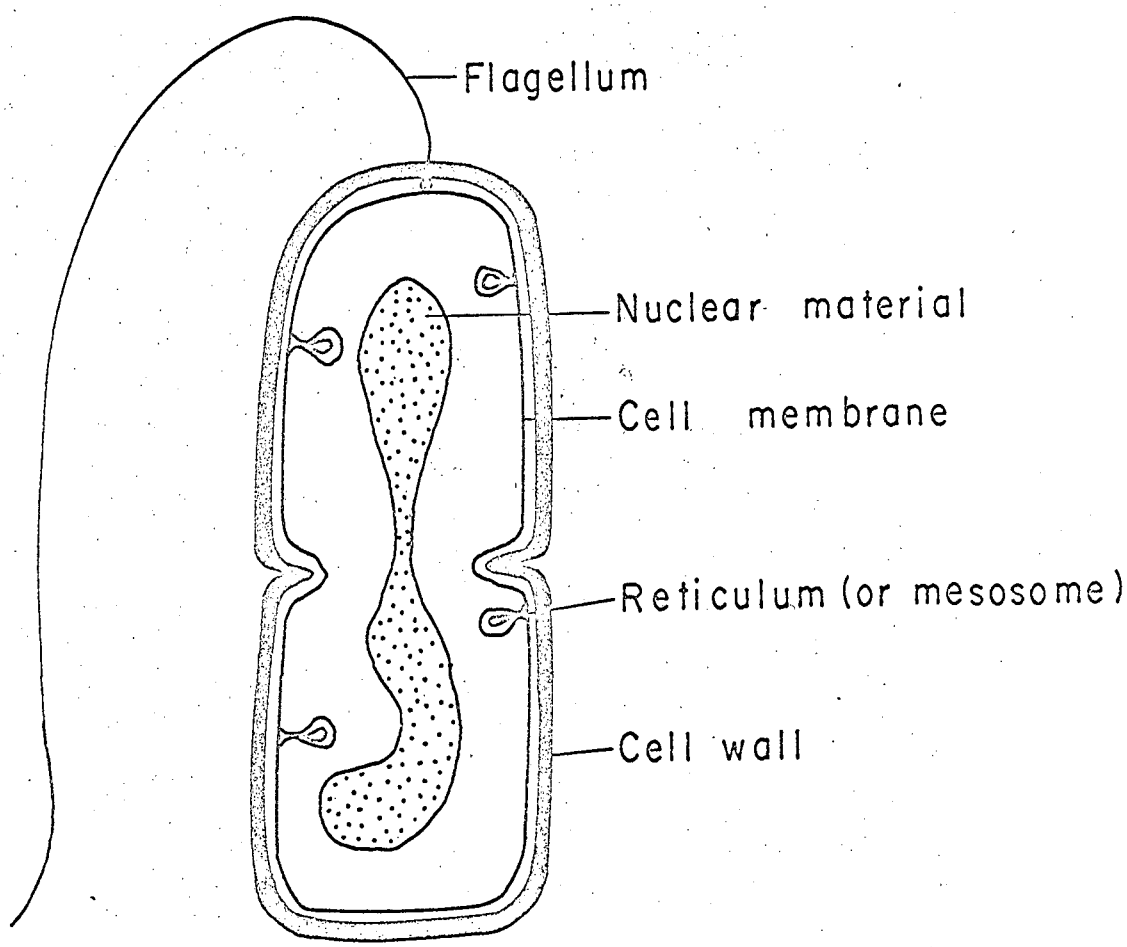

XBL 671 — 244

Fig. 1. A typical bacterial cell.

Growth of cells in a culture may be either balanced or unbalanced, as may be the culture itself. In balanced culture growth, the culture is in a steady state and the distribution of the physiological states of individual cells thus remains constant even though some individual cells are not in a steady-state cyclic condition themselves. A chemostat culture (i.e., a culture grown in a continuous stirred-tank reactor) at steady-state and low feed rates gives a steady-state culture in balanced growth although a significant percentage of the cells may be in a non-viable, unbalanced growth leading towards a non-growing condition. Batch culture at low cell concentration, on the other hand, are unsteady-state cultures of cyclical steady-state cells in balanced growth that are limited in growth by the constantly changing medium in which they are suspended. Kinetic analysis of both types of culture is thus complicated by an unsteady-state, non-cyclic phenomenon in individual cell growth processes in continuous culture and in the environment of the cells in batch culture.

Another complication in modeling is caused by the many couplings of different metabolic pathways, and the many side reactions important to the life of the bacterial cell. Also, many reaction mechanisms to the life of the cell are not completely understood.[2] Finally, because a large number of processes can be limiting it should be apparent that a rigorously complete kinetic model is far beyond our reach at this point. Thus we try to select the crucial variables of greatest economic interest and study their relation to kinetics while holding other variables constant. The choice of crucial variables will depend on the nature of the need for a kinetic study and one must be very careful to select all crucial variables in such studies.

The most common crucial variables up to the present are cell dry weight concentration, concentration of the limiting nutrient, and concentration of the desired product(s). Other variables that are now beginning to be recognized are average cell composition, more detailed

analysis of the cells' environment and the distribution of cellular properties among the individuals in a population. One such important variable is the cell size concentration distribution. Measurement of this variable by an electronic technique will be discussed in detail in the last part of this dissertation.

III. CLASSIFICATION SCHEMES IN BACTERIAL KINETICS

Different organisms show different types of kinetic behavior, and a number of authors have approached the problem of classification of kinetic behavior of different microbial processes as a first step in kinetic analysis of the processes. Table I shows the scheme proposed by Gaden.[4] He suggested that three types of relationships between carbohydrate (or substrate) consumption and product formation existed, ranging from direct coupling as in the ethanol fermentation to no association as in penecillin production.

At about the same time, Maxon proposed classification by the scheme shown in Table II. The relation between growth and product formation formed the basis for his method of classification.

Deindoerfer points out three approaches to classification: phenomenological, thermodynamic, and kinetic.[7] The methods of both Gaden and Maxon fall into the first category. The studies of Calam et al., into the penecillin process are cited by Deindoerfer as an example of the thermodynamic approach.[7] Calam et al., measured activation energies of rate-limiting steps for growth, respiration, and biosynthesis.[8] They argued that rate-limiting steps for each of the three functions studied represented three different enzyme systems. However, as pointed out by Deindoerfer, the evidence is strongly presumptive but not conclusive.[7]

The model proposed by Luedeking and Piret is an example of a kinetic approach to classification of microbial product formation.[10]

Deindoerfer also proposed a new method of organization shown in Table III.[7] Fermentation type reactions are classified according to the kinetic relation between product formation and substrate consumption.

More recently, Tsuchiya et al. have proposed a new way of classifying mathematical models.[11] Table IV shows the proposed scheme. In their system, a segregated model is one which recognizes the distribution of different physiological states among the cells in the population, while a distributed model treats the culture as if it were a continuum

Table I. Classification of microbial processes according to Gaden.[4]

Type	Specific rate relationships	Example
I	Product formation directly related to carbohydrate utilization	Ethanol fermentation
II	Product formation indirectly related to carbohydrate utilization	Citric acid fermentation
III	Product formation apparently not associated with carbohydrate utilization	Penecillin fermentation

Table II. Classification of microbial processes according to Maxon.[5]

Type	Specific rate relationships	Example
I	Product formation and growth are synonymous	Propagation of microorganisms
II	Product formation associated with growth	Ethanol fermentation
III	Product formation not associated with growth	Penecillin fermentation

Table III. Classification of microbial processes by type reactions by Deindoerfer[7]

Type	Description	Example
Simple	Nutrients converted to products in a fixed stoichiometry without accumulation of intermediates	Growth of yeast
Simultaneous	Nutrients converted to products in variable stoichiometric proportions without accumulation of intermediates	Conversion of sugar into cell protein and cell fat during batch growth of *Rhodotorula glutinis*
Consecutive	Nutrients converted to product(s) with accumulation of intermediate(s)	Gluconic acid fermentation by *Ps. ovalis*
Step-wise	Nutrients completely converted to intermediate before conversion to product or nutrients selectively converted to product	Diauxic growth of *E. coli*

Table IV. Classification of mathematical models of microbial growth by Tsuchiya et al.[11]

I. Model takes explicit account of organism-environment interactions

- A. Segregated
  - 1. Structured
  - 2. Unstructured
- B. Distributed
  - 1. Structured
  - 2. Unstructured

II. Model does not take explicit account of organism-environment interactions

with all cells in the culture assumed to have the same properties. A structured model is one that does not treat cultures as if they were simply constant composition, but rather recognizes at least two different compounds that make-up the cell and affect its metabolic activity.

Terui has also proposed a method of classifying fermentation processes. He first divides fermentations into the following three categories:[12] (1) Product formation via energy-producing reactions; (2) Product formation via reactions not acting as energy sources; and (3) Reactions not falling in either of the above categories. He then divides each category into three more classes: (a) simultaneous multiplication and product formation; (b) non-simultaneous multiplication and product formation; (c) those cases not classified by (a) or (b). Terui thus divides fermentations into 9 separate categories by this method.[12]

In Table V, we propose a method of classification of the kinetics of microbial cell systems. In this new scheme, distinctions are made between different systems on the basis of which step (or steps) is rate-limiting in the gross metabolism of the cells in the culture and hence limiting growth or product formation. Thus the transport to and from the cell of nutrients and products respectively may be rate-limiting, as may transport through the cell membrane for both nutrients and products. Rate limitation may also be caused by slow reactions within the cell or by product inhibition within the cell. In a state of balanced growth, the cells would simply be limited by the rate of one or more reactions in the cell when given an excess of all nutrients. Our method of classification differs from the other proposed schemes because it is quite possible that a given culture could pass through several phases with a different limiting step for each phase, thus falling under several different categories of classification. An example would be a mycelial culture. Just after germination of spores, one would expect a mycelial organism to reach and remain in balanced growth. However, as the mycelium

Table V. Classification of microbial processes on the basis of mass transfer and chemical reactions as limiting steps for metabolism.

Type	Limiting step	Example of limitation
I	Transport of nutrient to cell	Diffusion of oxygen into pellets in cultures of mycelial organisms
II	Reaction outside cell with outer surface of cell or with exoenzyme produced by cell	Decomposition of cellulose by microorganisms
III	Transport of nutrients into cell	Uptake of β-galactose by *E. coli*
IV	Reaction(s) in cell	Balanced growth in dilute cultures with excess of all nutrients
V	Product inhibition within cell	Lysine, threonine, and methionine production with *Micrococcus glutamicus*, inhibited by threonine and methionine in excess
VI	Transport of products out of cell	-
VII	Transport of products away from cell	Accumulation of inhibitory product within pellets of mycelia

began to develop into pellets, the increasing mycelial mass would tend to cause limitation by inadequate mass transfer to the innermost mycelial material to replace balanced growth. However, these conditions might at the same time stimulate antibiotic formation.

IV. PROPOSED MODELS

A. Reviews

In this section, a number of mathematical models that have been proposed will be reviewed critically. Literature reviews of bacterial kinetics already exist.[4,5,6,7,11,12,13] There are also three interesting reviews devoted or related to microbial growth.[14,15,16] Thus it is not our purpose to make an exhaustive study of kinetic models, but rather to trace the steps in the development of the field of bacterial kinetics.

B. Monod-Hinshelwood Period

1. General Remarks

The Monod-Hinshelwood period of bacterial kinetics extends from the late 1930's to the early 1960's. Both men played an early role during the period, establishing a method of modeling bacterial growth kinetics. Most of the kinetic models of this period treat cell growth and product formation for the cases limited by a single nutrient or product and none of them explicitly include the cell composition in the analysis. Also, in models of this type, no account is taken of the differences between individual cells. The models of this type can be arranged in the form

$$\frac{dX}{dt} = f(X,S,P) \tag{1}$$

$$\frac{dS}{dt} = g(X,S,P) \tag{2}$$

$$\frac{dP}{dt} = h(X,S,P) \tag{3}$$

where X = cell mass concentration or cell number concentration

S = concentration of limiting substrate

P = concentration of inhibitory product

and, f(X,S,P), g(X,S,P), and h(X,S,P) are the kinetic parameters of growth, substrate consumption, and product formation respectively. Division of these equations by X gives the equations for the specific rates of growth, substrate consumption, and product formation. Specific rates are the rates per unit dry mass of cells or per cell. The three equations are usually simplified by assuming the following equations apply

$$\frac{dS}{dt} = - K_1 \frac{dX}{dt} = - K_1 \; f(X,S,P) \tag{4}$$

$$\frac{dP}{dt} = K_2 \frac{dX}{dt} = K_2 \; f(X,S,P) \tag{5}$$

The assumptions inherent in these equations are that substrate consumption and product formation are directly proportional to growth. These assumptions hold only for growth-associated processes. (Simple type reaction according to Deindoerfer).[7] Thus this simplification (of constant yields) limits the usefulness of the equations to be described in this section to a restricted number of bacterial cell systems. The simplest form that could be assumed is that of a constant specific growth rate, thus implying that the effects of substrate and product concentrations do not affect the specific growth rate. Such an assumption is best applied to the region of exponential growth of a culture and may not apply to periods before or after exponential growth.

2. Substrate-limited Models

These models are of the first type, substrate-limited, which were first proposed by Monod in 1942. Monod proposed that the specific growth rate, μ, was related to the concentration of limiting nutrient, S, by the equations[17]

$$\mu = \frac{1}{X} \frac{dX}{dt} \tag{6}$$

$$\frac{d\mu}{dS} = \alpha \; (1 - \mu) \tag{7}$$

He then assumed the following approximate solution to the differential Eq. (7)

$$\mu = \frac{\mu_m S}{(K + S)} \tag{8}$$

where μ_m = maximum specific growth rate, constant

K = constant

A similar result, commonly known as the Michaelis-Menton equation, maybe derived on the basis of enzyme kinetics.[18b] This two parameter form gives an almost linear dependence of the growth rate on the substrate concentration at low substrate or nutrient concentrations, changing to a constant maximum growth rate at high substrate concentrations.

Teissier proposed that a more general solution of Eq. (7) be used.[19] The equation had the form

$$\mu = \mu_m(1 - \exp(-S/K)) \tag{9}$$

An empirical, but more general form was proposed by Moser.[20]

$$\mu = \frac{\mu_m}{(1 + KS^{-B})} \tag{10}$$

Note that Moser has added a third parameter to be used in fitting the data. More recently, two workers have proposed kinetic models that relate cell concentration as well as limiting substrate concentration to the specific growth rate.[21,22] Contois showed that the following model was superior to the Monod equation in fitting his data.[21]

$$\mu = \frac{\mu_m S}{BX + S} \tag{11}$$

This equation was suggested by the fact that regardless of the reactor feed concentration of the limiting substrate, S_o, the same maximum growth

rate in continuous culture was obtained. Because the Monod equation for specific growth rate at washout has the form

$$\mu_c = \frac{\mu_m S_o}{K + S_o} \tag{12}$$

It can be seen that K must be proportional to the inlet substrate concentration S_o as follows:

$$K = b\ S_o \tag{13}$$

and

$$CS = CS_o - X \tag{14}$$

By rearrangement and substitution, Eq. (11) is the result. As pointed out by Contois, this equation could result from production of inhibitory products, because the concentration of inhibitory products produced would probably be directly proportional to the amount of cells produced. On the other hand, higher cell densities might increase the energy expended per cell in the uptake of nutrients, giving the same form. It's also possible that this population term is a different way of accounting for endogeneous metabolism.

More recently, Fujimoto has proposed another model that relates the rate of substrate consumption to both the concentration of limiting substrate and the population density by the following equation

$$-\frac{dS}{dt} = K_m S \frac{S/X}{1/K + X/S} \tag{15}$$

When the cell yield from substrate is constant, the growth rate is given by the equation

$$\frac{dX}{dt} = -y\frac{dS}{dt} = \mu X$$

$$= \mu_m X \frac{S/X}{k + S/X} \tag{16}$$

The model is attractive because in different limiting cases, it reduces to the Monod equation (Eq. (8)), the model of Contois (Eq. (11)), or to the Verhulst-Pearl equation (Eq. (22)). However, Fujimoto did not perform the experiments necessary to demonstrate the overall superiority of his model, although he did perform several batch experiments to show that his model would fit batch data and also would account for inoculum size. Because the Monod equation is widely used at this time, it would be advisable to perform experiments designed to test the various different models.

Deindoerfer has pointed out that (1) various models for enzyme kinetics can be simplified to give the Monod equation and (2) that in many industrial fermentations, no single compound limits growth or product formation during the entire course of the fermentation. This should be kept in mind during modeling of cellular processes.

3. Product-limited Models

Several models have been proposed to describe the case of product-limited cultures. Hinshelwood first proposed the following equation to describe inhibitory effects[23]

$$\frac{1}{N}\frac{dN}{dt} = \mu_m(1 - aP) \tag{17}$$

where N = cells/ml

μ_m = maximum specific growth rate

P = concentration of inhibitory product

a = constant

He further assumed that the specific rate of formation of inhibitory product was a constant[23]

$$\frac{1}{N}\frac{dP}{dt} = r \tag{18}$$

Reid integrated Eqs. (17) and (18) to give the following equations[24]

$$\frac{1}{N}\frac{dN}{dt} = \sqrt{\mu_m^{\,2} + 2\ a\ r\ \mu_m(N_o - N)} \tag{19}$$

$$N_m - N_o = \mu_m/2\ a\ r \tag{20}$$

where N_o = initial cell concentration
N_m = maximum cell concentration

Recently, Finn has shown the if N_o is negligible, these equations simplify to give[25]

$$\frac{1}{N}\frac{dN}{dt} = \mu_m(1 - N/N_m)^{1/2} \tag{21}$$

Another model used in the general area of population growth and in particular in bacterial growth is the simple logistic equation, which was originally used by Pearl to model the population of the United States.[26,27] It has the form

$$\frac{1}{N}\frac{dN}{dt} = \mu_m(1 - N/N_m) \tag{22}$$

which when integrated gives the form

$$N = \frac{N_m}{1 + \exp(-\mu_m(t - t_o))} \tag{23}$$

The model of Luedeking and Piret for product formation is now in wide use for the case of product limited cultures. They proposed the following form[28]

$$\frac{dP}{dt} = \alpha\frac{dX}{dt} + \beta\ X \tag{24}$$

The first term on the right hand side of Eq. (24) is meant to account for growth associated product formation and the second term for non-growth

associated product formation. Rearrangement with insertion of the definition of the specific growth rate gives the following equation

$$\frac{1}{X}\frac{dP}{dt} = \alpha\,\mu + \beta \tag{25}$$

Equation (25) predicts that a graph of the specific rate of product formation, $\frac{1}{X}\frac{dP}{dt}$, versus the specific growth rate, $\frac{1}{X}\frac{dX}{dt}$, should be linear. This was observed to be the case with the lactic acid fermentation.[28] A relation between specific growth rate and cell concentration is also needed to use the model to predict culture behavior. As a second relation, Luedeking and Piret used the graphical correlation technique of Adams and Hungate (simply a plot of cell number versus specific growth rate, as measured from batch culture growth data).[29] Prediction of continuous culture performance from batch data by this method is not always successful, as was shown by Humphrey.[30] The equations for specific growth rate that were discussed earlier could also be used, with the degree of success dependent on the system.

4. Models in Which Both Product and Substrate Control Rates

Chen et al. have demonstrated that product and substrate simultaneously affect product formation by *Septomyxa affinis* during the dehydrogenation of steroids.[31] Working with non-growth systems, they showed that dehydrogenation rates could not be fit with a simple substrate-limited model, requiring instead the following equation

$$-\frac{dS}{dt} = \frac{(K_r E_o K_s)\,S}{(1 + K_s S + K_p P)} \tag{26}$$

where K_s = adsorption equilibrium constant
= inverse of Monod constant
K_p = desorption equilibrium constant
E_o = total mass of enzyme
K_r = reaction rate constant for rate of enxyme-substrate complex formation

They showed that assuming constant yields, Eq. (26) could be integrated to give the following form

$$K_r E_o t = (1/K_s(1 + K_p(a + P_o)))\ln(a/(a-x) + (1 - K_p/K_s))x \qquad (27)$$

where a = initial substrate concentration

x = amount of substrate reacted at time t

P_o = initial product concentration

More recently, Maxon and Chen have successfully simulated complicated fermentations, including some with semi-continuous substrate addition using models again based on enzyme kinetics.[32] For example, growth rates on glucose with inhibition by neomycin can be modeled by the equation

$$\frac{d(\text{cells})}{dt} = \frac{k(\text{cells})(\text{glucose})}{1 + K_1(\text{glucose}) + K_2(\text{neomycin})} \qquad (28)$$

Also, they model catabolite repressions in the conversion of glucosamine to compound Z, a reaction which is first order with respect to glucosamine but inhibited by glucose, with the equation

$$\frac{dZ}{dt} = \frac{k(\text{glucosamine})}{1 + K(\text{glucose})} \qquad (29)$$

Their models, which are oriented towards describing product formation, have been used successfully in a number of important industrial fermentations.

C. More Elaborate Approaches

1. Remarks

The models just discussed all treated substrate consumption, cell proliferation, and product formation as variables dependent only on cell concentration, substrate concentration, and product concentration. No attempt was made to include such important variables as the cell age distribution or the cell composition. By eliminating these variables from consideration, the resulting unstructured, distributed models were much simpler to use, being easier to manipulate; they also have fewer parameters to evaluate and thus require less experimental data for the evaluation of the parameters. Along with the progress of the last 15 years in understanding of the processes of cell growth, proliferation, and metabolism came advances in modeling of these processes.

2. Culture Age

One noteworthy approach was started by Shu.[33] He proposed a model that accounted for what he called the physiological age of culture and its effect on the metabolic activities of the culture by use of an equation for the rate of product formation of the following form:[33]

$$\frac{dP}{dt} = \sum_i A_i \exp(-K_i\theta) \qquad (30)$$

where θ = cell age defined as the time elapsed since birth by division of an existing parent cell

A_i, K_i = constants

His model distinguishes between mother and daughter cells; the age of the mother cell continues to increase after formation of a daughter cell by birth, while the daughter cell has age zero at the time of separation from the mother cell. His model is thus more appropriate for the budding of yeast and the growth of mycelial organisms than for binary fission of bacteria, although recent work by Maruyama and Hayashi with B. megaterium suggests that a portion of the bacteria in a culture may be aged by

division, eventually becoming non-viable.[34] Shu developed his model for both batch and continuous culture systems and showed that it would apply to batch cultures in both the lactic acid and lysine fermentations.[33]

Kobayashi has shown recently that the model could also be applied to a variety of batch and continuous culture systems, including multistage systems.

3. Statistics of Cell Division

Another important type of approach to kinetics of bacterial growth was begun by Kelly and Rahn in 1932.[36] They measured the distribution of times between successive divisions in individual bacteria. As they and many others have shown, there is often a wide distribution of cell division times in a culture of bacteria. Rahn proposed that cell division occurs after a group of cellular elements, pictured as genes, have been replicated.[37] Each element was modeled as replicating by a first-order reaction and was therefore random in time. Finney and Martin refined the statistical aspects of Rahn's model.[38] Kendall treated the process of cell division as resulting from the completion of a number of necessary steps, each a random Markov (stochastic) process.[39] The convolution or concatenation of those steps determines the division age distribution that cells achieve before dividing.[39] Later, Kendall combined his previous model with Rahn's model in a general theory.[40] Recently, considerable research has gone on along both experimental[41,42,43,44,46] and theoretical lines.[41,42,45,46]

Powell analyzed the affects of cell age distributions on continuous as well as batch culture.[41] He showed that the age distribution in continuous culture must in general be different from the distribution in batch culture.[41] He also showed that younger cells will always be present in the greatest number in growing cultures. Correlations between sister cells does not affect the growth rate of a culture, but mother-daughter correlations do.[41] In 1958 Powell published data and observations on the patterns of bacterial generation times of four species of bacteria

under several sets of conditions.[42] He obtained positive correlations between the generation times of sisters, cousins, and perhaps second cousins, showing that the effect of an ancestor is felt through two or three generations. Correlations between mothers and daughters were small, partly he points out, because of bias due to the interval between fission of cytoplasm and fission of cell wall. He found that the coefficient of variation was not constant for a given species, but that it was stable under given conditions, possible being related to the chemical complexity of the growth medium.

Kubitschek has shown that E. coli B/r, Hela cells, yeast, and a protozoan had cell generation rates (reciprocal of generation time) that could be treated as normal distributions when these populations were in balanced growth.[43] Sister rates are thus correlated, while mother and daughter are not unless daughter cells divide unusually soon after birth. These daughter cells usually had mother cells with long generation times. The correlations negate the hypothesis of Rahn and Kendall, which assumed independence of cell divisions.[43]

Schaechter et al. made measurements of growth, cell, and nuclear division in bacteria.[44] They found that the size at division was critical, in the sense that the coefficient of variation of size was smaller than the coefficient of variation of age at division. They found further that the critical size of bacteria at division changes monotonically, and without increase in its coefficient of variation, throughout the reorganization that accompanies a shift of a growing culture from one medium to another medium in which the growth rate and bacterial size are different. This last fact is an interesting contrast to Powell's finding that the coefficient of variation of generation times were not constant.[42] Koch and Schaechter proposed a model based on their measurements and the measurements of others that assumes that cell growth is deterministic, that the mean cell size at division is under cellular and environmental control, that the distribution of sizes of cells at division has a small coefficient of variation, and is independent of size at previous divisions,

and that the cell divides into nearly equal halves.[45] Their model explains the experimentally observed sister-sister generation time correlation and the negative mother-daughter generation time correlation. The magnitude of observed coefficients of variation of generation times result from the fact that the mass variable enters twice into determining the generation time, once when determining the cell size when the cell is formed and again when the cell divides. Deviations from the model are explained as being due to deviations from equal partition of cell components on division. Another likely source is the inherently statistical nature of many cellular processes which depend on small numbers of molecular events as discussed by Powell.[42]

Powell and Errington made further measurements of bacterial generation times and showed that complex media gave rise to a greater dispersion of generation time than simple media and that there is positive association between the generation times of second cousins.[46] They disputed the earlier observations of Kubitschek that generation rates are normally distributed.[43]

4. Segregated Models of Culture Kinetics

Some recent models of bacterial kinetics have included the differences in the rates of growth and metabolism of individual cells and have modeled these effects by making assumptions about their statistical distribution among the members of the population. One of these models was proposed by Frederickson and Tsuchiya.[47] They model the kinetics of growth of bacteria that are assumed to divide by binary fission and produce no spores. Cell age is defined as the time elapsed since the cell was formed by separation from another cell by binary fission. Cell age and its distribution, clock time, and dilution rate in the case of continuous culture are considered as the only independent variables and other variables such as metabolic rates and the cell size distribution are derived from these independent variables. An important feature of their model is that cell death is included as a possible event in the life of the cell.

The relation of their model to other models and the stability of the model system in continuous culture is discussed. Tsuchiya, Frederickson, and Aris have recently refined their derivation of this model and have proposed a new, more general model.[11]

Terui has proposed a simpler (and more easily applied) model for the adaptation of yeast to maltose.[12] By assuming that the adaptation lag time of the cells in the population has a normal distribution, a sigmoidal form (as in an autocatalytic reaction) is obtained from the time integral for the probability of adaptation in any cell. Good agreement is obtained with experimental results.[12] The model is consistent with the observations of Benzer, who did phage tests on the production of galactosidase by E. coli.[48] He observed a random distribution for the adaptation when the adaptive substrate was the only carbon source.

Currently, Terui has offered further experimental evidence for high model for adaptation by showing that the distribution of times of volume increase of yeast cells (resulting from adaptation to maltose) are normally distributed as had been postulated.[13] Using the standard deviations obtained with these optical measurements on individual cells, he was able to predict the gross kinetics of the adaptation of the culture.

In this recent work, he has also produced a model that works well for describing glucamylase producing activity in a 3-stage continuous reactor system. The first vessel was used mainly for growth, the second for glucamylase production, and the third for recovery of residual activity of mycelia. Rates of increased glucamylase activity in batch culture were found to be fit well by the form for monomolecular catalaysis

$$f(\theta) = \frac{E_m - E_o}{1 + a \exp(-k\theta)} + E_o \qquad (31)$$

where $f(\theta)$ = activity of glucamylase at age θ

θ = time elapsed with mycelia in glucamylase producing environment

E_o = initial glucamylase activity
E_m = maximum glucamylase activity
a,k = constants

A similar model is applied to the shift-down of glucamylase activity in the third vessel. Predicted steady-state values were in good agreement with observed values and further good matching was obtained for the unsteady-state values in the second vessel. Good agreement in predicting the unsteady-state values was not obtained in the third vessel, possibly due to overaging of mycelia in that vessel.

5. Structured Models of Microbial Populations

In the last section models were presented that took cognizance of the effects of the cell age distribution. In this section several models will be discussed that deal with the effects of the cell composition. The first model to be discussed was proposed by Yeisley and Pollard and differs from the other models discussed in that it models a single cell rather than a culture.[49] A set of seven differential equations is proposed that represent the processes of ribosomal, protein, and nucleic acid synthesis in the bacterial cell and one base in part on measurements of real systems. The model cell is simulated by an analog computer model of the set of equations and five steady-state solutions were found by trial-and-error. These solutions are defined as a combination of rate parameters which yields simultaneous doubling of all components of the cell. Such a definition is probably not operationally correct because some components are probably doubled before others in the living cell. One example is DNA (deoxy-ribonucleic acid), which in some cases is known to be replicated in considerably less than one generation time in growing cells. Yeisley and Pollard considered this alternative behavior in their model and in fact showed that it increased the stability of the model to disturbances in initial composition of the model cell. Stresses were modeled by changing the initial concentration of one or more components and following the system through several generations to see if the system returned to the steady-

state concentrations of all components. Fast readout and decay of messenger RNA was found to give greater stability. The study showed the value of the analog computer model approach to studying kinetics of cellular growth.

Ramkrishna, Fredrickson, and Tsuchiya recently proposed two models of microbial culture growth.[9] Their first model was considered to be unstructured because it did not recognize different components of the composition, but it is considered here because it distinguished between viable and non-viable cells. They call it the Staling effect model because inhibitor is assumed to be produced by cells during growth and thus is further assumed to combine with viable cell mass to produce non-viable cell mass. The equations thus have the form

$$V + a_S S \rightarrow 2V + a_T T + \ldots \tag{32}$$

$$V + T \rightarrow N + (1 + a_{T1})T + \ldots \tag{33}$$

where V = viable cell mass

N = non-viable cell mass

S = substrate

T = inhibitor

a_S, a_T, a_{T1} = stoichiometric coeffients

The dots in the reactions represent byproducts released to the medium. They assume growth rate to be related to the substrate concentration by the Monod equation and death to be given by a second order expression, the product of viable cell concentration and inhibitor concentration. Batch growth, substrate consumption, and inhibitor production show all characteristics shown by real cultures except a lag phase. The model gives different effects for different inoculum sizes and for different initial substrate concentrations. The model is shown to predict oscillatory behavior in continuous culture under special conditions of high feed substrate concentrations and long holding times.

The second model presented by Ramkrishna et al. was structured.[9] The cellular mass was viewed as being composed of two classes of compounds that could be thought of respectively as nucleic acids and the rest of the viable biomass. Both components were inactivated by inhibitors in a manner similar to that in their previous model. Second order kinetic expressions were assumed for reaction rates of formation of both components. Their second model could explain most phenomena observed in batch and continuous culture that were not predicted by their earlier model including the lag phase in batch culture and stability limit and unstable behavior near washout in continuous culture.

V. DATA ANALYSIS

A. Introduction

As can be seen from the foregoing literature survey, time derivatives of batch culture data are very often needed for kinetic analysis of the data. While graphical differentiation of the data is straight forward, it is tedious and relatively inaccurate, the results often depending on the brand of french curves used in drawing the lines through the data. Numerical differentiation through interpolation formulae offers an improvement, but is very sensitive to scatter in the data and assumes nothing is known about the functional form of the equation(s) describing the system studied. Also, data must be taken frequently for interpolation to work.

For the measurements of slopes of batch culture kinetic data, it appeared logical to adopt a generalized, integrated form of a popular kinetic model. Most mathematical models can not be integrated to give the dependent variable in an explicit form. Use of the equations from those models is thus very inconvenient for either curve-fitting or application of the fitted curve. An exception is the simple logistic equation discussed earlier. It has the integrated form

$$y = \frac{K}{1 + \exp(a_o + a_1 t)} \tag{34}$$

where y = dependent variable, e.g., cell concentration

K = final value of dependent variable (if final value is not zero

t = time

a_o, a_1 = constants

As pointed out be Dewitt, a generalized form of the logistic equation provides a very flexible form for fitting of sigmoidal data such as that obtained in filtration.[50] The generalized form is

$$y = \frac{K}{1 + \exp(F(t_1))} \tag{35}$$

where $F(t)$ = a polynomial in time

$= a_o + a_1 t_1 + a_2 t_1^2 + \ldots + a_n t_1^n$

$(t_1) = t - t_L$

t = time

t_L = length of lag phase

Two additional advantages of this model with regard to bacterial kinetics are that first, the value of y at large values of time is K or zero and second, at low values of y/K, exponential growth is well approximated, gradually going over to product-inhibited growth at large time values. Equation (36) shows the dependence of the specific growth rate on values of y and t.

$$\frac{1}{y}\frac{dy}{dt} = -(1 - y/K)(+ a_1 + 2a_2 t_1 + 3a_3 t_1^2 - \ldots + na_n t_1^{n-1}) \tag{36}$$

Because our batch culture kinetic data came from a system known to have product inhibition (sulfide) the generalized logistic equation was attractive and it was selected as the model of choice for representing the batch data.

B. Properties of the Model

Properties of the proposed model were discussed by Dewitt.[50] An outline of the properties will be given here.

Equation (36) can be rearranged to give the following form

$$\frac{dy}{dt} = - y(1 - y/K)\ F'(t) \tag{37}$$

Because y is always greater than zero and less than K, the sign of the first derivative, dy/dt, is determined by $F'(t)$, which may take on successively positive and negative values at various times values.

Points of inflection of Eq. (35) occur at intersections with Eq. (38)

$$y = K/2 \left(1 - \frac{F''(x)}{(F'(x))^2}\right) \tag{38}$$

Depending on the number of terms in $F'(t)$ and their signs, a number of relative maxima and minima may be obtained. For example, for $F(t)$ a fifth degree polynomial, $F(t) = a_o + a_1 t + a_2 t^2 + a_3 t^3 + a_4 t^4 + a_5 t^5$, and up to 3 relative minima and 3 relative maxima may be obtained, as shown in Fig. 2. In Fig. 2, at low values of the independent variable, lower order terms predominate, with higher order terms becoming the determining factors at high values of the independent variables. For the case shown, a_1, a_3, and a_5 have negative values while a_o, a_2, and a_4 have positive values. Of course, the values of a_o, a_1, ... a_n can take on any values desired to obtain curves of the desired type. The curve just shown demonstrates maximum degree of flexibility for a fifth order polynomial. In general, the maximum number of relative minima and maxima in the first quadrant may be at most one greater than the degree of the polynomial. The highest order term ultimately determines the asymptotes of the curve. Thus there are four possible results because a_n may be positive or negative and n may be odd or even. Figure 3 shows the four possible cases. Note that all values of the dependent variable lie between $y = K$ and $y = 0$. For the modeling of bacterial growth, n was always chosen as odd, values of 1, 3, and 5 being chosen, so that only curves of the second and the fourth types shown in Fig. 3 were used. Because the microbial growth is limited to the first quadrant, these two cases proved adequate to give the two desired alternatives of an asymptotic approach to a constant at large values of time and the case of an asymptotic approach to a zero value at large values of time. The first case could represent product concentrations versus time, while the second case could represent viable cell count versus time, which would approach zero concentration at

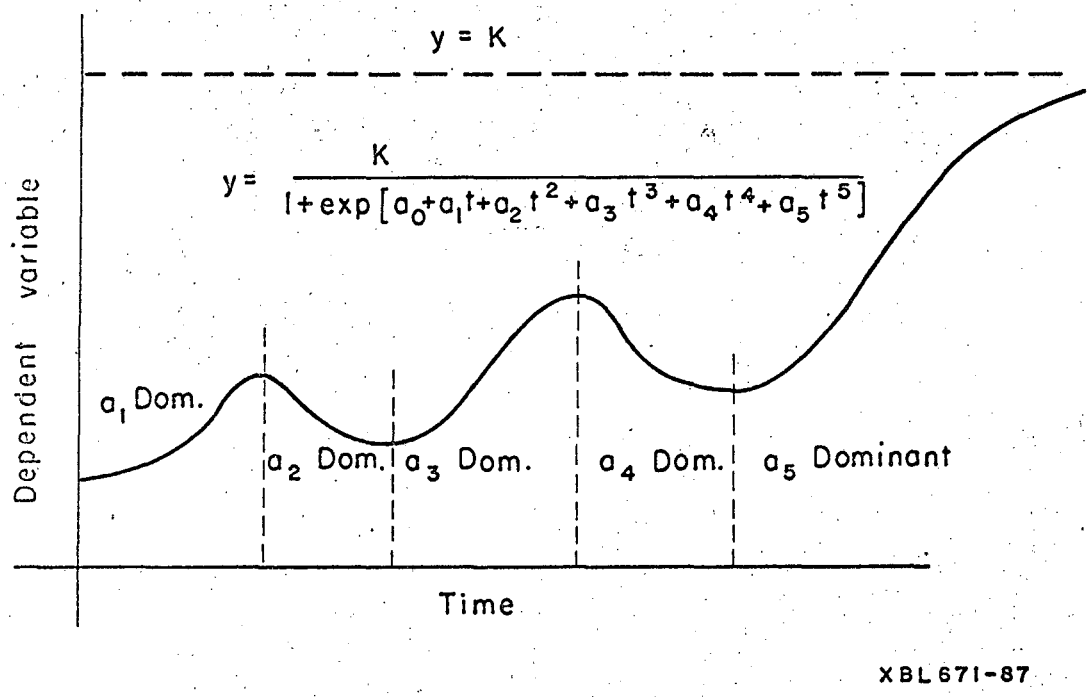

Fig. 2. Typical plot of fifth degree fitting equation versus time.

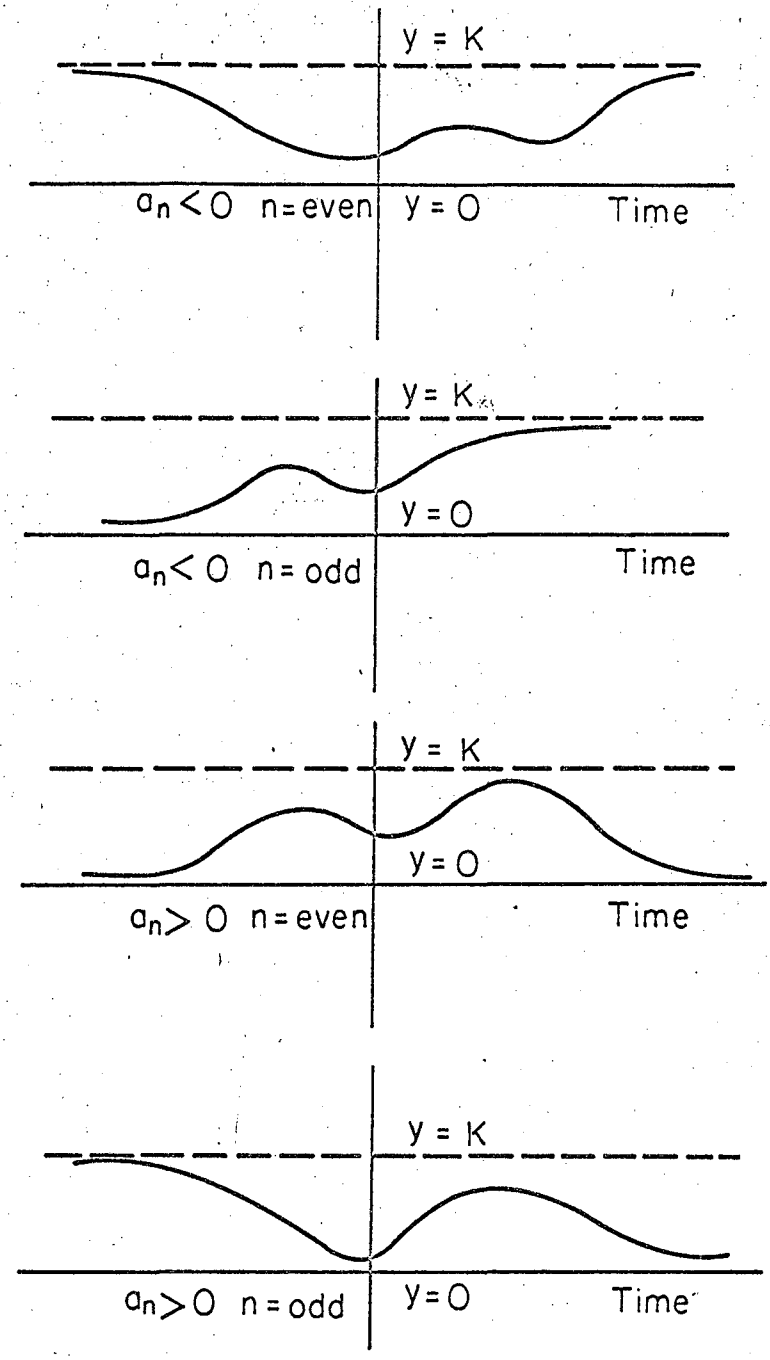

XBL 671-245

Fig. 3. Possible limiting cases for fitting model at large positive and negative values of independent variable.

very long incubation times. The flexibility of the model thus appears to be adequate to fit all types of batch culture data including data from complex fermentations. However, the non-linear least squares technique does not always succeed in fitting complex data, as will be discussed shortly.

C. Computer Program

To reduce the labor of fitting the equation to the data, a computer program in Chippewa Fortran was written for use with a Control Data 6600 Computer. A method of non-linear least squares curve-fitting was used to fit the equation to the data. The method is that given by Scarborough.[51] A linear least squares method will not work because the generalized logistic equation is non-linear in the coefficients to be computed. The non-linear method consists of making initial guesses for the values of the coefficients and correcting these initial guesses by repeated iteration until a desired degree of convergence is reached. The technique of making initial guesses is given in Appendix I. Corrections are obtained by assuming a Taylor series expansion of the fitting function in its coefficients, analogous to the Newton-Raphson technique of seeking roots of a non-linear equation. The method and a detailed outline of the computer program is given in Appendix II. A brief description of the program is presented here. Figure 4 shows the program in outline form. Several groups of data may be analyzed in sequence. During analysis of a group, the following sequence of events is followed: First, the data to which a curve is to be fit are read into the computer, along with standard deviations of the data, a time lag if required, and equally-spaced estimates of dependent variable for use in making estimates of the initial values of the parameters of the fitting equation. Weighting functions are calculated from the standard deviations and the data, standard deviations, and the weights of the data are printed out.

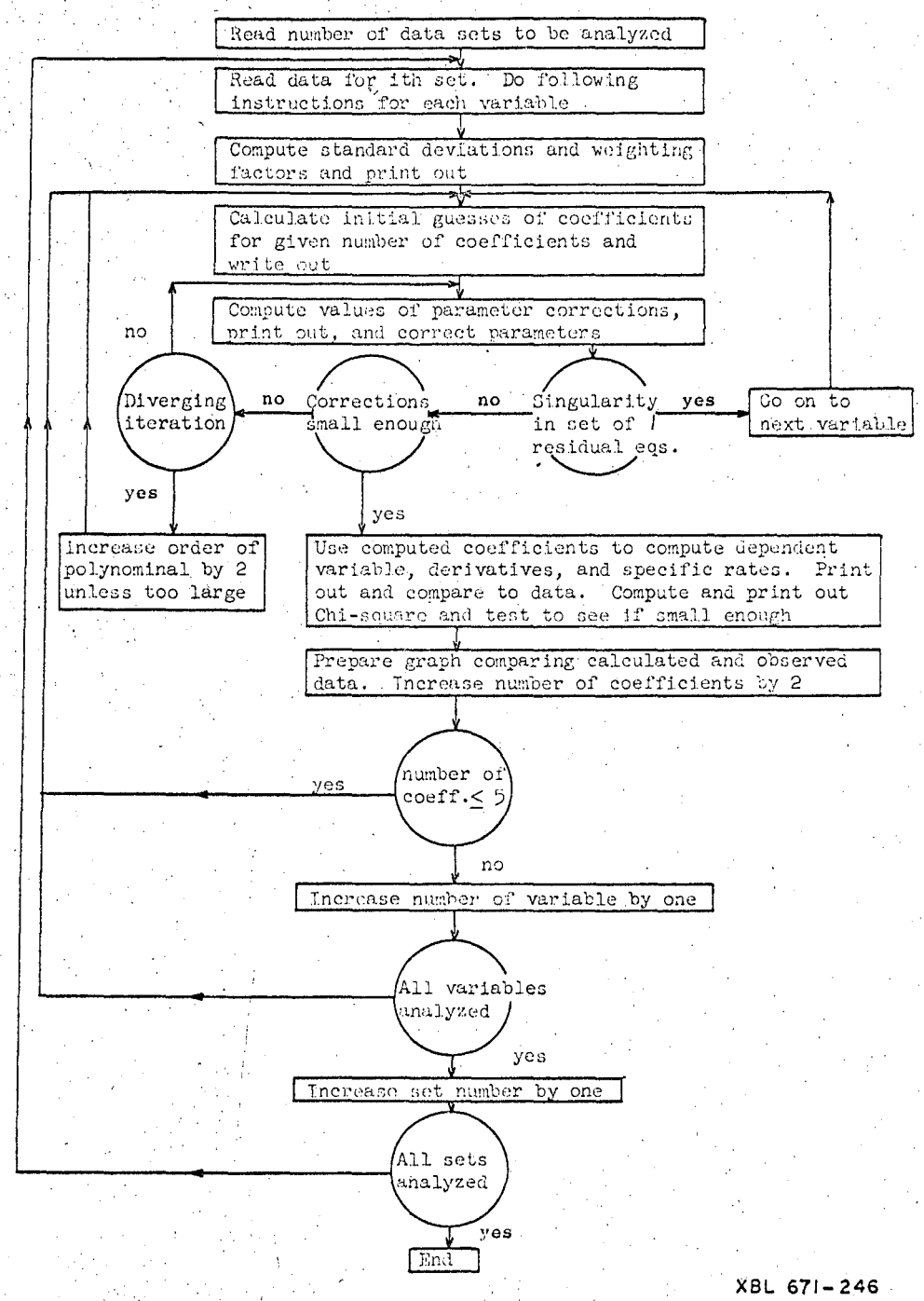

Fig. 4. Schematic outline of curve-fitting computer program

If the time lag is not zero, the coordinates are shifted so that in the new coordinate system, $t' = t - t_L$, where t' = new time scale, t = real time scale, and t_L = length of the lag phase. The value of the dependent variable at $t = t_L$ is assumed to be the average of all data values for $t \leq t_L$ and the fitting of the equation to the remaining data is done in the new coordinates.

Estimates of the corrections to the estimated values of the fitting parameters are computed for $F(t) = a_o + a_1 t'$ and the values of the parameters are corrected. This process is continued until the sum of the absolute magnitude of the ratio of the changes in the coefficients to their absolute value is less than .001. The values of the corrections and the corrected parameters are printed out at each step. At each tenth step, the values of the data and the corresponding values calculated with the fit equation are compared in a table. A maximum of 100 iterations is allowed to reach the desired convergence on the fit parameters. After the fitted values are obtained, the data and the values computed with the fitting equation are compared. Then the calculated derivatives and specific rates are calculated at regular intervals and printed-out also. Finally, a graph is prepared comparing the original data points with the line connecting the values calculated using the fitted equation. The process, starting with estimation of parameters and optimization by iteration, is repeated for third and fifth degree polynomials, provided that the number of data warrant it and that the additional terms are necessary to improve the fit to the data. The next variable in that group of data is then analyzed by the same procedure, until the last variable has been analyzed. The next set of data is analyzed. Cell concentration data must always be analyzed first because the fitted values of cell concentration are needed in computation of specific rates of change in later variables. The graphs prepared by the computer are very helpful in decisions about the adequacy of the equations fitted with the program. Chi-square values are also computed to assist in judgment of the goodness of fit.

D. Tests of Curve-fitting Model

Both synthetic and experimental data were supplied to the computer program to test the curve-fitting technique. The tests are discussed in this section.

1. Test #1

To test the effectiveness of the computer program in obtaining a good fit of the data, data were calculated with the following equation

$$y = \frac{1.04 \times 10^8}{1 + \exp(3.33-1.47(t-1))} \qquad t \geq 1 \qquad (39a)$$

$$y = \frac{1.04 \times 10^8}{1 + \exp(3.33)} \qquad t \leq 1 \qquad (39b)$$

Note that a time lag of 1.0 time units was assumed. Representative points were calculated from Eq. (39) and are listed in Table VI under "Original dependent variable". These data were then supplied to the curve-fitting program, which fit the following equation to the data

$$\begin{aligned} y &= \frac{1.045 \times 10^8}{1 + \exp(3.331-1.391(t-1))} \qquad t > 1 \\ y &= 3.60 \qquad t \leq 1 \end{aligned} \qquad (40)$$

The results calculated with Eq. (40) are compared with those obtained with Eq. (39) in Table VI and in Fig. 5. Agreement is good in both the figure and the table, signifying correct iteration to the desired result. Note also the good agreement between coefficients in Eq. (39) and Eq. (40).

2. Test #2

The second test was achieved by use of data for an imaginary system that had a period of exponential increase of cell concentration followed by a phase of constant cell concentration. Data values are listed in Table VII. The exponential data were from a table of exponentials. Plotting specific growth rates on semi-log paper, the first

Table VI. Original and calculated values, dummy data

Independent variable	Original dependent variable	Calculated dependent variable
0.0	3.6×10^6	3.600×10^6
1.0	3.60×10^6	3.600×10^6
2.0	1.32×10^7	1.314×10^7
3.0	3.80×10^7	3.829×10^7
4.0	7.34×10^7	7.307×10^7
5.0	9.45×10^7	9.440×10^7
6.0	10.15×10^7	10.180×10^7

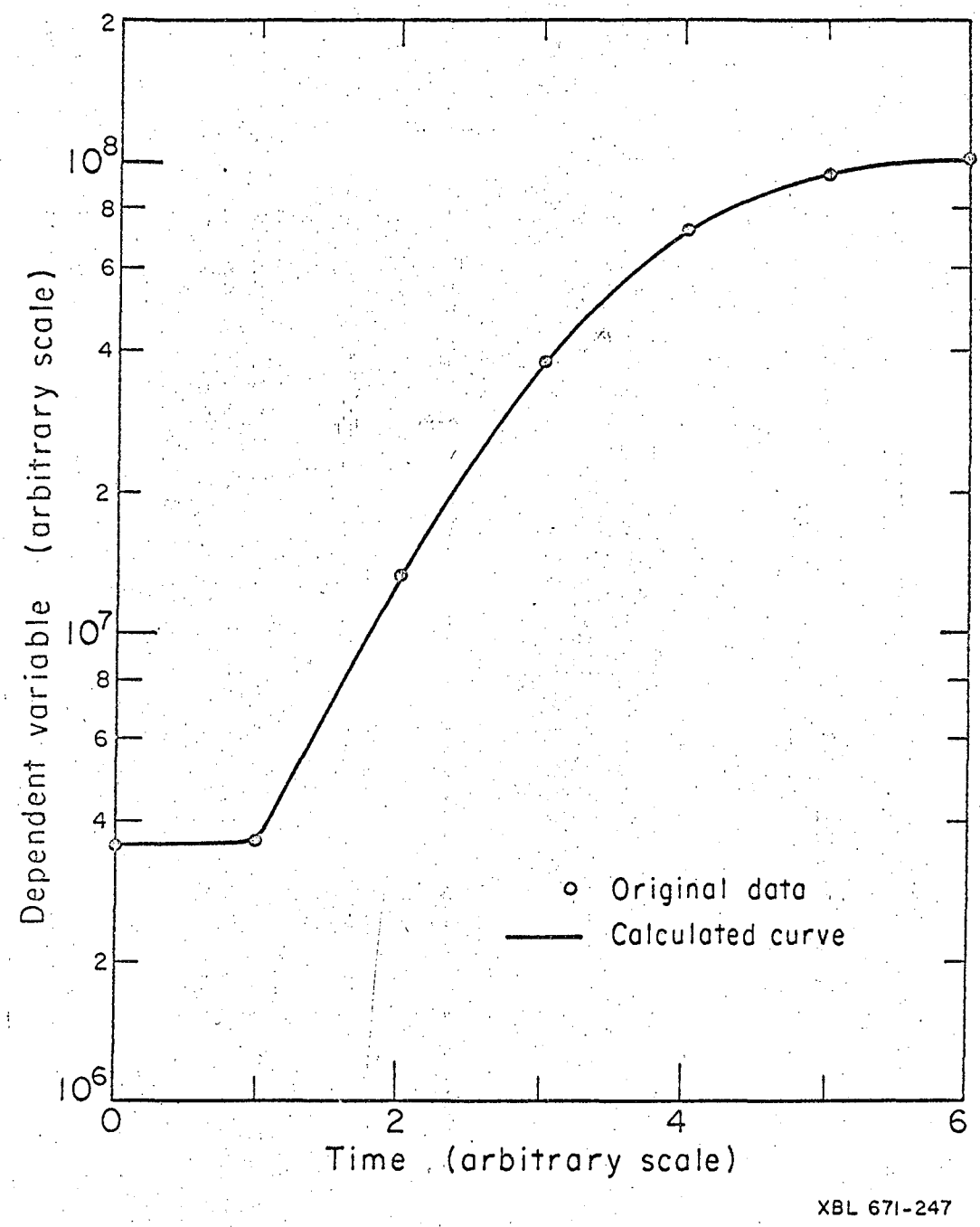

Fig. 5. A comparison of original and fit values, test #1.

Table VII. Data of test #2

Independent variable	Dependent variable		
	Given	Calculated, F(t) first degree	Calculated F(t) fifth degree
0	1.0000	1.0000	1.0000
1	1.6487	1.5838	1.6773
2	2.7183	2.7022	2.6915
3	4.4817	4.5952	4.4136
4	7.3891	7.7706	7.4159
5	12.182	13.019	12.406
6	20.086	21.485	20.194
7	33.115	34.615	32.395
8	54.598	53.794	53.921
9	90.017	79.486	93.892
10	148.41	110.19	138.12
11	148.41	142.24	150.88
12	148.41	171.30	151.47

period was a straight line of positive slope and it was followed by a period with a horizontal straight line. The slope discontinuity prevented the continuous function from fitting the curve perfectly and provided a stress on the model. These hypothetical results would never be achieved in practice, but a close approach would be made by a culture growing on a synthetic medium limited by a carbon source if the inoculum were a young adapted and exponentially growing culture that would give a zero lag phase. Cell mass versus time would most likely follow a course well approximated by an exponential and a resting phase, although cell number might not, there being a tendency for cell division to continue for a short period even after exhaustion of the carbon source. Figure 6 and Table VII compare the exponential model to the curves fit by the computer for the cases of a first degree polynomial, equivalent to the Verhulst-Pearl equation and a fifth degree polynomial in the generalized form of the equation. The first degree equation is satisfactory in the low values of cell concentration, but it is inadequate at high cell concentrations. In the case of the fifth degree polynomial, the fit is good. The equations fit to the data are, respectively,

$$N = \frac{239.966}{1 + \exp(5.5530-0.5389)} \tag{41}$$

$$N = \frac{151.473}{1+\exp(5.01945-.60037t+.10757t^2-.040219t^3+.0059485t^4-.00031375t^5)} \tag{42}$$

Use of Eq. (42) is clearly inconvenient without use of a computer or desk calculator. The fit of the specific growth rates calculated by computer are compared to the exponential model in Fig. 7 and Table VIII. As can be seen, the first degree equation again fails, particularly at high values of time and cell concentration, but the fifth degree equation does a good job of representing the general form of the variation of the specific growth rate with time. In the fifth degree case, better results could be obtained by smoothing of the specific growth rate data obtained by computer.

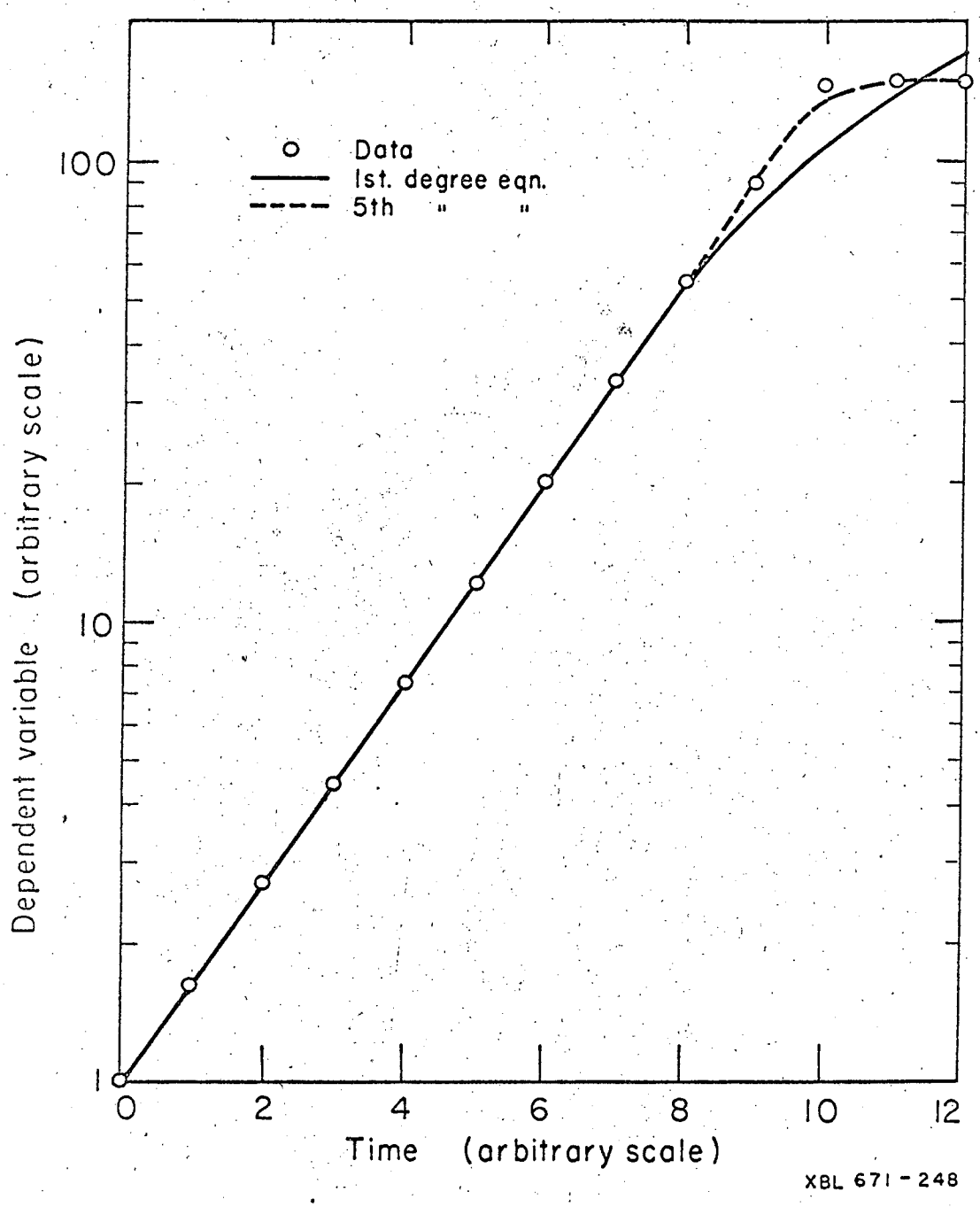

Fig. 6. A comparison of exponential test data with first and fifth degree fitted curves.

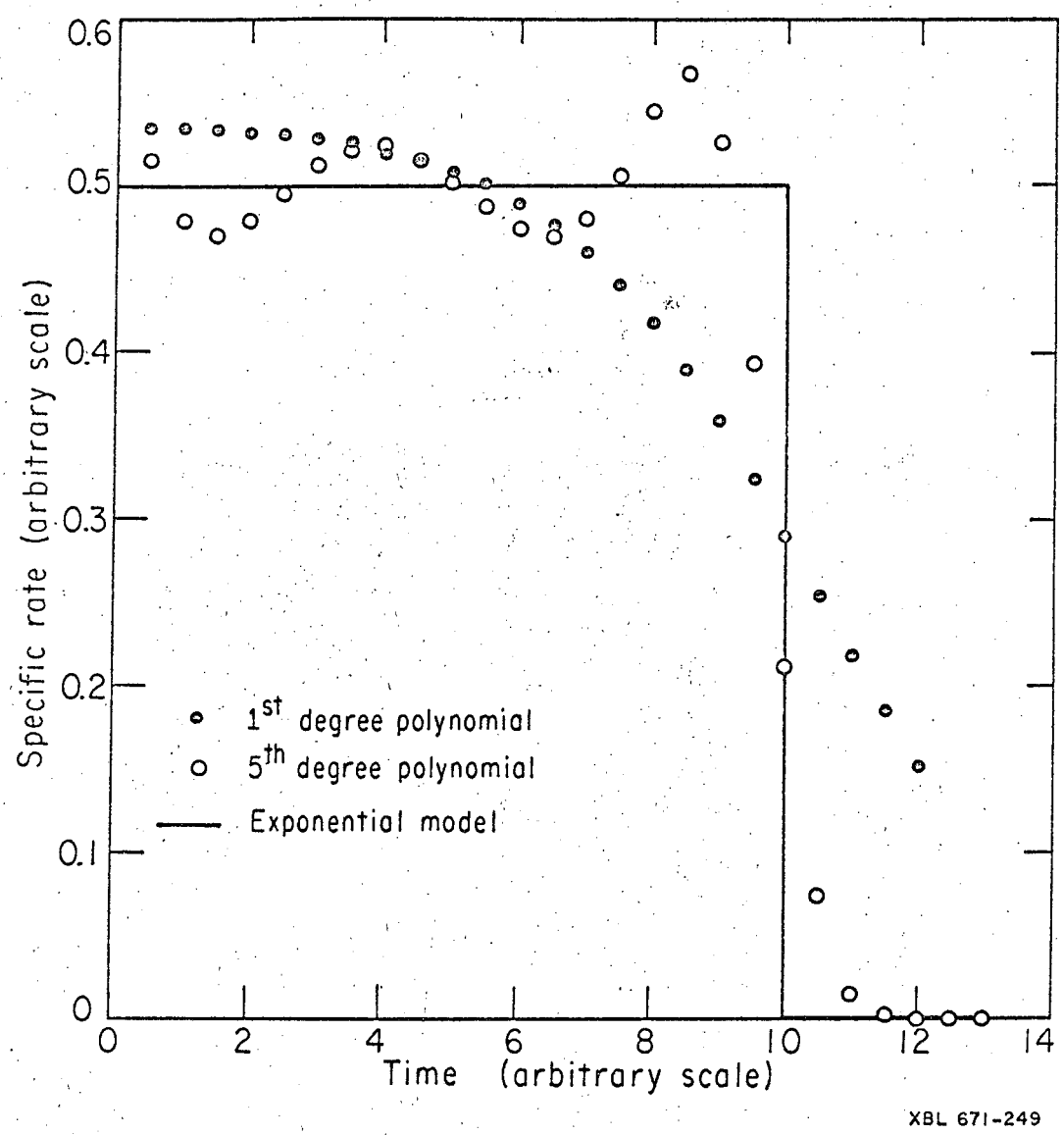

Fig. 7. A comparison of the specific growth rates of the exponential model with values calculated from the first and fifth degree fitted equations.

Table VIII. Specific growth rates, test # 2

Independent variable	Time derivative of dependent variable		
	Given	Calculated, F(t) first degree	Calculated, F(t) fifth degree
0	0.5	--	--
1	"	.535	.478
2	"	.533	.479
3	"	.529	.510
4	"	.521	.522
5	"	.510	.503
6	"	.491	.474
7	"	.461	.481
8	"	.418	.544
9	"	.360	.526
10	--	.291	.212
11	0	.219	.0162
12	0	.154	.00012

3. Test #3

To further test the computer program, a composite model system was devised in which the cell concentration was chosen to vary with time in a manner described by three different functional forms in three different regions of time. In this way, it was possible to have a lag phase, an exponential phase, and a phase of decline. Also, the true derivatives of the composite model could be directly calculated and compared with the computer fit results. The following functions were chosen: For times of 0 to 2 hr, the cell concentration was given by the equation

$$N_1 = 10^4 + 5 \times 10^3 t^3 \tag{43}$$

representing the lag phase. From t = 2 hr and t = 8.3341 hr, the exponential phase, an equation of the following form was chosen

$$N_2 = 4.53589 \times 10^3 \exp(1.2\ t) \tag{44}$$

For a decline phase, an equation of the following form was used

$$N_3 = \frac{1.2507 \times 10^8}{1 + 0.02798/(t-8)^2} \tag{45}$$

Besides giving periods of lagging, exponential, and declining growth, the constants were chosen so that the functions and their first derivatives would match at the points of contact, with t = 2 hr for the contact of lagging and exponential growth and t = 8.3341 hr for the interface between the exponential and declining phases of growth. Thus

$$N_1 = N_2$$

$$\frac{dN_1}{dt} = \frac{dN_2}{dt} \qquad \text{at } t = 2 \text{ hr} \tag{46}$$

$$N_2 = N_3$$

$$\frac{dN_2}{dt} = \frac{dN_3}{dt} \qquad \text{at } t = 8.3341 \text{ hr} \tag{47}$$

The constants were also chosen to represent those that one might obtain with a typical bacterium such as E. coli, having a lag and acceleration phase totaling 2 hrs and an exponential growth doubling time of 34.6 min. The composite model is plotted versus time in Fig. 8 and compared to the curve obtained by the computer fit. Agreement is very good for the fifth degree polynomial curve shown. Agreement is also in evidence in Table IX. It was not as good for first and third degree polynomials which are not shown. The fifth degree equation was as follows:

$$N = \frac{1.2571 \times 10^8}{1+\exp(9.4819+.04694t-.56051t^2+.11041t^3-.0083856t^4+.000132399t^5)} \tag{48}$$

Figure 9 compares original and fitted values of specific growth rate. The results are also listed in Table X. Fitted values are shown as points while the curve represents the values for the composite model. Agreement is good, particularly in the phases of lagging and declining growth, which were introduced to serve as stresses for the fitting equation.

Again, smoothing of the calculated specific growth rates for intermediate values of time improves the accuracy of the calculated specific growth rate.

Eye-balling of slopes was compared to the original data to test the accuracy of graphical methods. Three persons were commissioned to calculated specific growth rates graphically for comparison with the computer calculated data. The data are plotted in Fig. 10 and are listed in Table XI. Agreement is about equal to that obtained with the computer curve fitting program at high and low values of time.

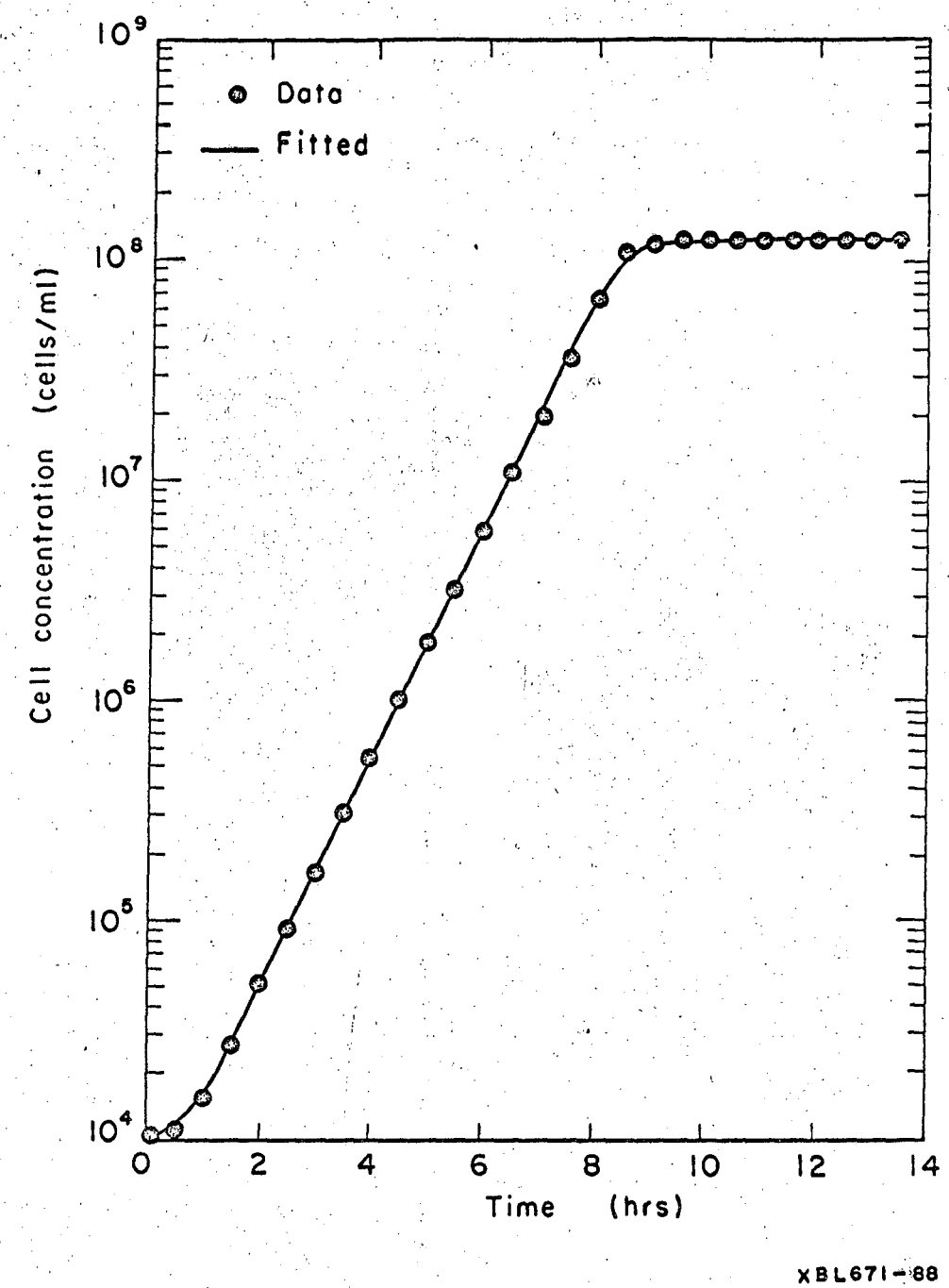

Fig. 8. A comparison of the composite model data with a fitted fifth degree curve.

Table IX. Data of test #3

Independent variable	Dependent variable: Original data	Dependent variable: Computed fit (5th degree polynomial)
0.0	1.0×10^4	1.0×10^4
0.5	1.0625×10^4	$1.1135 \quad 10^4$
1.0	1.5000×10^4	1.5879×10^4
1.5	2.6875×10^4	2.6050×10^4
2.0	5.0000×10^4	4.662×10^4
2.5	9.1106×10^4	8.7284×10^4
3.0	1.6601×10^5	1.6566×10^5
3.5	3.0248×10^5	3.1200×10^5
4.0	5.5116×10^5	5.7599×10^5
4.5	1.0043×10^6	1.0393×10^6
5.0	1.8299×10^6	1.8419×10^6
5.5	3.3343×10^6	3.2450×10^6
6.0	6.0755×10^6	5.7817×10^6
6.5	1.107×10^7	1.0611×10^7
7.0	2.0171×10^7	2.0248×10^7
7.5	3.6755×10^7	3.9253×10^7
8.0	6.6972×10^7	7.0529×10^7
8.334	1.0000×10^8	9.3358×10^7
8.5	1.1248×10^8	1.0291×10^8
9.0	1.2167×10^8	1.2004×10^8
9.5	1.2353×10^8	1.2482×10^8
10.0	1.2420×10^8	1.2562×10^8
10.5	1.2451×10^8	1.2571×10^8
11.0	1.2468×10^8	1.2571×10^8
11.5	1.2479×10^8	1.2571×10^8
12.0	1.2485×10^8	1.2571×10^8
12.5	1.2490×10^8	1.2571×10^8
13.0	1.2493×10^8	1.2571×10^8
13.5	1.2500×10^8	1.2571×10^8

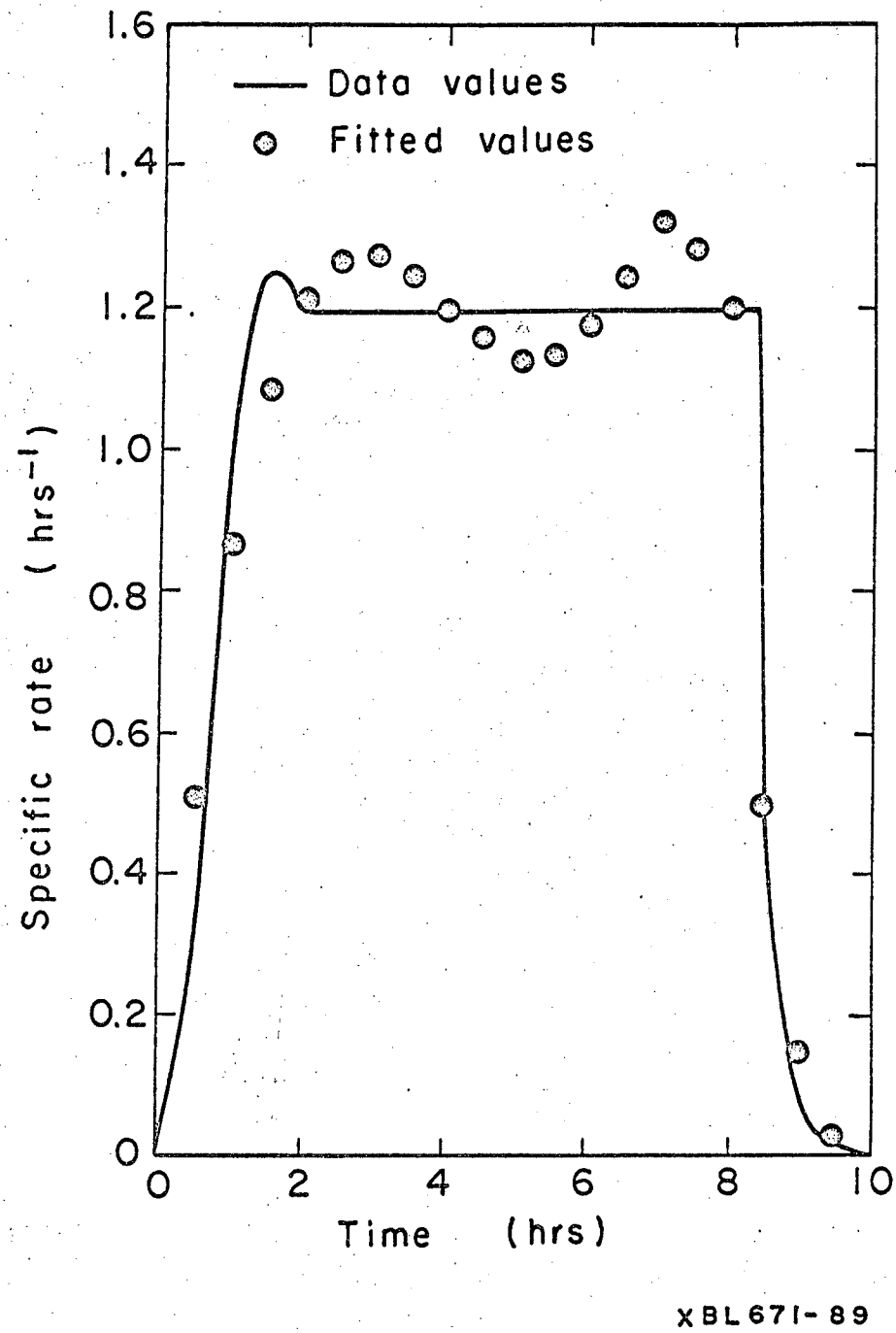

Fig. 9. Comparison of specific growth rates calculated from the composite model with values calculated from the derivative of the fitted curve.

Table X. Specific growth rates, test #3

Independent variable	Specific growth rate	
	Original data	Computed fit (5th degree polynomial)
0	--	--
0.5	.3529	.5287
1.0	1.0000	.8695
1.5	1.2558	1.0928
2.0	1.2000	1.2214
2.5	"	1.2767
3.0	"	1.2793
3.5	"	1.2486
4.0	"	1.2031
4.5	"	1.1596
5.0	"	1.1335
5.5	"	1.1375
6.0	"	1.1792
6.5	"	1.2534
7.0	"	1.3250
7.5	"	1.2923
8.0	"	1.0002
8.5	.4027	.5056
9.0	0.0544	0.1540
9.5	0.0164	0.0295
10.0	0.0069	0.0036
10.5	0.0036	0.00027
11.0	0.0021	0
11.5	0.0013	--
12.0	0.0009	--
12.5	0.0006	--
13.0	0.0004	--
13.5	0.0003	--
14.0	0.0003	--
14.5	0.0002	--

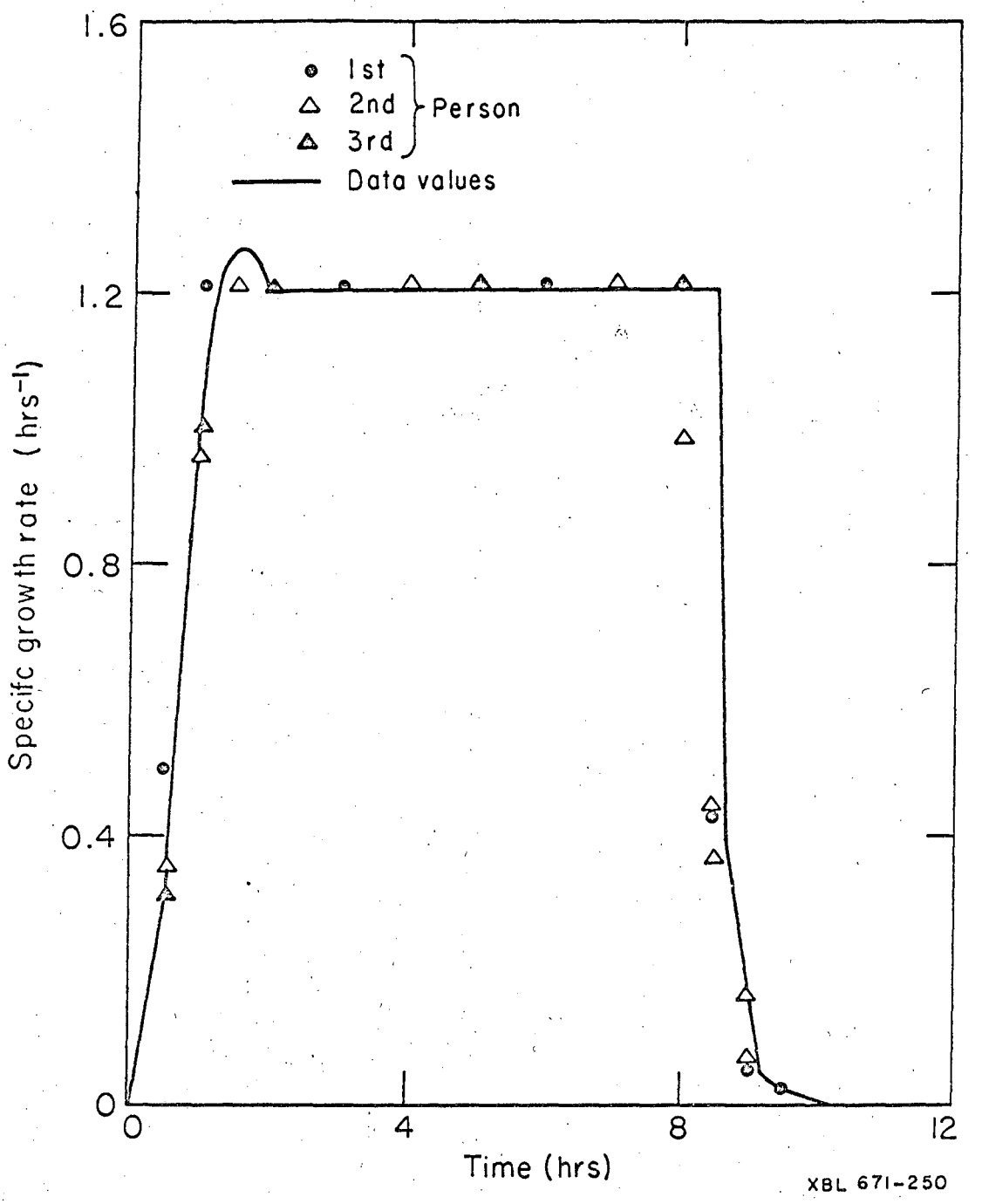

Fig. 10. Comparison of specific growth rates calculated from the composite model with values determined graphically.

Table XI. Specific growth rates obtained graphically, test #3

Independent variable	Original data	Specific growth rate		
		1st person	2nd person	3rd person
0	--	--	--	--
0.5	0.3529	0.501	0.362	0.322
1.0	1.0000	1.212	0.961	1.036
1.5	1.2558	1.212	1.212	1.215
2.0	1.2000	1.212	1.212	1.215
8.0	1.2000	1.212	0.982	1.215
8.334	1.2000	1.212	--	1.215
8.5	0.4027	0.428	0.436	0.366
9.0	0.0544	0.054	0.161	0.068
9.5	0.0164	0.020	--	0.021
10.0	0.0069	0.0095	--	0.007

At intermediate values of time, where the exponential function dominated, graphically calculated data were at least as good as smoothed computer fit results. Computer calculated of slopes should compare more favorably when used with data without a true exponential form. The computer fit also has the advantage of summarizing the data in the form of an equation. A final advantage is that no bias is introduced into the results from the subjective errors of judgment in graphically measured slopes.

4. Test #4

As a further test, the program was applied to the batch culture kinetic data of Luedeking.[52] Luedeking had studied the lactic acid producing Lactobacillus delbruckii system, which was product-limited. Because the Verhulst-Pearl equation was derived assuming product limitation, one expects good results in fitting the model to the data. A comparison of the fit made by comparing both the cell concentration versus time and the growth rate versus time in Figs. 11 and 12, respectively, shows good agreement between observed and calculated values. The points in the two figures are the data values and graphically calculated slopes, respectively, of Luedeking.[52] The line in Fig. 11 is the locus of the equation

$$N = \frac{9.4906}{1+\exp(4.6029-.4622t+.10374t^2-.03135t^3+.003279t^4-1.192\times10^{-4}t^5)} \tag{49}$$

The line in Fig. 12 is the first time derivative of Eq. (49). The observed and fitted values are also compared in Table XII. Good agreement can be seen in both figures between the experimental data and graphical slopes and the computer fit equation and its derivative.

5. Test #5

The first four tests were made using data that approached a positive, non-zero constant at large values of the independent variable. However, as was pointed out in the section on the mathematical properties

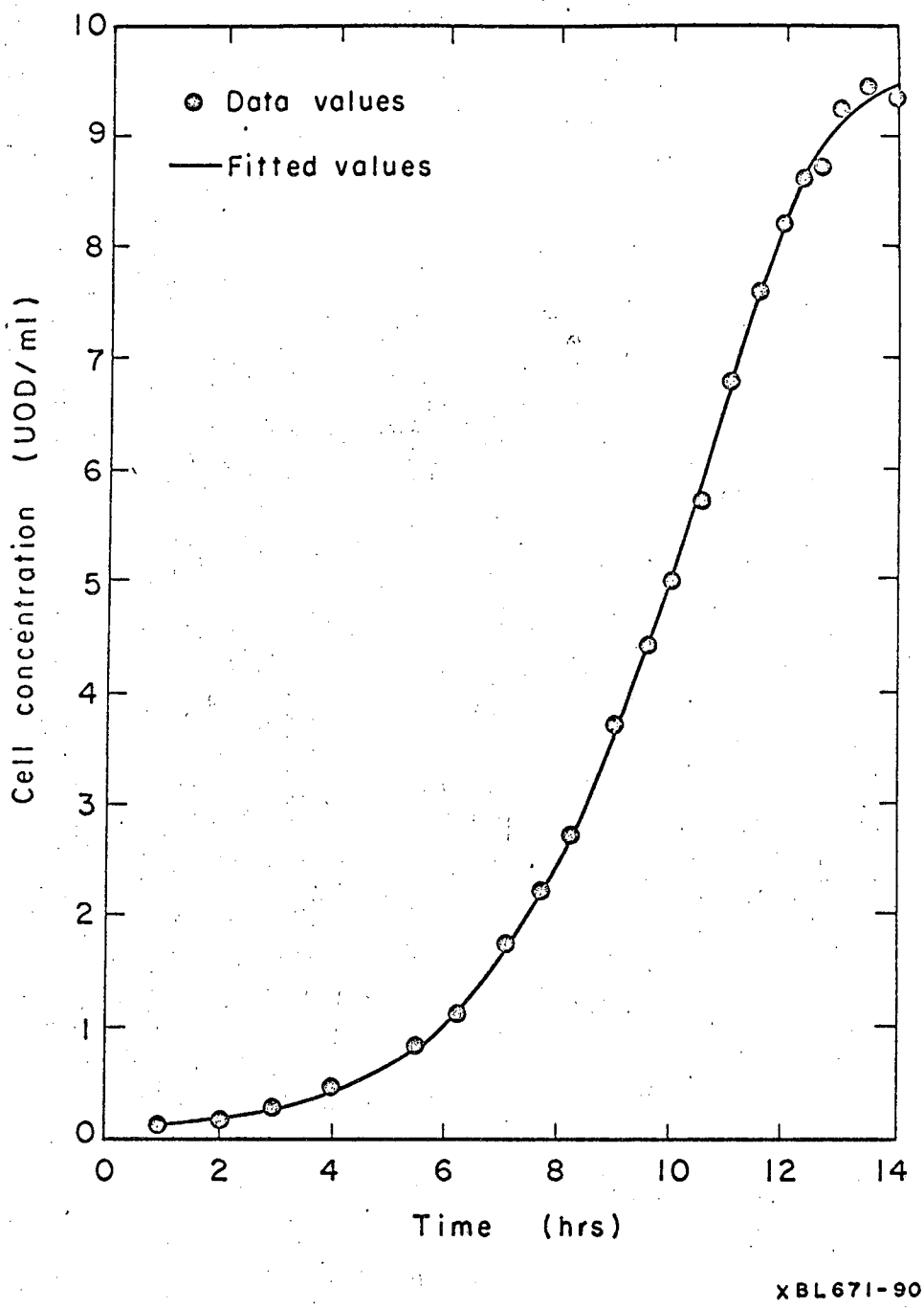

Fig. 11. Comparison of cell concentration data (run 13) of Luedeking[52] with fitted fifth degree curve.

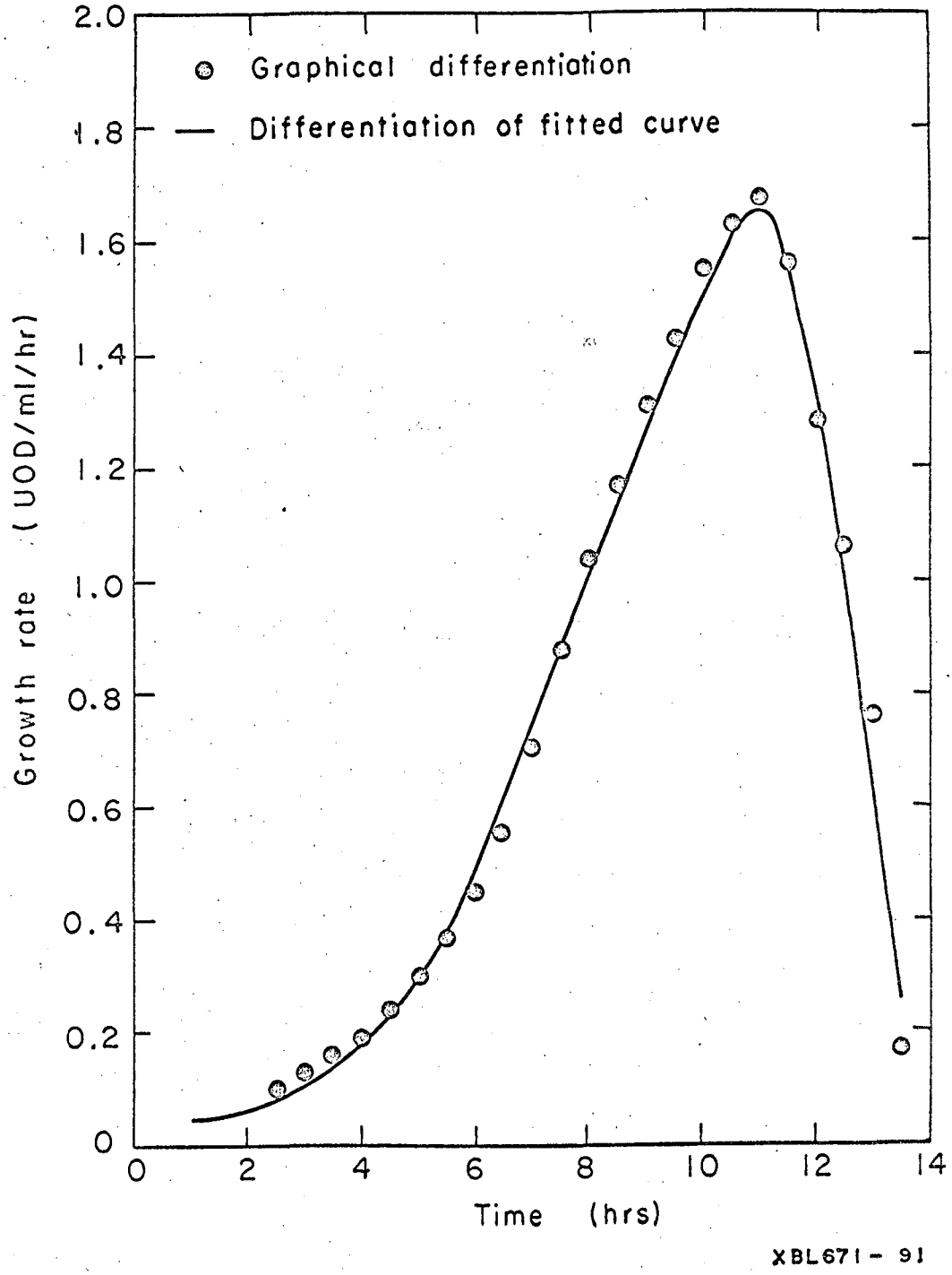

Fig. 12. Comparison of graphically measured growth rate of Luedeking[52] with values calculated as derivatives of the fitted curve.

Table XII. Comparison of observed and graphically measured values with computer calculated values (observed data is from run of Luedeking[52])

Time (hrs)	Observed cell conc. (UOD/ml)	Calculated cell conc. (UOD/ml)	Graphical growth rate (UOD/ml/hr)	Computer calculated growth rate (UOD/ml/hr)
1.0	0.123	0.138	-	0.046
2.0	0.139	0.190	-	0.061
2.5	-	-	0.10	0.077
3.0	0.283	0.268	0.13	0.099
3.5	-	-	0.16	0.130
4.0	0.442	0.400	0.19	0.172
4.5	-	-	0.24	0.228
5.0	-	-	0.30	0.300
5.5	0.82	0.802	0.37	0.389
6.0	-	-	0.45	0.496
6.25	1.12	1.154	-	-
6.50	-	-	0.56	0.618
7.0	-	-	0.71	0.750
7.17	1.77	1.773	-	-
7.50	-	-	0.88	0.885
7.70	2.24	2.23	-	-
8.00	-	-	1.04	1.019
8.25	2.73	2.79	-	-
8.50	-	-	1.17	1.147
9.0	3.77	3.67	1.31	1.271
9.50	-	-	1.43	1.393
9.53	4.43	4.38	-	-
10.00	5.00	5.07	1.55	1.512
10.50	5.72	5.85	1.63	1.612
11.00	6.78	6.67	1.68	1.653
11.50	7.51	7.48	1.56	1.578
12.00	8.23	8.22	1.29	1.340

Table XII (continued)

Time (hrs)	Observed cell conc. (UOD/ml)	Calculated cell conc. (UOD/ml)	Graphical growth rate (UOD/ml/hr)	Computer calculated growth rate (UOD/ml/hr)
12.33	8.63	8.62	-	-
12.50	-	-	1.06	0.965
12.67	8.78	8.95	-	-
13.00	9.27	9.18	0.76	0.564
13.50	9.49	9.38	0.17	0.257
14.00	9.38	9.46	-	-

the model can approach zero at large times. This property is important because variables such as viable count tend to fall off to zero values in the post-exponential phase. Also, intermediate products can accumulate in the early phases of a culture and then be consumed before the fermentation is complete. An example is the diphasic biooxidation of glucose to 5 ketogluconic acid by Acetobacter suboxydans, which shows an accumulation of gluconic acid.

Synthetic data were assumed with a lag phase of 10.5 time units and having a bell-shaped curve. The data were then analyzed. Table XIII and Fig. 13 compares the test data and the fit equation. The fit equation has the form

$$y = \frac{1.3805 \times 10^{8}}{1+\exp(4.5593-.86477t_1-.64989t_1^{2}+.1008t_1^{3})} \qquad (50)$$

$$t_1 = t - 10.5 \text{ hr}$$

Good agreement between the test data and Eq. (50) is evident.

Thus the bell-shaped curve may be added to the list of curves that the model is capable of fitting.

6. Test #6

Because the model has the capability of giving complex curves (as shown in the section on the mathematical properties of the model), it was decided to test the model with data from complex batch culture. The data of Hosler and Johnson for the penecillin fermentation provide a suitable example.[53] In their experiment, mycelial nitrogen showed diauxie at intermediate incubation times and fell off at long incubation times. The computer program fit a third degree model to the data with the following form:

$$y = \frac{2369.4}{1+\exp(3.1794-.05681t-3.37\times10^{-4}t^{2}+4.66\times10^{-6}t^{3})} \qquad (51)$$

Table XIII. Comparison of synthetic data and computer fit values, bell-shaped curve

Independent variable	Dependent variable	
	Original data	Fitted values
0	2.1000×10^6	2.1000×10^6
10.5	"	"
11.0	"	2.5397×10^6
11.5	5.0210×10^6	5.6976×10^6
12.0	1.5620×10^7	1.4531×10^7
12.5	4.2250×10^7	3.6143×10^7
13.0	8.1530×10^7	7.2110×10^7
13.5	1.1090×10^8	1.0516×10^8
14.0	1.2440×10^8	1.2308×10^8
14.5	1.2950×10^8	1.3048×10^8
15.0	1.3140×10^8	1.3317×10^8
15.5	1.3140×10^8	1.3364×10^8
16.0	1.2970×10^8	1.3202×10^8
16.5	1.2260×10^8	1.2492×10^8
17.0	9.0400×10^7	9.6335×10^7
17.5	2.9880×10^7	3.1074×10^7
18.0	2.3310×10^6	2.3806×10^6
18.5	6.8590×10^4	6.5128×10^4

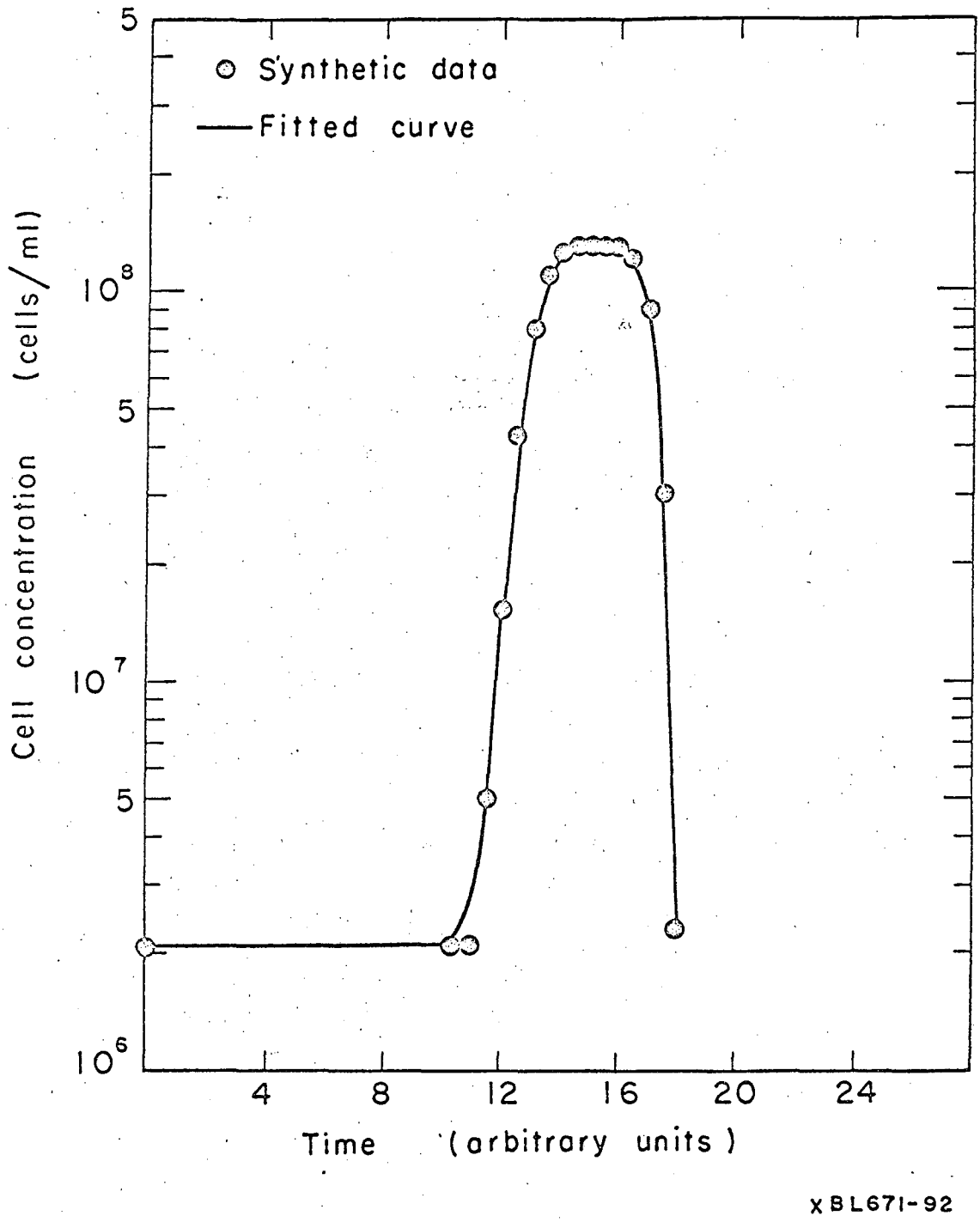

Fig. 13. Comparison of bell-shaped data with fitted equation.

Table XIV and Fig. 14 compare observed and fitted data. Agreement is poor. The bad results are partly due to the paucity of data points, partly to the irregular shpae of the data, and partly to the low number of coefficients in the fitting curve. There were too few points for fitting of the data satisfactorily with a higher order equation.

7. Test #7

The seventh and last test was made with data measured by Monod growing Escherichia coli in a medium containing glucose and sorbitol both a concentrations of 100 mg/l. First, cell growth was on only glucose. Then, after all glucose had been consumed, a short lag and then growth on sorbitol ensued. This phenomenon of consecutive utilization of substrates with an intervening lag is called diauxie. Figure 15 and Table XV compare the observed data with values calculated from what are referred to as the one part model and the two part model. The one part model fitted the data with a single equation. The equation obtained had the form

$$y = \frac{66.374}{1 + \exp(3.2298 - 0.8449t)} \qquad (52)$$

The locus of Eq. (52) is the solid curve in Fig. 15. As can be seen, the one part model did not give a good fit, showing no plateau at either intermediate or large times. To increase the quality of the fit, the data were broken into two parts and two separate equations were used to describe the two parts. With this approach, results were very good. For times less than 3.6 hrs, Eq. (53) was applied

$$y = \frac{29.62}{1+\exp(2.387-.7017t+.6046t^2-1.313t^3+.7225t^4-.1285t^5)} \qquad (53)$$

For times greater than 3.6 hrs, Eq. (54) was used to fit the data

$$y = 29.0+\frac{29.500}{1+\exp(4.0603-.0597(t-3.6)-1.626(t-3.6)^2-1.1903(t-3.6)^3)} \qquad (54)$$

Table XIV. Comparison of fitted curve with data of Hosler and Johnson[52]

Time (hours)	Mycelial nitrogen	
	Observed (mg/liter)	Calculated (mg/liter)
0	100	100.0
16	200	235.7
28	-	-
30	900	508.5
40	920	804.3
45	920	871.0
50	-	-
53	1010	1235.1
67	1690	1603.8
75	2000	1738.1
90	1800	1849.4
115	1600	1598.3

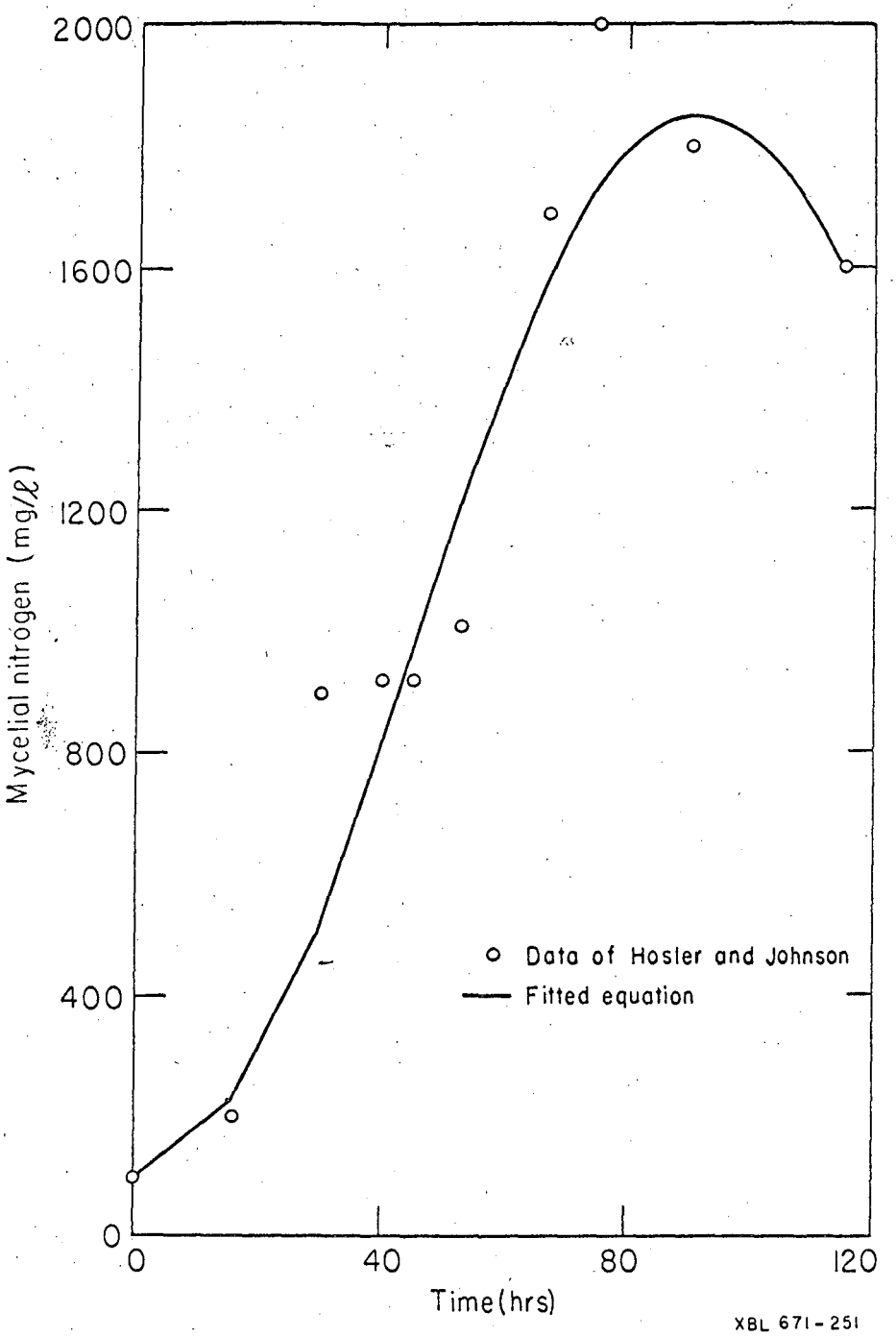

Fig. 14. Mycelial nitrogen concentration in the penecillin fermentation compared with values calculated from the fitted curve.

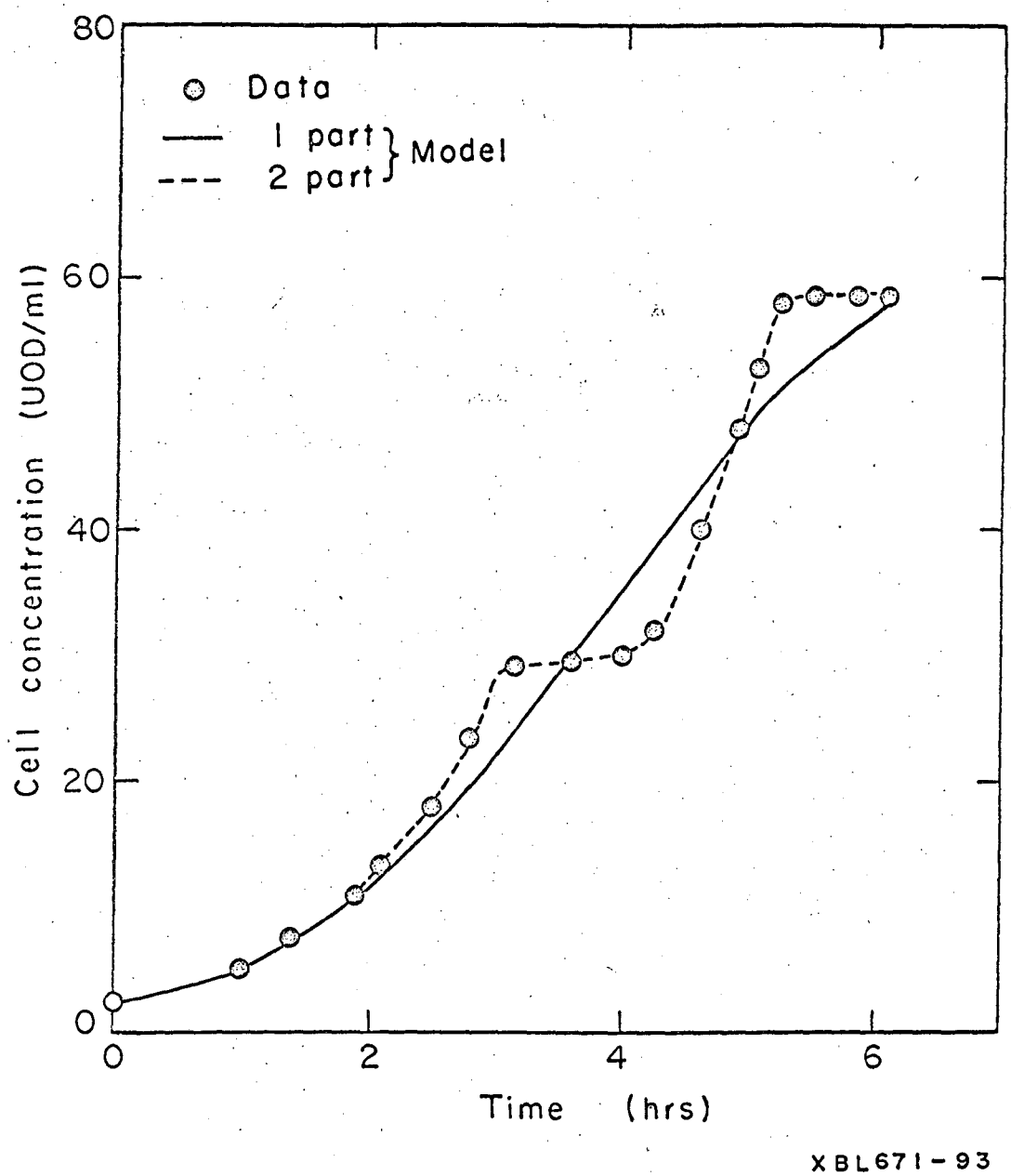

Fig. 15. Cell concentration versus time in diauxic batch culture compared with one-part and two-part fitted curves.

Table XV. Comparison of diauxie data of Monod[13] with fitted data

Time (hours)	Data of Monod	Optical density 1-part model	Optical density 2-part model	
0	2.5	2.50	2.500	Part 1
1.00	5.0	5.60	5.100	
1.40	7.8	7.59	7.565	
1.90	11.0	10.92	11.444	
2.10	13.5	12.55	13.179	
2.50	18.0	16.36	17.964	
2.80	23.5	19.68	23.614	
3.15	29.0	24.00	28.820	
3.60	29.5	30.07	29.621	
			29.500	Part 2
4.00	30.0	35.67	30.000	
4.25	32.0	39.11	32.000	
4.60	40.0	43.71	40.000	
4.90	48.0	47.33	48.000	
5.05	53.0	49.00	53.000	
5.25	58.0	51.08	58.000	
5.50	58.5	53.42	58.500	
5.85	58.5	56.23	58.500	
6.10	58.5	57.92	58.500	

Excellent agreement was found between model and data, as shown by Fig. 15, where the two part model is represented by the dashed curve , and in Table XV.

8. Conclusions

The preceding results demonstrate the usefulness and flexibility of the generalized form of the Verhulst-Pearl equation in fitting a variety of real and synthetic batch culture data. Agreement between data and fitted equations is particularly good for simple fermentations such as those discussed in the first four tests. Lag phases are handled quite effectively by the program as could be seen in the fifth test of the program, which also showed that the program could represent results with zero value asymptotes at large values of the independent variable. Adequate fit was also obtained in the second test, despite the discontinuity in the slope, although improvement in the measurement of slopes would result from smoothing of the rate versus time curves calculated with the fitted model.

The definition of closeness of fit is on a well-defined quantitative basis provided the standard deviations of the data to be fit are known, because the program automatically computes Chi-square values for all distributions. The closeness of fit can then be read from a set of statistical tables. However, in the results presented here, the standard deviations were unknown so the Chi-square values were not used in evaluating results. Instead, the subjective method of visual inspection was used.

9. Recommendations for the use of the Curve Fitting Computer Program

The computer program is listed and the functions of the various parts of the program are discussed in detail in Appendices I and II. Table XVI lists the order in which data are read with the curve-fitting program. Details of the input format of the data are given in Appendix II. Standard deviations for each dependent variable are read as coefficients α_j, β_j, and γ_j in Eq. (55).

Table XVI. Order of reading of data for computer curve-fitting program

A. Initially,

1. Read-in table of Chi-square values for testing closeness of fit.
2. Read labels for axes of computer plotted figures.
3. Read number of runs to be analyzed.

B. For each run,

1. Read number of runs now being analyzed, number of samples in run, and number of dependent variables in run.
2. Read (independent variable, dependent variables) for each sample.
3. Read coefficients of variance equation (Eq. (55)) for each dependent variable in run.
4. Read estimated numerator of Eq. (35) for each variable in run.
5. Read length of lag phase for run.
6. Read three equally spaced data and value of spacing for each dependent variable (see Appendix I).

$$\sigma^2(y_{ij}) = \alpha_j + \beta_j y_{ij} + \gamma_j y_{ij}^2 \qquad (55)$$

where $\sigma^2(y_{ij})$ = variance of jth dependent variable at ith datum
y_{ij} = ith datum of jth dependent variable
α_j, β_j, γ_j = coefficients of jth dependent variable

Equation (55) is used by the computer program to calculate standard deviations of each datum. The calculated variances are then used to compute the weighting factors for each datum with Eq. (56).

$$W_{ij} = 1/\sigma^2(y_{ij}) \qquad (56)$$

= weighting factor of ith datum of jth dependent variable

These weighting factors determine the relative weights given the various data in the fitting of an equation to the data. Weighting factors are also used to calculated values of Chi-square for the comparison of the actual data to the values calculated from the fitted equation, using Eq. (57)

$$\chi^2 = \sum_i W_i (y^*_{ij} - y_{ij})^2 \qquad (57)$$

where y^*_{ij} = calculated jth dependent variable at value of independent variable corresponding to the ith datum

It is clear that the values of α_j, β_j, and γ_j thus strongly affect the resulting fitted equation and the judgment of the closeness of fit (i.e., values of Chi-square). Therefore, accurate values of the coefficients are important to the curve-fitting technique. When such values are unavailable it is customary to assign arbitrary positive values to α_j for data with a moderate range of values of the dependent variable. When the range of dependent variable is large, as in cell counts, it is customary to assign an arbitrary positive value to γ_j instead.

When the culture to be analyzed shows a lag phase, the length of the lag phase is estimated by eye and read into the computer along with the other data. The program then shifts the abscissa of the data to coincide with the end of the lag phase before performing the curve-fitting of the data. Data taken during the lag phase is averaged. The value of the dependent variable at the end of the lag phase is then set equal to the mean value of the data taken during the lag phase and is treated as a datum in the subsequent curve fitting. The weight assigned to this lag phase datum is then proportional to the number of data averaged.

Equally-spaced values of each dependent variable and the spacing are also read into the program for each run. These values are then used along with the initial value of the dependent variable by the program to make initial estimates using the equations of Appendix I. These estimated coefficients are then used as a starting point for iteration to the best-fitting final values. Because the convergence of the iteration to the correct values is dependent on the starting point of the iteration, it is suggested that the estimates be made from a smoothed curve through the data to be fitted and that the spacing be chosen so that most of the range of the data is covered by the selected points.

As was shown, fit of the modified logistic equation to simple fermentation data is straightforward. For more complex cases, fit is often bad. If such is the case, good results can sometimes be obtained by breaking the observed data into two or more parts and analyzing each separately, as was done with the diauxie data of Monod. It has been found that the second and higher parts of a multi-part model are fitted best if the coordinates are shifted prior to fitting equations to the data. For example, see Eq. (54). However, the initial value of the dependent variable should not be absolute zero, although it may be as small as desired.

As a final note, these computer fit equations should not be used to extrapolate outside the range of variables to which the equations were fitted.

APPENDIX I

ESTIMATION OF COEFFICIENTS IN THE GENERALIZED LOGISTIC EQUATION

Accurate initial guesses for the values of the coefficients increase the likelyhood that the iterative curve-fitting technique used will converge to the correct values and reduces the number of iterations required. Assuming that a fairly good estimate can be made for K, we define

$$G(t,y) = \ln\left(\frac{K - y}{y}\right)$$
$$= a_o + a_1 t + a_2 t^2 + a_3 t^3 + a_4 t^4 + \ldots$$

Assume that the initial value $G(0,y_o)$, and three equally spaced values $G(t_1,y_1)$, $G(t_2,y_2)$, and $G(t_3,y_3)$ are known ($t_3 = 3t_1$ and $t_2 = 2t_1$). Then the following equations may be derived to make initial guesses of the coefficients a_o, a_1, etc.

<u>For $F(t) = a_o + a_1 t$</u>

$$a_o = G_o$$
$$a_1 = (G_1 - G_o)/t_1$$

<u>For $F(t) = a_o + a_1 t + a_2 t^2$</u>

$$a_o = G_o$$
$$a_1 = (4(G_1 - G_o) - (G_2 - G_o))/2t_1$$
$$a_2 = ((G_2 - G_o) - 2(G_1 - G_o))/2t_1^2$$

<u>For $F(t) = a_o + a_1 t + a_2 t^2 + a_3 t^3$</u>

Defining $B_1 = G_1 - G_o$

$$B_2 = G_2 - G_o$$
$$B_3 = G_2 - G_o$$

$$a_1 = (3B_1 - 1.5\ B_2 + B_3/3)/t_1$$

$$a_2 = (4B_2 - B_3 - 5B_1)/2t_1^{\ 2}$$

$$a_3 = (B_3 - 3B_2 + 3B_1)/6t_1^{\ 3}$$

These equations were used in the computer program to make initial guesses of the coefficients from given equally-spaced data. For fitting of F(t) for fourth and fifth degree cases, zero values of a_4 and a_5 were used for the initial guess.

APPENDIX II

DESCRIPTION OF CURVE-FITTING COMPUTER PROGRAM

The method and computer program to be described here is designed to fit equations to the sigmoidal curves obtained in batch culture kinetic experiments. The equations to be fit belong to a class that we call generalized logistic equations. The equations have the form of Eq. (35)

$$y = \frac{K}{1 + \exp(F(t))} \tag{35}$$

where K = constant

y = dependent variable, e.g., cell or substrate concentration

$F(t)$ = polynomial in time

$= a_o + a_1 t + a_2 t^2 + \ldots a_m t^m$

t = time

Dewitt proposed that equations of this form be used in the analysis of filtration data and any other data for which the dependent variables occur in sigmoidal forms.[50]

Determination of the constants in Eq. (35), $K, a_o, a_1 \ldots a_m$ is very tedious by hand because Eq. (35) is not linear in the constants. The equation can be rearranged to the following form, which is linear in the constants a_o, $a_1 \ldots a_m$ but not in K

$$a = \ln\left(\frac{K - y}{y}\right) = a_o + a_1 t + a_2 t^2 + \ldots + a_m t^m \tag{58}$$

Equation (58) was the form we first used for least squares curve fitting, estimating the value of K from graphs of the data, thereby making possible calculation of z from the data. Fitting of the new dependent variable z to t thus became a simple linear least squares problem to determine a_o, a_1, ... a_m. However, this proved unsatisfactory for two reasons. First, the value of K could not be estimated accurately when there was a significant amount of experimental error present. Second, if

data had not been obtained for the stationary phase of the culture growth, it was almost impossible to choose the best value for K by eye. To avoid these difficulties, the program was rewritten using a non-linear least squares technique, thus permitting calculation of optimal values of K as well as $a_o, a_1, \ldots a_m$.

The non-linear least squares method was derived from the general method proposed by Scarborough.[51] It is first assumed that random errors occur in the measurement of the dependent variable only and thus that the independent variable (time) is always measured with absolute accuracy. The dependent variable is expanded using a Taylor series in terms of corrections to the coefficients to be determined. Optimal corrections are then determined using a linear least squares technique, the coefficients are corrected, and the procedure repeated until all corrections have become very small compared to the coefficients themselves.

Reviewing the procedure in more detail, let

$$y = f(t,a,b,c,\ldots l) \tag{59}$$

represent the equation to be fit to the data with y the dependent variable, t the independent variable, and a,b,c,...l the coefficients to be determined. If $a_o, b_o, c_o, \ldots l_o$ are the approximate values of the coefficients to be determined then we can write

$$\begin{aligned} a &= a_o + \alpha \\ b &= b_o + \beta \\ c &= c_o + \gamma \\ &\vdots \\ l &= l_o + \xi \end{aligned} \tag{60}$$

and $y^* = f(t, a_o, b_o, \ldots l_o)$ (61)

Equation (61) can be written for each of the n data values of (t_i, y_i).

$$\begin{aligned} y_1^* &= f(t_1, a_o, b_o, \ldots l_o) \\ y_2^* &= f(t_2, a_o, b_o, \ldots l_o) \\ &\vdots \\ y_n^* &= f(t_n, a_o, b_o, \ldots l_o) \end{aligned} \tag{62}$$

The residuals or errors, v_i that we want to minimize are of the form

$$\begin{aligned} v_1 &= f(t_1, a, b, c, \ldots l) - y_1 \\ v_2 &= f(t_2, a, b, c, \ldots l) - y_2 \\ &\vdots \\ v_n &= f(t_n, a, b, c, \ldots l) - y_n \end{aligned} \tag{63}$$

where y_i is the value of y observed at time t_i. Combining Eqs. (60) with Eqs. (63), we obtain

$$v_i = f(t_i, a_o + \alpha, b_o + \beta, c_o + \gamma, \ldots l_o + \xi) - y_i \tag{64}$$

Expanding the right-hand side of Eq. (64) by Taylor's theorem

$$v_i + y_i = f(t_i, a_o, b_o, \ldots l_o) + \alpha \frac{\partial f_i}{\partial a}\Big|_o + \beta \frac{\partial f_i}{\partial b}\Big|_o + \ldots \xi \frac{\partial f_i}{\partial l}\Big|_o \tag{65}$$

where $\frac{\partial f_i}{\partial a}\Big|_o = \frac{\partial f}{\partial a}\Big|_{\substack{t = t_i \\ a = a_o \\ \vdots \\ l = l_o}}$

and so on.

Rearranging, neglecting higher coefficients, and substituting for $f(t_i, a_o, b_o, \ldots l_o)$ using Eq. (61), we obtain

$$
\begin{aligned}
v_1 &= \alpha\frac{\partial f_1}{\partial a}\Big|_o + \beta\frac{\partial f_1}{\partial b}\Big|_o + \ldots + \xi\frac{\partial f_1}{\partial l}\Big|_o + r_1 \\
v_2 &= \alpha\frac{\partial f_2}{\partial a}\Big|_o + \beta\frac{\partial f_2}{\partial b}\Big|_o + \ldots + \xi\frac{\partial f_2}{\partial l}\Big|_o + r_2 \\
&\vdots \\
v_n &= \alpha\frac{\partial f_n}{\partial a}\Big|_o + \beta\frac{\partial f_n}{\partial b}\Big|_o + \ldots + \xi\frac{\partial f_n}{\partial l}\Big|_o + r_n
\end{aligned}
\tag{66}
$$

where $r_i = y_i^* - y_i$

Equations (65) are linear in α, β, $\gamma, \ldots \xi$ and the problem has thus been reduced to a simple least squares problem that can be solved with a standard program library subroutine.

Applying this technique to the generalized Verhulst-Pearl equation, the coefficients K, a_o, $a_1, \ldots a_m$ are the coefficients to be determined and the derivative of the dependent variable with respect to each of these coefficients is needed. Thus

$$
\begin{aligned}
\frac{\partial y}{\partial K} &= y/K \\
\frac{\partial y}{\partial a_o} &= (y - K)(y/K) \\
\frac{\partial y}{\partial a_1} &= \frac{\partial y}{\partial a_o}\, t \\
\frac{\partial y}{\partial a_2} &= \frac{\partial y}{\partial a_1}\, t \\
\frac{\partial y}{\partial a_3} &= \frac{\partial y}{\partial a_2}\, t \\
&\vdots \\
\frac{\partial y}{\partial a_n} &= \frac{\partial y}{\partial a_{n-1}}\, t
\end{aligned}
\tag{67}
$$

The residual equations for this system arise when Eqs. (67) are substituted into Eqs. (66). Weighting factors for each datum are calculated as the reciprocal of the variance calculated for that datum.

A computer program was written in Chippewa Fortran to use this method to curve-fit. A block diagram in Fig. 16 of the program, called BATFIT, shows the relation of CULT, the main program to its various subroutines. The majority of the calculations pertaining to the curve fitting is done by CULT. Subroutine CHI is used to tabulate values of Chi-square for up to 100 degrees of freedom for use in testing the goodness of fit of the fitted curve. CULT calls on the second subroutine LSQS to do the least squares determination of the corrections to the coefficients. The subroutine IP is used by LSQS. Subroutines CCNEXT through CCUNPK comprise a standard set of library subroutines that are used to plot any given set of data. In BATFIT, CULT uses this so-called Cal Comp plotter to compare calculated and observed values by plotting them together versus time. Our explanation of the programs used will be limited to the main program CULT and subroutine CHI because LSQS, IP, and CCNEXT through CCUNPK are subroutine available from the Computer Center, Lawrence Radiation Laboratory, University of California, Berkeley, California.

CULT and CHI are listed in Table XVI. The important variables in the computer program are defined in Table XVII. The definitions are given in order of appearance in the program except where it is helpful to change the order. In Table XVIII, the function of each part of CULT is discussed in turn. By referring first to the brief outline of the program in the text and then studying Tables XVI, XVII, and XVIII, it should be possible for the interested reader to understand the workings of the main program.

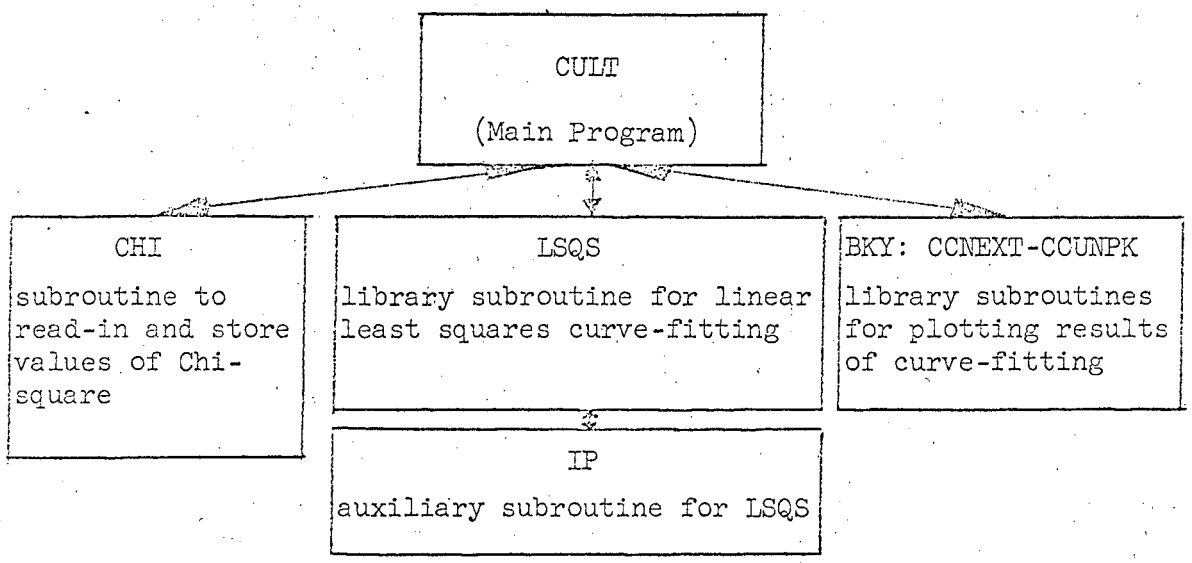

Fig. 16. Relationship between main computer program and its subroutines.

Table XVII. Program CULT and
Subroutine CHI

```
                PROGRAM CULT(INPUT,OUTPUT,TAPE2=INPUT,TAPE3=OUTPUT,TAPE98,TAPE99)
000066          DIMENSION A(100,7), ALPHA(7), BETA(7), SIG(100,7), W(100,7), XK(7)
000066          DIMENSION VAR1(7), DER1(7), C(100),B(100,8),CC(8)
000066          DIMENSION YC(100), X(100)
000066          DIMENSION ZC(100), GAMMA(7)
000066          DIMENSION Z(100,7)
000066          DIMENSION TEST(104)
000066          DIMENSION AINIT(7),F(100,7),T(100),WT(100,7),AC(7),SG(7)
000066          DIMENSION EX(4,7)
000066          DIMENSION ISIT(7)
000066          COMMON/CCPOOL/XMIN,XMAX,YMIN,YMAX,CCXMIN,CCXMAX,CCYMIN,CCYMAX
000066          COMMON/CCFACT/FACTOR
000066          DATA IOC/1/
          C
          C        SUBROUTINE CHI STORES IN THE ARRAY TEST TABLED CHI-SQUARE VALUES
          C        FOR 1 THROUGH 100 DEGREES OF FREEDOM AT THE 95 PERCENT LEVEL.
          C
000066          CALL CHI( TEST )
000070          CALL CCBGN
          C
          C        VAR1, VAR2, DER1, DER2, VS ARE USED TO LABEL THE CALCOMP PLOTS.
          C
000071          READ(2,12) (VAR1(I), I=1,7)
000102          READ(2,12) (DER1(I), I=1,7)
000113          READ(2,12) VAR2, DER2, VS
000124     12   FORMAT(7A10)
          C
          C        N            THE NUMBER OF RUNS TO BE ANALYZED
          C
000124          READ(2,1) N
000131      1   FORMAT(I5)
          C
          C        IRUN         THE RUN NOW BEING ANALYZED
          C        NSAM         NUMBER OF SAMPLES IN IRUN
          C        NVAR         NUMBER OF DEPENDENT VARIABLES IN IRUN
          C
000131      7   READ(2,2) IRUN, NSAM, NVAR
000142      2   FORMAT(3I5)
          C
          C        ID           DAYS IN ITH INDEPENDENT VARIABLE
          C        HRS          HOURS IN ITH INDEPENDENT VARIABLE
          C                     X(I) = ID + HRS/24.
          C        A            ARRAY OF DEPENDENT VARIABLES.
          C                     I INDEX RUNS THROUGH ALL SAMPLES.
          C                     J INDEX RUNS THROUGH NO. OF DEPENDENT VARIABLES.
          C
000142          DO4 I=1,NSAM
000144          READ(2,3) X(I),(A(I,J),J=1,NVAR)
000162        3 FORMAT(F10.3,E10.7,6F10.3)
000162      4   CONTINUE
          C
          C        ALPHA, BETA, AND GAMMA ARE USED TO DETERMINE THE VARIANCE
          C                 OF EACH DEPENDENT VARIABLE.
          C
000165          READ(2,5) (ALPHA(I), BETA(I), GAMMA(I), I=1,NVAR)
000203      5   FORMAT(8F10.4)
          C
          C        XK(I) IS THE LIMIT OF THE ITH VARIABLE AS TIME GOES TO INFINITY.
          C
000203          READ(2,14) (XK(I), I=1,NVAR)
000215       14 FORMAT(7E10.5)
```

```
000215          READ(2,5) TLAG
000222          READ (2,98) ((EX(M,J),M=1,4),J=1,NVAR)
000241       98 FORMAT(4E10.3)
000241          DO 8 I=1,NSAM
000243          DO 8 J=1,NVAR
000244          SIG(I,J)=0.
000247          W(I,J)=0.
000251          IF( A(I,J) .EQ. 0.0) GO TO 8
000252          SIG(I,J)=ALPHA(J)+BETA(J)*A(I,J)+GAMMA(J)*A(I,J)**2
000261          X2 = XK(J)**2
000263          W(I,J)=1./SIG(I,J)
000266     8    CONTINUE
000273          WRITE(3,304)
000276     304  FORMAT(///,10X, 2H I, 3X, 2H J, 3X, 7H A(I,J), 8X, 9H SIG(I,J),
               16X, 7H W(I,J), 8X,/)
000276          DO303 I=1,NSAM
000300          DO303 J=1,NVAR
000301          WRITE(3,305) I, J, A(I,J), SIG(I,J), W(I,J)
000323     305  FORMAT(10X, 2I5, 3(E13.6, 2X))
000323     303  CONTINUE
          C
          C        TLAG IS THE ESTIMATED LENGTH OF THE LAG PHASE.  THE FIT EQUATION
          C        IS APPLIED ONLY TO THE DATA FOR TIME GREATER THAN TLAG
          C        AINIT(J) IS THE INITIAL VALUE OF THE JTH VARIABLE AND
          C        SG(J) IS THE VARIANCE OF THE INITIAL VALUE
          C
000330          DO 86 J=1,7
000332          SG(J)=0.
000333          ISIT(J)=0.
000334       86 AINIT(J)=0.
000337          DO 82 II=1,6
000340          IF(TLAG.EQ.X(II)) GO TO 83
000342          IF(TLAG.LT.X(II)) GO TO 108
000344       82 CONTINUE
000346      108 II=II-1
000350       83 IF(II.LE.1) GO TO 104
000353          DO 84 I=1,IT
000354          DO 84 J=1,NVAR
000355          IF(A(I,J).EQ.0.) GO TO 84
000360          IF(A(I,J).GT.0.) ISIT(J)=ISIT(J)+1
000365          AINIT(J)=AINIT(J)+A(I,J)/FLOAT(IT)
000372          SG(J)=SG(J)+SIG(I,J)/FLOAT(IT)
000377       84 CONTINUE
000404          DO 131 J=1,NVAR
000406          IF(IT.EQ.ISIT(J)) GO TO 131
000410          CALC=FLOAT(IT)/FLOAT(ISIT(J))
000413          AINIT(J)=CALC*AINIT(J)
000415          SG(J)=CALC*SG(J)
000416      131 CONTINUE
000421          GO TO 105
000421      104 DO 109 J=1,NVAR
000423          AINIT(J)=A(1,J)
000426          SG(J)=SIG(1,J)
000430      109 CONTINUE
000432      105 DO 87 J=1,NVAR
000434          F(1,J)=AINIT(J)
000440          T(1)=0.
000440          NSAMT=NSAM-IT+1
000443          DO 87 I=2,NSAMT
000444          ITI=IT+I-1
000447          F(I,J)=A(ITI,J)
000454          T(I)=X(ITI)-TLAG
```

```
000457      87 CONTINUE
000463         WRITE(3,98) (AINIT(J),XK(J),J=1,NVAR)
000477         IF( IGO .GT. 1) GO TO 9
000503         WRITE(3,6) N
000510    6    FORMAT(1H1, 20X, I5, 22H RUNS WILL BE ANALYZED//)
000510    9    CONTINUE
000510         WRITE(3,10) IRUN
000515   10    FORMAT(1H0, 10X, 8H RUN NO.,I5)
000515         WRITE(3,11) NSAM
000522   11    FORMAT( /, 10X, 21H NUMBER OF SAMPLES IS, I4)
000522         WRITE(3,81) TLAG
000527      81 FORMAT(/,10X,25H LENGTH OF LAG PHASE IS  ,E12.4)
         C
         C        CYCLE THROUGH THIS LOOP ONCE FOR EACH DEPENDENT VARIABLE
         C        IN A PARTICULAR RUN
         C
000527         DO13 J=1,NVAR
000531         XKOLD=XK(J)
000533         K = 0
         C
         C        DETERMINE THE MINIMUM AND MAXIMUM FUNCTIONAL VALUES WHICH
         C        WILL BE NEEDED FOR THE CALCOMP PLOTS.
000534         L=1
000535         YMIN = A(L,J)
000540         YMAX = A(L,J)
000542         DO39 L=2,NSAM
000543         IF( A(L,J) .EQ. 0.0) GO TO 39
000546         K = K+1
000550         IF( A(L,J) .LT. YMIN) YMIN = A(L,J)
000555         IF( A(L,J) .GT. YMAX) YMAX = A(L,J)
000565   39    CONTINUE
000570         NPTS = K
000571         YMIN=0.
000572         ZZZ = (YMAX-YMIN)/10.0
000575         YMAX=YMAX+2.*ZZZ
000600         IYMAX=YMAX/2.
000601         YMAX=2.*FLOAT(IYMAX)
000603         XMIN = X(1)
000605         XMAX = X(NSAM)
         C
         C        THIS PART MAKES INITIAL ESTIMATES OF COEFFICIENTS
         C        FROM EQUALLY SPACED DATA EX(1,J),EX(2,J),AND EX(3,J)
         C        ICO IS THE NUMBER OF COEFFICIENTS IN THE POLYNOMIAL  OF THE
         C        EQUATION BEING FIT TO THE DATA
         C
000607         NITER = 0
000610         ICO=2
000611         II=ICO-1
000613         ALP=ALOG((XK(J)-AINIT(J))/AINIT(J))
000621         BB1=ALOG((XK(J)-EX(1,J))/EX(1,J))-ALP
000631         BB2=ALOG((XK(J)-EX(2,J))/EX(2,J))-ALP
000642         BB3=ALOG((XK(J)-EX(3,J))/EX(3,J))-ALP
000653         AC(1)=ALOG(XK(J)/AINIT(J)-1.)
000661         AC(2)=BB2/(2.*EX(4,J))
000666         GO TO 90
000666     100 NITER=0
000667         NWRITE=0
000670         IF(ICO.EQ.3) GO TO 101
000672         IF(ICO.EQ. 4) GO TO 102
000674         IF(ICO.GE.5) GO TO 103
000676     101 AC(2)=(2.*BB1-.5*BB2)/EX(4,J)
000705         AC(1)=ALOG(XK(J)/AINIT(J)-1.)
```

```
000713          AC(3)=(BB2-2.*BB1)/(2.*EX(4,J)**2)
000722          GO TO 90
000722      102 AC(2)=(3.*BB1-1.5*BB2+.333333*BB3)/EX(4,J)
000733          AC(1)=ALOG(XK(J)/AINIT(J)-1.)
000740          AC(3)=(2.*BB2-2.5*BB1-.5*BB3)/EX(4,J)**2
000751          AC(4)=(BB3+3.*BB1-3.*BB2)/(6.*EX(4,J)**3)
000761          GO TO 90
000761      103 DO 88 L=5,7
000763          AC(L)=0.
000764       88 CONTINUE
000766       90 WRITE(3,91)  I1,XK(J),(AC(L),L=1,100)
001004       91 FORMAT(//,10X,27H FOR A POLYNOMIAL OF DEGREE,I2,16H ESTIMATED XK I
             1S,E13.6,27H ESTIMATED COEFFICIENTS ARE,/5X,7(E13.6,4X))
          C
          C     THIS PART CALCULATES FUNCTIONAL VALUES BASED ON THE LATEST
          C     ESTIMATES OF THE COEFFICIENTS
          C
001004          WT(1,J)=1./SG(J)
001010          YY=0.
001011          DO 93 L=1,100
001013          K1=L-1
001015          YY=YY+AC(L)*T(1)**K1
001022       93 CONTINUE
001024          IF(T(1).LE.0) YY=AC(1)
001027          Z(1,J)=XK(J)/(1.+EXP(YY))
001037          NSAMT=NSAM-IT+1
001041          DO 89 I=2,NSAMT
001043          II=1+I-1
001046          WT(I,J)=1./SIG(ITT,J)
001053          IF(F(I,J).EQ.0.) WT(I,J)=0.
001056          YY=0.
001057          DO 92 L=1,100
001061          K1=L-1
001063          YY=YY+AC(L)*T(I)**K1
001071       92 CONTINUE
001073          IF(T(I).LE.0.) YY=AC(1)
001077          YY=AMAX1(-600.,AMIN1(600.,YY))
001107          Z(I,J)=XK(J)/(1.+EXP(YY))
001116       89 CONTINUE
001120          NWRITE=NWRITE+1
001121          IF(NWRITE.LT.10) GO TO 110
001123          WRITE(3,26)
001126          WRITE(3,28) (T(I),F(I,J),WT(I,J),Z(I,J),I=1,NSAMT)
001153      110 CONTINUE
          C
          C
          C        IN THE LOOP DO16, AN OVERDETERMINED SYSTEM OF EQUATIONS
          C        IS SET UP OF THE FORM  B*CC = C.
          C     B IS A NSAMT*7 MATRIX
          C     C IS A NSAMT*1 VECTOR
          C     CC WILL BE CORRECTIONS TO XK AND COEFFICIENTS AC
          C
001153          DO 16 I=1,NSAMT
001155          DO 123 K=1,8
001156          B(I,K)=0.
001162      123 CONTINUE
001164          IF(F(I,J).EQ.0.0) C(I)=0.
001170          IF(F(I,J).EQ.0.0) GO TO 16
001172          RW1J=SQRT(WT(I,J))
001175          C(I)=RW1J*(F(I,J)-Z(I,J))
001204          B(I,1)=RW1J*Z(I,J)/XK(J)
001210          B(I,2)=B(I,1)*(Z(I,J)-XK(J))
```

```
00121 5          DO 94 K=3,8
00121 7          B(I,K)=B(I,K-1)*T(I)
00122 7       94 CONTINUE
00123 1    16    CONTINUE
00123 4          IEND = 1
00123 5          IF(NWRITE.LT.10) GO TO 40
00123 7          IF( J .EQ. 1) GO TO 38
00124 1          WRITE(3,21) J
00124 6    21    FORMAT(1H1,10X, 20H FIT OF VARIABLE NO., I2)
00124 6          NWRITE=0
00124 7          GO TO 40
00125 0    38    WRITE(3,41) J
00125 5       41 FORMAT(1H1,10X,20H FIT OF VARIABLE NO.,I2)
00125 5          NWRITE=0
00125 6    40    CONTINUE
         C
         C          WILL MAKE FITS OF DEGREE TWO TO SIX UNLESS A CHI-SQUARE
         C          GOODNESS OF FIT TEST IS PASSED BY A FIT OF DEGREE LESS
         C          THAN SIX
         C
         C
         C          LSGS SOLVES THE OVERDETERMINED SYSTEM OF EQUATIONS  B * CC = C.
         C
00125 6          IDCC=ICC+1
00126 0          CALL LSGS(B,CC,C,NSAMT,IDCC,1,KERR,9)
00126 6          IF( KERR .EQ. 0) GO TO 15
00126 7          WRITE(3,17)
00127 2    17    FORMAT(//, 20X, 55H THE SYSTEM WAS FOUND TO BE SINGULAR WHEN OF TH
               1E FORM -, /)
00127 2          DO19 K=1,NSAM
00127 4          WRITE(3,27) (B(K,L), L=1,I), C(K)
00131 2    27    FORMAT(8(3X, E13.6))
00131 2    19    CONTINUE
00131 5          GO TO 13
00131 5    15    CONTINUE
00131 5          I1=ICC-1
00131 7          WRITE(3,95)I1,(CC(L),L=1,IDCC)
00133 3       95 FORMAT(//,10X,27H FOR A POLYNOMIAL OF DEGREE,I2,45H THE COEFFICIEN
               1T CORRECTIONS WERE FOUND TO BE,/4X,8(E12.5,2X))
00133 3          XK(J)=XK(J)+.35*CC(1)
00133 7          NITER=NITER+1
00134 1          CHECK=0.
00134 2          DO 96 L=1,ICC
00134 3          AC(L)=AC(L)+.35*CC(L+1)
00134 6          IF(AC(L).EQ.0.)GO TO 96
00134 7          CHECK=CHECK+ABS(CC(L+1)/AC(L))
00135 3       96 CONTINUE
00135 6          BLOSTOP=ABS(XK(J))
00136 0          XB=XKOLD/5.
00136 2          BX=2.*XKOLD
00136 4          IF(BLOSTOP.GE.BX.OR.XB.GE.BLOSTOP) GO TO 120
00137 3          CZECH=2.*ALOG(XK(J)/AINIT(J)-1.)
00140 2          ACK=CABS(AC(1))
00140 4          IF(ACK.GE.CZECH) GO TO 120
00140 6          GO TO 121
00140 7      120 IF(ICC.GE.5) GO TO 13
00141 2          IDF=NPTS-ICC-1
00141 4          IF(IDF.LE.2) GO TO 13
00141 6          ICC=ICC+2
00141 7          I1=ICC-1
00142 0          XK(J)=XKOLD
00142 2          PRINT 122,BLOSTOP
```

```
00142 7      122 FORMAT(22H WHOA BESSIE,8LCSTOP =,E16.6)
00142 7          PRINT 124,ACK
00143 4      124 FORMAT(13H ABS(AC(1)) =,E16.6)
00143 4          GO TO 100
00143 5      121 CONTINUE
          C
          C          BLCSTOP IS AN INDEX OF DIVERGENCE IN THE ITERATION
          C          NITER IS THE NUMBER OF ITERATIONS PERFORMED SO FAR IN
          C          THE NON-LINEAR LEAST SQUARES FIT PRESENTLY BEING MADE
          C          AND CHECK IS AN INDEX OF THE DEGREE OF CONVERGENCE OF THE
          C          ITERATION ON THE COEFFICIENTS AC AND XK
          C
00143 5          IF(NITER.GE.100) GO TO 107
00144 0          IF(CHECK.GE. .001) GO TO 90
00144 2      107 CONTINUE
00144 2          WRITE(3,200) II,XK(J),(AC(L),L=1,ICO)
00146 0      200FORMAT(//,10X,27H FOR A POLYNOMIAL OF DEGREE,I2,5H XK =,E13.6,38H
               1AND THE COEFFICIENTS WERE FOUND TO BE,/5X,7(E13.6,4X))
00146 0          SUM = 0.0
00146 1          SUM1 = 0.0
00146 2          YC(1) = CC(1)
          C
          C          IN THE LOOP DO22, FUNCTIONAL VALUES ARE DETERMINED ACCORDING TO
          C          THE FIT JUST MADE - FUNCTIONAL VALUES CORRESPONDING TO BOTH THE
          C          ORIGINAL DATA (ZC) AND THE TRANSFORMED DATA(YC).
          C          ERROR SUMS OF SQUARES ARE DETERMINED FOR BOTH THE ORIGINAL(SUM)
          C          AND THE TRANSFORMED(SUM1) DATA.
          C
00146 3          DO 22 L=1,NSAM
00146 5          YC(L) = 0.0
00146 6          ZC(L) = 0.0
00146 7          IF( A(L,J) .EQ. 0.0) GO TO 22
00147 2          IF(X(L).LE.TLAG) GO TO 56
00147 5          DO 23 K=1,ICO
00147 6          K1 = K-1
00150 0       23 YC(L)=YC(L)+AC(K)*((X(L)-TLAG)**K1)
00151 1          YC(L)=AMAX1(-600.,AMIN1(600.,YC(L)))
00152 1          ZC(L) = XK(J)/(EXP(YC(L))+1.)
00152 6          SUM=SUM+(ZC(L)-A(L,J))**2/SIG(L,J)
00153 6          GO TO 22
00153 7       56 CONTINUE
00153 7          YC(L)=AC(1)
00154 1          ZC(L)=AINIT(J)
00154 3          SUM=SUM+(ZC(L)-A(L,J))**2/SIG(L,J)
00155 3       22 CONTINUE
00155 6          IDF=NPTS-ICO-1
00156 0          WRITE(3,24)SUM,IDF
00156 7       240FORMAT(10X,31H AND THE VALUE OF CHI-SQUARE IS,E16.9,7H WITH  ,I5,2
               1X,19H DEGREES OF FREEDOM)
00156 7          WRITE(3,25)
00157 2       25 FORMAT(//, 10X, 36H TABLE OF DATA AND THE FITTED POINTS/)
00157 2          WRITE(3,26)
00157 5       260FORMAT(15X,10H INC.VAR.,10X,10H DEP. VAR.,10X,11H POLYNOMIAL,9X,17
               1H CALCD. DEP. VAR.,/)
00157 5          WRITE(3,28) (X(K),A(K,J),YC(K),ZC(K),K=1,NSAM)
00162 0       28 FORMAT(15X,4(E16.9,4X))
          C
          C THIS PART CALCULATES THE GROWTH RATE AND THE SPECIFIC GROWTH RATE
          C
00162 0          IF(J.GT.1) GO TO 70
00162 4          NDAYS=2.*X(NSAM)+2.
00162 7          DIMENSION DYDT(100),YCC(100),ZCC(100),DZDT(100),SRATE(100),XDAYS(1
```

```
              100),YCC(100),ZCC(100)
00627           DO 60 L=1,NHDAYS
00631           KD=L
00632           XDAYS(L)=KD/2.-.5
00635           IF(XDAYS(L).LE.TLAG) GO TO 77
00640           YCC(L)=0.
00641           DYDT(L)=0.
00642           ZCC(L)=0.
00643           DO 61 K=1,ICO
00644           K1=K-1
00646           YCC(L)=YCC(L)+AC(K)*(XDAYS(L)-TLAG)**K1
00654        61 CONTINUE
00657           YCC(L)=AMAX1(-600.,AMIN1(600.,YCC(L)))
00667           ZCC(L)=XK(J)/(EXP(YCC(L))+1.)
00674           DO 62 K=2,ICO
00676           AK1=K-1
00700           K2=K-2
00702           DYDT(L)=DYDT(L)+AK1*AC(K)*(XDAYS(L)-TLAG)**K2
00711        62 CONTINUE
00714           SRATE(L)=(ZCC(L)-XK(J))*DYDT(L)/XK(J)
00721           DZDT(L)=ZCC(L)*SRATE(L)
00723           GO TO 60
00723        77 YCC(L)=AC(1)
00725           ZCC(L)=AINIT(J)
00727           DYDT(L)=0.
00730           DZDT(L)=0.
00731           SRATE(L)=0.
00732        60 CONTINUE
          C
          C THIS PART PRINTS CALCULATED GROWTH RATES
          C
00735           WRITE(3,51)
00740        51 FORMAT(/51H TABLE OF CALCULATED DERIVATIVES AND SPECIFIC RATES)
00740           WRITE (3,52)
00743        52FORMAT(/15X,10H IND. VAR.,10X,10H DEP. VAR.,9X,15H DER. DEP. VAR.,
              15X,14H SPECIFIC RATE/)
00743           WRITE (3,53) (XDAYS(L),ZCC(L),DZDT(L),SRATE(L),L=1,NHDAYS)
00763        53 FORMAT(15X,4(E16.9,4X))
00763           GO TO 76
          C
          C THIS PART CALCULATES DERIVATIVES AND SPECIFIC RATES FOR ALL OTHER
          C          DEPENDENT VARIABLES
          C
00764        70 DO 75 L=1,NHDAYS
00766           IF(XDAYS(L).LE.TLAG) GO TO 78
00771           YCD(L)=0.
00772           DYDT(L)=0.
00773           ZCD(L)=0.
00774           DO 71 K=1,ICO
00775           K1=K-1
00777           YCD(L)=YCD(L)+AC(K)*(XDAYS(L)-TLAG)**K1
00005        71 CONTINUE
00010           YCD(L)=AMAX1(-600.,AMIN1(600.,YCD(L)))
00020           ZCD(L)=XK(J)/(EXP(YCD(L))+1.)
00025           DO 72 K=2,ICO
00027           AK1=K-1
00031           K2=K-2
00033           DYDT(L)=DYDT(L)+AK1*AC(K)*(XDAYS(L)-TLAG)**K2
00042        72 CONTINUE
00045           DZDT(L)=ZCD(L)*(ZCD(L)-XK(J))*DYDT(L)/XK(J)
00052           SRATE(L)=DZDT(L)/ZCD(L)
00054           GO TO 75
```

```
00205 5      78 YCD(L)=AC(1)
00205 7          ZCD(L)=AINIT(J)
00206 1          DYDT(L)=0.
00206 2          DZDT(L)=0.
00206 3          SRATE(L)=0.
00206 4      75 CONTINUE
         C
         C THIS PART PRINTS CALCULATED RATES FOR VARIABLES OTHER THAN CELL CONCN.
         C
00206 7          WRITE(3,51)
00207 2          WRITE(3,52)
00207 5          WRITE(3,53) (XDAYS(L),ZCD(L),DZDT(L),SRATE(L),L=1,NHDAYS)
00211 5      76 CONTINUE
         C
         C          TEST TO DETERMINE THE GOODNESS OF FIT
         C
00211 5   31     CONTINUE
00211 5          CALL CCGRID(10, 10, 6HLABELS, 10, 10)
00212 1          WRITE(58, 32) VAR1(J1, VAR2, VS
00213 2   32     FORMAT(10X, 3A10)
00213 2          CALL CCLTR(200., 10., 0, 2)
         C
         C          THE LOOP DO33, PLOTS THE ORIGINAL NONZERO DATA AS DIAMONDS.
         C
00213 5          DO33 I=1,NSAM
00213 7          IF( A(I,J) .EQ. 0.0) GO TO 33
00214 2          CALL CCPLOT(X(I), A(I,J), 1, 6HNOJOIN, 6, 1)
00214 7   33     CONTINUE
         C
         C          PLOT THE LATEST FIT MADE.
         C
00215 2          I = 1
00215 3   35     IF( ZC(I) .EQ. 0.0) GO TO 34
00215 5          CALL CCPLOT(X(I), ZC(I), 1, 4HJOIN, 1, 11
00216 1          I = I+1
00216 3          GO TO 36
00216 3   34     I = I+1
00216 5          GO TO 35
00216 5   36     DO37 K=I,NSAM
00216 7          IF( ZC(K) .EQ. 0.0) GO TO 37
00217 0          CALL CCETC(X(K), ZC(K))
00217 2   37     CONTINUE
00217 5          CALL CCNEXT
00217 6          IF(IDF.LE.2) GO TO 13
00220 1          IF(ICC.GE.5) GO TO 13
00220 3          IF(SUM.LT.TEST(IDF))GO TO 13
00220 5          ICC=ICC+2
00220 7          II=ICC-1
00221 1          GO TO 100
00221 1   13     CONTINUE
00221 4          IGO = IGO+1
00221 5          IF( IGO .LE. N ) GO TO 7
00221 7          CALL CCEND
00222 0          STOP
00222 2          END
```

```
.CCLT

FUNCTION ASSIGNMENTS

STATEMENT ASSIGNMENTS
7       -  000132    8       -  000267    83      -  000351    108     -  000347
104     -  000422    84      -  000400    131     -  000417    105     -  000433
9       -  000511    39      -  000566    90      -  000767    100     -  000667
101     -  000677    102     -  000723    103     -  000762    110     -  001154
16      -  001232    40      -  001257    38      -  001251    15      -  001316
13      -  002212    96      -  001354    120     -  001410    121     -  001436
107     -  001443    22      -  001554    56      -  001540    70      -  001765
77      -  001724    60      -  001733    76      -  002116    78      -  002056
75      -  002065    31      -  002116    33      -  002150    34      -  002164
35      -  002154    36      -  002166    37      -  002173

VARIABLE ASSIGNMENTS
A       -  002641    ALPHA   -  004135    BETA    -  004144    SIG     -  004153
B       -  005447    XK      -  006743    VAR1    -  006752    DER1    -  006761
C       -  006770    8       -  007134    CC      -  010574    YC      -  010604
X       -  010750    ZC      -  011114    GAMMA   -  011260    Z       -  011267
TEST    -  012563    AINIT   -  012733    F       -  012742    T       -  014236
WT      -  014402    AC      -  015676    SG      -  015705    EX      -  015714
ISIT    -  015750    IGO     -  015757    I       -  015760    VAR2    -  015761
DER2    -  015762    VS      -  015763    N       -  015764    IRUN    -  015765
NSAM    -  015766    NVAR    -  015767    J       -  015770    TLAG    -  015771
M       -  015772    X2      -  015773    IT      -  015774    CALC    -  015775
NSAMI   -  015776    IIT     -  015777    XKOLD   -  016000    K       -  016001
L       -  016002    YMIN    -  002632    YMAX    -  002633    NPTS    -  016003
ZZZ     -  016004    IYMAX   -  016005    XMIN    -  002630    XMAX    -  002631
NITER   -  016006    ICO     -  016007    II      -  016010    ALP     -  016011
BB1     -  016012    BB2     -  016013    BB3     -  016014    NWRITE  -  016015
YY      -  016016    K1      -  016017    RWIJ    -  016020    IEND    -  016021
IECO    -  016022    KERR    -  016023    CHECK   -  016024    BLOSTOP-   016025
XB      -  016026    BX      -  016027    CZECH   -  016030    ACK     -  016031
IDF     -  016032    SUN     -  016033    SUM1    -  016034    NHDAYS  -  016035
DYDT    -  016036    YCC     -  016202    ZCC     -  016346    DZDT    -  016512
SRATE   -  016658    XDAYS   -  017022    YCD     -  017166    ZCD     -  017332
RC      -  017476    AK1     -  017477    K2      -  017500

START OF CONSTANTS
002225

START OF TEMPORARIES
002552

START OF INDIRECTS
002611
```

```
                SUBROUTINE CHI( TEST)
017505          DIMENSION TEST(104)
017505          I1 = 1
017506     2    I2 = I1+7
017510          READ(2,1) (TEST(I), I=I1,I2)
017524     1    FORMAT(8F10.2)
017524          I1 = I2+1
017526          IF( I2 .LT. 100) GO TO 2
017530          RETURN
017530          END
```

```
CH1

FUNCTION ASSIGNMENTS

STATEMENT ASSIGNMENTS
2       -  017507

VARIABLE ASSIGNMENTS
TEST    -  017503    11      -  017542    12      -  017543    I       -  017544

START OF CONSTANTS
017533

START OF TEMPORARIES
017537

START OF INDIRECTS
017542
```

Table XVII: Definition of variables in computer program*

Symbol	Definition
A(I,J)	Array of dependent variables, with I index running over all samples and J index running over all dependent variables (e.g., cell concentration, substrate concentration, etc.)
SIG(I,J)	Variance for each data point for same array as above
ALPHA(J), BETA(J)**, GAMMA(J)	Coefficients for calculation of variance by the equation $SIG(I,J) = ALPHA(J)+BETA(J)\cdot A(I,J)+GAMMA(J)\cdot A(I,J)^2$
W(I,J)	Weighting factor for Jth variable of Ith sample
XK(J)	Value of numerator of right hand side of fitting equation (= K in Eq. (35))
VAR1(J), DER1(J), VAR2**, DER2**, VS	Labels for coordinate axes of graphs prepared by computer
C(I),B(I,J), CC(J)	Parameters calculated from data and fitting equation using approximate values for coefficients. For use by subroutine LSQS in calculating corrections for coefficients
X(I)	Value of independent variable (time) corresponding to Ith sample
YC(I), ZC(I)	Values of fit polynomial and fit equation (Eq. (35)) for the Ith sample time, respectively
IDF**	Number of degrees of freedom of fitted equation (=NPTS-ICO-1)
NPTS**	Number of non-zero data points for Jth variable

*In order of appearance in program except where noted othewise(**)

Symbol	Definition
ICO**	Number of coefficients in polynomial to be determined in fitting equation
TEST(IDF)	Chi-square value for 95% confidence at IDF degrees of freedom
SUM**	Weighted error sum of squares
TLAG**	Length of lag phase
AINIT(J)	Initial value of Jth variable; averaged value of all observations taken at X(I) $\leq$ TLAG
SG(J)**	Variance of initial value of Jth variable
IT	Value of index I for the last (in time) datum in the lag phase
ISIT(J)	Number of data points of Jth variable observed during lag phase; used for weighting initial value of Jth variable during curve-fitting
ITT	Index used in shift of coordinates in case of a non-zero TLAG ITT = IT + I -1
T(I)	Ith value of independent variable (time) shifted for lag phase (T(I)=X(ITT) - TLAG)
F(I,J)	Ith value of Jth dependent variable in new coordinate system (F(1,J) = AINIT(J), F(I,J) + A(ITT,J), I>1)
WT(I,J)	Weighting factor of Ith datum of Jth dependent variable
AC(L)	Current estimate of Lth coefficient in fitting equation
EX(M,J)	For M $\leq$ 3; Mth estimated (or observed) value of equally spaced data. For M = 4, spacing in time between estimated dependent variables
XMIN, XMAX, YMIN, YMAX, CCXMIN,CCXMAX, CCYMIN,CCYMAX	Minimum and maximum expected values of independent and dependent variables for use in plotting by computer
N	Number of runs (groups of data) to be analyzed
IRUN	Run now being analyzed

Symbol	Definition
NSAM	Number of samples in IRUN
NVAR	Number of dependent variables in IRUN
IGO**	Number of runs being analyzed
NWRITE	Number of iterations performed since last write-out of observed and calculated values of dependent variable
CHECK	Parameter to estimate degree of convergence of iteration; total sum of fractional changes in all coefficients
BLOSTOP, ACK	Indices of divergence of iterative procedure
SUM	Weighted error sum of squares (i.e., Chi-square value) of difference between observed and calculated values of dependent variable

Table XVIII: Detailed outline of curve-fitting computer program

Storage Locations (in octal base number system)	Function of section
66-70	Provision of space in program for subscripted variables; Common and Data assignments; read-in of Chi-square values for 1 through 100 degrees of freedom at the 95% confidence level
70-124	Read-in labels for axes of graphs (to be prepared for visual comparison of data and points calculated with the fitted equation)
124-131	Read-in number of experiments or runs to be analyzed
131-241	Read-in of data for a given run
241-273	Calculation of variances and weighting factors for each data point for all variables under consideration
273-327	Write-out table of A(I,J), SIG(I,J), and W(I,J)
330-431	Determine: (1) IT, the value of index I for the last datum in the lag phase; (2) all AINIT(J), the mean initial values for the different dependent variables; (3) All SG(J), variances of initial values
432-462	Perform transformation of coordinates from X(I) base to T(I) base
463-527	Write-out N(if first run), IRUN, NSAM, TLAG
527-2211	Do the following instructions once for each (Jth) variable in the Ith run
527-605	Calculate XMIN, XMAX, YMIN, and YMAX
607-765	Calculate first estimates of coefficients if number of terms in denominator polynomial (F(t) in text) is less than or equal to 4. For coefficients above the fourth, set initial estimates to zero
766-1004	Write-out newly estimated coefficients

Storage Locations	Function of section
1004-1117	Compute new values of calculated dependent variable Z(I,J) using newly improved estimates of coefficients in fitting equation
1120-1153	Write-out the calculated results of every tenth iteration
1153-1231	Calculate values of functions C(I) and B(I,K) for use in performing least-squares determination of corrections to coefficients
1233-1256	Write-out J value if number of iterations, NITER, is greater than or equal to ten
1256-1315	Call least squares program to calculate corrections to coefficient, test system of equations for singularity. Transfer to fitting of next variable if singularity exists.
1315-1333	Write-out coefficient corrections
1333-1353	Increase NITER by one, add .035 x coefficient corrections to coefficients, and calculate CHECK, a variable used to measure the rate of change of the coefficients
1355-1435	Check for divergence of iteration by determining if absolute values of calculated coefficients are far removed from expected values
1435-1437	If number of iterations, NITER is greater than or equal to 100, stop iterations and proceed to write-out part of program
1440-1441	If CHECK, convergence criterion, is larger than .001, perform another iteration
1442-1462	Write-out degree of polynomial and final estimate of coefficients. Set zero initial value for error sum of squares, SUM

Storage Locations	Function of Section
1463-1555	At each data point where non-zero data exists, calculate value of polynomial and of dependent variable; compute weighted error sum of squares
1556-1620	Write-out Chi-square and degrees of freedom; write-out table of independent variable and calculated and observed dependent variables
1620-1734	Calculate at every 1/2 time unit for the first variable (some index of cell concentration) and write-out independent variable, dependent variable, growth rate (time derivative of cell concentration equation) and specific growth rate (growth rate divided by cell concentration)
1735-1763	Write-out table of calculated values
1764-2066	Calculate at 1/2 time unit intervals the values of the dependent variable for $J \geq 2$, the time derivative of the variable, and the specific rate of change of the variable
2026-2115	Write-out calculated values
2115-2134	Plot grid on plain paper and label axes
2135-2147	Plot original non-zero data as diamonds
2152-2174	Plot on same grid calculated dependent variables of latest fit by joining adjacent points with straight line sections
2175	Advance plotter to prepare to plot next graph
2176-2211	Start on next variable if number of degrees of freedom less than or equal to 2, or if number of coefficients greater than or equal to five or if Chi-square is sufficiently small. If none of above, increase number of coefficients by two and return to statement 100
2214-2216	Increase IGO by one and go on to next run unless have finished all runs
2217-2222	Complete graphs, stop, end

REFERENCES

1. R. E. Ecker and M. Schaechter, Bacterial Growth Under Conditions of Limited Nutrition, Ann. N. Y. Acad. Sci. 102, 549 (1963).

2. H. V. Wyatt, Cations, Enzymes, and Control of Cell Metabolism, J. Theoret. Biol. 6, 441 (1964).

3. A. D. Brown, Aspects of Bacterial Response to the Ionic Environment, Bact. Rev. 28, 296 (1964).

4. E. L. Gaden, Jr., Chem. and Ind. (Review), 154 (1955) (Gaden-Ref. 6).

5. W. D. Maxon, Appl. Microbiol. (Review) 3, 110 (1955)(Deindoerfer-Ref. 7).

6. E. L. Gaden, Jr., Fermentation Process Kinetics, J. Biochem. Microbiol. Technol. Eng. 1, 413 (1959).

7. Fred H. Deindoerfer, Fermentaion Kinetics and Model Processes, in Adv. Appl. Microbiol. 2, 321 (1960).

8. C. T. Calam, N. Driver, and R. H. Bowers, J. Appl. Chem. (London) 1, 209 (1951)(Deindoerfer-Ref. 7).

9. D. Ramkrishna, A. G. Fredrickson, and H. M. Tsuchiya, The Dynamics of Microbial Growth, J. Ferm. Technol. 44, 203 (1965).

10. R. Luedeking and E. L. Piret, J. Biochem. Microbiol. Techn. Eng. 1, 393 (1959).

11. H. M. Tsuchiya, A. G. Fredrickson, and R. Aris, Dynamics of Microbial Cell Populations, Adv. Chem. Eng. 6, (1966).

12. Gyozo Terui, Some Problems of Fermentation Technology, Lawrence Radiation Laboratory Translation 1192, 1965.

13. Gyozo Terui, Some Problems of Fermentation Kinetics, J. Ferm. Technol. 44, 242 (1966).

14. J. Monod, Ann. Rev. Microbiol. 3, 371 (1949).

15. C. B. Van Neil, The Kinetics of Growth of Microorganisms, in The Chemistry and Physiology of Growth, edited by A. K. Parpart (Princeton University Press, 1949), Chap. 5, pp. 91.

16. Thomas W. James, Continuous Culture of Microorganisms, Ann. Rev. Microbiol. 15, 27 (1961).

17. J. Monod, Récherches sur la croissance des cultures bactériennes (Masson et Cie, Paris, France, 1942).

18a. Sir Cyril Hinshelwood, The Chemical Kinetics of the Bacterial Cell (Oxford, The Clarendon Press, 1946).

18b. L. Michaelis and M. L. Menten, Biochem. Z. 49, 333 (1913).

19. G. Teissier, Rev. Sci. No. 3208 (extract) 209 (1942)(Deindoerfer-Ref. 7).

20. H. Moser, The Dynamics of Bacterial Populations Maintained in the Chemostat, Carnegie Inst. Wash. Publ. No. 614.

21. D. E. Contois, Kinetics of Bacterial Growth: Relationship between Population Density and Specific Growth Rate of Continuous Cultures, J. Gen. Microbiol. 21, 40 (1959).

22. Yoshinori Fujimoto, Kinetics of Microbial Growth and Substrate Consumption, J. Theoret. Biol. 5, 171 (1963).

23. Sir Cyril Hinshelwood, The Chemical Kinetics of the Bacterial Cell (The Clarendon Press, Oxford, 1946).

24. A. T. Reid, Bull. Math. Biophys. 14, 313 (1952).

25. R. K. Finn, Inhibitory Cell Products: Their Formation and Some New Methods of Removal, J. Ferm. Technol. 44, 305 (1966).

26. P. F. Verhulst, Mem. Acad. Roy. Bruxelles 18, 1 (1844); 20, 1 (1846).

27. R. Pearl and L. J. Reed, Proc. Natl. Acad. Sci. 6, 275 (1920).

28. R. Luedeking and E. L. Piret, J. Biochem. Microbiol. Technol. Eng. 1, 393 (1959).

29. S. L. Adams and R. E. Hungate, Ind. Eng. Chem. 42, 1815 (1950).

30. Arthur E. Humphrey, Some Observations of Continuous Fermentation, I.A.M. Symposia on Microbiology, Tokyo, 215 (1963).

31. J. W. Chen, H. J. Koepsell, and W. D. Maxon, Kinetics of 1-Dehyrogenation of Steroids by Septomyxa affinis, Biotech. Bioeng. 4, 65 (1962).

32. W. D. Maxon and J. W. Chen, Kinetics of Fermentation Product Formation, J. Ferm. Technol. 44, 255 (1966).

33. Ping Shu, Mathematical Models for the Product Accumulation in Microbiological Processes, J. Biochem. Microbiol. Technol. Eng. 3, 95 (1961).

34. Yoichi Maruyama and Keiko Hayashi, Some Aspects of Cell Age Distribution Function, J. Ferm. Technol. 44, 227 (1966).

35. Jiroh Kobayashi, The Fermentation Characteristics from the Point of View of Apparent Age and its Application to Continuous Fermentation, J. Ferm. Technol. 44, 233 (1966).

36. C. D. Kelly and O. Rahn, The Growth Rate of Individual Bacterial Cells, J. Bact. 23, 147 (1932).

37. O. Rahn, A Chemical Explanation of the Variability of the Growth Rate, J. Gen. Physiol. 15, 257 (1931-2).

38. D. J. Finny and L. Martin, A. Re-examination of Rahn's Data on the Number of Genes in Bacteria, Biometrics 7, 133 (1951)(Koch and Schaechter-Ref. 45).

39. D. G. Kendall, On the Role of Variable Generation Time in the Development of a Stochastic Birth Process, Biometrika 35, 316 (1948) (Koch and Schaechter-Ref. 45).

40. D. G. Kendall, On the Choice of a Mathematical Model to Represent Normal Bacterial Growth, J. Roy. Statist. Soc. B. 14, 41 (1952) (Koch and Schaechter-Ref. 45).

41. E. O. Powell, Growth Rate and Generation Time of Bacteria, with Special Reference to Continuous Culture, J. Gen. Microbiol. 15, 492 (1956).

42. E. O. Powell, An Outline of the Pattern of Bacterial Generation Times, J. Gen. Microbiol. 18, 382 (1958).

43. H. E. Kubitschek, Normal Distribution of Cell Generation Rate, Exptl. Cell Res. 26, 439 (1960).

44. M. Schaechter, J. P. Williamson, J. R. Hood, and A. L. Koch, Growth, Cell and Nuclear Division in Some Bacteria, J. Gen. Microbiol. 29, 421 (1962).

45. A. L. Koch and M. Schaechter, A Model for Statistics of the Cell Division Process, J. Gen. Microbiol. 29, 435 (1962).

46. E. O. Powell and F. P. Errington, Generation Times of Individual Bacteria: Some Corroborative Measurements, J. Gen. Microbiol. 31, 315 (1963).

47. A. G. Fredrickson and H. M. Tsuchiya, Continuous Propagation of Microorganisms, Am. Inst. Chem. Eng. J. 9, 459 (1963).

48. S. Benzer, Biochem. Biphys. Acta 11, 383 (1953).

49. Warren G. Yeisley and Ernest C. Pollard, An Analog Computer Study of Differential Equations Concerned with Bacterial Cell Synthesis, J. Theoret. Biol. 7, 485 (1964).

50. C. C. Dewitt, Correlation of Rate Data, Ind. Eng. Chem. 35, 695 (1943).

51. J. B. Scarborough, Numerical Mathematical Analysis, 4th Ed. (The Hohns Hopkins Press, Baltimore, 1958), pp. 478.

52. R. L. Luedeking, The Lactic Acid Fermentation at Controlled pH: Kinetics of the Batch Process and Continuous Flow Theory and Experiments (Ph.D. thesis), University of Minnesota, Minneapolis, Minnesota, 1956).

53. Peter Hosler and Marvin J. Johnson, Penicillin from Chemically Defined Media, Ind. Eng. Chem. 45, 871 (1953).

PART II: SULFATE REDUCTION BY BACTERIA

I. SUMMARY

This section is primarily concerned with studies on the rates of growth and sulfate reduction by a strain of Desulfovibrio able to tolerate high concentrations of sodium chloride. Effects of all components of the growth media on batch culture growth were studied to determine optimal concentrations of each component. A computer was used to fit equations to the batch data, thus permitting more accurate determination of the metabolic rates.

Mixing, reduced sulfide concentrations, and pH control were shown to increase rates of growth and sulfide production. A continuous culture system was built and used to measure the growth kinetics in continuous culture. Anomalous specific growth rates observed during washout of the continuous reactor system could be explained by postulating wall growth by bacteria. Most batch and all continuous culture data could be correlated well by the logistic equation.

Batch culture and continuous culture data were correlated by plotting specific rate of sulfide production versus specific growth rate, but the straight line predicted by the Luedeking-Piret model gave only rough correlation. Instead, the data seemed to be divided into three distinct regions: (1) at low specific growth rates, a region involving unusually large mean cell size due to accumulation of cell reserve material; (2) at intermediate specific growth rates, a region of constant rate of specific sulfide formation per cell dry weight; (3) at high specific growth rates, a region of very high specific sulfide production rates, presumably due to uncoupling of energy production (sulfide production) and biosynthesis (specific growth rate).

It was not possible to obtain a completely satisfactory and general correlation of specific growth rates and specific sulfide production rates with the system variables. However, the Luedeking-Piret type of linear correlation seems satisfactory over a sufficient range to be useful for preliminary scale-up of systems using these organisms for sulfate reduction.

II. INTRODUCTION

Many bacteria reduce sulfates during the synthesis of sulfur-containing amino acids ("assimilatory" sulfate reduction). But by sulfate-reducing bacteria one usually means only those bacteria whose major energy-yielding metabolic reactions are linked to the reduction of the sulfate to the sulfide ion ("dissimilatory" sulfate reduction). Only a few specialized bacterial species are capable of this dissimilatory sulfate reduction, but they occur widely in nature, being found in deep marine deposits, in lakes, rivers and streams, soil, sewage, swamps, oil and sulfur deposits, industrial wastes and cooling waters, and particularly around buried iron structures. The versatility of sulfate reducing bacteria is evident from the different types of environments in which they can live, withstanding wide ranges of pH, temperature, redox potential, salinity, and hydrostatic pressure.

Until recently, sulfate-reducing bacteria were classified under the genus Desulfovibrio, with the exception of a few sulfate-reducing clostridia. Three species were recognized: D. desulfuricans (Beijerick) was the name given to common fresh-water strains; Marine and salt tolerant sulfate-reducers were called D. aestaurii (van Delden); D. rubentschickii (Baars) was the designation given to a strain able to utilize acetate as a sole carbon and energy source. The original culture of D. rubentschickii was lost and all efforts since to isolate such an organism have failed to find it.

Other sulfate-reducing bacteria have been discovered recently and buoyant density measurements of the DNA of these and the other sulfate-reducing bacteria has led to a revised taxonomy.[1] Sulfate-reducers are now classified as either Desulfotomaculum species or Desulfovibrio species, the former being comprised of spore-forming sulfate-reducing bacteria. Further subdivision of Desulfovibrio into three distinct groups is proposed on the basis of buoyant density measurements on DNA and on the results of inhibitor studies. This second part of this thesis will be concerned with a salt-tolerant strain of Desulfovibrio.

Desulfovibrios are gram negative, obligately anaerobic vibrio or spiriloid organisms, usually motile with polar flagella. Their metabolism is analogous to that of the aerobic acetic acid bacteria in that both have a cytochrome electron transport system, the major difference being that sulfate is the terminal electron acceptor in one case and oxygen in the other. Thus just as in aerobic metabolism, a physiological separation occurs between the metabolism of carbon and the reduction of sulfate.[2]

Strains or species differ somewhat as to the type of organic compounds they can utilize as the energy-yielding oxidizable substrates. However, as a class, sulfate reducers utilize a large variety of organic compounds, including lactate, malate, citrate, pyruvate, tartrate, fatty acids ranging from formic to stearic, amino acids, peptone, simple alcohols above methyl, glycerol, monosaccharides, certain disaccharides, possibly petroleum hydrocarbons, and some others.[3,4]

Complete reviews of the metabolism and ecology of Desulfovibrio have been presented previously by Leban and Wilke,[5] and more recently by Postgate.[1]

Because of their widespread occurance, sulfate-reducing bacteria make important geochemical changes such as the formation of sulfur, sulfide, and soda deposits. They also perform important biochemical duties in the sulfur and carbon cycle and in the creation of reducing environments. Though man has often been dismayed by their presence in the past, usually because of the foul odor and corrosive action of hydrogen sulfide, more recently he has made use of their biochemical abilities. Applications to data include purification of wastes, production of elemental sulfur, and release of petroleum from shale formations.[6]

A new application for the sulfate-reducing bacteria was proposed by Leban and Wilke.[5] They suggested use of sulfate-reducing bacteria for the removal of sulfate from sodium chloride brines. Sulfate is usually the main impurity in natural salt brines and it interferes with many of their uses. Leban and Wilke isolated a salt tolerant culture of sulfate-

reducing bacteria that they identified as a strain of Desulfovibrio aestaurii. They also obtained important information on some basic aspects of the physiology of the organisms in batch culture and estimated their performance in continuous culture.

This paper reports further research into the physiology of these bacteria in batch culture and preliminary results of continuous culture experiments. To obtain higher growth rates, a chemically defined medium for culture of a fresh-water sulfate-reducer developed by MacPherson and Miller[7] was tested and modified for use with the salt-tolerant strain used here.

The effects of variables such as concentrations of nutrients and products on the growth kinetics are also needed to evaluate potential uses of these organisms. These effects were studied and the results were correlated for a number of important variables.

III. METHODS

A. Organism

The salt-tolerant sulfate-reducing bacteria isolated by Leban and Wilke were used throughout this work. A detailed discussion of the isolation of the organism may be found in their work.[5] Tentative identification of the organism as Desulfovibrio desulfuricans is proposed, pending reorganization of the taxonomy of sulfate-reducing bacteria. This classification is discussed briefly in Appendix I in relation to current findings.

In the early part of this work, stock cultures were maintained in bottles with ground glass stoppers and stored at room temperature with monthly transfers to fresh media. Present practice is to store the cultures at 10°C in test tubes sealed with vaspar (50% paraffin waxes, 50% petroleum jelly). The cultures were grown in Medium E. Prior to kinetic experiments with media other than Medium E, the culture was adapted to the new medium by one or more transfers through a medium similar or identical in composition to the medium to be used in the experiment.

Crude electron microscope photographs of the organism have been taken using the negative staining technique of Zwillenberg.[8] (The method is described in Appendix IIG) The two photographs shown in Fig. 1 were made at a magnification of about 11,000X. The stain had penetrated the cell membrane in all photographs studied, as shown by the uniformly dark appearance of the cell. The penetration of the dye is probably due to the fact that the culture photographed was an old one. Figure 1(a) shows a cell with one long polar flagella and a second flagella that may be associated with the other end of the cell, although that cannot be determined from this photograph. A layer of material about 0.1-μ thick can also be seen to cover parts of the cell. It is possible that the unknown material is the polysaccharide gum known to be formed by sulfate-reducers.[9] Figure 1(b) shows a dividing cell next to a polyvinyltoluene latex sphere (supplied by the Dow Chemical Company, Bioproducts Division,

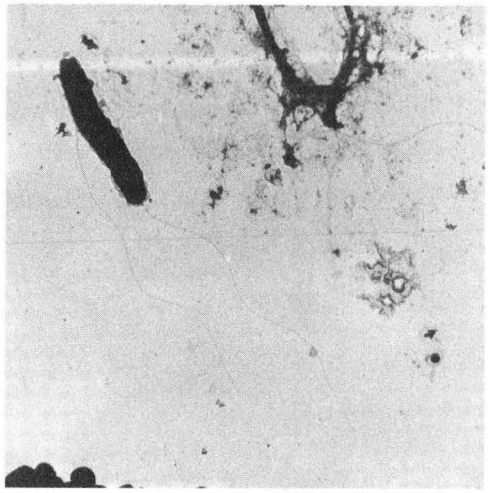

(a)

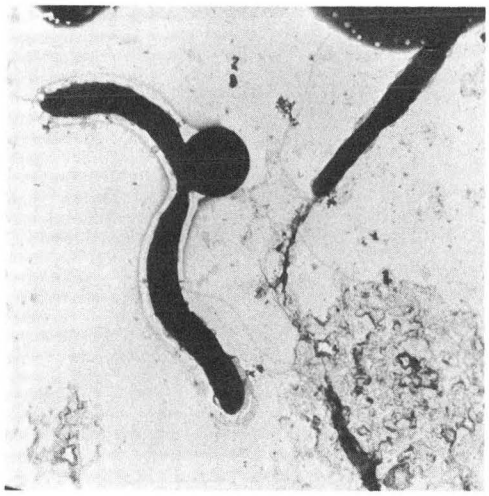

XBB 671-395

(b)

Fig. 1. Electron microscope photographs of sulfate-reducing bacteria.

Midland, Michigan) with a diameter of about 1.3 μ. Measurements of these and other photographs taken with the electron microscope showed that the fixed cells had diameters of 0.47 to 0.59 μ, ranged from about 3 to 4.5 μ in length, and had flagella as long as 8 μ. (Cell length was measured from septum to either end when a cell was seen to be dividing.)

B. Batch Culture Methods

Batch kinetic experiments were usually performed in 65-ml glass-stoppered bottles using the technique described by Leban and Wilke.[5] Briefly, the method consists of preparation of about a liter of sterile medium (method described in Appendix II), followed by inoculation with an adapted culture of sulfate-reducing bacteria. The normal inoculum size was 1 to 2 ml of a young culture (about 5×10^7 bacteria per ml) for each 100 ml of sterile medium. After mixing to insure uniformity, the inoculated medium is distributed to a number of sterile and chemically clean glass reagent bottles fitted with ground-glass stoppers. Each bottle is over-filled before fitting the stopper to be certain that no gas phase exists in contact with the culture liquid. Aseptic technique is used throughout to prevent contamination by other organisms. The bottles are stored in an incubator that maintains the temperature within 0.1° of 30°C. During kinetic experiments, each bottle was shaken at least once a day. At about daily intervals, one of the bottles was removed and measurements made on its contents. The sulfide content was determined by titration, and a bacterial count was made with a Petroff-Hausser counting chamber, as described in Appendix II. A cumulative amount of sulfide produced in any incubation period was obtained as the difference between the sulfide concentration measured after that period and the concentration of sulfide in the sample taken immediately after inoculation. Dry weight concentration of cells, sulfate concentration, pH, and redox potential were also measured with some samples.

A limited number of batch experiments were conducted in the reactor system discussed in the next section. The techniques of these experiments were identical to continuous culture techniques to be discussed, except no medium was supplied to the reactor after filling and inoculation.

C. Continuous Culture Methods

Continuous culture was the other type of experimental procedure used to obtain information about kinetics of growth and metabolism. The continuous culture method differs from batch culture methods in that when operating normally, sterile nutrient is continuously added to the reactor vessel while cells and spent nutrient are removed from it at the same volumetric rate. The first continuous culture experiments discussed here were performed with an apparatus that had a number of disadvantages so the evolution of the apparatus used will be discussed concurrently with the method of operation.

1. Early Continuous Culture Apparatus

The reactor is constructed of glass and contains 2.3 liters of liquid when operating. The reactor is jacketed to allow temperature control. Stirring is achieved with a Teflon-coated bar magnet. Baffling is achieved by vertical crimps in the walls. Mixing was sufficient to completely disperse an ink drop in about four seconds.

Figure 2 is a flow diagram of the system. Separate supplies of hydrogen sulfide and nitrogen gas were used to control the sulfide concentration in the reactor. Regulation of the flows was achieved by monitoring rotameters while manipulating pressure regulators and needle valves. Gases entering and leaving the reactor were passed through a sterilized glass-wool filter. Fresh medium was fed to the reactor with a peristaltic pump. Rates were monitored with rotameters and by collection. Feed was introduced close to the liquid level to reduce splashing. Level control was maintained in the reactor by an overflow line.

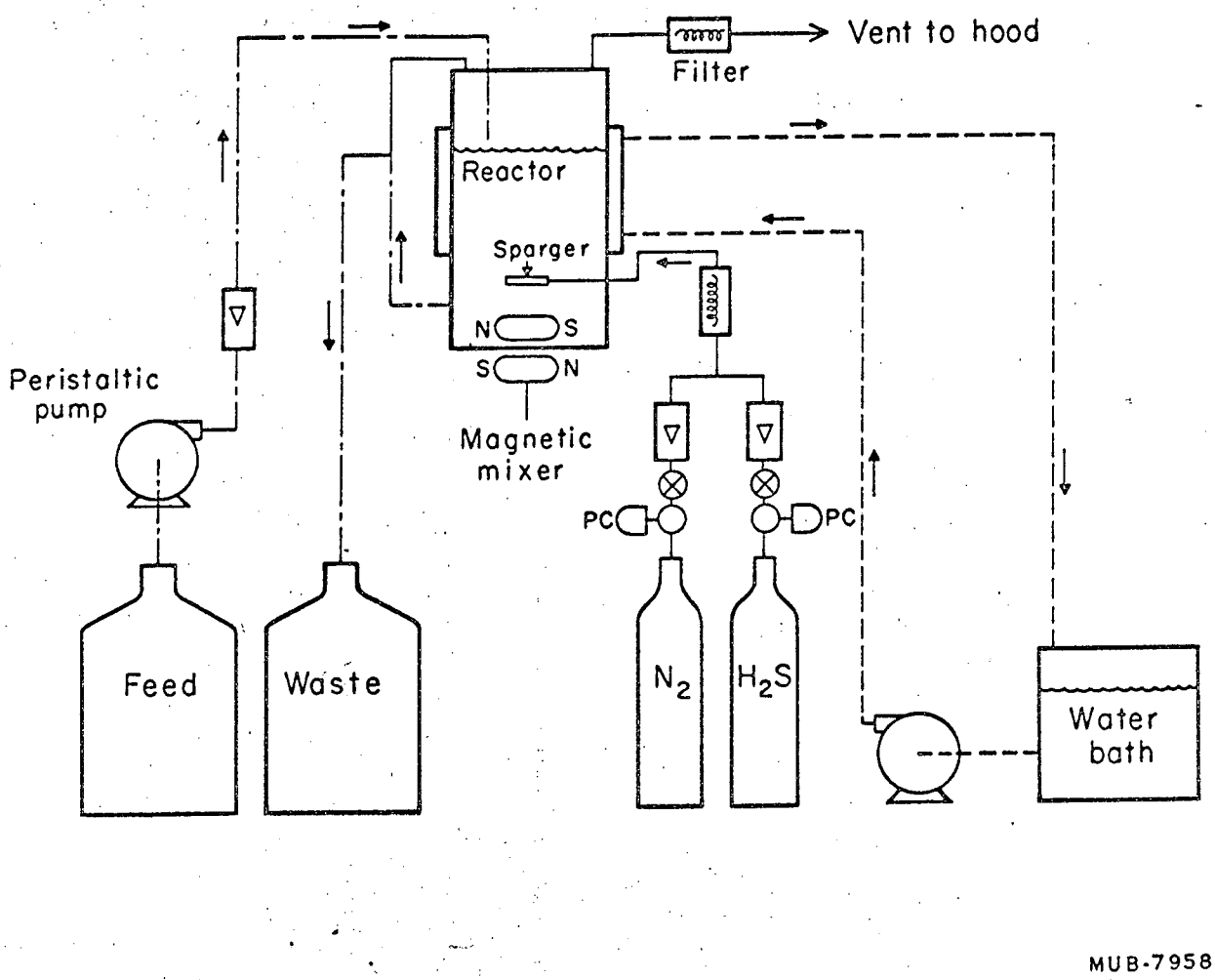

Fig. 2. Flowsheet of early continuous reactor system.

Temperature control was maintained within $\pm 0.1^{\circ}C$ in the reactor by flowing constant temperature water through the water jacket of the reactor. All lines were constructed of glass or polyvinyl chloride tubing with Teflon stopcocks. Sterilization of the system was accomplished with ethylene oxide gas.

After sterilization and rinsing with the medium, more sterilized nutrient solution was added to the 20-liter feed supply and a continuous culture experiment begun by filling the reactor to the 2.3-liter mark and inoculating with a culture of sulfate-reducing bacteria. The cell concentration was allowed to reach a sufficiently high value to indicate exponential growth had begun and continuous addition of nutrient solution, nitrogen gas, and hydrogen sulfide gas to the reactor was begun. Cell concentration and sulfide concentration, as well as flow rates and temperature were monitored several times daily until steady values were reached. At the steady-state, pH, cell concentration by optical count, cell dry weight concentration, sulfate concentration, sulfide concentration, and flow rates were measured. At the completion of the measurements, the liquid feed rate was changed to a new value and the procedure begun again. All experiments were performed at a temperature of $30^{\circ}C$. Difficulty was met in obtaining and maintaining steady-states because of the lack of pH control and because of difficulties with flow and temperature controls, so that measurements at only three true steady-states were made before modification.

2. Improved Continuous Culture Apparatus

The improved continuous culture apparatus was designed to allow continuous measurement, control, and recording of pH, continuous recording of redox potential and optical density of the culture, control of carbonate concentration, and improved control of temperature and sulfide concentration. A flow diagram of the improved system is shown in Fig. 3.

The reactor is the same cylindrical glass vessel of 2.3-liter capacity fitted with a removable ground-glass top, with pH and redox

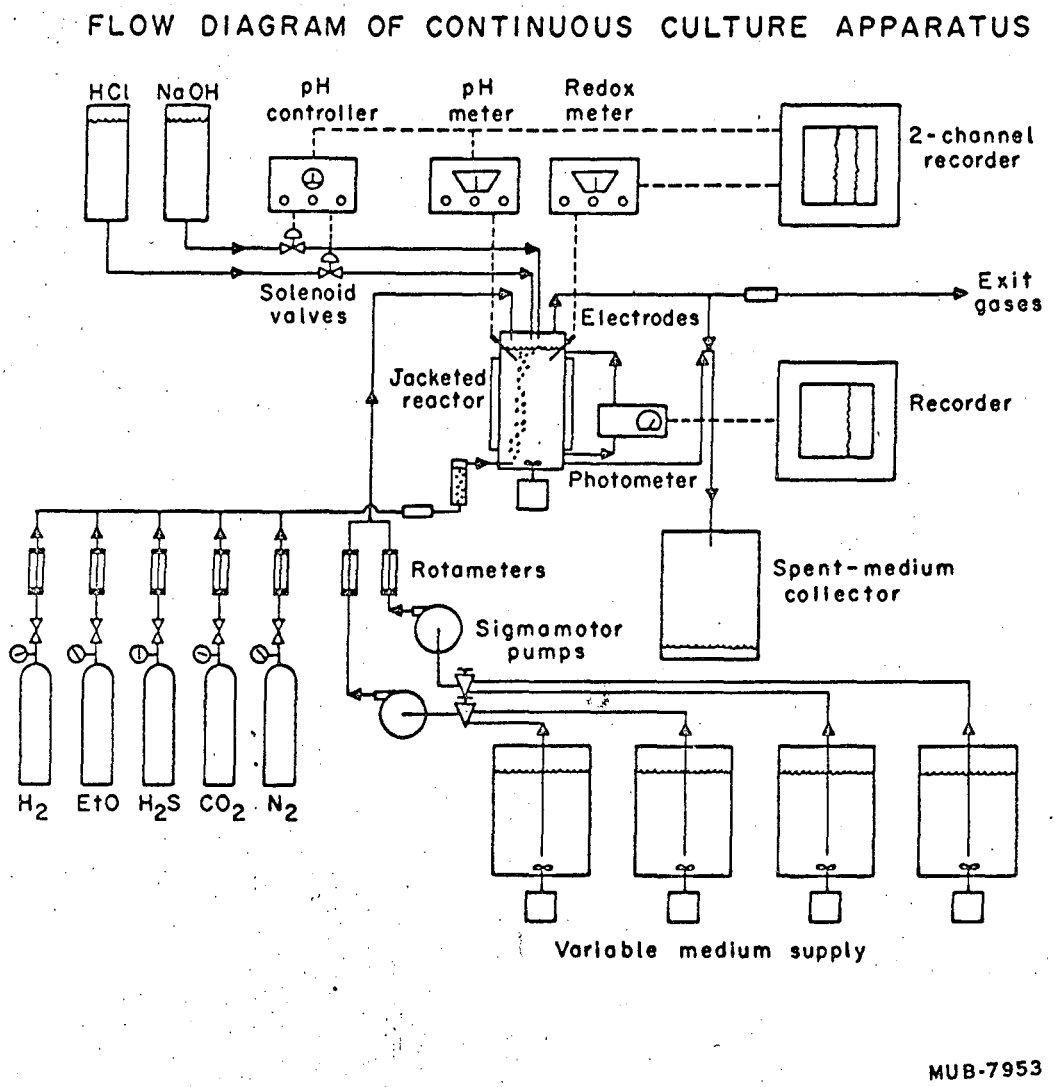

Fig. 3. Flowsheet of modified continuous reactor system.

electrodes added. Water at a constant temperature is circulated through a jacket on the reactor. An inoculating culture may be added through either or two serum caps. Samples may be withdrawn through the serum caps or by opening of Teflon stopcock in a glass sampling line. Similar stopcocks are on the gas inlet port and the medium outlet port. (Stopcocks, serum caps, and similar details are not shown on the flow diagram.) Using ground-glass joints, electrodes for pH and redox measurement are mounted through the wall of the reactor at a 45 deg angle with the wall. Acid and base for pH control are introduced through capillary tubing sealed into a serum cap in the top of the reactor. Gases are brought in through a porous glass sparger near the bottom of the reactor. Agitation is effected by a 3-in. magnetic stirring bar. The stirring action also pumps a stream of the fluid in the reactor through a spectrophotometer cell in an external leg. The output of the spectrophotometer is displayed on a potentiometric recorder, providing a continuous record of cell concentration.

The level in the reactor is controlled by an overflow leg connected to the lower part of the reactor. Spent medium can be collected in either of two 20-liter bottles.

Four 20-liter glass bottles serve to supply the reactor with medium. Each bottle can contain a medium of different composition so that the composition of the reactor feed may be varied. The bottles can be filled quite rapidly through a permanently-installed filling system without disturbing the operation of the reactor. Medium is sterilized by passage through a sterile stainless steel Millipore filter assembly directly into the appropriate medium bottle. Details of the filling system are not included on the flow sheet. In order to retard growth of any contaminating organisms in the medium prior to use, it is kept at about 8°C by passing refrigerated water through cooling coils in each medium bottle.

The medium is pumped from the bottles to the reactor through one or both of two Sigmamotor peristaltic pumps. One pump is used when low

flow rates are required, while the other is used for delivering higher rates. By adjusting the rates of the two pumps, the two streams may be blended to give a medium of the desired composition and flow rate. Flow rates are monitored with rotameters. The entire medium supply system, including the filling lines, is sterilized in place with ethylene oxide. In preliminary tests, no contamination was encountered.

Gaseous nitrogen, carbon dioxide, hydrogen sulfide, hydrogen, and ethylene oxide can be introduced singly or in combination through a porous glass sparger near the bottom of the reactor. The sparger breaks the gas stream into fine bubbles, providing good mass transfer with the liquid in the reactor. The flow rate of each gas is controlled with a needle valve and a rotameter. All rotameters are mounted on a single panel for quick reference. Before entering the reactor the gases pass through a bacteriological filter and through a water saturator, which helps reduce evaporation losses in the reactor. Exit gases are vented to a hood through a bacteriological filter. Samples of the exit gas may be readily taken for analysis.

The pH and redox potential of the reactor solution are measured continuously. The redox potential is measured with a Beckman Zeromatic pH Meter and recorded on one channel of a 2-channel redorder.

A Leeds and Northrup Model 7501 expanded Scale pH Meter with Beckman pH electrodes is used for pH measurement and control. The output of the meter is sent to the second channel of the 2-channel recorder for recording of a 2-pH unit span full-scale.

The output from the pH meter is also used as the control signal for a bidirectional controller that was built following the design appearing in an article by Cotman and Smith,[10] who reported control to within ±0.02-pH units. The controller governs the on-off actions of solenoid valves which allow acid or base to flow into the reactor for pH correction. The set point and control span are selected by the turn of appropriate dials.

Figure 4 shows the equipment as mounted in the laboratory.

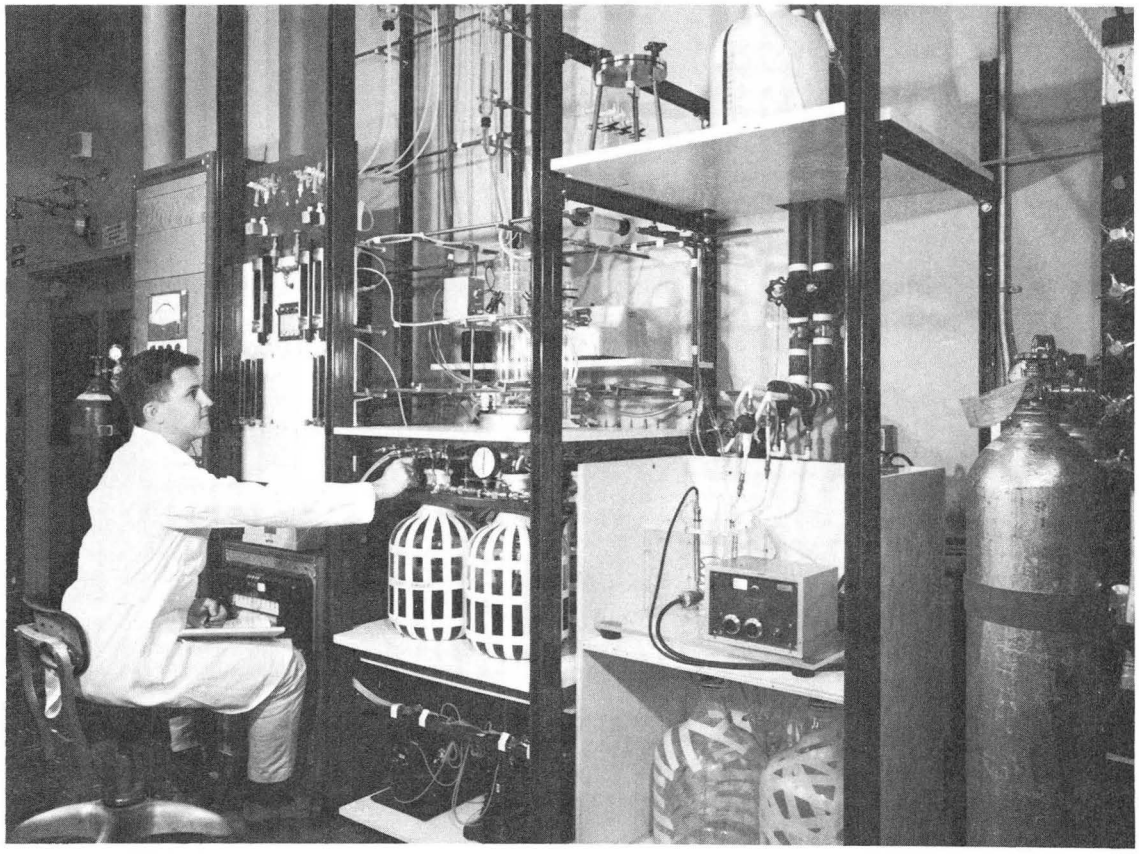

ZN-5163

Fig. 4. Photograph of continuous reactor system.

D. Data Analysis

Most of the batch experiments were analyzed by computer fit of the data to the generalized logistic equation discussed in Part I of this work. The generalized logistic equation, Eq. (35) of Part I, has the following form

$$y = \frac{K}{1 + \exp(a_0+a_1t_1+a_2t_1^2+a_3t_1^3+a_4t_1^4+a_5t_1^5)} \qquad (1)$$

where y = dependent variable

$t_1 = t - t_L$

t = time

t_L = length of lag phase, chosen by eye

$a_0, a_1, a_2, a_3, a_4, a_5$ = constants.

All or some of the batch data of Figs. 7, 8, 13, 21, and 44 were analyzed prior to development of the generalized logistic equation. The growth curves were drawn by eye and rates were determined by graphical differentiation. The remaining batch culture curves are based on the logistic equation and are shown in the figures in addition to being summarized in Tables XXIII and XXXI. The generalized logistic equation was found to fit the data well in most of the cases studied. The rate of change of each variable was then computed at regular time intervals and the results tabulated. Chi-square values were computed to test the closeness of fit of the equations. When the probability that the Chi-square value was due to chance was greater than or equal to 95%, the computer program stopped with a generalized logistic equation of the degree just fit. Otherwise, the program fitted the generalized logistic equation for first, third, and fifth degree polynomials. The probability that the Chi-square values obtained were due to chance are listed in Tables XXIII and XXXI. Probabilities were greater than 50% in all but three of the

batch cultures in which the logistic equation was used to calculate rates. When the probability of fit was low, the highest degree equation fit to the data was used if visual inspection showed that the data seemed to be fairly represented by the fitted curve.

IV. RESULTS

A. Development of Medium M

In a nutritional study of a fresh-water strain of sulfate-reducing bacteria, MacPherson and Miller reported the development of a chemically defined culture medium that did not form a precipitate on autoclaving as did Medium E,[7] which was used in earlier studies.[5] The compositions of MacPherson's Medium and Medium E are given in Appendix II. A nonprecipitating medium is important in a kinetic study because it is desirable to know the concentrations of all chemical species present. Experiments were designed to test MacPherson's Medium with the salt-tolerant strain isolated by Leban and Wilke.[5] Because the medium had been developed for a fresh-water of sulfate-reducing bacteria, some changes in the medium composition were anticipated and a study of the effects of each component of the medium was made to obtain a medium giving optimum growth and sulfate reduction. In the first set of experiments, ten sets of culture media were prepared with different compositions and each were inoculated with an identical quantity of a single culture adapted to grow in MacPherson's medium modified by the addition of 10% (w/v) sodium chloride. One of the ten sets of media had the same composition as that given in Appendix II. In each of eight of the nine other sets, the concentration of one component had been reduced by one half. In the remaining set, the concentration of yeast extract was reduced to zero. After inoculation, total counts and sulfide concentrations were measured daily in each set of media until full growth and high sulfide concentrations were reached. Tables I through X, which are given in Appendix III, list the results. Cell yields were calculated by averaging the counts made for each culture after cell concentrations had about reached their maximum values. The values obtained are listed in Table XI. The interpretation of these data follows in Sections 1 through 5. A second set of experiments was performed to obtain additional information about the effect of the concentrations of lactic acid and yeast extract. The results of the second set are listed in Tables XII

Table XI. Cell yield for reduced concentrations of various components of MacPherson's medium

	Modification	yield (10^8 cells/ml)
	none	1.09
no effect	1/2 KH_2PO_4	1.08
	1/2 NH_4Cl	1.10
moderate effect	1/2 $FeSO_4$	0.90
	1/2 $CaCl_2$	0.99
	1/2 $MgSO_4$	0.97
	1/2 Na_2SO_4	0.93
	1/2 lactic acid	1.35
greatest effect	1/2 yeast extract	0.45
	no yeast extract	0.01

through XVII and yields of sulfide and cells are listed in Tables XVIII and XIX. Tables XII through XVII are in Appendix III. The results are discussed in Sections 4 and 5. A third set of experiments was performed to study the effect of pH. The results are listed in Tables XX, XXI, and XXII in Appendix III. Section 6 discusses the effect of the initial pH of the medium, and the last section summarizes the changes made in MacPherson's medium as a result of the experiments discussed.

1. Effect of Potassium Phosphate, Ammonium Chloride, and Ferrous Sulfate

Sulfide concentration is plotted versus time in Fig. 5 for the first four batch experiments (unmodified, Table I; 1/2 KH_2PO_4, Table II; 1/2 NH_4Cl, Table III; 1/2 $FeSO_4$, Table IV). As shown by the graph, sulfide production was not significantly reduced during the period of the experiment by halving the concentrations of potassium phosphate, ammonium chloride, and ferrous sulfate in MacPherson's medium.

Also, cell yield for reduced concentrations of potassium phosphate and ammonium chloride was not significantly different from the value obtained in unmodified MacPherson's medium, as shown in Table XI. Table XI also shows that cell yield was reduced from 1.09×10^8 cells/ml (for the unmodified medium) to a value of 0.90×10^8 cells/ml by halving the initial concentration of ferrous sulfate.

Because the effects of halving the concentrations of potassium phosphate, ammonium chloride, and ferrous sulfate were slight, the concentrations of these components were kept at their original values in future experiments.

2. Effect of Magnesium Sulfate and Calcium Chloride

Figure 6 is a graph of sulfide concentration versus time for the first, fifth, and sixth batch experiments (unmodified medium, Table I; 1/2 $CaCl_2$, Table V; 1/2 $MgSO_4$, Table VI). By comparison to the sulfide curve for unmodified medium, it is clear that lowering the concentration of either calcium chloride or magnesium sulfate reduces the rate of sulfide

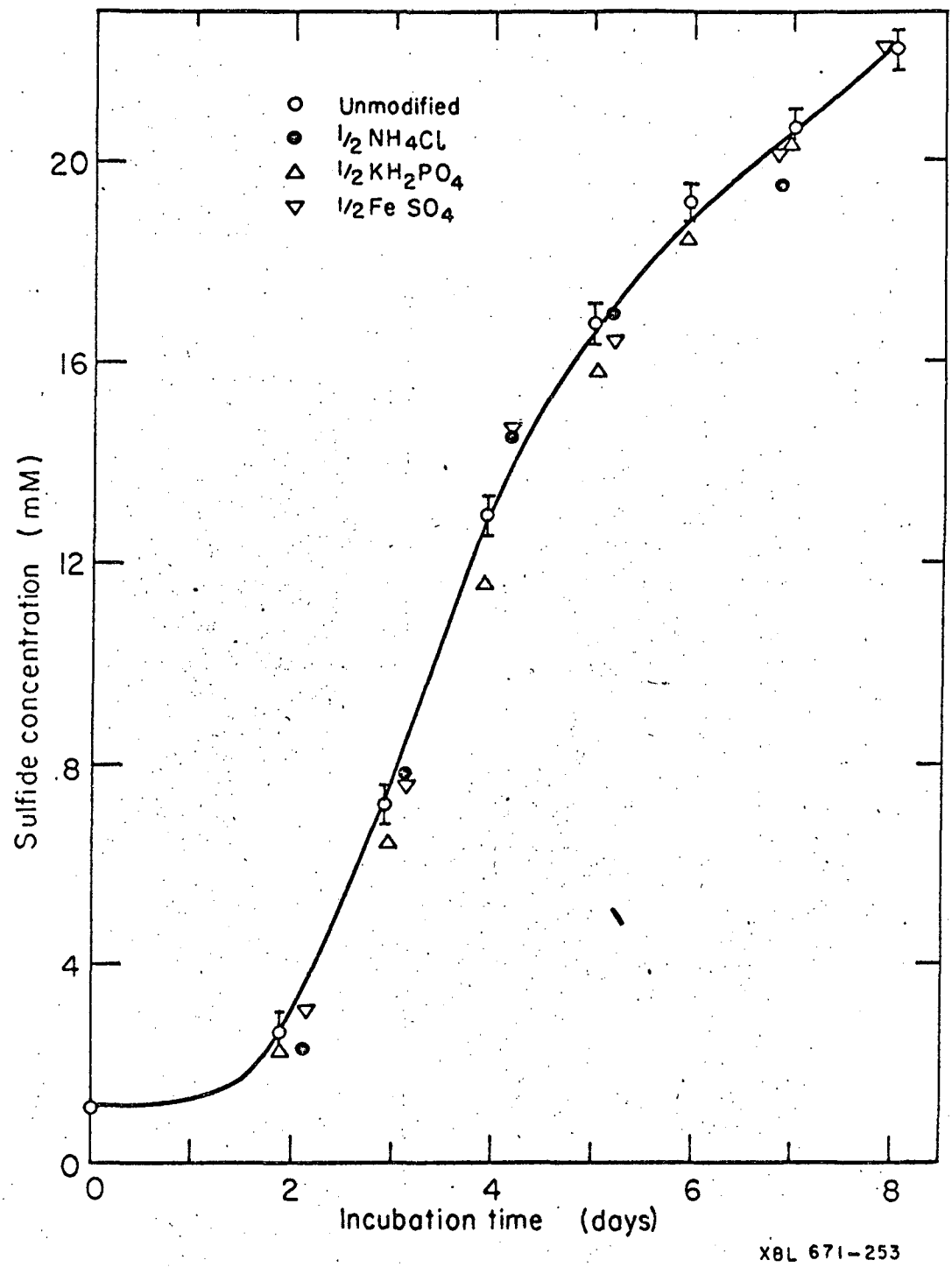

Fig. 5. Sulfide concentration versus incubation time.

Table XVIII. Cell yields in modified medium M

Modification	Cell yield (10^8 cells/ml)	Sulfide yield (mM)
0.1% yeast extract	1.23	24.1
100 mM lactic acid 0.1% yeast extract	1.28	25.6
0.2% yeast extract	2.52	27.6
0.3% yeast extract	2.54	32.0
0.5% yeast extract	2.34	28.8
1.0% yeast extract	3.69	31.9
Initial pH = 7.60 0.25% yeast extract	2.77	23.6
Initial pH = 7.99 0.25% yeast extract	2.67	23.3
Initial pH = 8.60 0.25% yeast extract	2.83	24.8

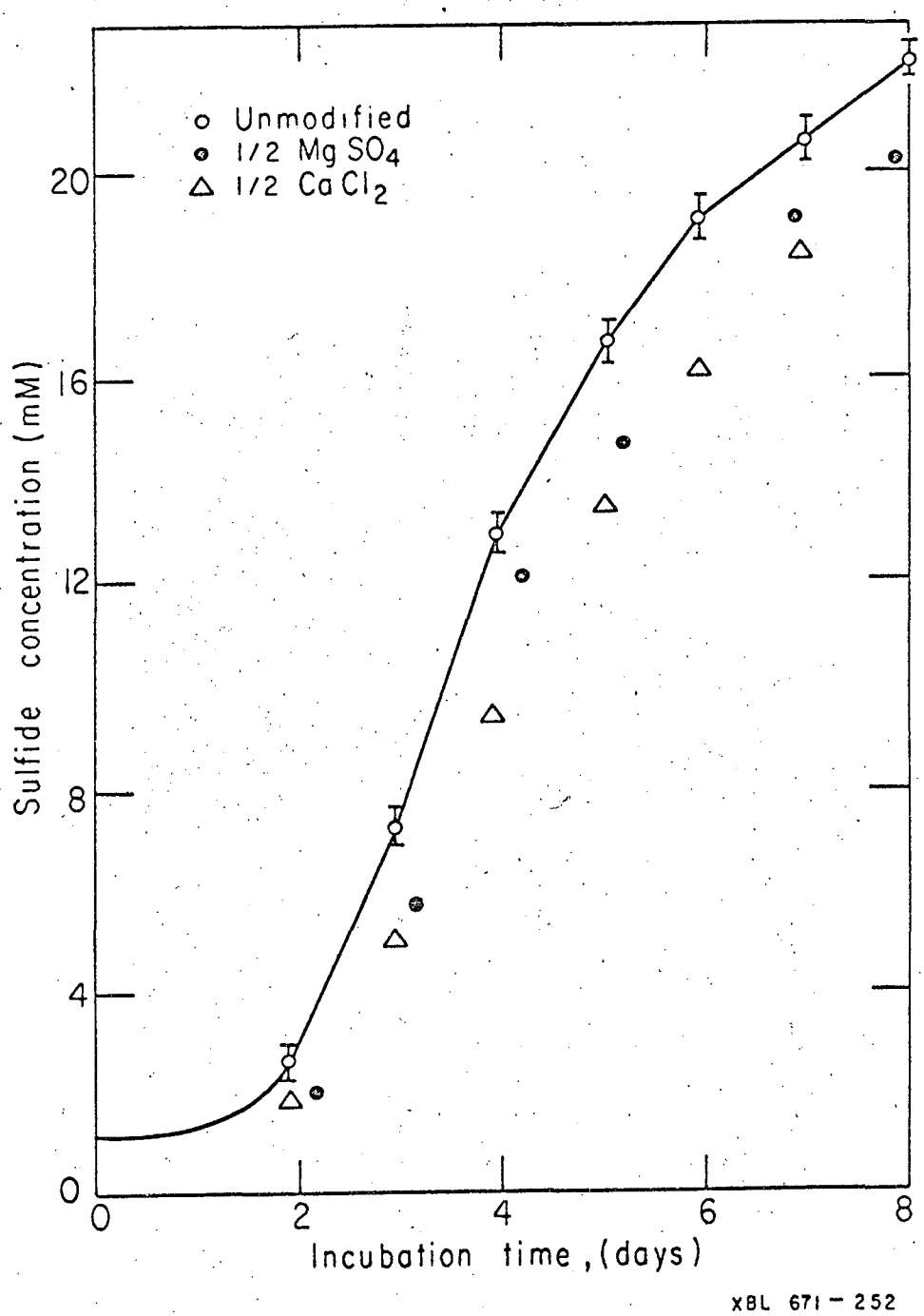

Fig. 6. Sulfide concentration versus incubation time.

production. Also, reference to Table XI shows that cell yield was moderately reduced by the reduced concentrations of calcium and magnesium salts. Therefore, to prevent limitation of growth by either of these components, they were added at twice their concentrations in MacPherson's medium in future experiments. This change decreased the maximum rate of sulfide production, as shown in Fig. 11 by comparing rates obtained with 100 mM lactic acid before the change (circles) with the rates after the concentrations of calcium and magnesium salts were doubled (triangles with apices down). Figure 12 shows that the maximum specific growth rate was increased by the change in the concentrations of calcium and magnesium salts.

3. Effect of Sodium Sulfate

Figure 7 shows the effect of reducing the initial concentration of sodium sulfate by one half in the seventh culture. Both cell yield and sulfate reduction were decreased, although the change did not seem to have an effect on the rates of growth and sulfate reduction until a sulfate concentration of about 4 mM/l was reached. An attempt was made to fit the Michaelis-Menten[11] model for substrate-limited enzyme kinetics to the specific rate of sulfate-reduction by graphically measuring slopes of the sulfide production curve and estimating sulfate concentrations from sulfide concentrations and the initial sulfate concentrations. The model was fit to the data in the conventional manner of plotting the reciprocal of the specific rate of sulfate reduction against the reciprocal of the sulfate concentration. The best line through the data is given by Eq. (2) as shown in Fig. 8.

$$\frac{1}{N}\frac{d(SO_4^{--})}{dt} = \text{specific rate of sulfate reduction}$$

$$= -2.5 \times 10^{-10} \frac{(SO_4^{--})}{17 + (SO_4^{--})} \qquad (2)$$

where N = cell concentration in cells/l

(SO_4^{--}) = sulfate concentration in mM

t = time in days.

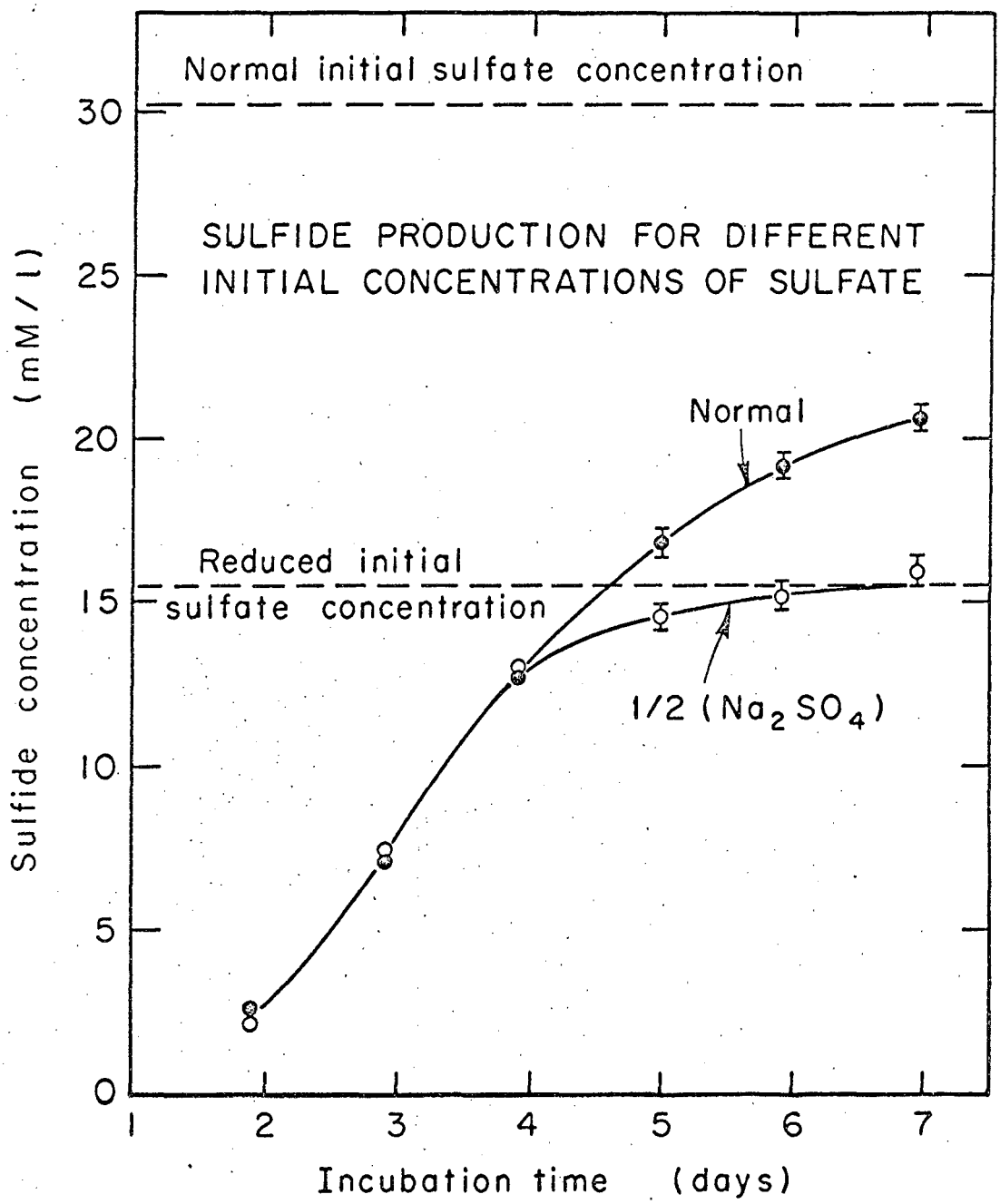

MUB-7952

Fig. 7. Sulfide concentration versus incubation time.

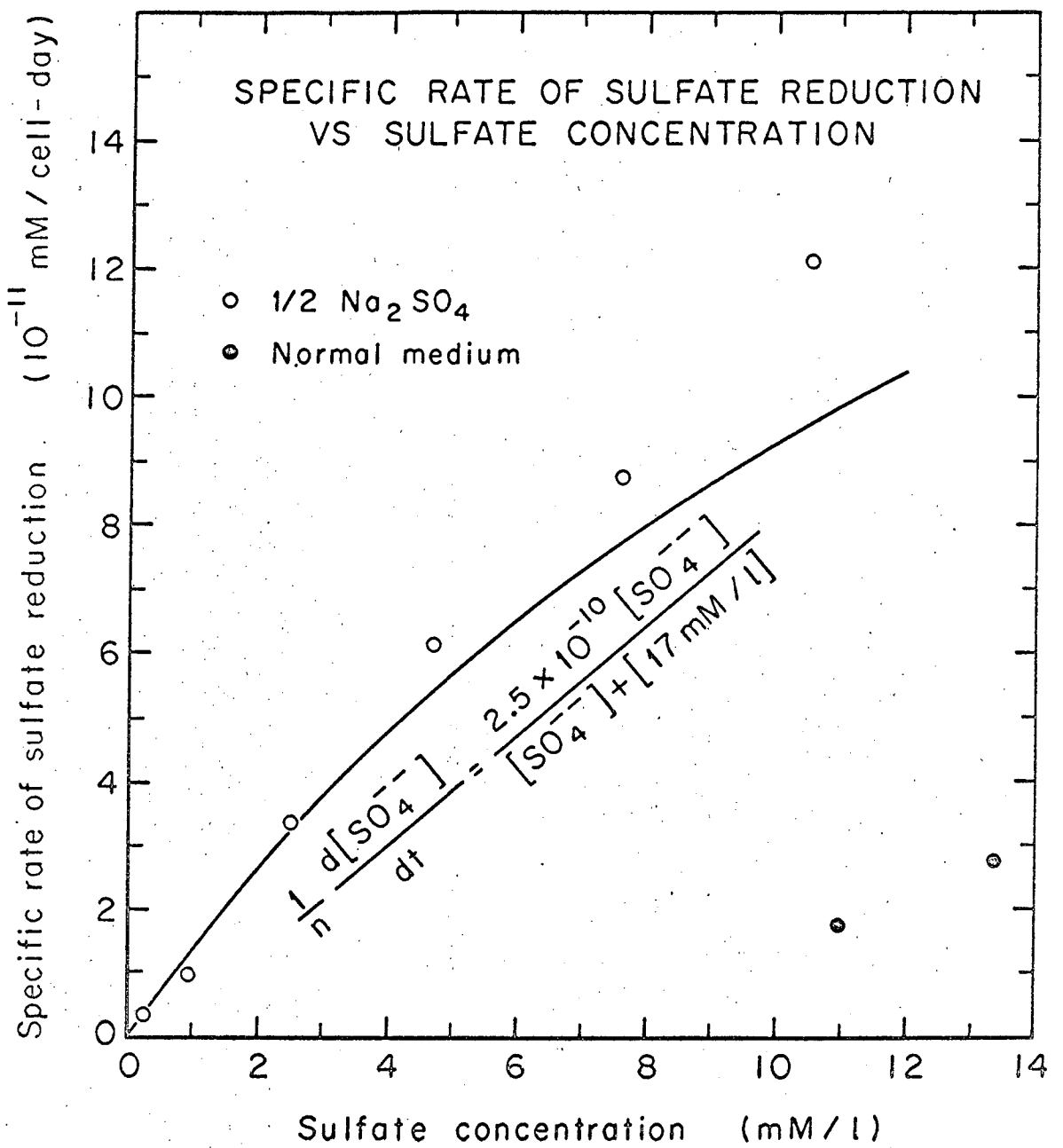

MUB-7957

Fig. 8. Specific rate of sulfate reduction versus sulfate concentration.

Agreement with the observed data is best for low sulfate concentrations, as would be expected. Specific rates calculated from the data for the unmodified medium are much lower than those for the case where sulfate is initially present at a lower concentration. Possible causes for failure of the model to apply at higher sulfate concentrations include the effects of yeast extract, of sulfide concentration, and of the phase of growth of the organisms (because the data were calculated with data from both exponential phase and post-exponential phase cultures). Further discussion of these other effects is given later in this report.

4. Effect of Lactic Acid

Figures 9 and 10 show the effect of the initial concentrations of lactic acid on sulfide production. A longer lag phase in the production of sulfide occurred at a lactic acid concentration of 100 mM as shown in Fig. 9. Figures 11 and 12 show the effects on the specific rate of sulfide formation and on the specific growth rate. The curves in Figs. 9 and 10 and the rates in Figs. 11 and 12 were calculated by computer analysis of the data as described in the Methods Section. The coefficients are given in Table XXIII.

An initial concentration of lactic acid of 100 mM inhibited growth slightly. As shown in Table XI, a cell yield of 1.09×10^8 cells/ml developed in the same medium with an initial lactic acid concentration of 50 mM. Table XVIII shows that no significant changes in cell yield or sulfide yield occurred when initial lactic acid concentrations of 85 and 100 mM were compared in the second set of experiments. Rates of sulfide production were higher at the reduced lactic acid concentrations in both sets of experiments as shown by Fig. 11. Growth rates were also higher at lower lactic acid concentrations, as shown by Fig. 12.

In all other runs during the second set of experiments and in all experiments afterwards, an initial lactic acid concentration of 85 mM was used because it gave high rates of growth and sulfate reduction without a loss in the yield of sulfide.

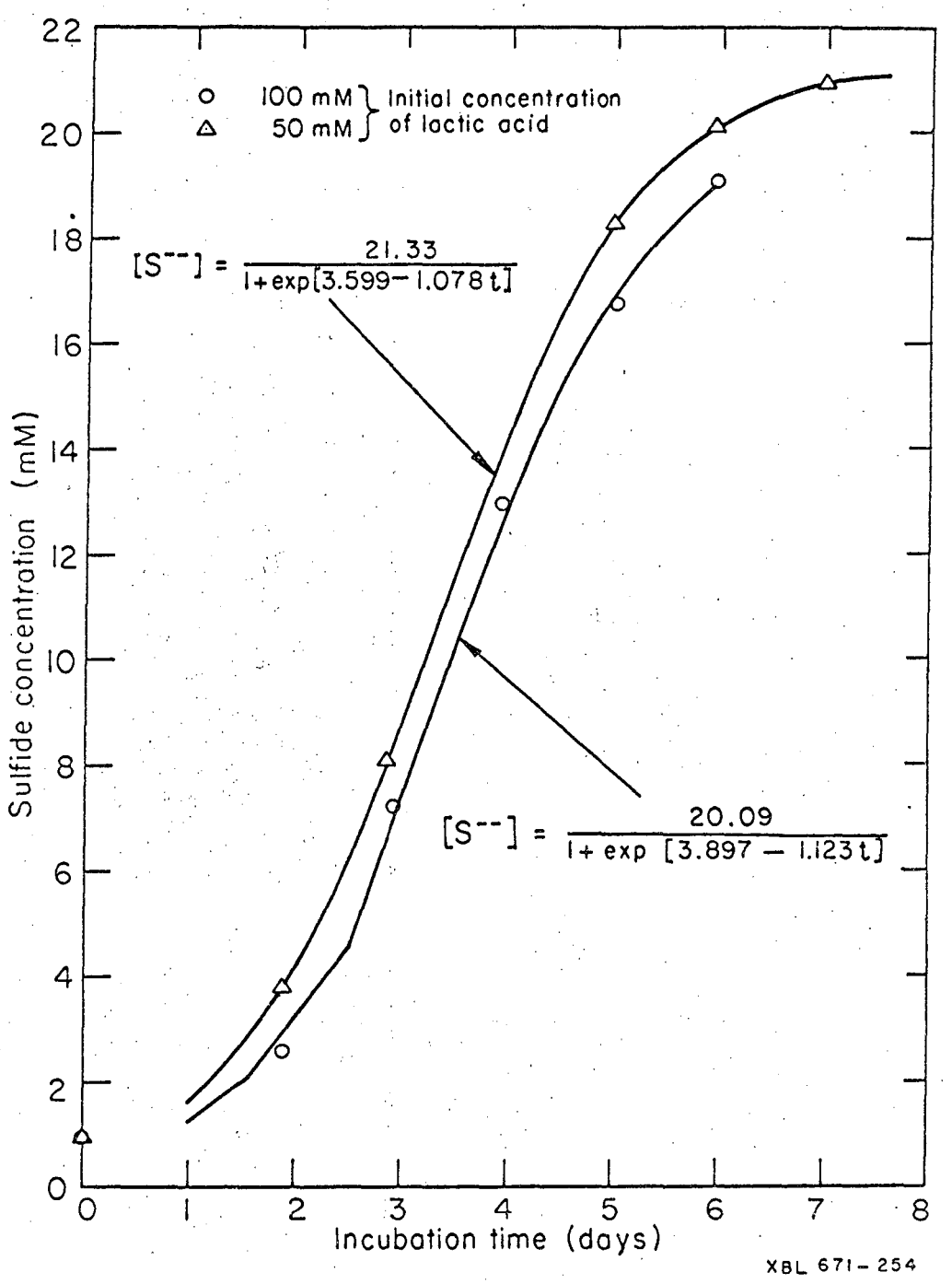

Fig. 9. Sulfide concentration versus incubation time.

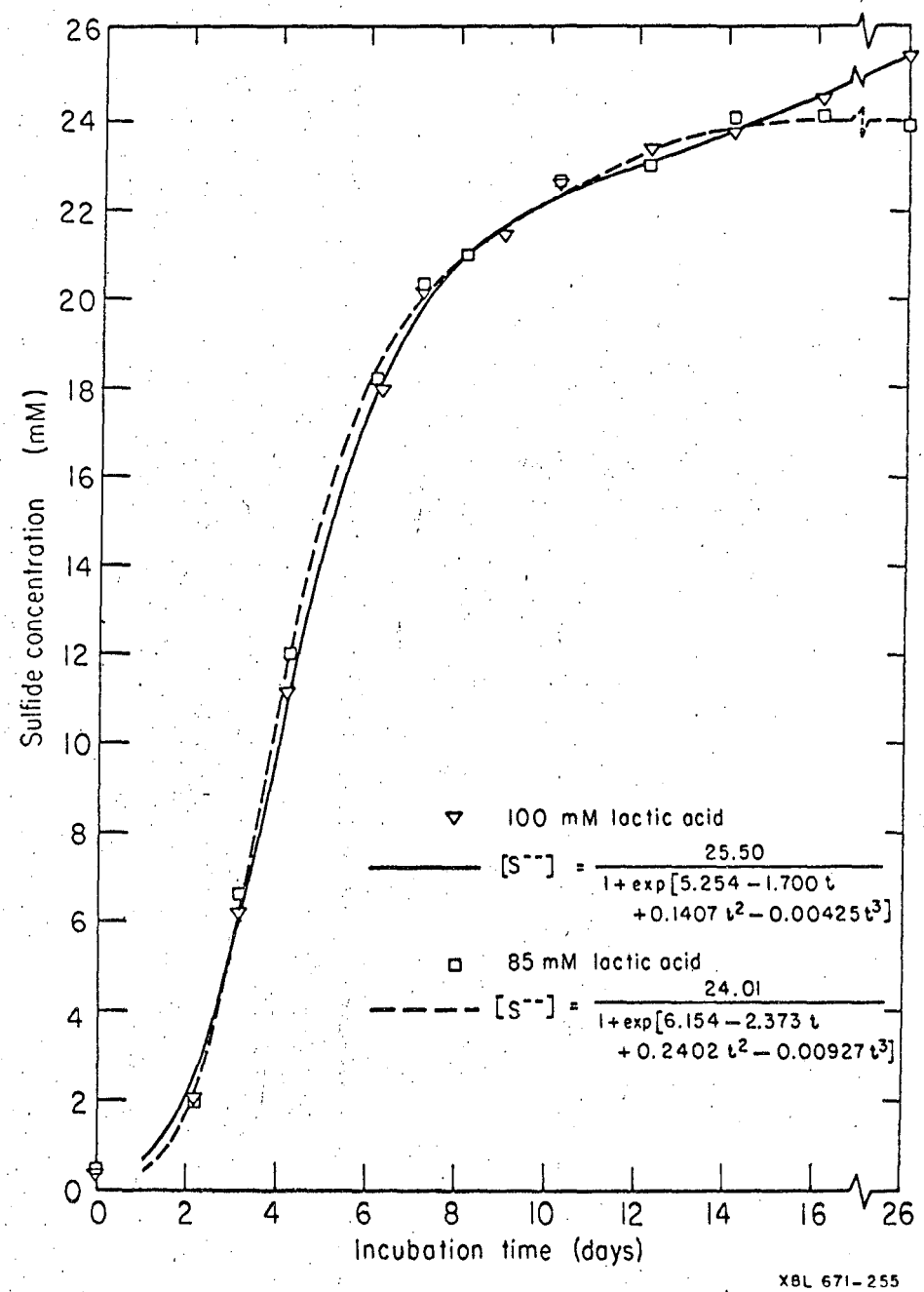

Fig. 10. Sulfide concentration versus incubation time.

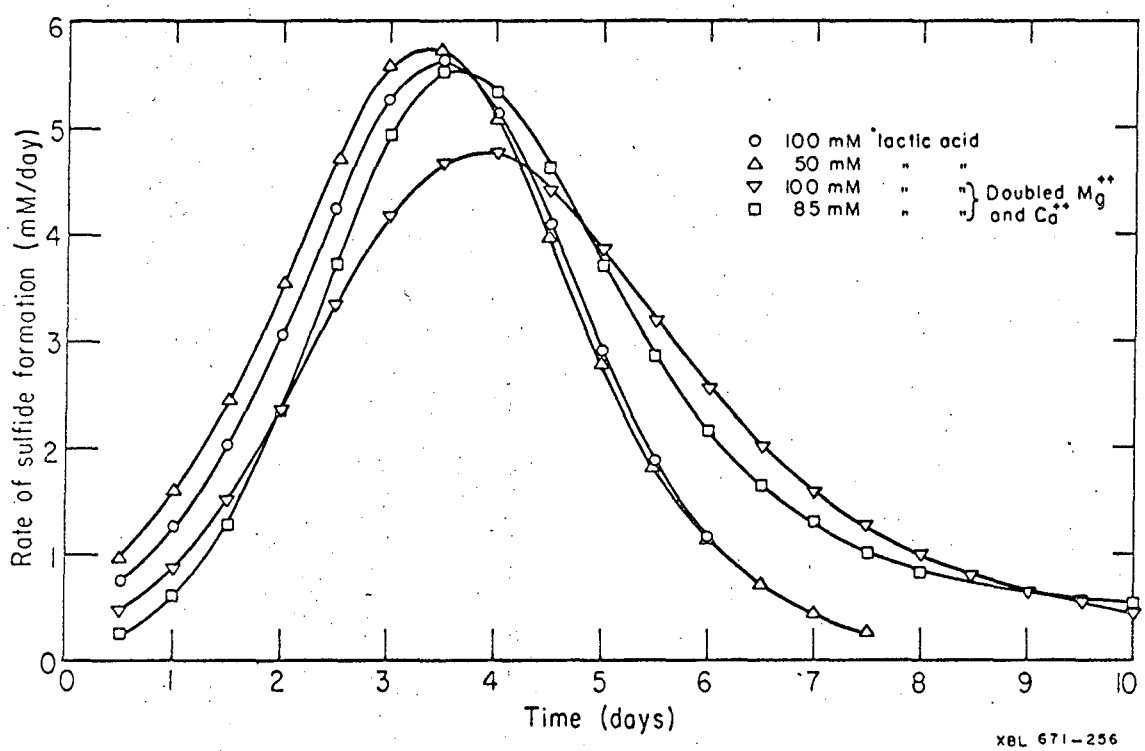

Fig. 11. Rate of sulfide formation versus time.

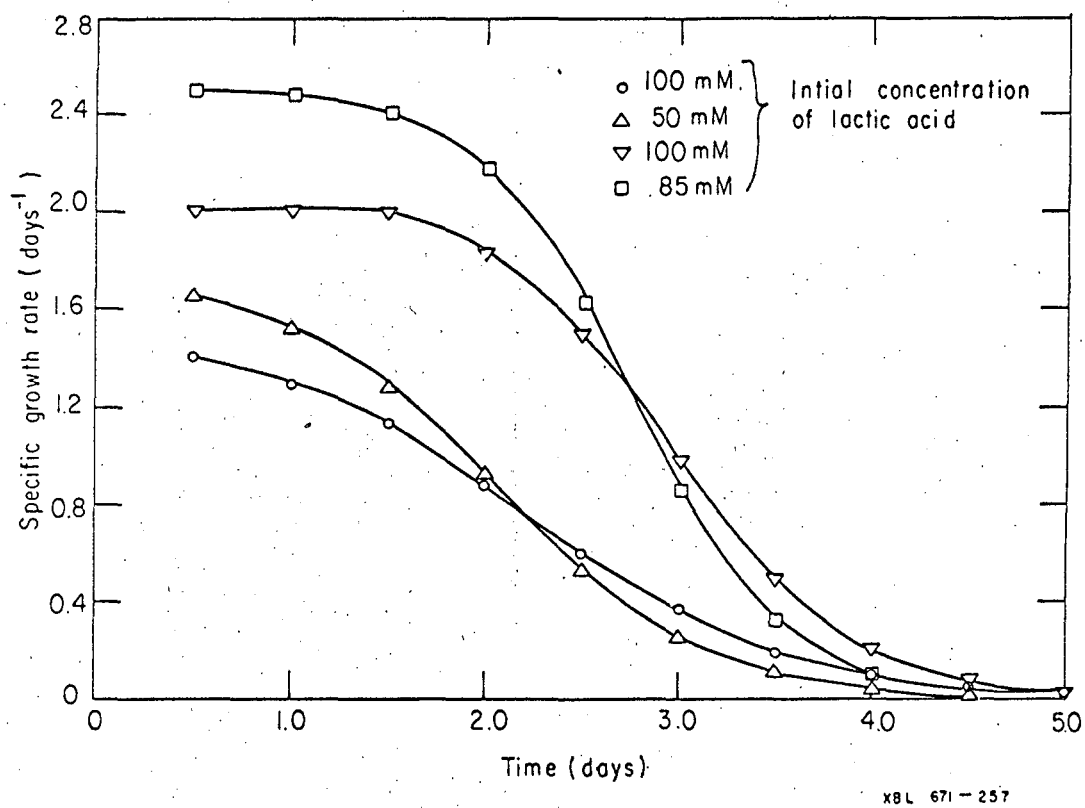

Fig. 12. Specific growth rate versus incubation time.

5. Effect of Yeast Extract

In the first set of experiments with MacPherson's medium, batch growth was monitored at initial concentrations of yeast extract of 0, 0.05, and 0.10 % (w/v). The results are listed in Tables I, IX, and X. Sulfide production for those three experiments is shown in Fig. 13. Sulfide production was reduced in both quantity and rate of formation when yeast extract was present at one half the normal initial concentration. No measurable sulfide formation occurred when no yeast extract was present. Cell yields were also strongly dependent on yeast extract concentration, as shown by Tables XI, XVIII, and XIX. Because the kinetics were strongly affected by the yeast extract concentration, the effects of yeast extract were investigated further in the second set of experiments. Batch growth data in modified MacPherson's medium* were obtained at initial concentrations of 0.1, 0.2, 0.3, 0.5, and 1.0% (w/v) yeast extract and are given in Tables XII, XIV, XV, XVI, and XVII, respectively. Batch sulfide curves at the different concentrations are compared to 0.1% yeast extract in Figs. 14 and 15. Overall yields of sulfide are increased as can be seen from the graphs and from Table XVIII. Table XIX shows that cell yield increased with increased yeast extract concentration when measured by either dry weights or optical counts. Dry weight measurements were made after four days of batch growth. However, they do not represent the maximum yield obtainable at 0.5 and 1.0% yeast extract because growth was still continuing in those cases four days after inoculation. Specific growth rates, however, were reduced by increased concentration. This is shown by Figs. 16 and 17. Specific growth rates were calculated with the computer program discussed in the methods section of this report and showed a regular pattern when plotted versus time in Fig. 16, with the exception of

---

*Calcium and magnesium salts were present at twice their concentration in the first set of experiments for the reasons given in Section A.2 and lactic acid was reduced to 85 mM as explained in Section A.4.

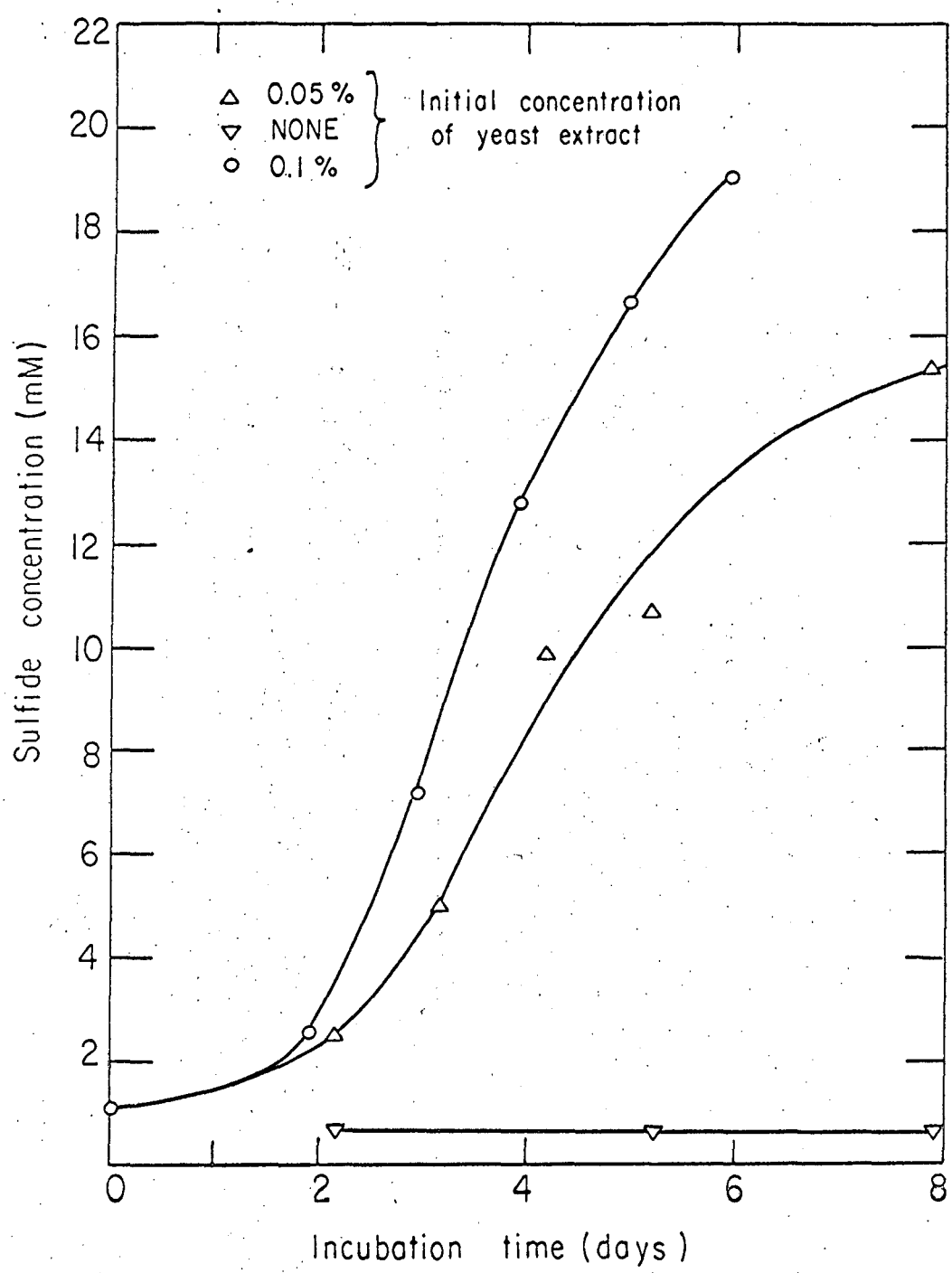

XBL 671 — 258

Fig. 13. Sulfide concentration versus incubation time.

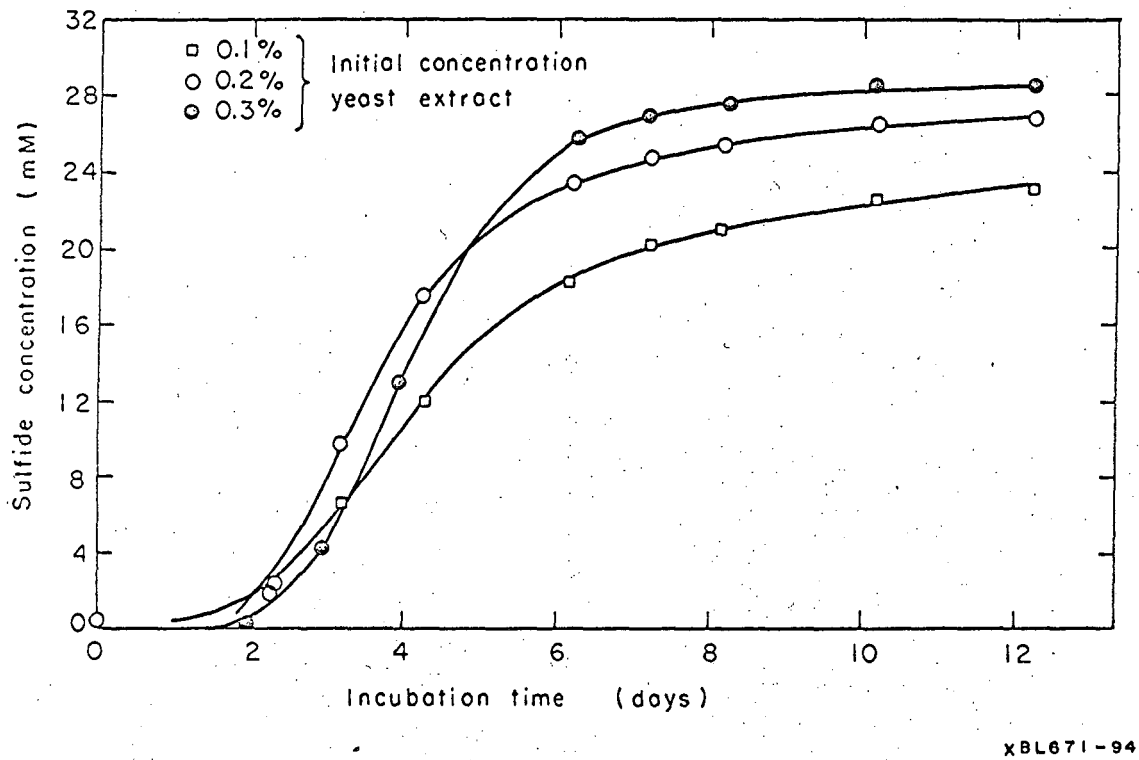

Fig. 14. Sulfide concentration versus incubation time.

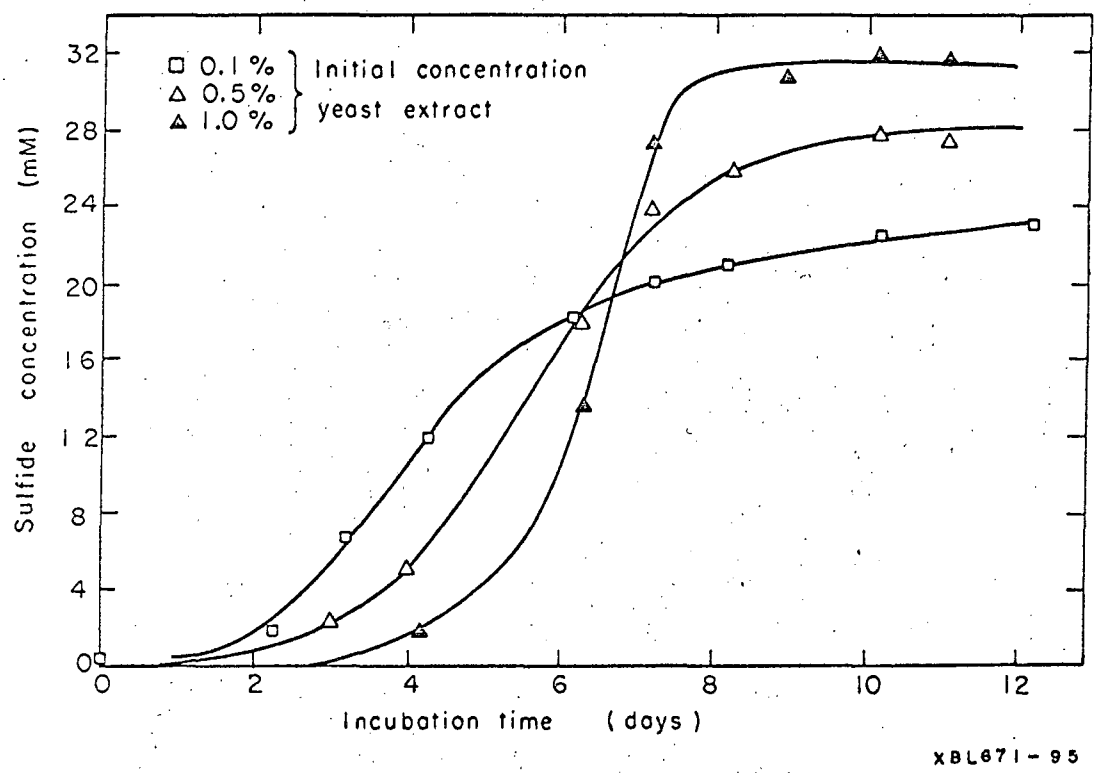

Fig. 15. Sulfide concentration versus incubation time.

Table XIX. The effect of yeast extract on yields in modified MacPherson's medium

Initial concentration of yeast extract %(w/v)	Maximum growth rate $days^{-1}$	Cell yield 10^8 cells/ml	Dry weight after 4 days g/l	Sulfide after 16 days mM
0.0	-	0.011	-	-
0.05	-	0.45	-	-
0.1	2.50	1.23	0.066	23.7
0.2	2.41	2.52	0.140	27.1
0.3	2.27	2.54	0.180	27.7
0.5	1.59	2.34	0.174	27.2
1.0	0.76	3.69	0.286	28.7

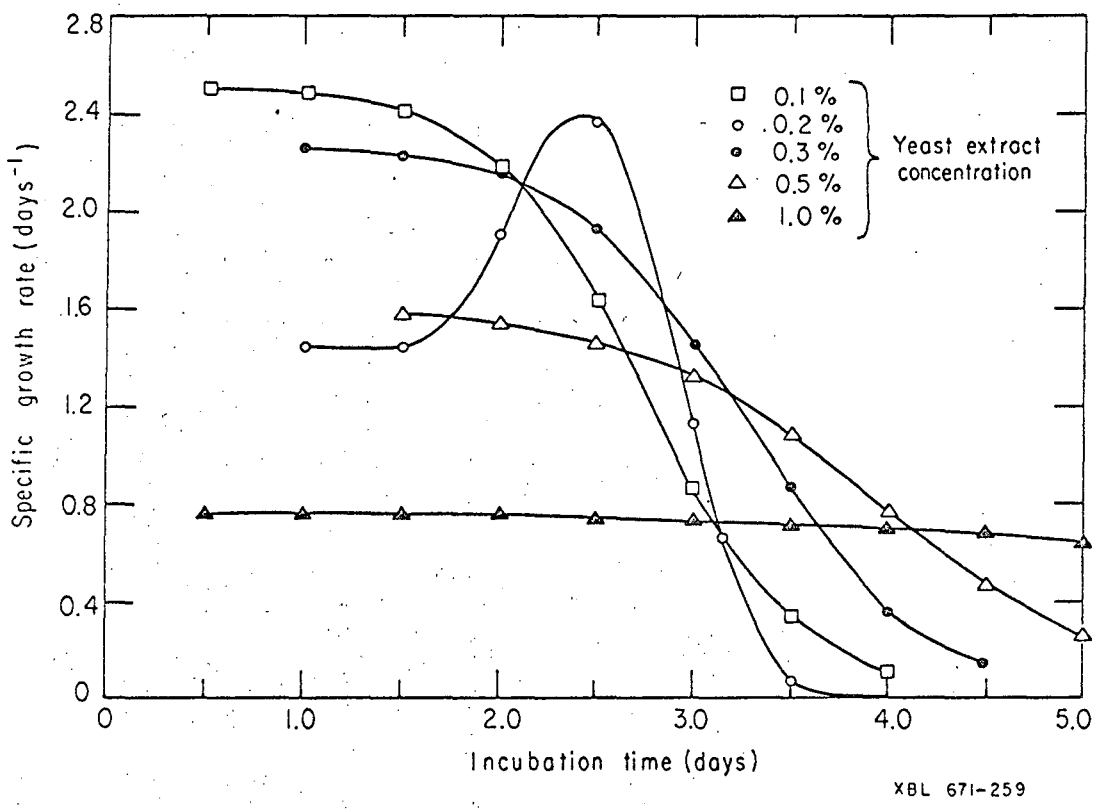

Fig. 16. Specific growth rate versus incubation time.

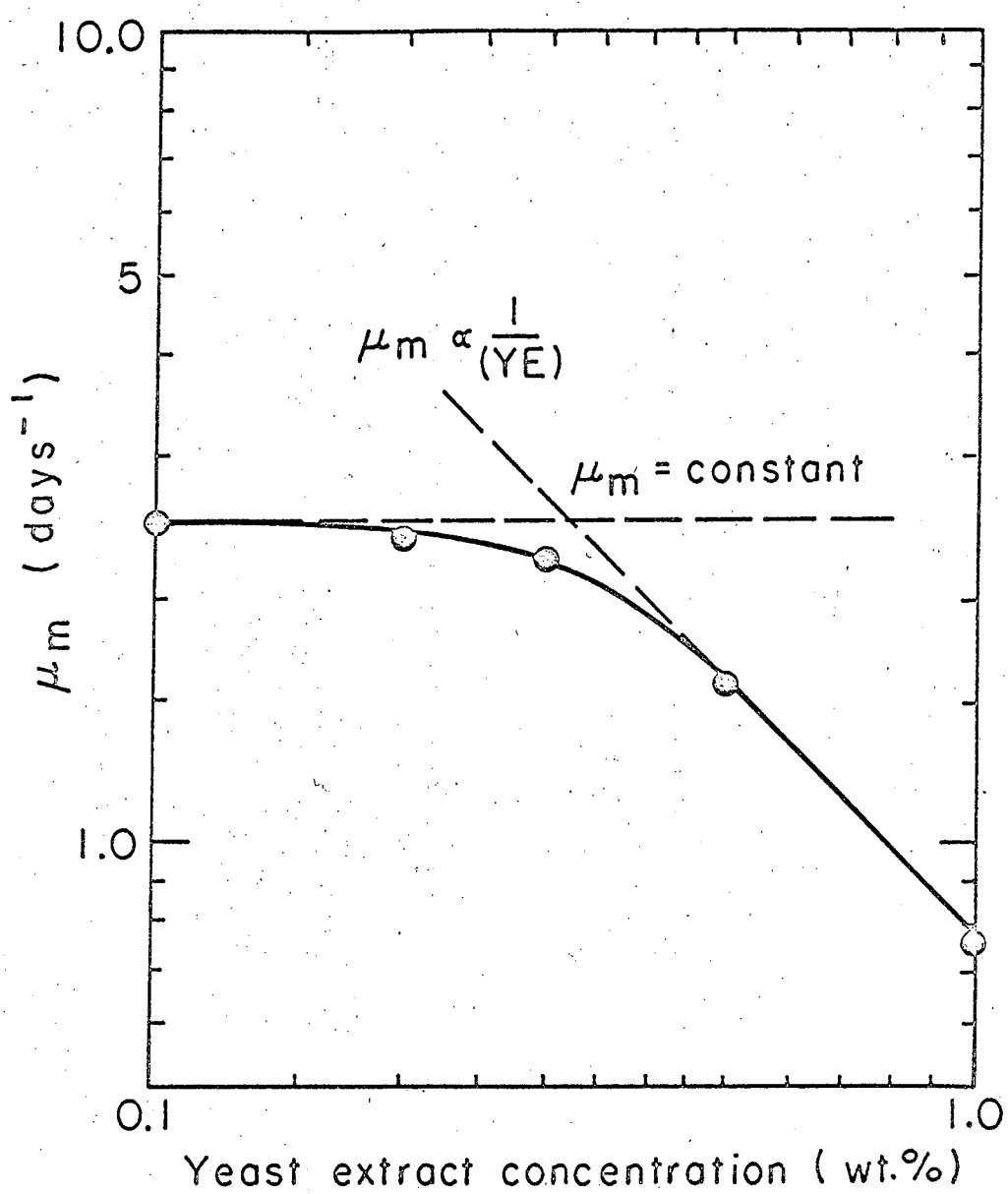

XBL671-96

Fig. 17. Maximum specific growth rate versus yeast extract concentration.

the curve for a yeast extract concentration of 0.2%. The coefficients of the fit equations are given in Table XXIII. The irregular behavior of that case (yeast extract = 0.2%) may be due to a poor fit to the data by the equation used to calculate specific rates. The maximum growth rates correlate well with the yeast extract concentration when plotted on log-log paper as shown in Fig. 17. Maximum growth rates are fairly constant at 0.1, 0.2, and 0.3% (w/v) yeast extract, but fall off rapidly at higher or lower concentrations.

Another apparent trend is the increasing lag in growth and sulfide formation with yeast extract concentrations above 0.2%. This trend can be seen in Figs. 14 and 15 and also in Figs. 16 and 18. The lags are most pronounced at yeast extract concentrations of 0.5 and 1.0%.

Figure 18 is a graph of the rate of sulfide formation versus incubation time, and Fig. 19 is a plot of the maximum specific rate of sulfide formation versus yeast extract concentration. Figure 18 shows that sulfide production rates for concentrations of 0.2 and 0.3% were the most similar of any two of the experiments.

It can be seen that yeast extract at all concentrations has an important effect on the kinetic behavior of sulfate-reducing bacteria. Increasing concentrations of yeast extract led to increasing values of cell yield and sulfide production. But specific growth rates were near their maximum at 0.1% yeast extract and appreciable reductions in specific growth rate and sulfide production rate were observed at concentration of 0.3% and above. On the basis of these results, it was concluded that changes in the yeast extract concentration would have the smallest effect at a value of 0.25% (w/v), and that concentration was adopted in all future experiments.

6. Effect of pH

The hydrogen ion activity is known to have an important influence on many biological rate processes. The next experiment illustrates the effect of pH on growth and sulfate-reduction in Medium M. Five liters

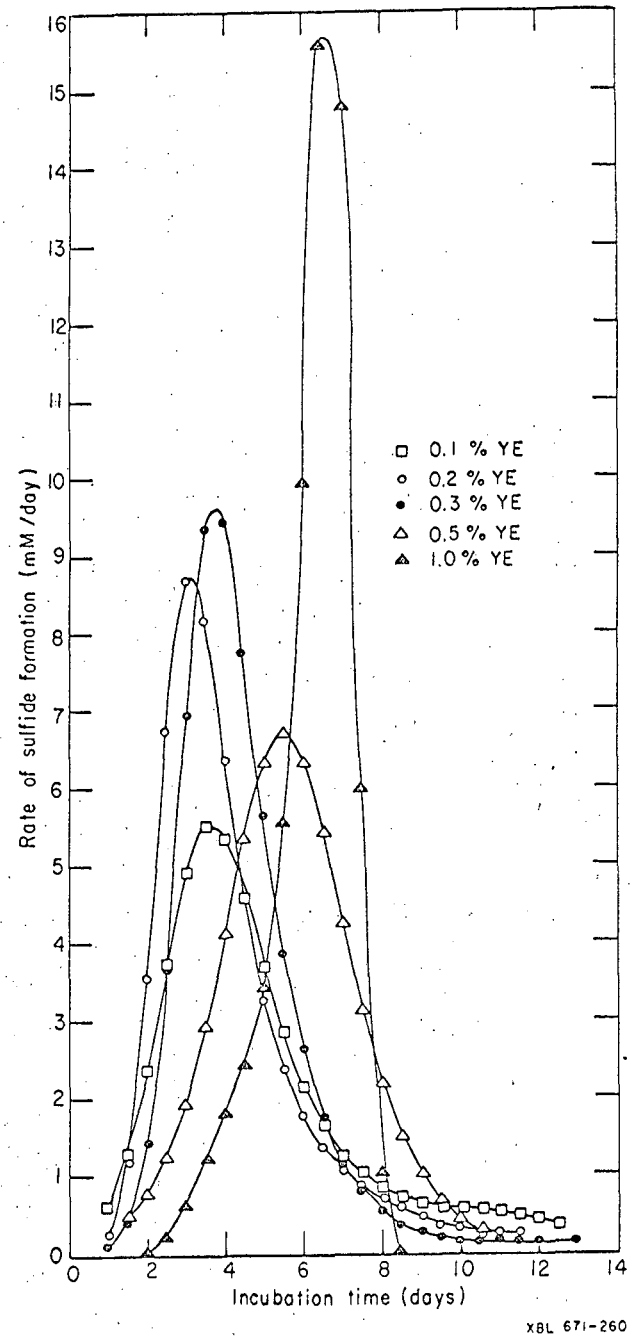

Fig. 18. Rate of sulfide formation versus incubation time.

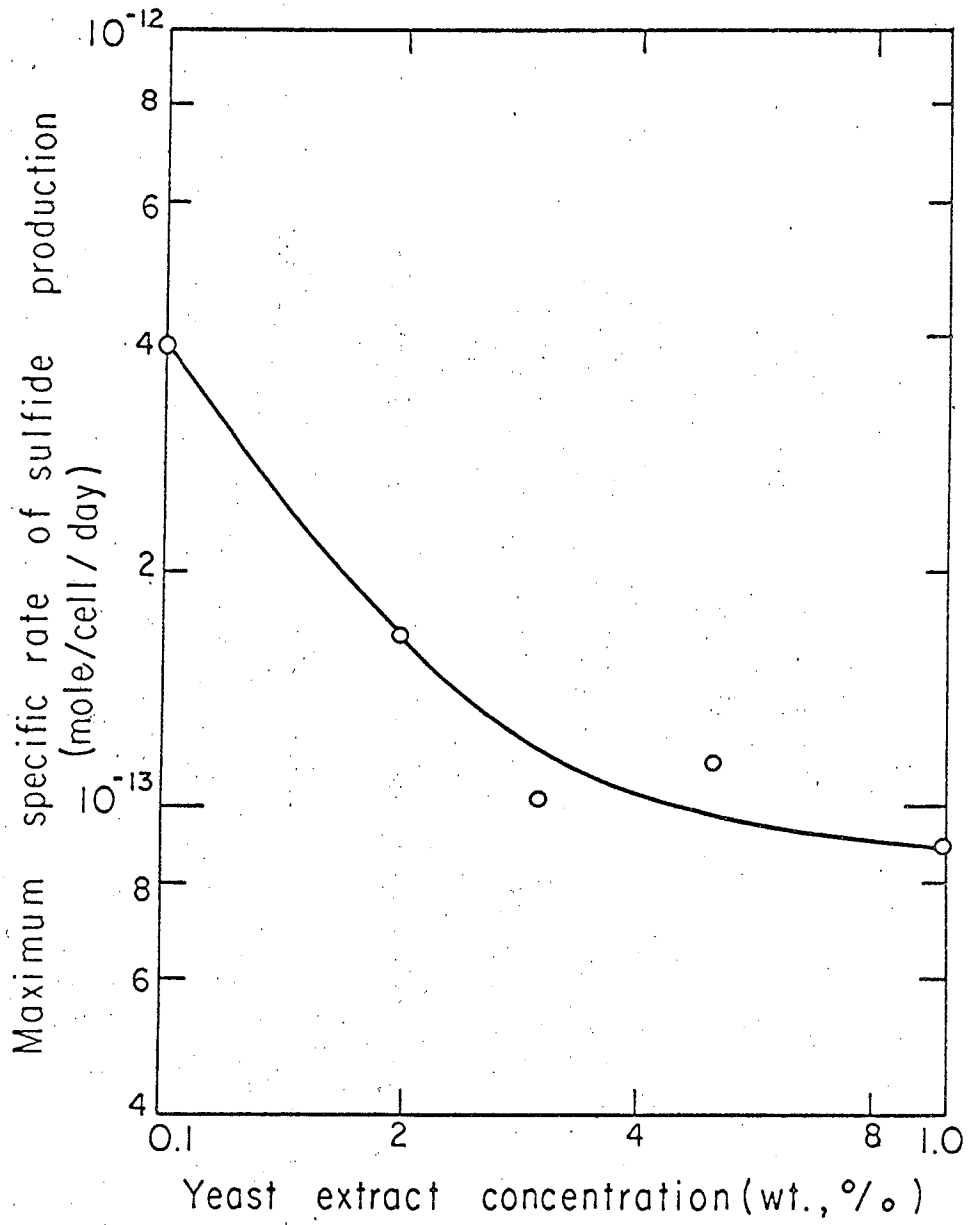

XBL 671 — 261

Fig. 19. Maximum specific rate of sulfide formation versus yeast extract concentration.

of medium was prepared and divided equally among five bottles. After sterilization, the pH of each bottle was adjusted to a different value using aseptic technique. The initial pH values chosen for the experiment were 6.40, 6.95, 7.60, 7.99, and 8.60. As before, optical count and sulfide concentration were monitored after inoculation and distribution among smaller bottles. Growth was obtained only at the three highest initial values of pH. The results are listed in Tables XIX, XX, and XXI in Appendix III for initial values of 7.60, 7.99, and 8.60. Figure 20 compares optical counts for these three cultures. The curves shown in Fig. 20 are those calculated with the equations given in Table XXII. In each case, the pH declined during the experiment, as shown in Fig. 22. Figure 21 is a comparison of sulfide production in the same three cultures. As is evident from the low probability of fit shown in Table XXIII, good fits were not obtained for the sulfide data, so the curves in Fig. 21 were placed by eye. The paucity of data and the high initial values of sulfide concentration are responsible for the poor fit by the logistic equation. It should also be noted that for short incubation times, the computer-fit growth curves are unreliable for initial pH values of 7.99 and 8.60. Values of the variables and rates of change at regular time intervals are shown in Tables XXIV, XXV, and XXVI. Values of optical count and specific growth rate in these tables were calculated with the appropriate equations in Table XXIII. Curves for sulfide production, and rate of sulfide production were determined graphically. Values of pH for intermediate incubation times were estimated by graphical interpolation.

Specific growth rates are plotted versus time in Fig. 23 and versus pH in Fig. 24. Maximum specific growth rates were lower than those observed in the preceding experiments with yeast extract. The high sulfide concentrations in these experiments may have caused inhibition. Specific growth rate is nearly independent of the initial pH for the data shown in Figs. 23 and 24, except for a shorter lag phase at an initial pH of 7.88. The shortened lag at the intermediate pH is also apparent in Figs. 20, 21, and 25. Sulfide production rates are plotted

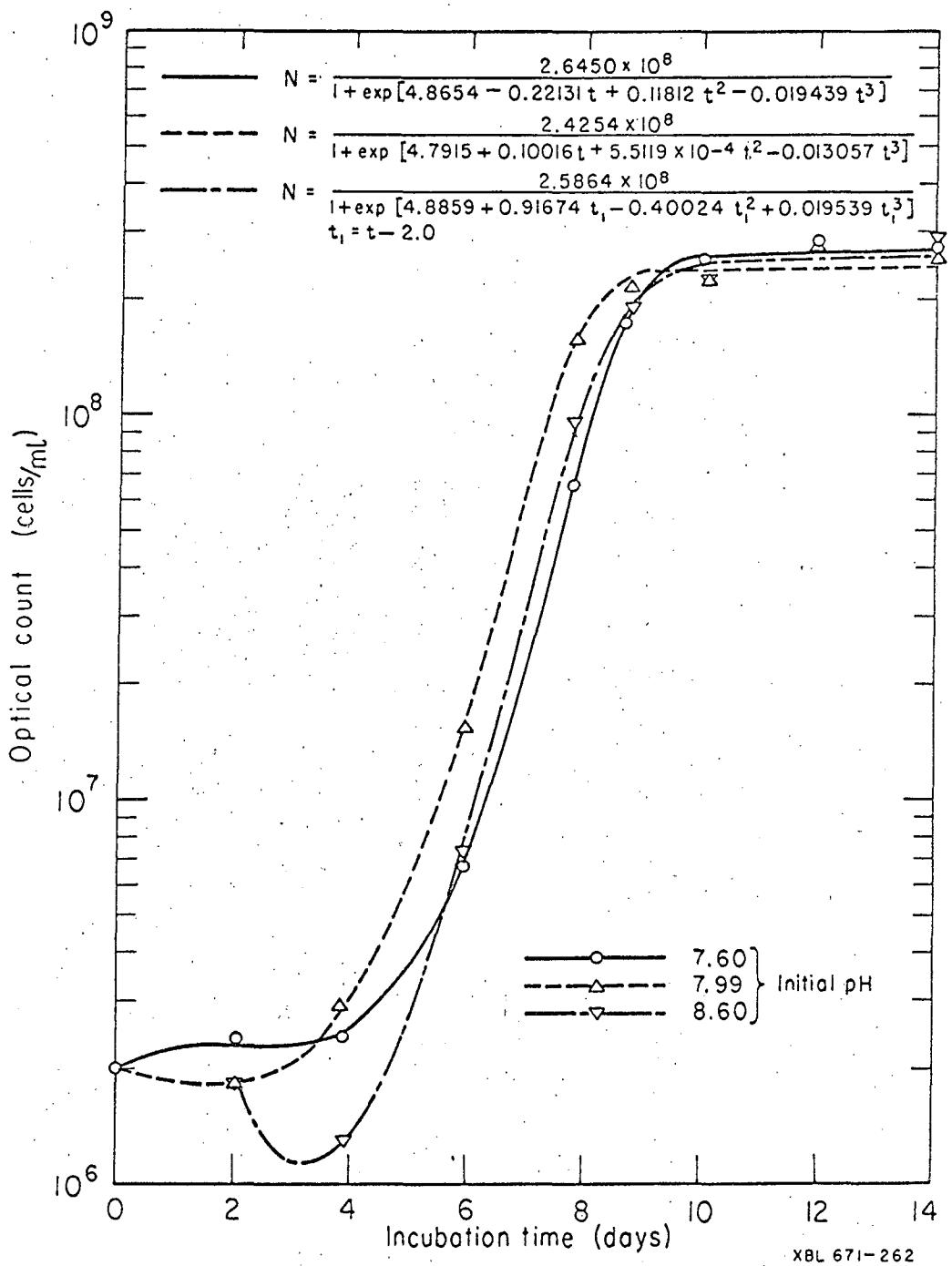

Fig. 20. Cell count versus incubation time.

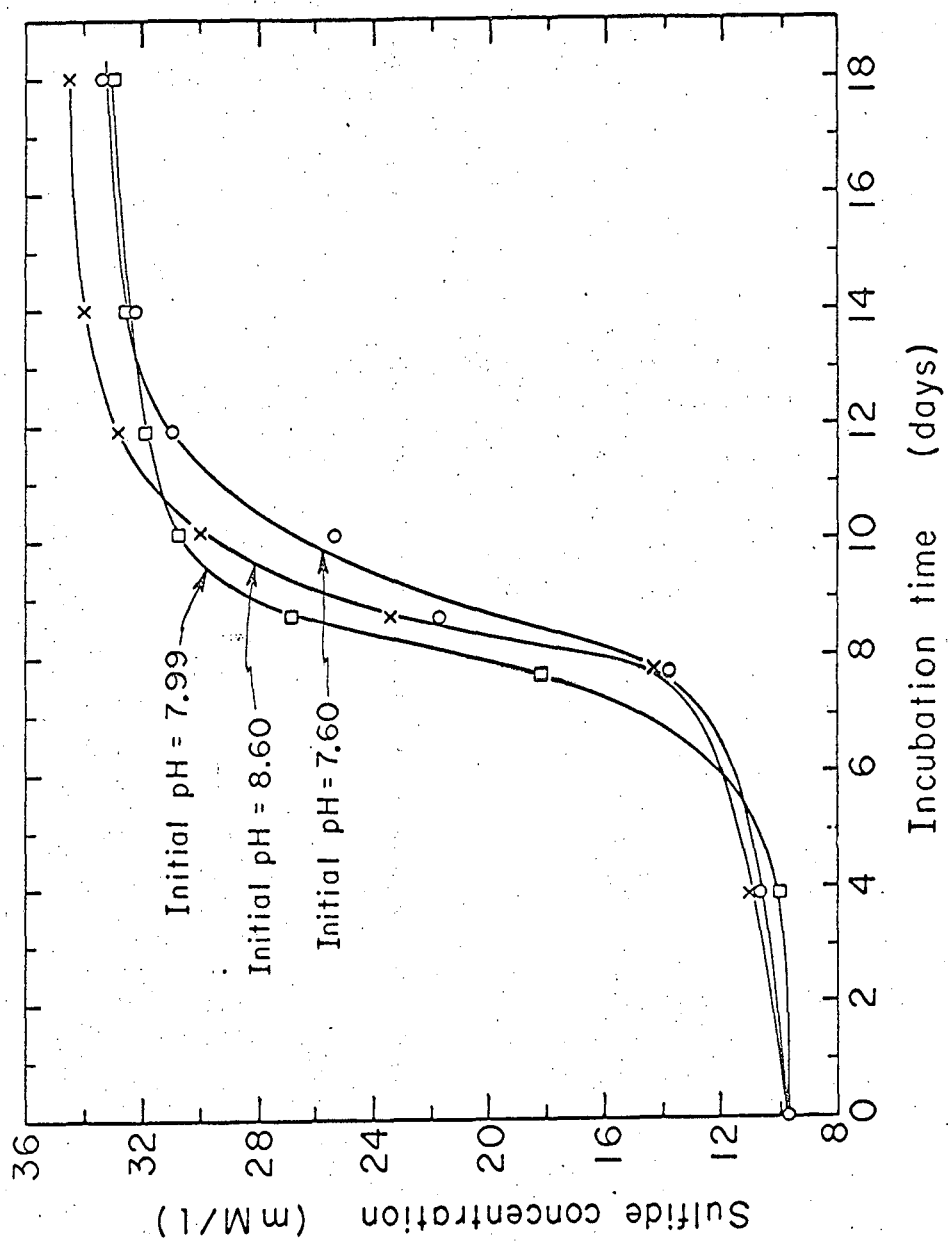

MUB-7951

Fig. 21. Sulfide concentration versus incubation time.

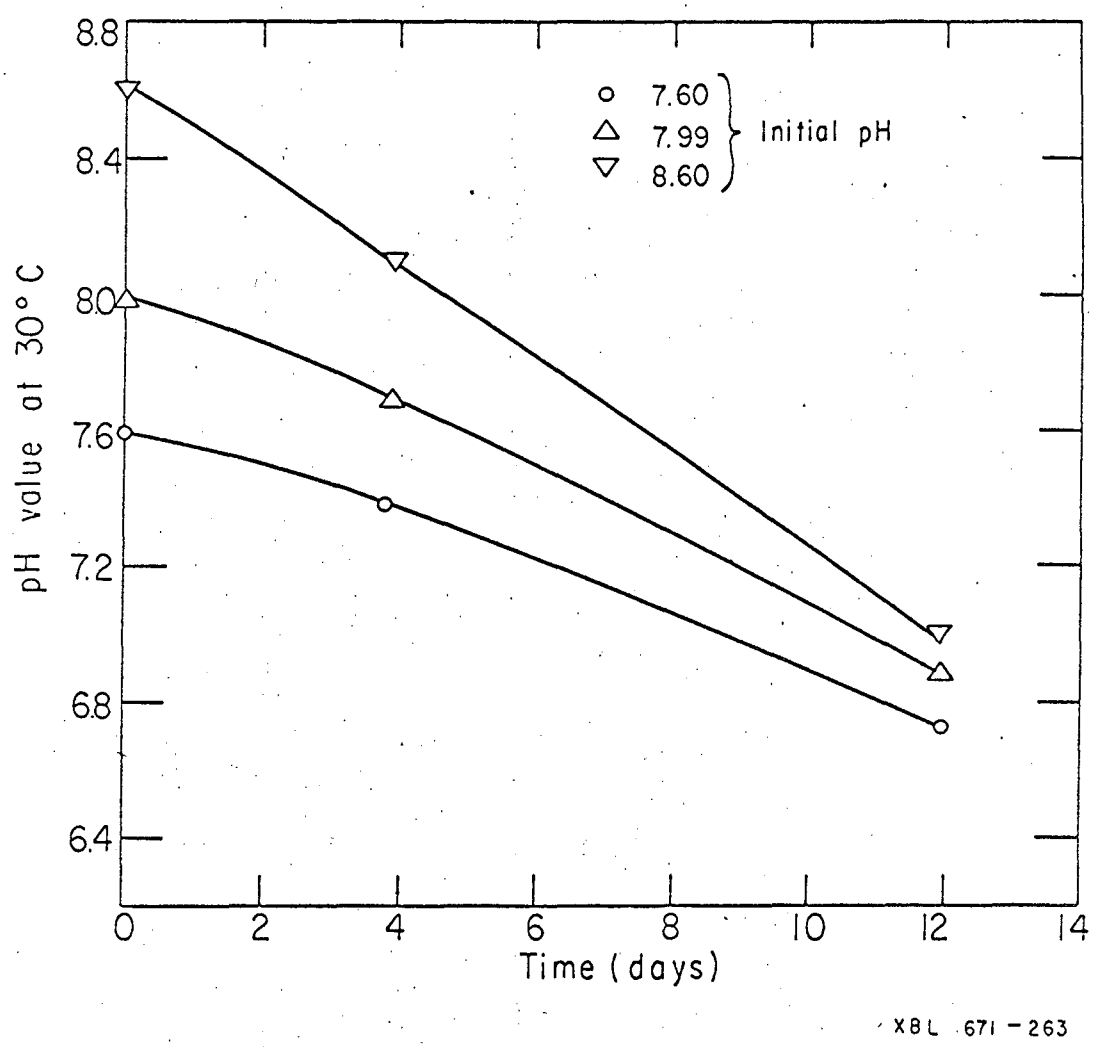

Fig. 22. pH value versus time.

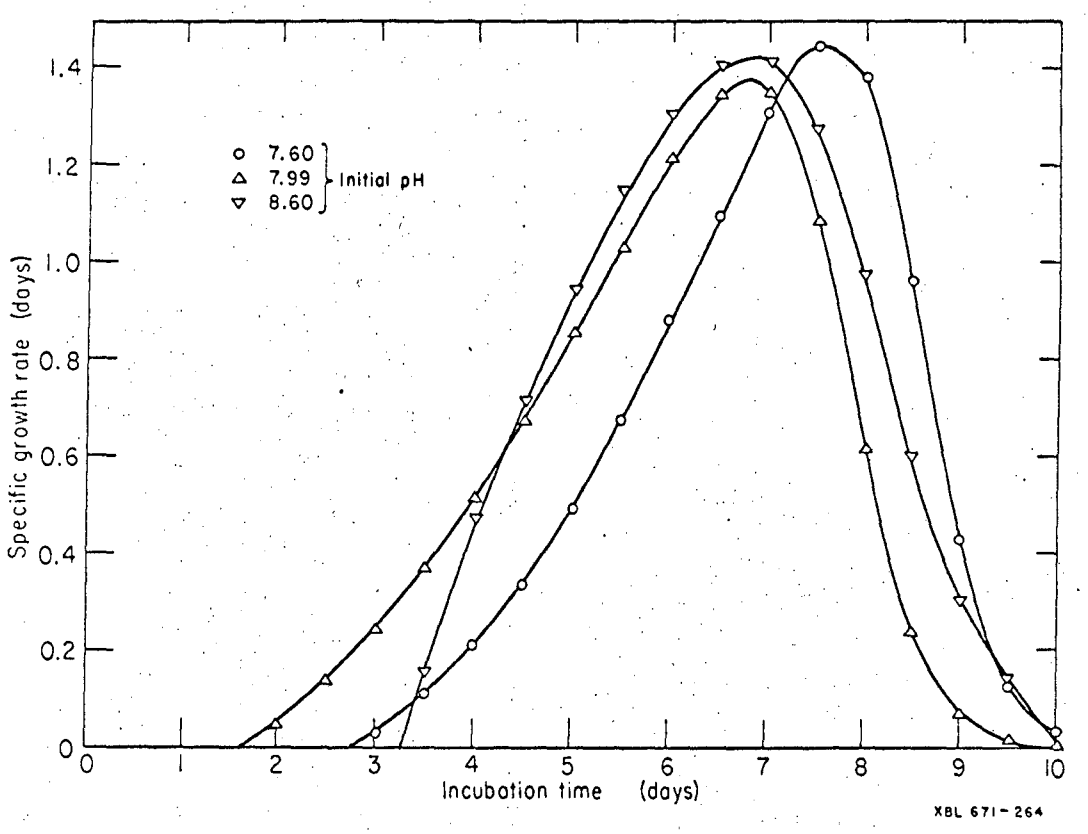

Fig. 23. Specific growth rate versus time.

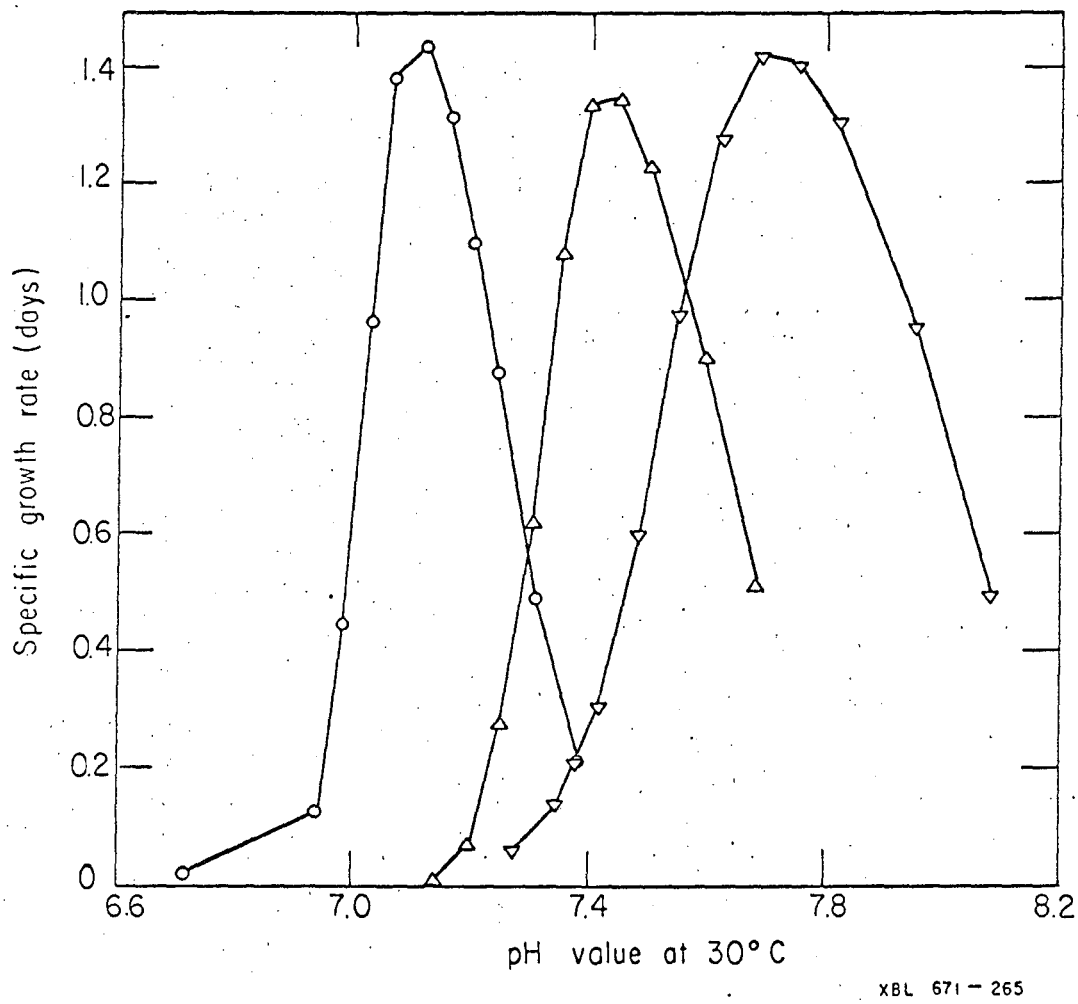

Fig. 24. Specific growth rate versus pH.

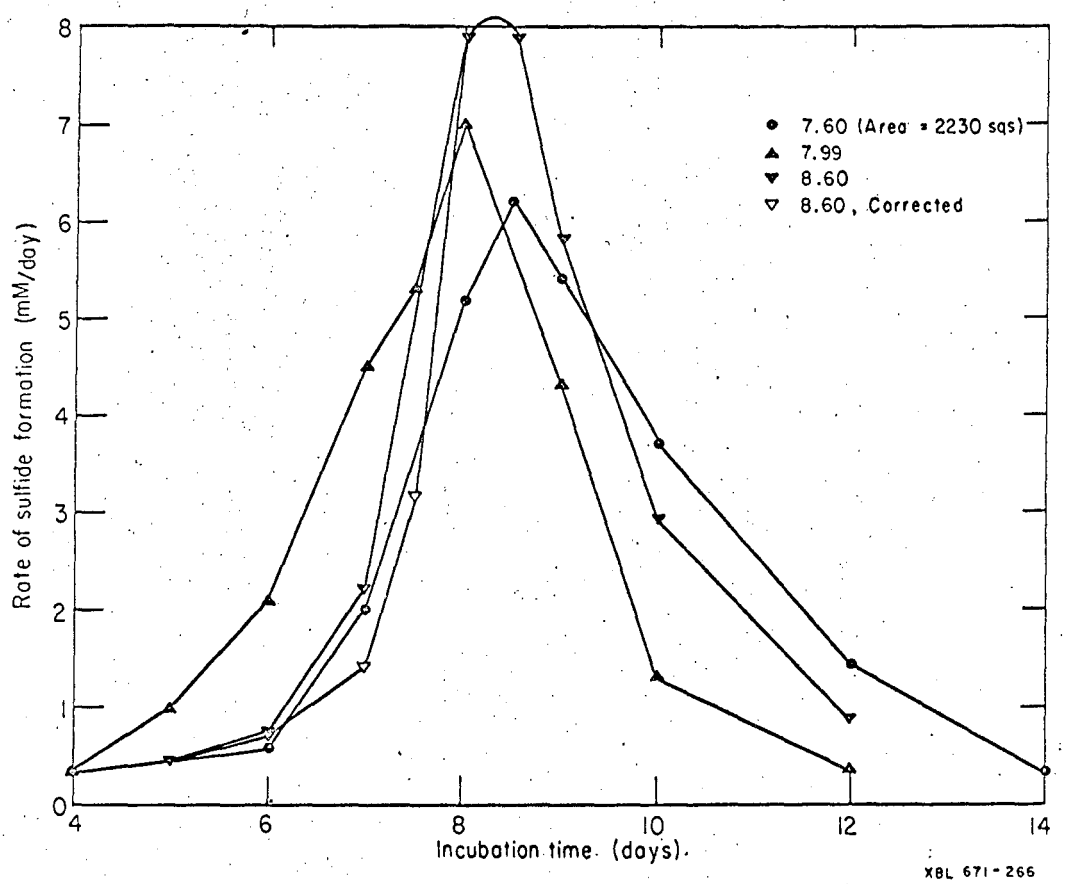

Fig. 25. Rate of sulfide formation versus incubation time.

versus time in Fig. 25. Sulfide production rates achieved somewhat higher values in the culture having an initial pH of 8.60, as shown in Fig. 25, and a slightly higher yield of sulfide was also obtained in that case, as shown in Fig. 21. The shorter lag phase obtained at an initial pH of 7.99 appeared to offer convenience in reducing required experimental time, and therefore Medium M was adjusted to an initial pH of 8.0 before use in all subsequent experiments.

7. Medium M

The preceding experiments with MacPherson's medium showed that several changes would improve growth and sulfate reduction by a salt tolerant strain of *Desulfovibrio*. The medium was therefore modified correspondingly for future work. This modified medium is designated as medium M throughout the remainder of this report. The changes in medium composition are summarized by a comparison of the original MacPherson's medium with medium M in Table XXVII. Medium M is probably still not completely optimal in all component concentrations for the strain of *Desulfovibrio* used here, because of the limited number of concentrations studied for each component of the medium, but the preceding experiments show that it is a good approximation to the optimal medium, with no single component strongly limiting growth or sulfate reduction at the chosen concentrations.

Table XXIII. Medium optimazation experiments: Coefficients of the generalized logistic equation corresponding to the growth and sulfide formation curves.

$$y = \frac{K}{1 + \exp(a_o + a_1 t_1 + a_2 t_1^2 + a_3 t_1^3 + a_4 t_1^4 + a_5 t_1^5)}, \quad t_1 = t - t_L$$

Data of table number	Variable	K	a_o/a_1	a_2/a_3	a_4/a_5	t_L	$P(\chi^2)$
I	cell concn.	1.0543×10^8 cells/ml	3.3528 -1.5118	- -	- -	0.0	> 70%
	sulfide	20.09mM	3.8967 -1.1234	- -	- -	0.0	50%
VIII	cell concn.	1.3699×10^8 cells/ml	3.6296 -1.7834	- -	- -	0.0	> 70%
	sulfide	21.33mM	3.5991 -1.0784	- -	- -	0.0	> 95%
XII	cell concn.	1.2483×10^8 cells/ml	6.9053 -2.5125	- -	- -	0.0	> 95%
	sulfide	24.01mM	6.4538 -2.3731	.2402 -.009275	- -	0.0	> 70%
XIII	cell concn.	1.5309×10^8 cells/ml	6.1428 -2.0897	- -	- -	0.0	> 70%
	sulfide	25.50mM	5.2535 -1.7001	.14071 -.004245	- -	0.0	> 50%
XIV	cell concn.	2.166×10^8 cells/ml	4.6671 -2.0485	.89492 -.40934	- -	0.5 days	> 10%
	sulfide	27.62mM	8.3043 -50269	1.1192 -.1387	.008788 -.0002223	0.5 days	> 98%

Table XXIII. (continued)

Data of table number	Variable	K	a_o/a_1	a_2/a_3	a_4/a_5	t_L	$P(X^2)$
XV	cell concn.	2.596×10^8 cells/ml	7.4853 -2.2743	- -	- -	0.0	> 85%
	sulfide	32.93mM	11.622 -.51167	.77709 -.05817	.0021179 -2.9676×10^{-5}	0.0	> 90%
XVI	cell concn.	2.197×10^8 cells/ml	4.6006 -1.6172	- -	- -	1.1 days	> 5%
	sulfide	28.33mM	4.5557 -1.0869	.015233 7.7657×10^{-5}	- -	1.1 days	> 5%
XVII	cell concn.	4.73×10^8 cells/ml	5.5022 -.7654	- -	- -	0.0	> 45%
	sulfide	31.55mM	21.9980 -10.3017	1.9084 -.13018	- -	0.0	> 30%
XX	cell	2.645×10^8 cells/ml	4.8654 -.2213	.1181 -.01944	- -	0.0	> 98%
	sulfide	32.59mM	.8330 -.02836	.01348 -.004701	- -	1.5	< 1%
XXI	cell	2.43×10^8 cells/ml	4.7915 .10016	$5.512 \quad 10^{-4}$ -.01306	- -	0.0	> 95%
	sulfide	32.12mM	.8371 -.5031	.2091 -.02112	- -	0.0	< 1%
XXII	cell concn.	2.586×10^8 cells/ml	4.8859 .01954	-.4002 -	-	2.0	> 80%

Table XXIV. Estimated concentrations and rates, initial pH = 7.60.

t Time (days)	pH	N Optical count (cells/ml)	μ Specific growth rate ($days^{-1}$)	$[S^{--}]$ sulfide (moles/ liter	$\frac{d[S^{--}]}{dt}$ Rate of sulfide moles/ liter day)	$\frac{1}{N}\frac{d[S^{--}]}{dt}$ Specific rate of sulfide formation (moles/cell day)
4.0	7.38	2.57×10^{6}	0.207	10.7	0.32	
4.5		2.94×10^{6}	0.335			
5.0	7.31	3.60×10^{6}	0.491	11.1		
5.5		4.82×10^{6}	0.674			
6.0	7.24	7.10×10^{6}	0.879	12.1	0.59	
6.5	7.20	1.16×10^{7}	1.099	12.2		
7.0	7.16	2.13×10^{7}	1.311	12.7	2.0	0.938
7.5	7.12	4.27×10^{7}	1.451	13.6		
8.0	7.07	8.77×10^{7}	1.380	15.8	5.2	0.593
8.5	7.03	1.60×10^{8}	0.962	18.2	6.2	0.388
9.0	6.98	2.25×10^{8}	0.424	21.8	5.4	0.240
9.5	6.94	2.55×10^{8}	0.122	24.2		
10.0	6.72	2.63×10^{8}	0.025	26.2	3.7	0.141
12.0		2.65×10^{8}	0	31.1	1.44	0.543
14.0		2.65×10^{8}	0	32.4	0.31	0.0117
18.0		2.65×10^{8}	0	33.3	0.14	0.0053

Table XXV. Estimated concentrations and rates, initial pH = 7.99.

t Time (Days)	pH	N Optical count (cells/ml)	μ Specific growth rate ($Days^{-1}$)	$[S^{--}]$ Sulfide concentration (moles/liter)	$\frac{d[S^{--}]}{dt}$ Rate of sulfide formation (moles/liter day)	$\frac{1}{N}\frac{d[S^{--}]}{dt}$ Specific rate of sulfide formation (moles/cell-day) $\times 10^{-13}$
3.0		2.09×10^{6}	0.247			
4.0	7.68	3.04×10^{6}	0.516	10.2	0.39	1.28
5.0	7.59	6.00×10^{6}	0.852	10.7	1.0	1.67
5.5		9.62×10^{6}	1.036			
6.0	7.50	1.69×10^{7}	1.213	12.1	2.1	1.24
6.5	7.45	3.21×10^{7}	1.343	13.1		
7.0	7.40	6.33×10^{7}	1.339	14.8	4.5	0.712
7.5	7.35	1.17×10^{8}	1.082	17.0	5.3	0.453
8.0	7.30	1.80×10^{8}	0.618	20.7	7.0	0.389
8.5	7.25	2.21×10^{8}	0.240	24.8		
9.0	7.20	2.37×10^{8}	0.068	28.0	4.3	0.181
9.5	7.14	2.41×10^{8}	0.015	29.7		
10.0	7.09	2.42×10^{8}	0.003	30.5	1.31	0.0541
11.0		2.43×10^{8}	0			
12.0	6.88	2.43×10^{8}	0		0.36	148
14.0		2.43×10^{8}	0		0.25	103

Table XXVI. Estimated concentrations and rates, initial pH = 8.60.

t Time (days)	pH	N Optical count (cells/ml)	μ Specific growth rate ($days^{-1}$)	$[S^{--}]$ sulfide (moles/ liter)	$\frac{d[S^{--}]}{dt}$ Rate of sulfide (moles/ liter day)	$\frac{1}{N}\frac{d[S^{--}]}{dt}$ Specific rate of sulfide formation (moles/cell day)
4.0	8.08	1.32×10^{6}	0.447	11.0	0.31	
4.5		1.76×10^{6}	0.713	11.2		2.35
5.0	7.95	2.67×10^{6}	0.947	11.4	0.42	1.57
5.5		4.52×10^{6}	1.147	11.7		
6.0	7.82	8.36×10^{6}	1.304	12.0	0.74	0.886
6.5	7.75	1.65×10^{7}	1.403	12.4		
7.0	7.69	3.35×10^{7}	1.411	13.0	2.2	0.656
7.5	7.62	6.60×10^{7}	1.276	13.8		
8.0	7.55	1.17×10^{8}	0.976	16.8	8.0	0.684
8.5	7.48	1.73×10^{8}	0.601	21.6	8.0	0.462
9.0	7.41	2.15×10^{8}	0.303	25.5	5.8	0.270
9.5	7.34	2.39×10^{8}	0.135	27.8		
10.0	7.27	2.50×10^{8}	0.057	29.5	2.9	0.116
11.0		2.57×10^{8}	0.010			
12.0	6.99	2.58×10^{8}	0.002		0.84	0.0326
14.0		2.59×10^{8}	0			

Table XXVII. Comparison of Mac Pherson's medium and medium M, concentration (grams/ℓ).

component	(Mac Pherson's medium)	(Medium M)
	.....	.....
Lactic acid	9.01	7.66
$CaCl_2$	0.056	0.111
$Mg\ 50_4 \cdot 7H_2O$	0.0616	0.123
Yeast extract	1.0	2.5
	pH = 7.2-7.4	pH = 8.0

The other components of the media are present in identical concentrations.

B. Effects of Mode of Cultivation

1. Effects of Sulfide Concentration, Mixing and pH Control

Inhibition by high sulfide concentrations has been postulated to explain reduced rates of growth and sulfate reduction in this work, as well as in other reports.[5,12] The hydrogen ion concentration was also shown to prevent initiation of growth at pH values below 7.0. Finally, sedimentation of some of the cells in old cultures in the polysaccharide gum formed on lactate medium has been observed in our experiments and by other workers.[8,9] This phenomenon may be partly responsible for the erratic counts obtained at high cell concentrations. Removal of cells would reduce sulfate reduction rates and decrease final yields of cells. It would also introduce an error in the kinetic analysis of the data. To minimize settling in bottle culture experiments, bottles had been shaken at daily intervals during experiments, but continuous stirring might give superior results. Three experiments were performed to test the effects of sulfide concentration, pH control, and mixing on batch culture kinetics. Two experiments were performed in the continuous reactor with mixing and with crude pH control (an electrode failure at the beginning of the experiment prevented use of the pH controller). In the third experiment, stripping with nitrogen was used to keep the sulfide concentration below 22 mM and sulfate reduction was followed by measuring sulfate concentrations gravimetrically. One deviation in technique from earlier experiments is that bottle experiments were started by rapidly filling the bottles with medium from the reactor that had been prepared by diluting an exponentially growing batch culture with fresh medium just before the start of the experiment. This technique is responsible for the shortened lag phases.

The results of the three experiments are given in Tables XXVIII, XXIX, and XXX. Coefficients of equations fitted to the data are given in Table XXXI. Batch growth data are compared in Fig. 26 and batch sulfide production curves (measured as decrease in sulfate concentration in the third experiment are plotted in Fig. 27. Sulfide concentrations in the third experiment are also shown in Fig. 27 by the inverted open tri-

angles denote sulfate removal for the same experiment. In both figures, the curves shown were calculated with the equations and coefficients given in Table XXXI. Note that the sulfide concentration in the second experiment was always about 10 mM or more greater than in the other two experiments at corresponding incubation times.

Figure 28 shows pH profiles and Fig. 29 shows profiles of redox potential for the three experiments. The irregularity of the pH profile for the reactor culture is due to the crude pH control exercised by periodic addition of sodium hydroxide and the removal of hydrogen on the third and fourth days. The redox potential profiles in Fig. 29 reflect the trends in sulfide concentration in the respective cultures. Sulfide was never below 12.8 mM in the second experiment, and the redox potential was accordingly low at a value of about -500 mV, showing only a slow decline with additional increase in sulfide concentration. In the other two experiments, redox potentials decreased steadily, approaching values of - 500 mV at about the same time that sulfide concentrations of about 12-16 mM were reached, leveling off afterwards.

Specific growth rates for the three experiments are plotted versus incubation time in Fig. 30. Rates of sulfide formation and specific rates of sulfide formation are shown plotted versus time in Figs. 31 and 32 for the three experiments. Specific growth rates under conditions of low sulfide concentration (circles and inverted triangles) were definitely higher than the rates obtained at high sulfide concentrations, as shown in Fig. 30. Note that the maximum specific growth rates obtained in the two experiments at low sulfide concentrations (2.33 $days^{-1}$ for reactor cultured and 2.47 $days^{-1}$ for bottle cultured) agreed well with the correlation in Fig. 17, which predicts a maximum specific growth rate of 2.36 $days^{-1}$ at 0.25% (w/v) yeast extract. Specific growth rates were also slightly higher and continued to slightly higher levels in the reactor cultured case (sulfide kept low, crude pH control, mixing) than in the experiment conducted in bottles at low sulfide concentrations. Specific rates of sulfate reduction, shown in Fig. 32, lead to similar conclusions

about the inhibitory effect of sulfide. Comparison of the maximum specific rates of sulfide formation with the values obtained in the yeast extract experiments shows fairly good agreement. Figure 19 predicts a value of 1.26×10^{-13} moles/cell-day and values of 1.21×10^{-13} moles/cell-day and 0.907×10^{-13} moles/cell-day were obtained in the two experiments at low sulfide concentrations discussed here. Improved rates were also obtained on mixing and control of pH, as is also apparent from Fig. 27.

Summarizing, sulfide was shown to be inhibitory at an initial concentration of 12.8 mM, and the combination of mixing and the control of pH and sulfide concentration was shown to give slightly improved cell yields, higher growth rates, and higher rates of sulfide formation than culturing in bottles. The inhibitory effects of sulfide have implications for the rates obtained in the pH experiments discussed earlier, in which initial sulfide concentrations were about 10 mM. Although the conclusions drawn there are still valid, the absolute values of rates of growth and sulfide formation are probably lower than they would have been at lower sulfide concentrations. Further evidence for inhibition in the pH experiments lies in the good agreement between the maximum specific growth rates measured in these experiments and the values obtained in the experiments on the effect of yeast extract. Also, the improved rates in the reactor suggest that comparison of results obtained in the experiments conducted in bottles with rates obtained in continuous culture may not be completely quantitative. Finally, comparison of the maximum specific growth rates obtained in the two experiments at low sulfide concentrations with those obtained in the yeast extract experiments show good agreement, and fair agreement with maximum specific sulfide formation rates.

2. Materials of Construction

During the course of continuous culture experiments, inhibition of growth was encountered and several possible causes were investigated by adding excess amounts of the suspected compounds to medium M and comparing batch growth of Desulfovibro in the test media with unmodified medium M.

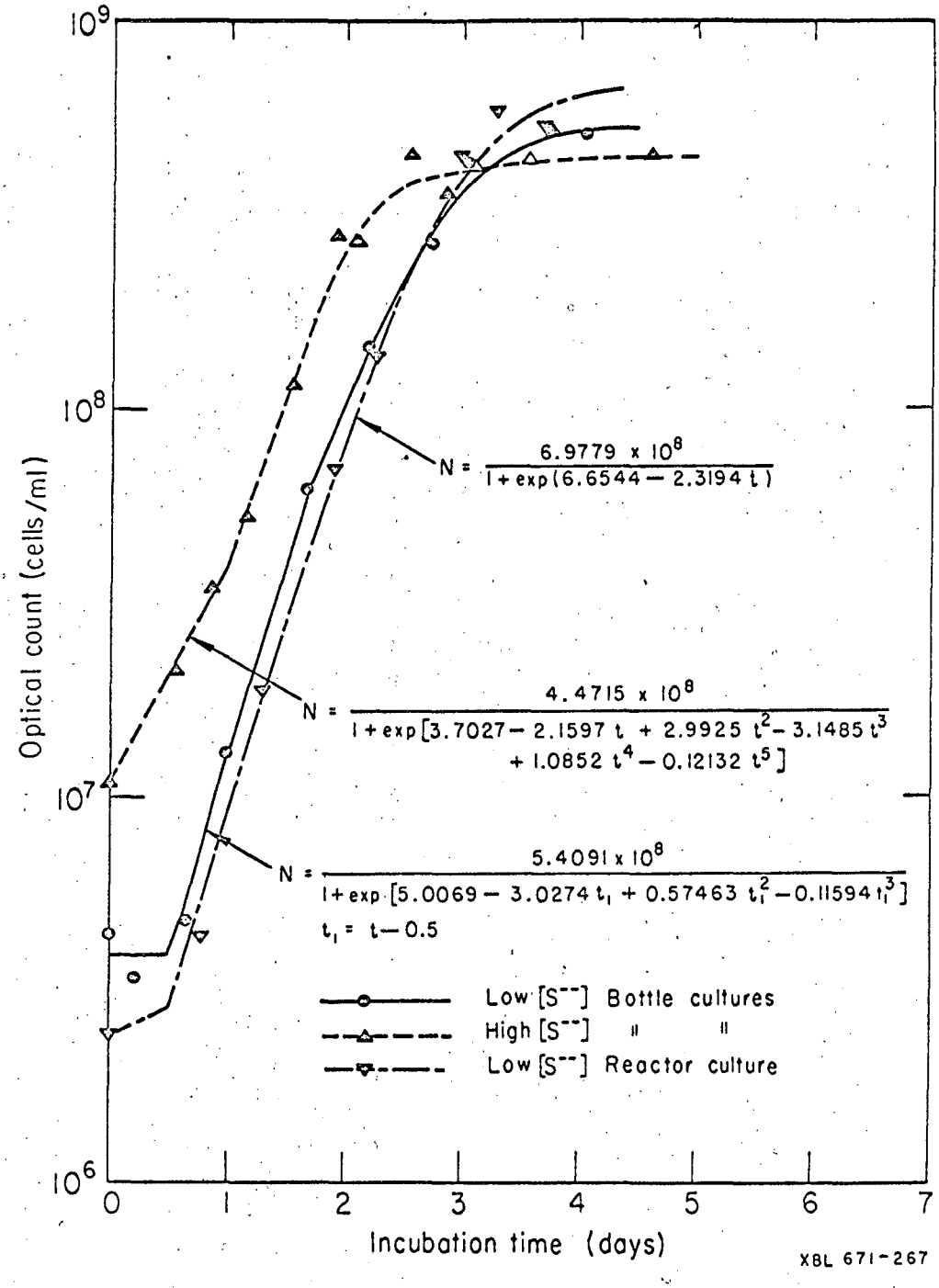

Fig. 26. Optical count versus incubation time.

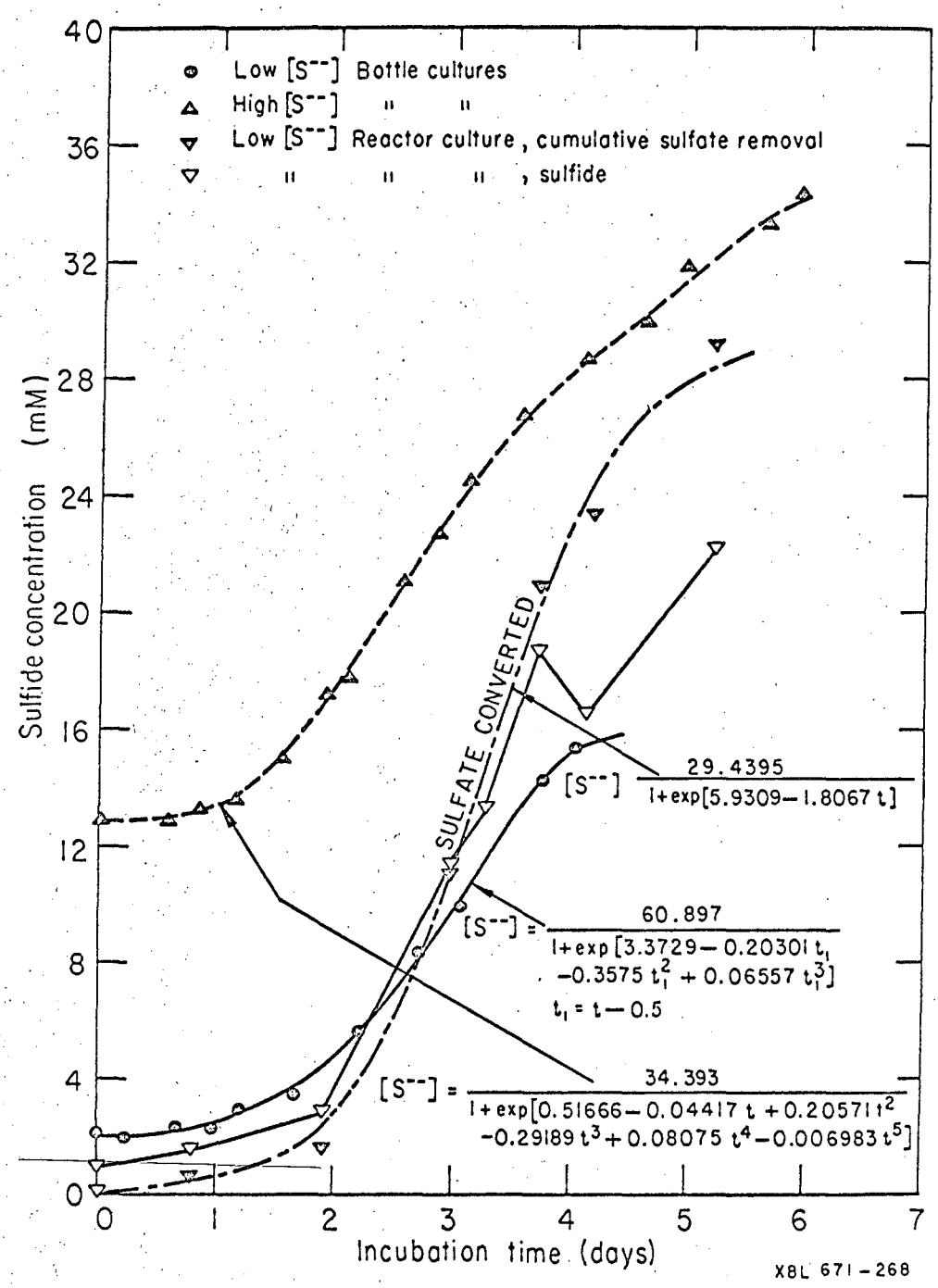

Fig. 27. Sulfide concentration versus incubation time.

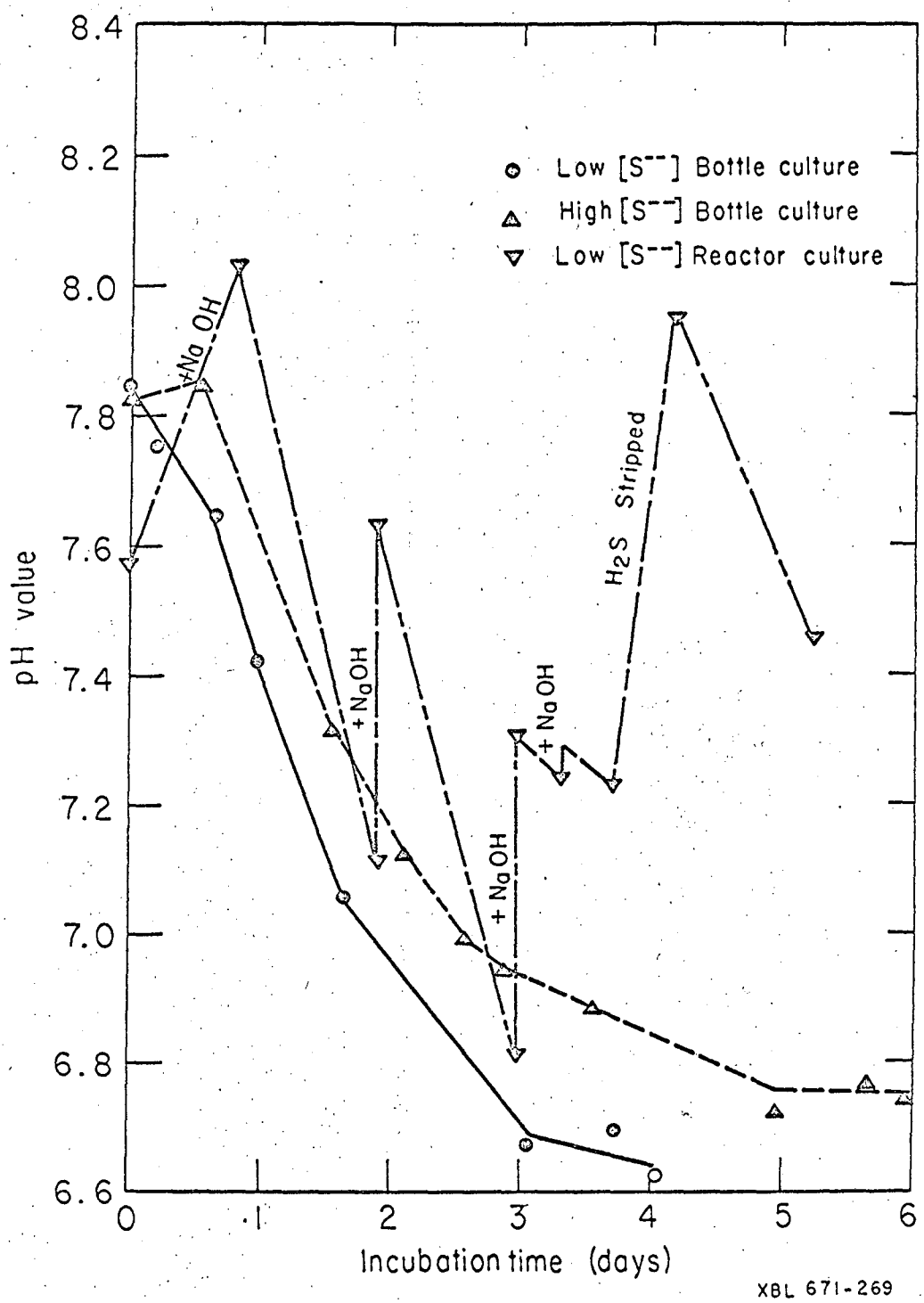

Fig. 28. pH versus incubation time.

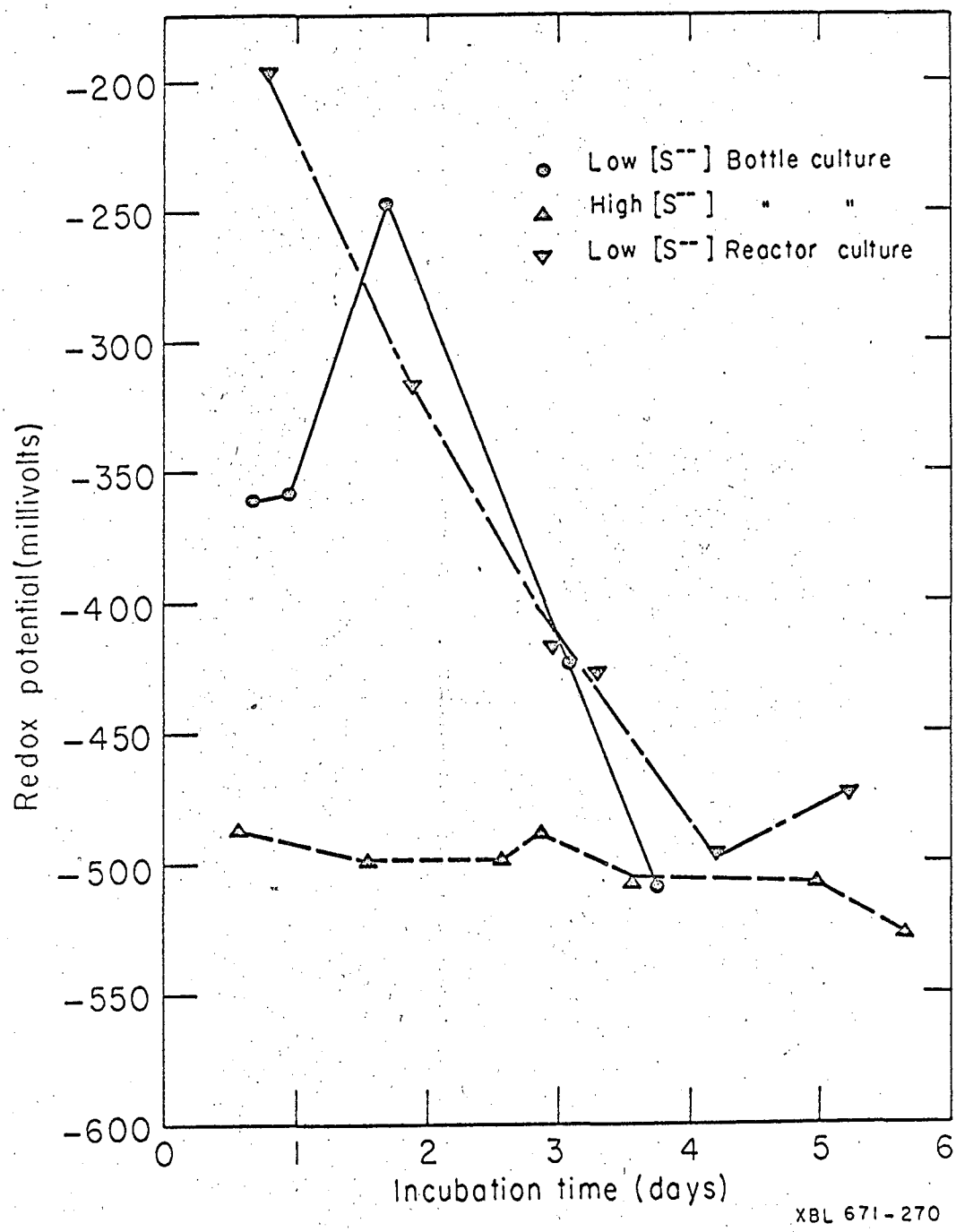

Fig. 29. Redox potential versus incubation time.

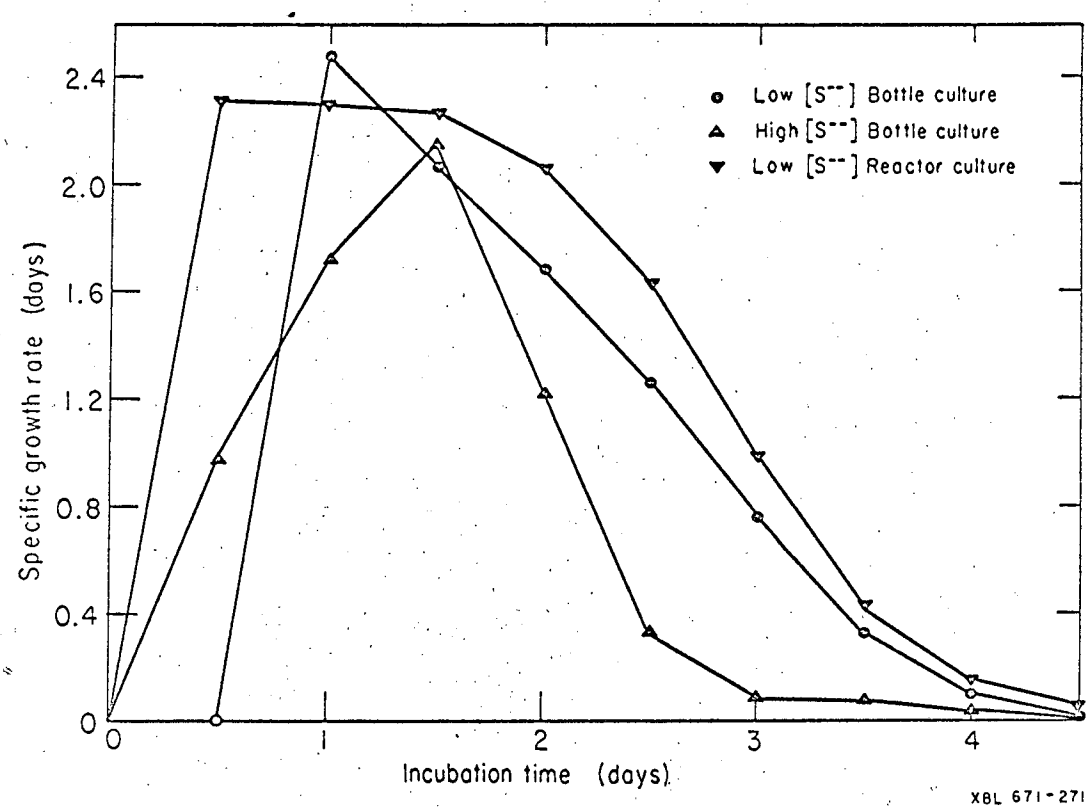

Fig. 30. Specific growth rate versus incubation time.

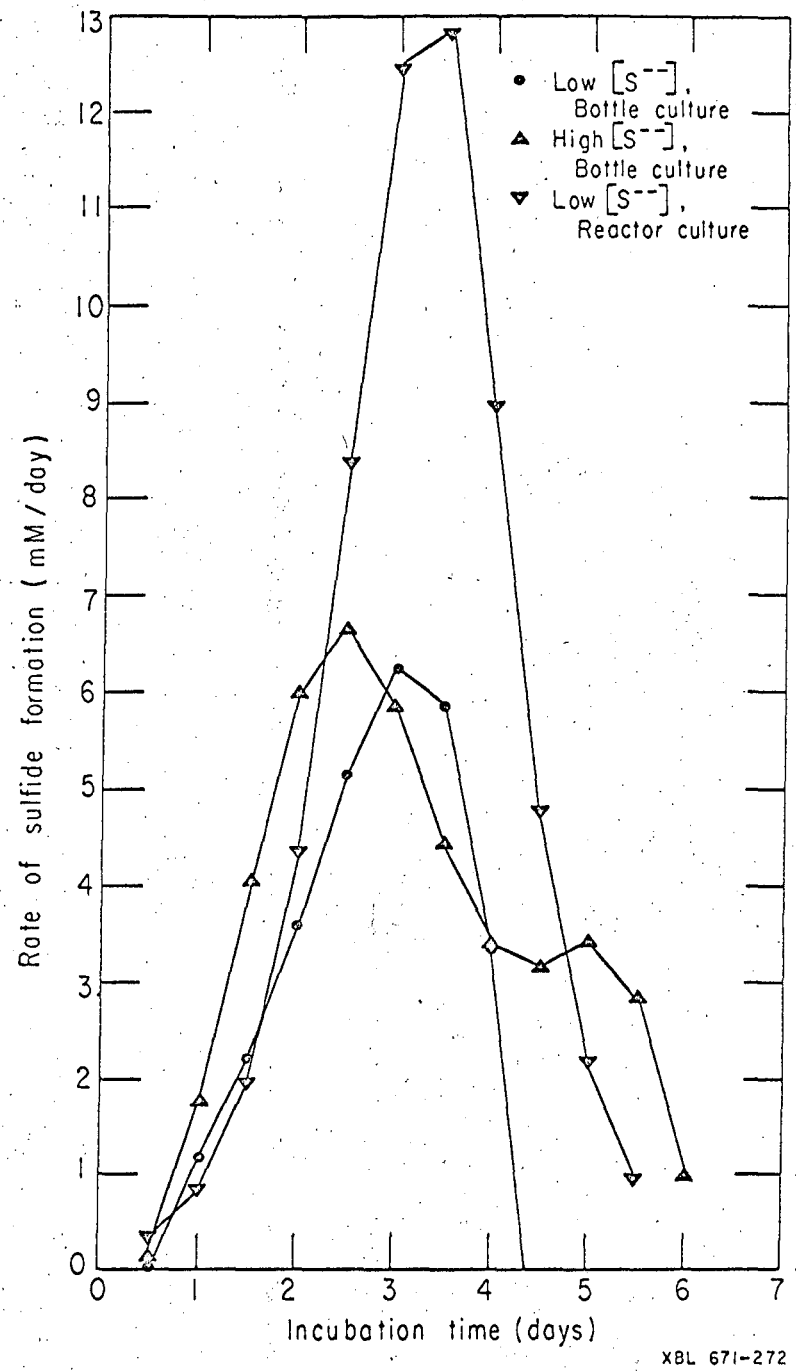

Fig. 31. Rate of sulfide formation versus incubation time.

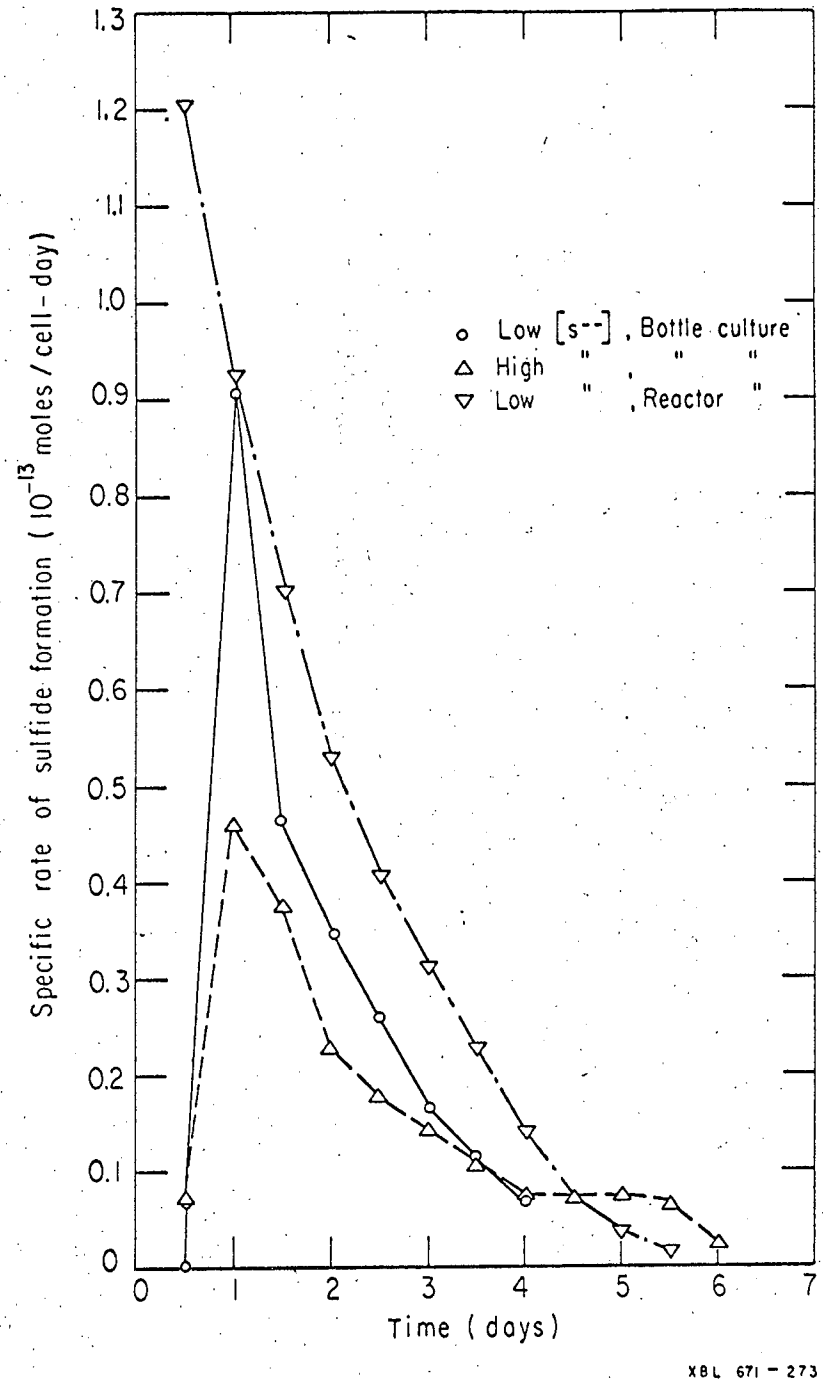

Fig. 32. Specific rate of sulfide formation versus incubation time.

Table XXVIII. Batch growth at low initial sulfide concentrations, bottle cultured.

Time (days)	Optical count (cells/ml)	Sulfide (mM)	pH (pH units)	Redox potential (millivolts)
0	4.40×10^{6}	2.09	7.85	-
0.2083	3.40×10^{6}	1.88	7.76	-
0.6667	4.80×10^{6}	2.25	7.65	-360
0.9792	1.30×10^{7}	2.20	7.43	-358
1.2083	-	2.94	-	-
1.6271	6.30×10^{7}	3.41	7.06	-246
2.2188	14.47×10^{7}	5.64	-	-
2.7292	26.30×10^{7}	8.34	-	-
3.0625	42.70×10^{7}	9.93	6.68	-448
3.7500	51.90×10^{7}	14.32	6.70	-510
4.0417	50.60×10^{7}	15.38	6.63	-

Table XXIX. Batch growth at high initial sulfide concentrations, bottle cultured.

Time (days)	Optical count (10^7 cells/ml)	Sulfide (millimoles/ liter)	pH (pH units)	Redox potential (millivolts)
0	1.08	12.85	7.83	-
0.5625	2.10	12.8_4	7.85	-486
0.8854	3.44	13.3_1	-	-
1.1667	5.30	13.4_7	-	-
1.5521	11.27	14.9_6	7.32	-498
1.9167	27.87	17.1_8	-	-
2.1042	26.90	17.7_1	7.13	-
2.5625	45.20	21.0_2	7.00	-498
2.8750	35.90	22.8_2	6.95	-478
3.1042	42.00	24.4_6	-	-
3.5729	44.27	26.7_5	6.89	-508
4.1146	-	28.6_4	-	-
4.6250	44.70	29.9_1	-	-
4.9583	-	31.8_2	6.73	-508
5.6458	-	33.3_6	6.78	-528
5.9375	-	34.2_6	6.75	-

Table XXX. Batch growth at four initial sulfide concentrations, reactor cultured.

Time (days)	Optical count (10^7 cells/ml)	Sulfide (milli-moles/liter)	Sulfate reduced (milli-moles/liter)	pH (pH units)	Redox potential (millivolts)
0	0.24	0.9	0.0	7.57	-
0.2604	0.55	-	-	-	-
0.7917	0.43	1.5	0.6	8.08	-198
1.2917	1.88	-	-	-	-
1.8958	6.98	2.8	1.4_4	7.10 → 7.63	-318
2.2708	13.76	-	-	-	-
2.9792	44.80	11.4	11.0	6.81 7.30	-418
3.2917	58.67	13.3	-	7.24	-428
3.7083	53.33	18.7	20.8_3	7.23	-
4.1667	43.67	16.5	23.2_8	7.95	-498
5.2083	36.00	22.2	29.0_6	7.45	-473

Table XXXI. Coefficients of growth and sulfide formation curves, made of cultivation experiments.

$$Y = Y_0 \quad t \leq t_L$$

$$Y = \frac{K}{1 + \exp[a_0 + a_1 t + a_2 t^2 + a_3 t^3 + a_4 t^4 + a_5 t^5]} \quad t > t_L$$

Data of table number	Y	K	a_o	a_1	a_2/a_4	a_3/a_5	T_L/Y_o	$P(X^2)$
XXVIII, bottle growth, low [5⁻]	cell concn.	5.4091×10^8	5.0669	-3.0274	.57463	-.11594	.5d 3.9×10^6	> 80%
	sulfide	60.8974	3.3729	-.20301	-.35753	.065571	.5d 1.985	> 80%
XXIX, bottle growth, high [5⁻]	cell concn.	4.4715×10^8	3.7027	-2.1597	2.9925 1.0852	-3.1485 -.12132	0 1.08×10^7	> 90%
	sulfide	34.3926	.51666	-.044170	.20571 .080748	-.29189 -.0069833	0 12.85	> 80%
XXX, reactor, low [5⁻]	cell concn.	6.9779×10^8	6.6544	-2.3194	- -	- -	0 2.4×10^6	> 75%
	sulfide	29.4395	5.9309	-1.8067	- -	- -	0 .01	-

The results are shown in Table XXXII. Cured epoxy putty added as small (0.8 cm) balls did not affect growth or morphology, while a one hundred-fold excess of the antifoam agent, Alkaterge C (Commerical Solvents, Terre Haute, Ind.), reduced growth only slightly, and did not alter morphology. Nickel powder, sterilized by dry heat and suspended in a culture inhibited growth and caused a change in cell morphology. The cooling coils in the nutrient supply bottles in the continuous culture apparatus, which had been nickel-plated, were replaced with stainless steel coils.

C. Continuous Culture Experiments

Continuous culture of sulfate-reducing bacteria is of value in either the study of their kinetics or the development of an industrial process using them. In the kinetic study, the continuous culture technique is valuable because greater accuracy can be obtained by the use of repetitive measurements on a steady-state culture and by computation of specific rates of growth and product formation without depending on the use of estimated slopes of experimental curves. In industrial applications of bacterial processes, the technique is important because no means exists of predicting with certainty the behavior of a continuous culture from batch culture data.

Steady-state and unsteady state continuous culture data were obtained using medium M and the reactor system described in the methods section for comparison with batch culture results. These results will now be described.

1. Maximum Growth Rate Experiment

An experiment was designed to measure the maximum growth rate of *Desulfovibrio* in both batch and continuous culture in medium M. The experiment was performed in the continuous reactor following the customary procedure outlined in the methods section. In the batch culture phase of the experiment, the reactor was filled with sterile medium M and inoculated with a young culture of *Desulfovibrio*. Cell concentrations were monitored

XXXII. Effects of antifoam agent and materials of contruction of reactor system

Material Tested	Growth after 2 days	Cell morphology
Control	+ + + + +	Normal
+ Nickel powder, 2g/ℓ	+ +	Smaller
+ Cured epoxy putty	+ + + + +	Normal
+ Alkaterage C (autoclaved separately), 5ml/ℓ	+ + + +	Normal

after exponential growth had begun. The reactor feed was off until a cell concentration of about 3.5×10^7 cells/ml was reached. At that time, the feed of medium M to the reactor was begun at a rate of 5.86 ml/min, corresponding to a dilution rate of 3.52 $days^{-1}$. The results are shown in Table XXXIII and Fig. 33. The high dilution rate caused washout of the cells and it was possible to determine the growth rates in the two periods from the following equations:

Batch growth period

$$\frac{dN}{dt} = \mu N$$

$$\ln\left(\frac{N}{N_o}\right) = \mu (t) \qquad (3)$$

Wash-out period

$$\frac{dN}{dt} = (\mu - D) N$$

$$\ln \left(\frac{N}{N^*}\right) = (\mu - D)(t - t^*) \qquad (4)$$

where t = time since end of lag phase

t^* = time at which feed to reactor was started

= specific growth rate

D = dilution rate during wash-out

N = cell concentration at time t

N_o = cell concentration at the end of the lag phase

N^* = cell concentration at beginning of wash-out

The foregoing equations depend on the assumption that the specific growth rate was constant. The growth rate would have been constant and at its maximum value provided that the cells were adapted to the medium and that the cell concentration was low enough so that the cells did not cause much change in their environment. Both conditions were met. The maximum cell concentrations attained in the experiment was less than 5×10^7 cells/ml, which is only about 10% of the final cell yield obtained with

Table XXXIII. Results of maximum growth rate experiment.

Rate experiment time	Optical count (cells/ml)	Reactor feed rate (ml/min)	Dilution rate ($days^{-1}$)
0	5.45×10^6	0	
4.5	7.78		
7.5	10.10	0	
20.5	30.30	0	
21.5	-	5.86	3.52
25.5	38.40	"	"
28.5	25.50	"	"
32.5	25.20	"	"
44.0	16.60	"	"
50.5	15.10	"	"
56.0	15.40	"	"

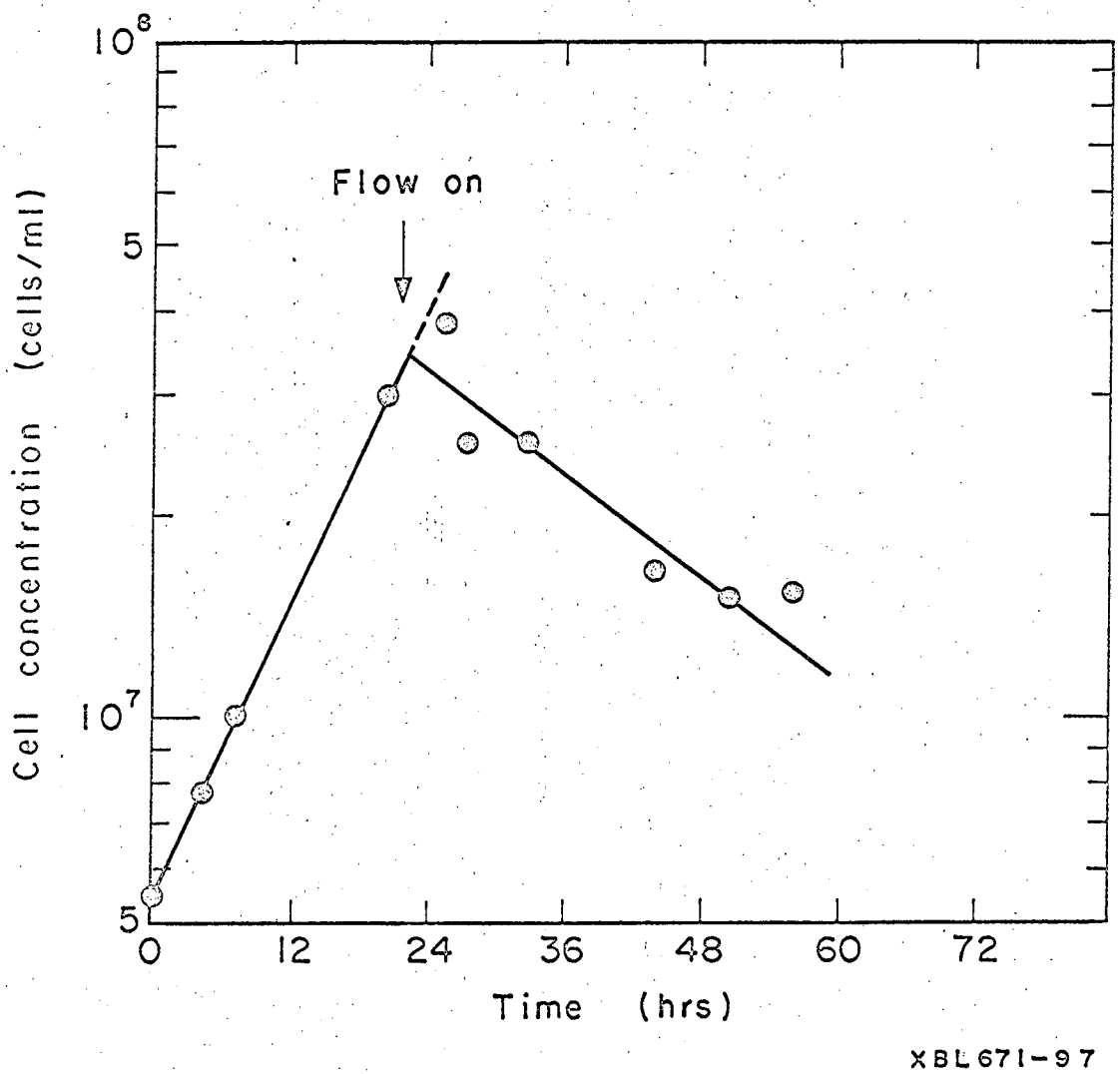

Fig. 33. Washout experiment to determine maximum growth rate.

medium M. Thus the kinetic properties of the cells' environment should not change much during the experiment, and the use of an exponentially growing culture eliminated the lag phase.

Both Eq. (3) for batch culture and Eq. (4) for wash-out predict that semi-logarithmic plots of cell concentration versus time should be linear with slopes of μ and (μ-D) respectively. Figure 33 is a semi-logarithmic plot of the data. Lines were drawn through the data for both portions of the experiment. The growth rates were computed from the slopes of the lines representing the two periods of the experiment. These growth rates are as follows:

μ_B = specific growth rate during batch growth phase
= 2.02 days^{-1}

μ_w = specific growth rate during wash-out phase
= 3.52 days^{-1} - 0.71 days^{-1}
= 2.81 days^{-1}

Thus the growth rate calculated from the wash-out experiment is 39% greater than the value for batch growth on the same medium, and neither agrees well with the value of 2.36 days^{-1} obtained in earlier batch experiments. An explanation could be based on the hypothesis that during wash-out, a limiting factor that had been quickly consumed during batch growth is present in the feed and allows a higher growth rate. However, such a hypothesis is not consistent with the observations that the growth rate was constant during the batch phase, when the cell concentration varied from 5.4×10^6/ml to more than 3.0×10^7 cells/ml, and second, that the cell concentration during the wash-out measurement was greater than 1.5×10^7 cells/ml, or nearly three times as large as the cell concentration at the beginning of the batch measurements. The constancy of the growth rate during batch culture suggests that any limiting factors could be acting only at higher or lower cell concentrations, i.e., greater or lesser degrees of nutrient consumption than were observed. The concentration of any hypothesized limiting factor during the wash-out portion

should have always been within the range of the values encountered during the batch experiment. Thus the growth rates should have been the same under both conditions.

A more plausible explanation is that a portion of the cells stick to the walls of the reactor and that during the period of falling cell concentration in the wash-out phase, some of the cells on the walls are resuspended and contribute to a higher cell count and thus an apparently higher growth rate. Although no visible wall growth developed during this experiment, at low dilution rates, it was common for an opaque greenish-black film of cells and precipitated ferrous sulfide to coat parts of the walls of the reactor after long periods of continuous operation at low feed rates. Problems of wall growth are not uncommon. Contois suspended small rubber disks in his reactor to prevent wall growth from forming.[13] W. D. Maxon has indicated that wall growth occurs in many industrial fermentations.[14] Munson and Bridges found that prototrophic revertants of E. coli WP2 could "take-over" a continuous culture because the revertants could stick to the walls.[5] In most of their work, the wall growth was sparse enough that it could not be seen unless the reactor was emptied.

The higher apparent growth rate observed during wash-out could be explained by the hypothesis that some of the cells stick to the walls of the reactor and that some of the cells formed by division of the cells attached to the wall are resuspended in the solution. The reactor will not wash-out as long as some cells remain attached to the wall. Because the mechanism and kinetics of adsorption of the bacteria to the wall is unknown, the simple hypothesis that the concentration on the wall is directly proportional to the concentration in the solution will be assumed. Then as shown in Appendix IV, the following equations would apply to the wash-out phase:

$$N_w = k\,N \tag{5}$$

$$\ln\left(\frac{N}{N_o}\right) = (\mu_{ap} - D)\,t \tag{6}$$

$$\mu_{ap} = \mu(1 + Ak/V) \tag{7}$$

Applying Eq. (7) to the wash-out phase, a value of 0.768 cm was obtained for k, which would predict from Eq. (5) that the reactor wall would be about 75% covered by a monolayer of cells at the maximum cell concentration obtained, which would not be unreasonable.

The original purpose of this experiment was to determine tha maximum growth rate under conditions of both batch and continuous cultivation and to show agreement between the two methods. Instead of agreement, a higher apparent growth rate was observed during wash-out conditions. Wall growth offers one explanation for the results and the possible effects of wall growth on the results of other continuous culture measurement will be discussed in the next section.

2. Steady-State Continuous Culture

Continuous culture kinetic data were obtained at five different growth rates by adjusting the flow rate of medium to the reactor to a desired value and monitoring cell concentration, sulfide, and other variables until constant values were obtained, or until at least 3 1/2 mean residence times had elapsed at constant feed rate and growth conditions. As in earlier experiments, 30°C was the cultivation temperature.

Cell concentration versus time is shown in Fig. 34 for the unsteady-state portion of a continuous culture experiment conducted at a dilution rate of 1.07 $days^{-1}$, and the data are listed in Table XXXIV. The reactor had been sterilized, rinsed, filled with sterile medium and inoculated with a culture of Desulfovibrio. The reactor was operated as a batch reactor until the culture was well into the exponential phase. The reactor was then partly emptied, refilled with fresh medium, and flow to the reactor begun at a rate of 1.85 ml/min. Flow slowed down slightly after 22 hrs because of replacement of worn tubing in the finger pumps, giving the slight inflection in the curve after 22 hrs. Steady-state values of variables were calculated as the averages of values observed at 68, 75, and 93.5 hrs after the initiation of the feed to the reactor and are shown in Table XXXV along with steady-state values obtained at four other reactor feed rates by similar techniques, with the exception that the

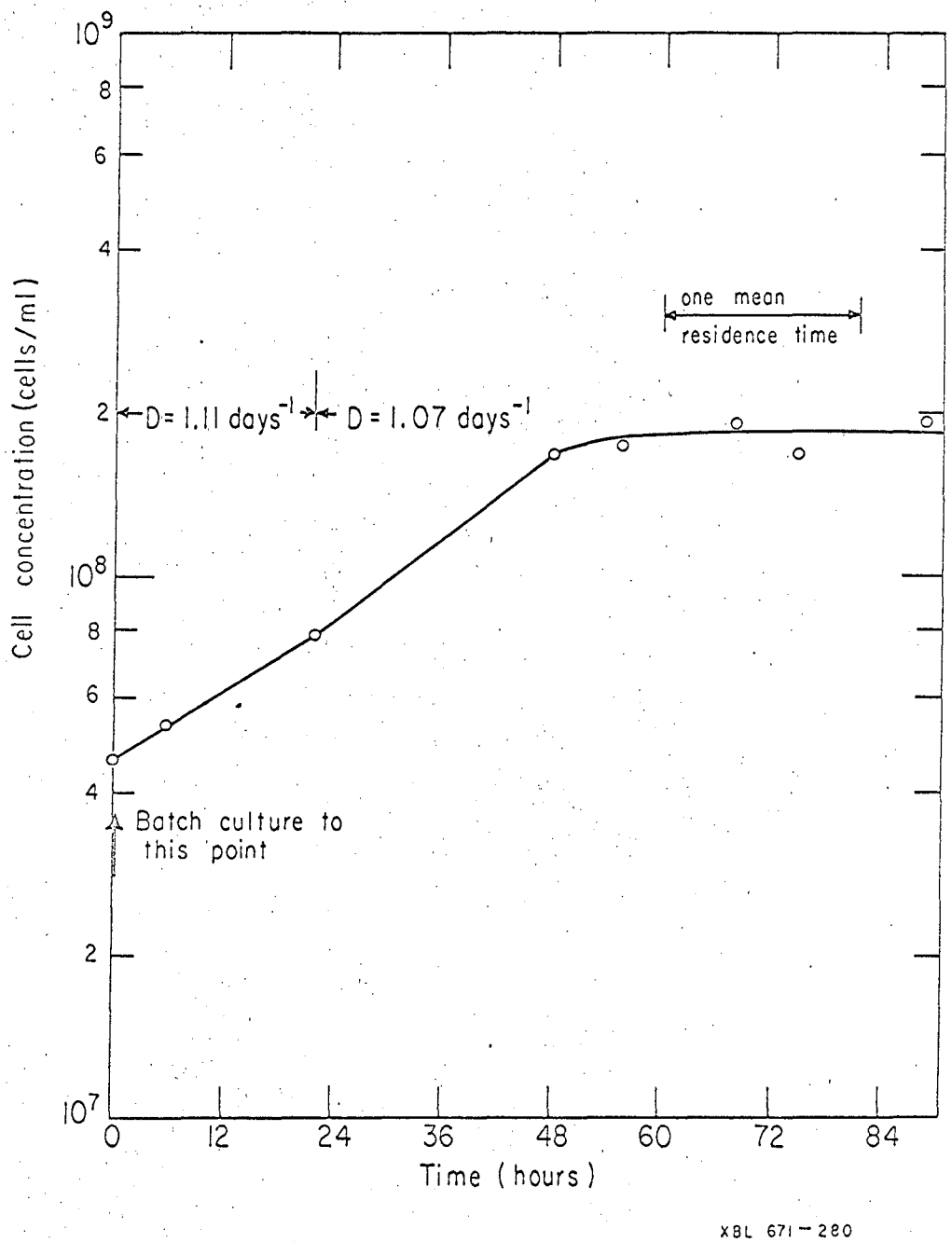

Fig. 34. Approach to the steady-state in continuous culture.

Table XXXIV. Data of a typical continuous culture experiment.

Time (hrs)	Cell count (cells/ml)	Dilution rate ($days^{-1}$)	Sulfide concentration (mM/liter)	EH (milli-volts)	pH
0	4.6×10^7	1.11	-	-	7.49
6	5.25 "	"	2.1	-380.	7.55
22	7.83 "	"	2.5	-380.	7.92
48.5	1.68×10^8	1.07	-	-	-
53.5	1.75 "	"	2.3	-460.	-
68.0	1.93 "	"	7.5	-560.	7.75
75.0	1.70 "	"	7.6	-540.	7.80
93.5	1.95 "	"	8.7	-	-

Table XXXV. Steady-state continuous culture data.

Date	Dilution rate ($days^{-1}$)	e_R*	cell count (10^7 cells/ml)	Dry weight concentration (g/l)	Mean cell dry weight (10^{-12} g/cell)	Feed sulfate concentration (mM/liter)	Reactor sulfate concentration (mM/liter)	Specific rate of sulfate reduction (mM/cell-day)	Sulfide concentration (mM/liter)	pH
11/4/64	0.130	3.5	31.9	0.395	1.24	31.5	0.2	1.27×10^{-11}	17.2	7.8
10/8/64	0.296	4.2	32.6	0.195	0.60	31.5	5.2	2.39 "	15.5	8.2
9/8/64	0.695	5.4	18.4	0.172	0.94	30.3	19.9	3.94 "	8.2	-
12/31/65	1.07	3.3	18.3	0.228	1.25	30.9	-	4.56 "	7.9	7.80
1/7/66	1.53	6.3	5.5	0.09	1.64	30.9	27.8	8.65 "	7.0	7.80

*Number of mean residence times to reach steady-state.

values obtained at the three lowest dilution rates were made in a single run in order of decreasing dilution rate. A fourth set of data (D = 0.387 $days^{-1}$) taken in the same series of runs was not included in Table XXXIV or in the kinetic analysis because the sample was taken prematurely, before a steady-state had been reached.

In addition to averaged optical counts and sulfide concentration, Table XXXV lists values of cell dry weight concentrations, sulfate concentration, number of mean residence times at constant flow rate prior to final sampling, and specific rates of sulfate reduction. Data at the first three growth rates in Table XXXV were obtained with the early version of the continuous culture apparatus; data at the two highest dilution rates were obtained at controlled pH with the improved continuous reactor system described in the methods section. Sulfate formation rates were calculated from measured sulfate concentrations in the steady-state reactor culture and the reactor feed using the following equation:

$$\left(\begin{array}{l}\text{specific rate of}\\ \text{sulfate reduction}\end{array}\right) = \frac{((SO_4^{--})_{feed} - (SO_4^{--})_{reactor})\ D}{N} \qquad (8)$$

= rate of sulfate reduction per cell per unit time

where D = dilution rate

The data measured at a dilution rate of 1.07 $days^{-1}$ did not include a reliable value of sulfate concentration. Therefore, sulfate reduced was equated to the concentration of sulfide produced by the culture in calculating the specific sulfate reduction rate in that case.

A correlation of continuous data is shown in Fig. 35, a graph of average cell mass versus specific growth rate. At specific growth rates greater than 0.29 $days^{-1}$, the average dry cell weight is a linear function of specific growth rate. Similar correlations of dry cell weight with specific growth rate have been observed by others using other bacteria.[16,17,18] The point of lowest specific growth rate deviates widely from the correlation. It is our opinion that sulfate, which is directly coupled to

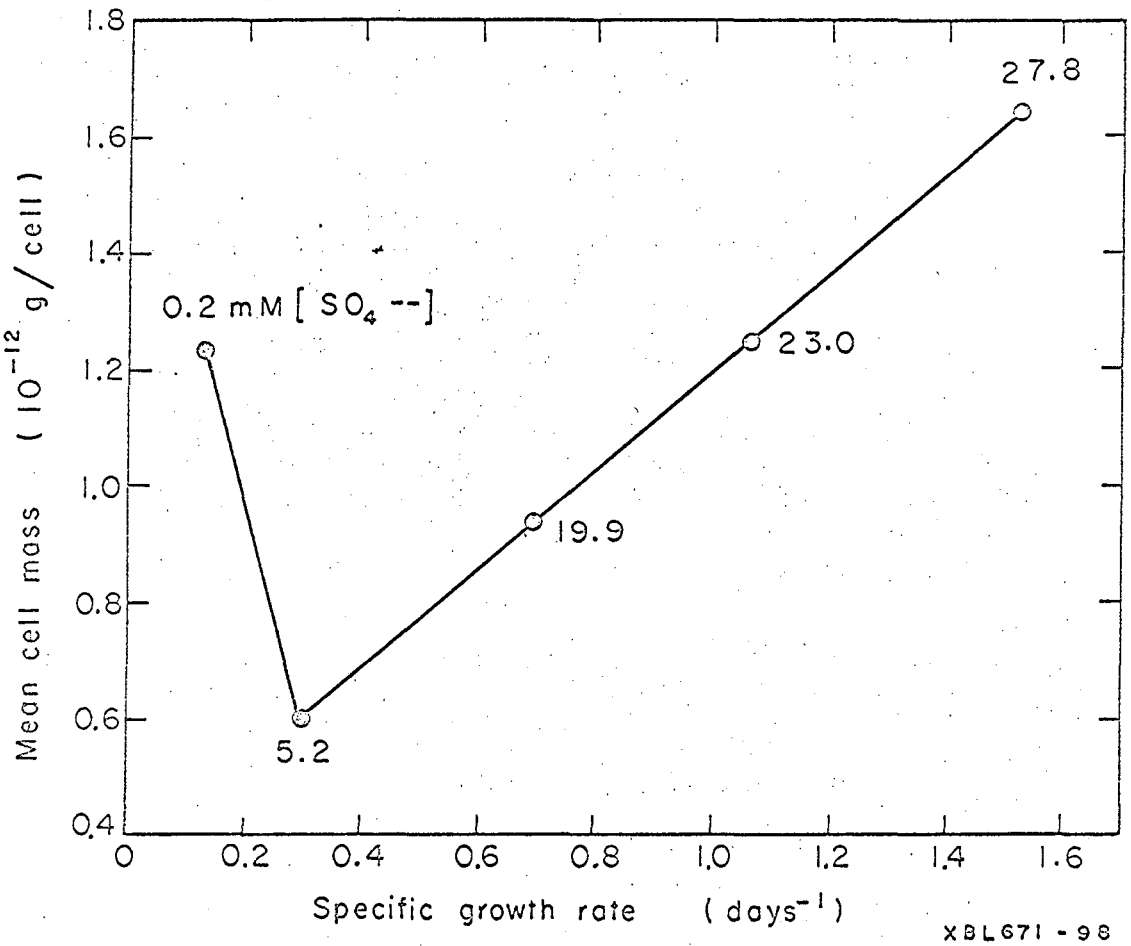

Fig. 35. Mean cell mass versus specific growth rate in continuous culture.

energy production, may be limiting cell growth at the lowest specific growth rate and that accumulation of carbon reserve material is responsible for the large increase in mean cell dry weight. Herbert[16] and Ecker and Schaechter[18] have shown that nitrogen-limited cultures accumulate carbon as reserve material at low growth rates, giving results similar to Fig. 35. At higher specific growth rates, some other substrate is probably limiting growth. Also, endogeneous metabolism is probably an important factor at the lower growth rates.

3. Effect of Wall Growth

At the steady-state in continuous culture, the specific growth rate is equal to the dilution rate provided that the reactor is perfectly mixed. With wall growth of the type hypothesized in Sec. C.1, the specific growth rate would be less than the dilution rate under steady-state conditions. Wall growth of the type hypothesized in Sec. C.1 would affect observed rates of sulfate reduction in addition to affecting growth rates. The correction factor is the same for both the specific growth rate and the specific rate of sulfate reduction and derives from the greater number of cells in the reactor than is predicted by the product of the reactor volume and the cell concentration in the effluent. It is of interest to assess the possible error in the present experiments due to wall growth. The results of the preceding wash-out experiments may be employed for this purpose. The apparent number of cells, η, in a perfectly mixed and homogeneous reactor is as follows:

$$\eta = V N \tag{9}$$

In a reactor with wall growth following Eq. (5), a term must be added for cells adhering to the walls.

$$\eta_T = V N + A k N$$
$$= (V + A k) N$$

where V = reactor volume

A = surface area of reactor in contact with culture

k = sticking coefficient

A correction factor η/η_T may be defined as the ratio of the apparent cell concentration in absence of wall growth to that with wall growth for a given reactor. Combining Eqs. (9) and (10) gives:

$$\eta/\eta_T = \frac{V\,N}{(V + A\,k)\,N} = \frac{1}{1 + A\,k/V} \tag{11}$$

For this system, it is assumed that $k = 0.77$ cm, as determined from the wash-out experiments described previously. Therefore for the reactor used in these studies with $A = 1200\ cm^2$ and $V = 2400\ cm^3$, $A\,k/V \doteq 0.384$, and the correction factor becomes

$$\eta/\eta_T = \frac{1}{1.384} = 0.72 \tag{12}$$

Apparent specific rates of growth and sulfate reduction deduced from the experimental data were corrected by the factor 0.72 from Eq. (12), and are compared to the apparent values in Table XXXVI. The correction factor is somewhat uncertain, because the hypothesized wall growth equation has not been tested by experiment. In view of the relatively small estimated effect of wall growth in relation to the various uncertainties involved in development of the correction and of other experimental factors it was decided to neglect wall growth in further treatment of the experimental results.

Table XXXVI. Specific growth rate and specific rate of sulfate reduction corrected for wall growth.

Dilution rate ($days^{-1}$)	Specific growth rate ($days^{-1}$)	Specific rate of sulfate reduction (mM/cell/day)	Corrected specific rate of sulfate reduction (mM/cell/day)
0.130	0.094	1.27×10^{-11}	0.92×10^{-11}
0.296	0.21	2.39 "	1.7 "
0.695	0.50	3.94 "	2.8 "
1.07	0.77	4.56 "	3.3 "
1.53	1.11	8.65 "	6.3 "

D. Kinetic Analysis

In this section, the batch and continuous data discussed in the preceding sections are compared and correlated where possible. The correlations are useful in design of systems employing sulfate-reducing bacteria. In addition, further interpretation of the experimental results is possible in some cases.

Figure 36 shows a correlation of cell yield versus specific growth rate for batch and continuous culture data. Cell yield is defined as the cell concentration at the given specific growth rate minus the initial cell concentration for batch cultures, and as the prevailing cell concentration in continuous culture. To produce a given cell ~~yield~~ yield, corresponding amounts of nutrients must be consumed, and metabolic products produced. Regardless of whether the rate of cell growth is limited by concentrations of required nutrients or of inhibitory products or both, the rate of growth should therefore be related to the cell yield produced in a given growth medium, because all changes in the concentrations of nutrients and inhibitory products result from cell growth. Data from any one run seems to correlate well by this method, but the results of different experiments are different from one another although similar in nature. Failure of the data from different runs to correlate with one another may be caused by differences in variables such as mixing, pH control, and sulfide concentration. Also, continuous and batch data may not necessarily correlate with one another because of the differences in the cell age distributions resulting from the two different means of culture.

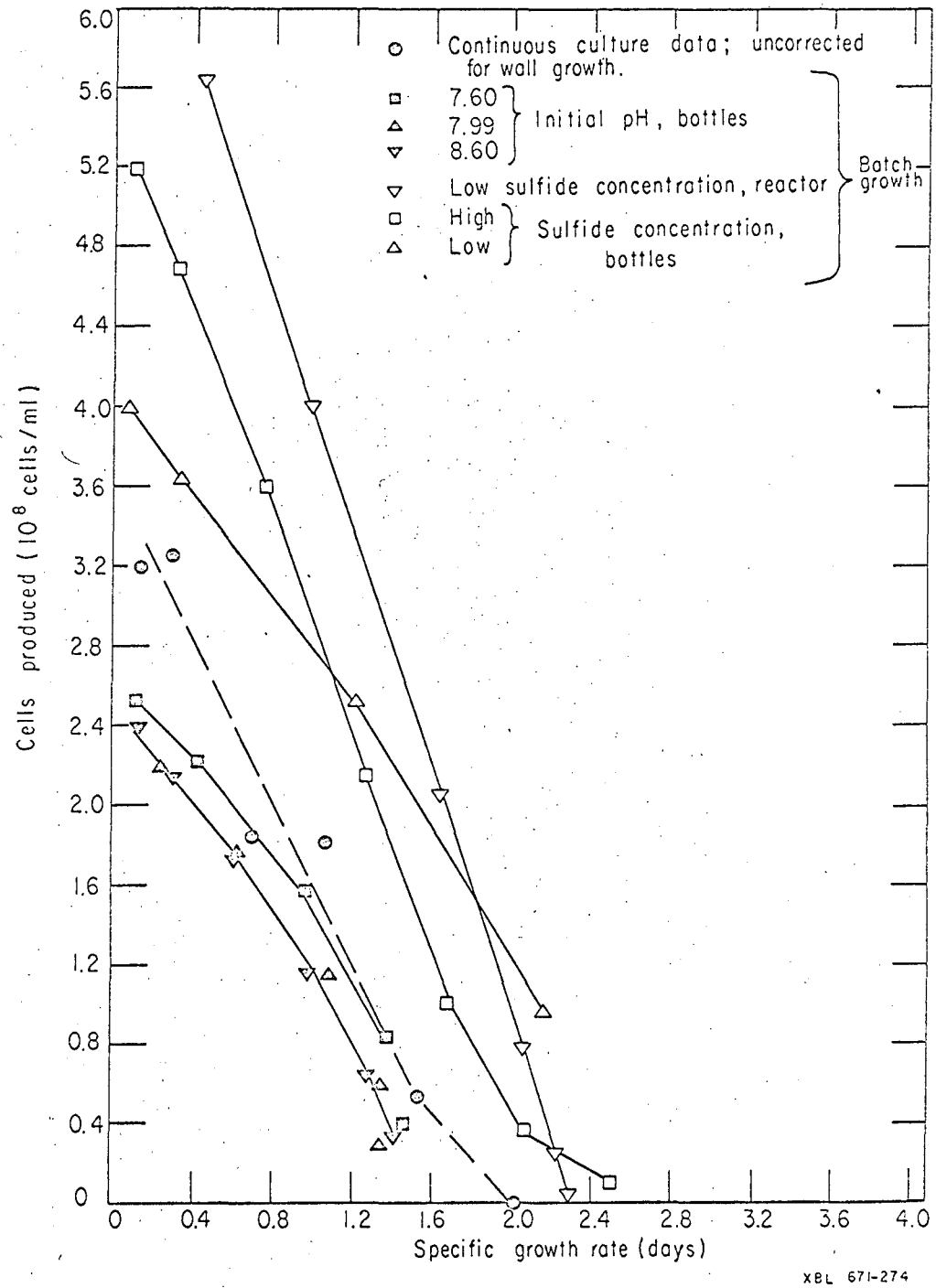

Fig. 36. Cell yield versus specific growth rate.

Models for product-limited cultures were discussed in Part I of this thesis. Two of the models discussed were the Hinshelwood-Reid equation and the simple logistic equation. Equation (1), the generalized logistic equation, reduces to the simple logistic equation when a_2, a_3, a_4, and a_5 are all zero, giving Eq. (13).

$$y = \frac{K}{1 + \exp(a_o + a_1 t_1)} \tag{13}$$

For possible correlation of the data, graphs of μ/μ_m versus $(1 - N/N_m)$ could be used to determine which of these two models fitted the data best. Equation (21) of Part I, representing the Hinshelwood-Reid equation, has the form,

$$\begin{aligned} \mu &= \frac{1}{N}\frac{dN}{dt} \\ &= \mu_m(1 - N/N_m)^{1/2} \end{aligned} \tag{14}$$

Equation (22) of Part I, which may be derived from the simple logistic equation, has the form

$$\mu = \mu_m(1 - N/N_m) \tag{15}$$

Equation (1), the generalized logistic equation, which was used in this work to determine rates from batch growth data, gives the form

$$\begin{aligned} \mu &= -(1 - N/N_m)(a_1 + 2a_2 t + 3a_3 t^2 + 4a_4 t^3 + 5a_5 t^4) \\ &= -(1 - N/N_m)\sum_{n=1}^{5} n a_n t^{n-1} \end{aligned} \tag{16}$$

When the three parameter form of Eq. (1) was used, $a_n = 0$ for $n = 2$, reducing Eq. (1) to the simple logistic equation and Eq. (16) to Eq. (15) with $\mu_m = -a_1$. The generalized logistic equation (Eq. (16)) is capable of approximating the Hinshelwood-Reid equation (Eq. (14)) when the latter is applicable.

A plot of μ/μ_m versus $(1 - N/N_m)$ should correlate data described by either the Hinshelwood-Reid equation or the simple logistic equation. Equation (14) predicts that the data will be correlated by a line with a slope of 1/2 on a log-log plot. Equation (15) predicts a straight line with slope of unity on a log-log plot, as does the three parameter form of Eq. (16). The more general Eq. (16) can be plotted in this manner for any individual experiment, but the relationship depends on the experimental time, and is thus unique for any single experiment. Several experiments under different conditions would not necessarily fit a single curve of μ/μ_m versus $(1 - N/N_m)$. True exponential growth would give a horizontal line with value $\mu/\mu_m = 1$.

Log-log plots of μ/μ_m versus $(1 - N/N_m)$ are shown in Figs. 37 and 38. The points shown for the batch data were calculated from equations of the form of Eq. (1) that were fit to the data by computer as discussed earlier. Continuous culture data were computed from the data of Sec. C neglecting the effects of wall growth. The points shown in Fig. 37 were calculated from the data of the pH experiment discussed in Sec. A.7. The points correlate well for all three cultures with best agreement between cultures having initial pH values of 7.60 and 7.99. Neither Eq. (13) nor Eq. (14) fit the points, although the points seem to have a slope parallel to the simple logistic equation over much of the range. Fig. 38 shows the continuous culture data and points calculated from the batch data of Sec. B.1. Agreement with the simple logistic equation is good in all cases but for the bottle cultures at high sulfide concentrations, where it was only fair. With the exception of the batch reactor experiment, which was fit with the three parameter form of Eq. (1), the data were fit with five or more parameters and thus would not necessarily be expected to follow the simple logistic equation. That they do to a fair approximation suggest the production of some inhibitory compound as postulated in the model. Sulfide is a likely candidate, because it is known to be an inhibitor as discussed in Sec. B.1. Specific growth rate is plotted versus sulfide concentration in Fig. 39 for data from the continuous culture experiments and the six batch experiments shown in

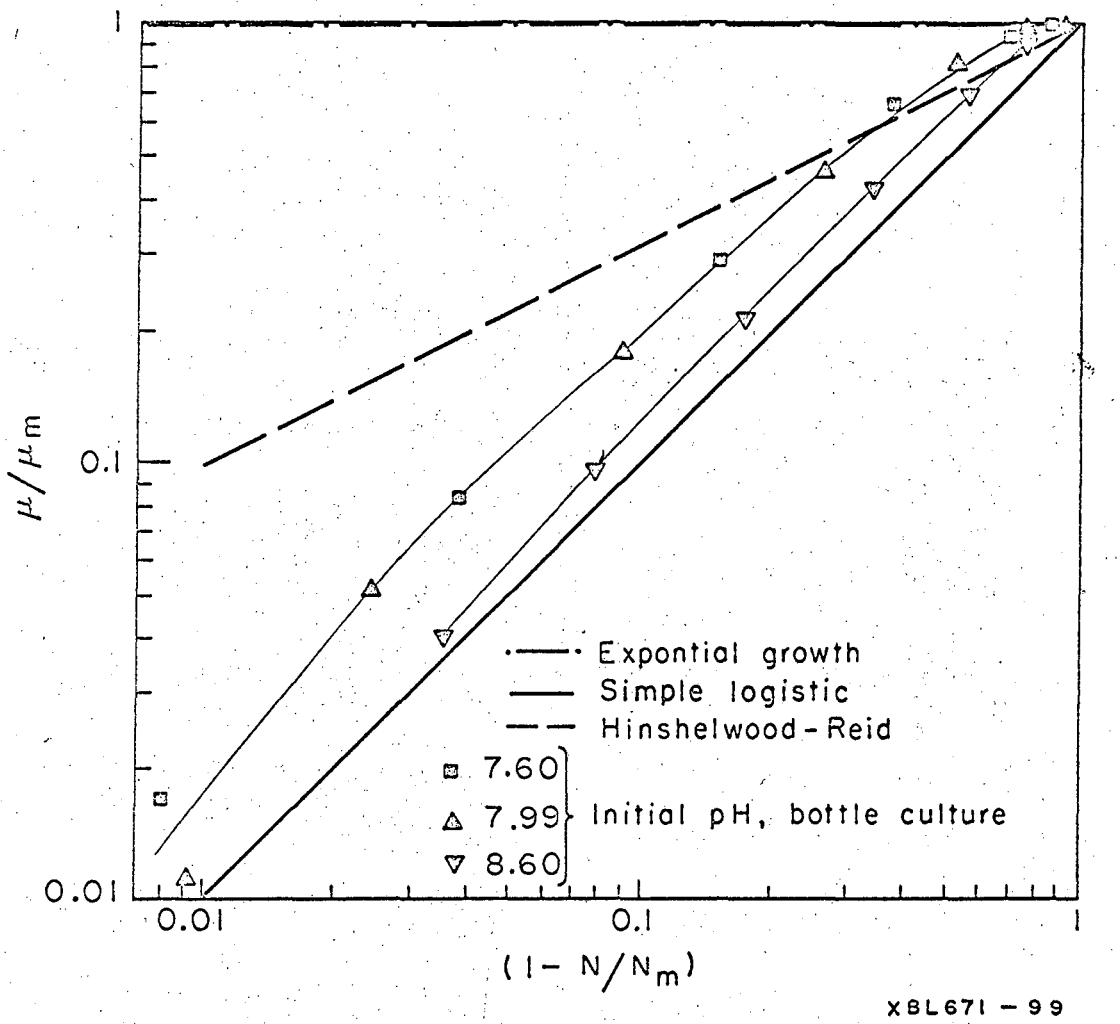

Fig. 37. μ/μ_m versus $(1 - N/N_m)$.

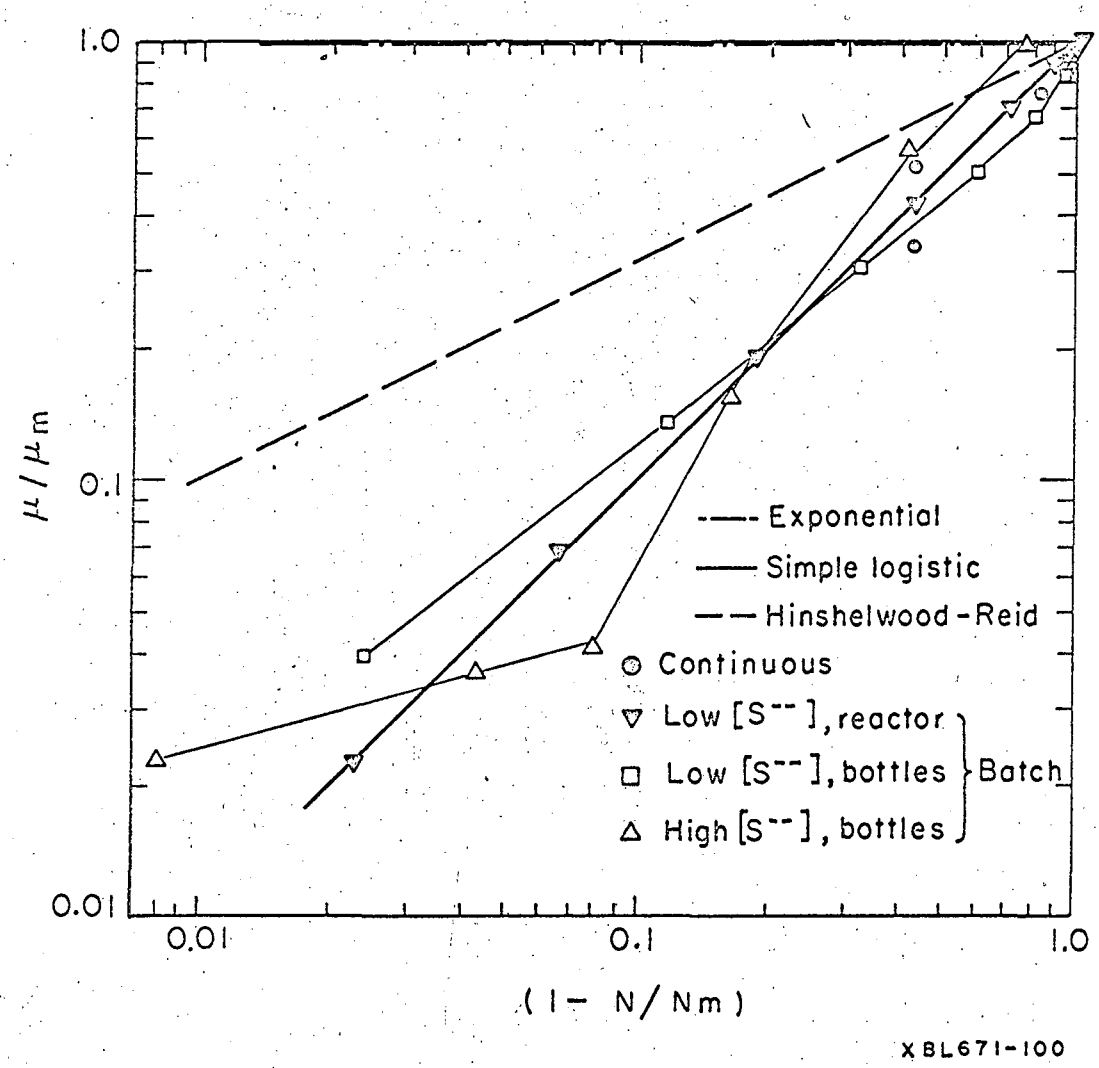

Fig. 38. μ/μ_m versus $(1 - N/N_m)$.

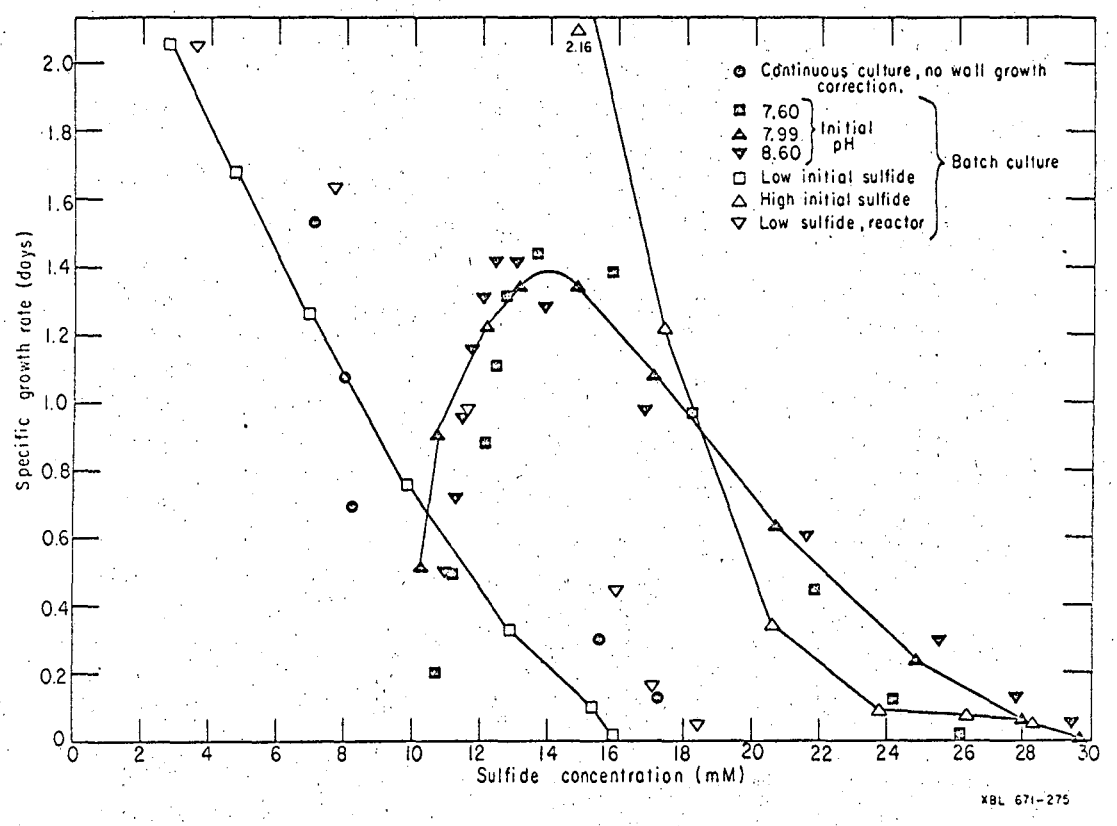

Fig. 39. Specific growth rate versus sulfide concentration.

Figs. 37 and 38. Correlation is best within the three batch runs in the pH experiments, but it is clear that other variables are also operative, because the specific growth rates cannot be correlated in a satisfactory manner by sulfide concentration alone. Another possible means of correlating the specific growth is by plotting it versus sulfate reduced as in Figs. 40 and 41. Reactor cultures, both batch and continuous, gave considerably higher sulfate reduction at low specific growth rates. A possible explanation of this behavior is that control of pH would permit longer sulfate reduction and mixing would help prevent precipitation of cells in old cultures by mucin formation. Agreement between batch experiments conducted in bottles was fair.

Productivity in batch and continuous culture in medium M are correlated with specific growth rates in Figs. 42 and 43. Productivity is defined as the rate of production of desired product, in this case sulfide, per unit volume per unit time. In the case of batch culture, this is simply the derivative of the sulfide versus time curve. In steady-state continuous culture, the productivity is the product of the dilution rate (specific growth rate) and the difference between the sulfide concentration in the inlet and the concentration in the outlet. The highest productivity was obtained in the batch culture experiment conducted in the reactor. Productivities in continuous culture were higher than in batch cultures conducted in bottles, with the exception of the run at an initial pH of 8.60 in the pH experiment.

Another means of correlating kinetic data also discussed in Part I is the method proposed by Luedeking and Piret.[24] They proposed the following equations be used:

$$\frac{dP}{dt} = \alpha\frac{dN}{dt} + \beta N \qquad (17)$$

where P is the concentration of fermentation product; α and β are fermentation constants fixed by the organism, substrate, temperature etc.

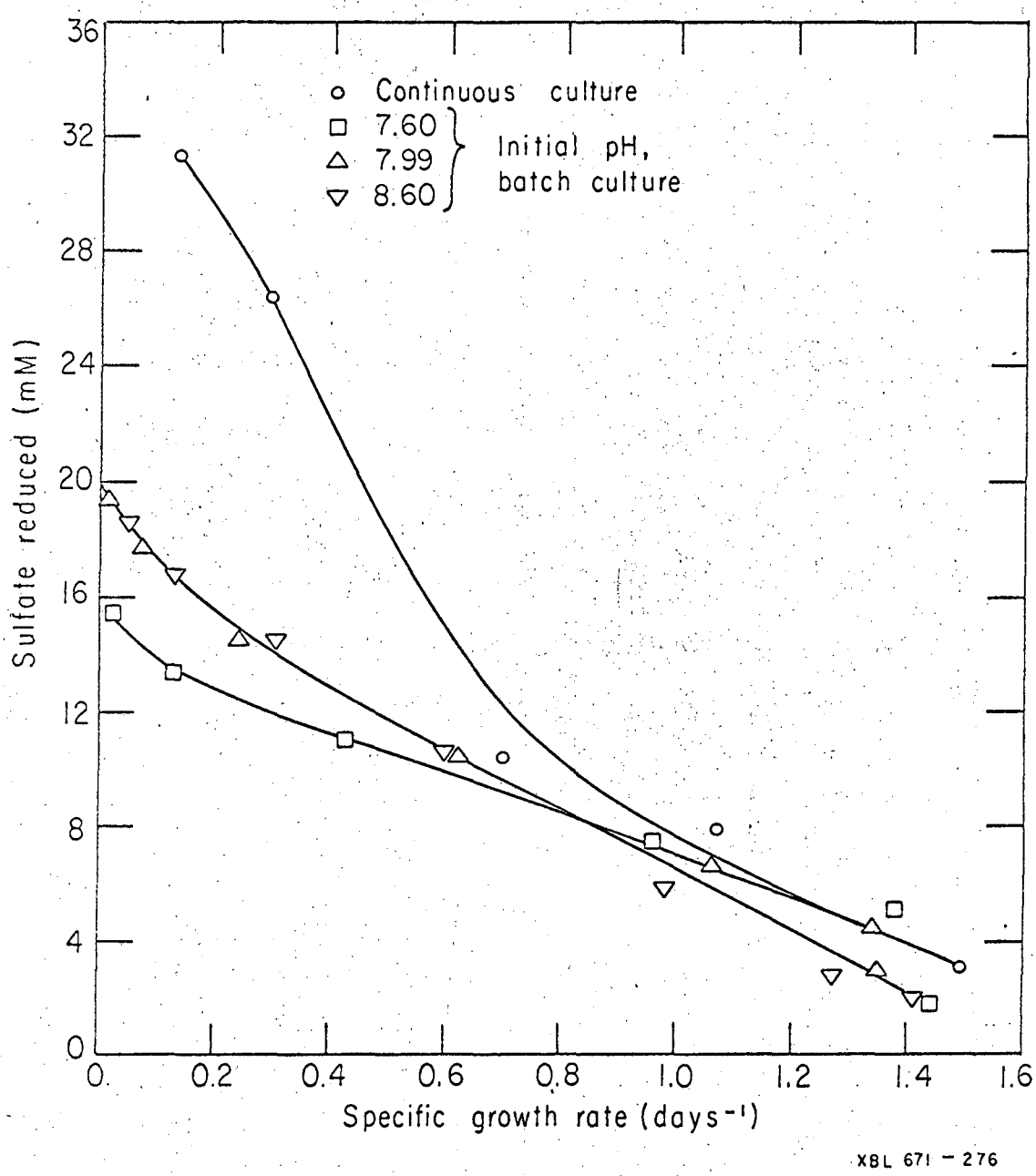

Fig. 40. Sulfate reduced versus specific growth rate.

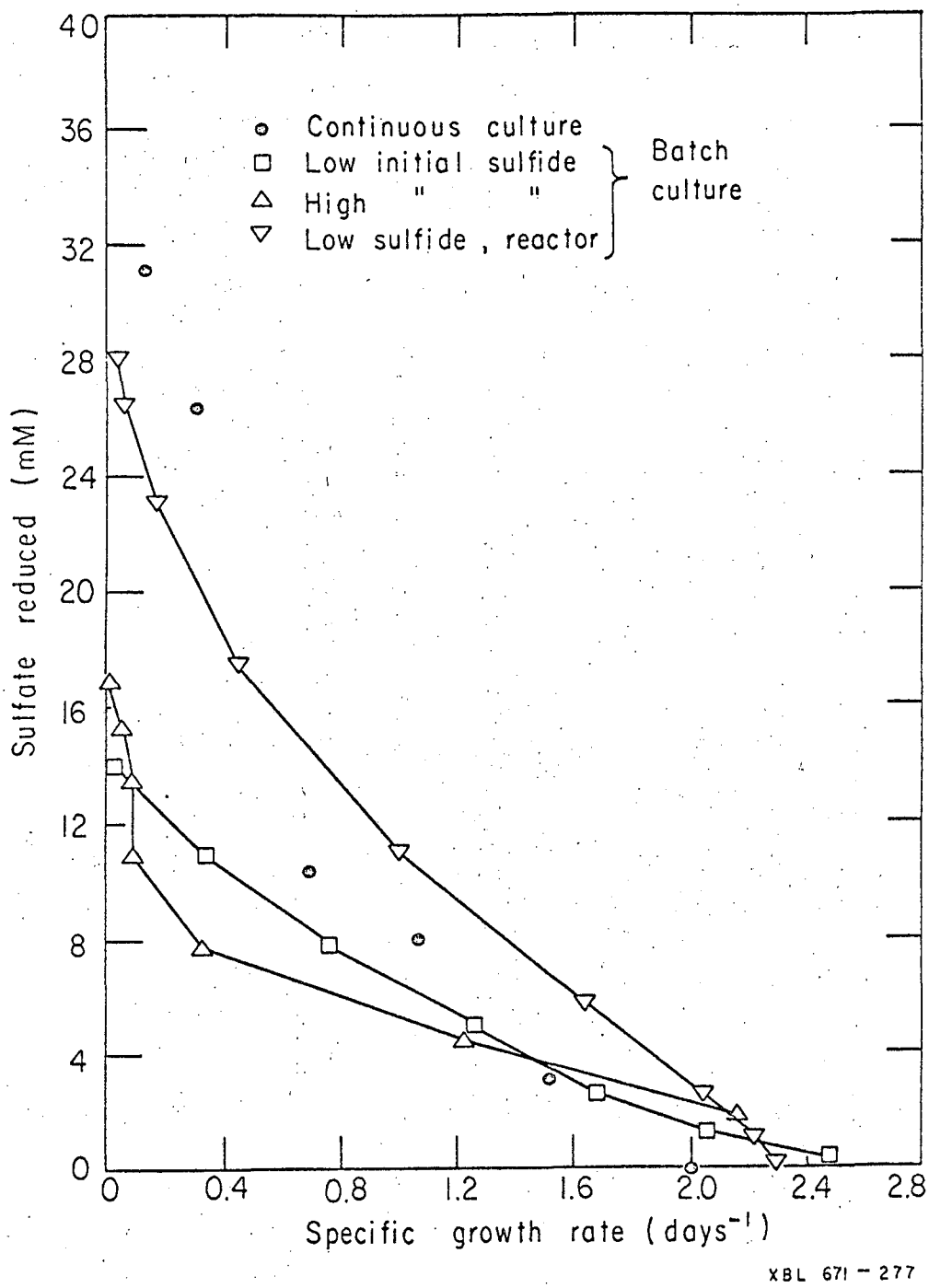

Fig. 41. Sulfate reduced versus specific growth rate.

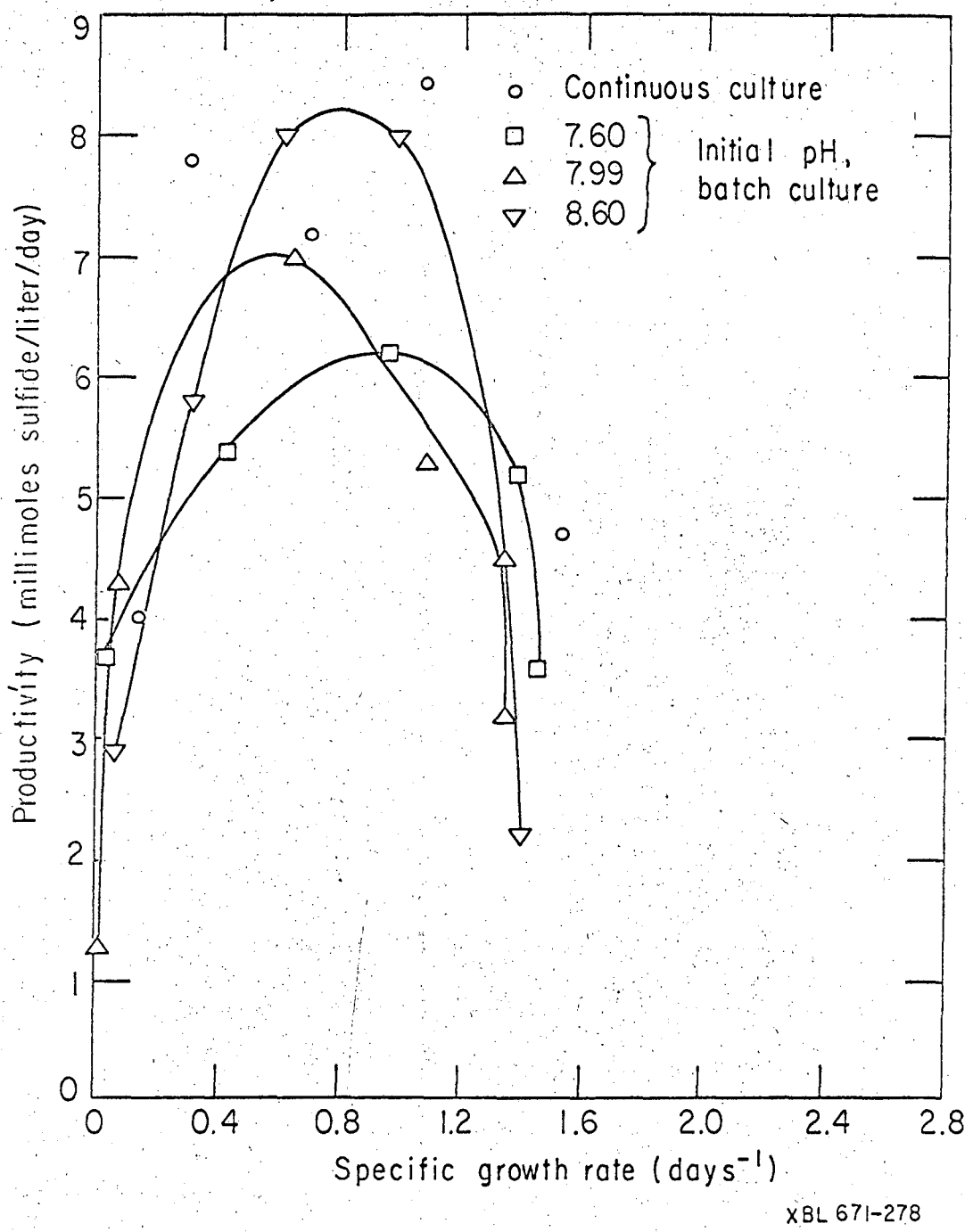

Fig. 42. Productivity versus specific growth rate.

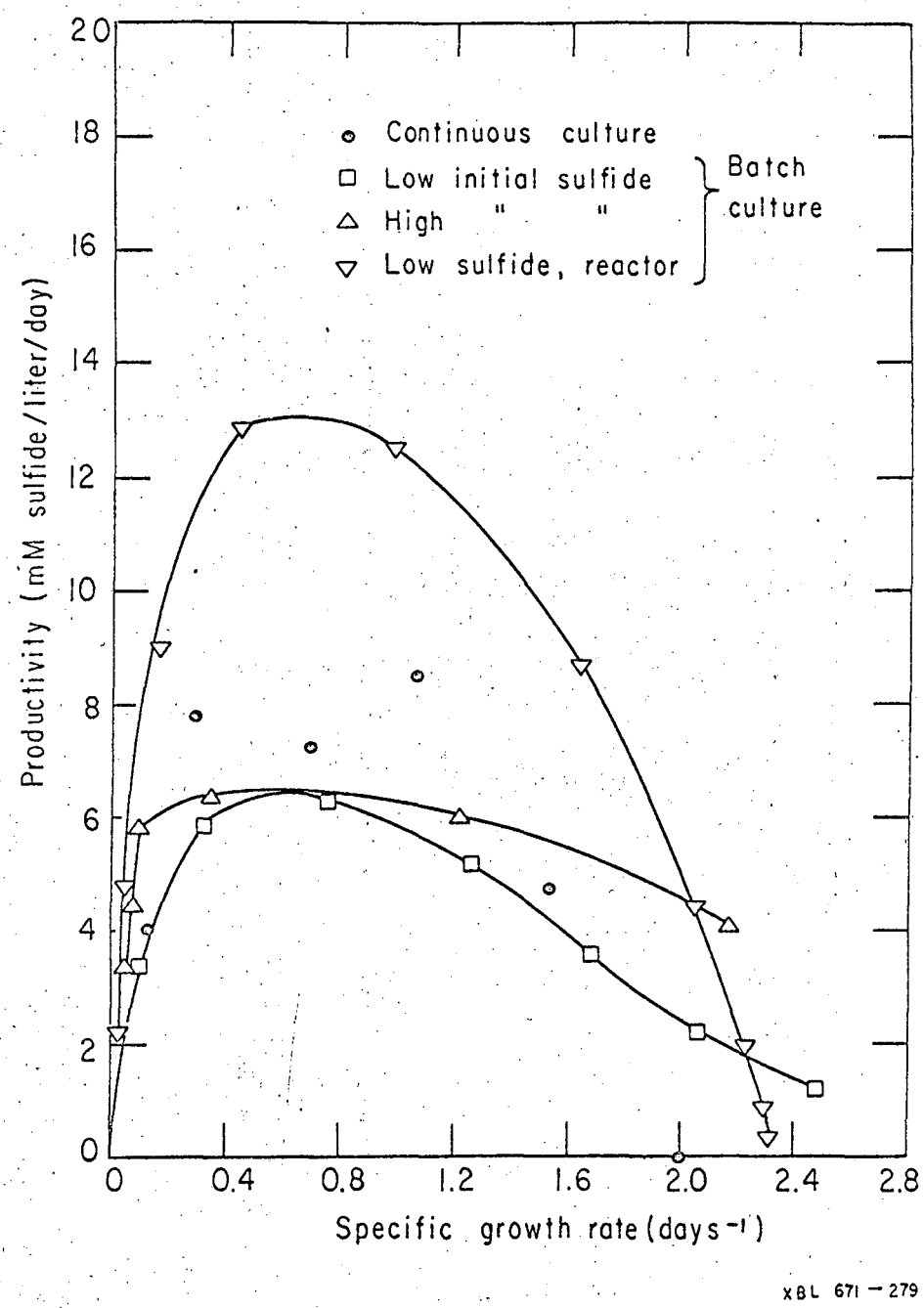

Fig. 43. Productivity versus specific growth rate.

The form of Eq. (17) was suggested by the fact that the energy derived from the product formation is consumed in two main processes: growth and basic metabolic activities. Growth rate per volume of culture is given by dN/dt, and the basic metabolic activities are proportional to the quantity of bacteria present, N.

In the case of lactic acid fermentation at constant pH, Eq. (17) was found to apply over the entire batch fermentation, except possibly in the lag phase and at the very end of the fermentation.[25] Similarity of the sulfate reduction process to the lactic acid fermentation lies in the formation of a single end product which is also toxic. In sulfate reduction the pH was not controlled in all experiments, but its variation is not as great as in the lactic acid fermentation. In the case of sulfate reduction, Eq. (17) can be written

$$\frac{d(H_2S)}{dt} = \alpha\frac{dN}{dt} + \beta N \tag{18}$$

Since the rate of product formation is proportional to the rate of substrate utilization, we have

$$\frac{d(H_2S)}{dt} = - E\frac{d(SO_4^{--})}{dt}, \tag{19}$$

where E is the efficiency of a fermentation process expressed as the ratio of product formed to substrate consumed, and is, for the present, assumed to be unity.

By substituting Eq. (19) in to Eq. (18) and rearranging one obtains

$$- \frac{1}{N}\frac{d(SO_4^{--})}{dt} = \alpha\mu + \beta \tag{20}$$

where $\frac{1}{N}\frac{d(SO_4^{--})}{dt}$ is the rate of sulfate reduction per bacterium.

By plotting sulfate reduction rate per bacterium versus growth rate, and by fitting the data with a line, the constants α and β can be obtained as the slope and the intercept of the line. Continuous data and

batch data of the three runs in the pH experiments are shown in Fig. 44. The solid line corresponds to that obtained by the authors in an earlier correlation based on a smaller number of data. The dashed line represents a possible more general correlation at higher specific growth rates. Employing the non-linear relation at the higher growth rates gives a fairly good correlation of both the batch and continuous data with a single curve over the range. Below a specific growth rate of 0.6 days^{-1}, the data were in agreement with a linear relationship corresponding to the Luedeking-Piret model expressed by the equation:

$$-\frac{1}{N}\frac{d(SO_4^{--})}{dt} = 10^{-13}(0.069 + 0.505\ \mu) \qquad (21)$$

Above a specific growth rate of 0.6 days^{-1} it appears necessary to employ the non-linear function. It should be noted that while the linear function appears to give a poor overall correlation, that the deviation from the line at high specific growth rates would have little influence in the employment of this correlation in the sizing of a continuous culture apparatus for sulfate reduction.

Figure 45 shows additional data taken approximately one year later than those described above. Although Medium M was used, a different stock of yeast extract was employed which may account for the somewhat lower rates of specific sulfide formation. These batch data do not agree well with Eq. (21) or with the continuous data. However, fair agreement was obtained with an earlier correlation obtained by Leban and Wilke for growth of the same strain of sulfate-reducing bacteria in medium E.[5] Their correlation had the form

$$-\frac{1}{N}\frac{d(SO_4^{--})}{dt} = 2.2 \times 10^{-14}\ \mu + 7.0 \times 10^{-15} \qquad (22)$$

Agreement is best for specific growth rates below a value of 2.0 days^{-1}. It is interesting that both Figs. 44 and 45 show the same intercept at zero growth rate indicating that the sulfate requirement for cell maintainence is independent of the medium composition. The Luedeking-Piret model

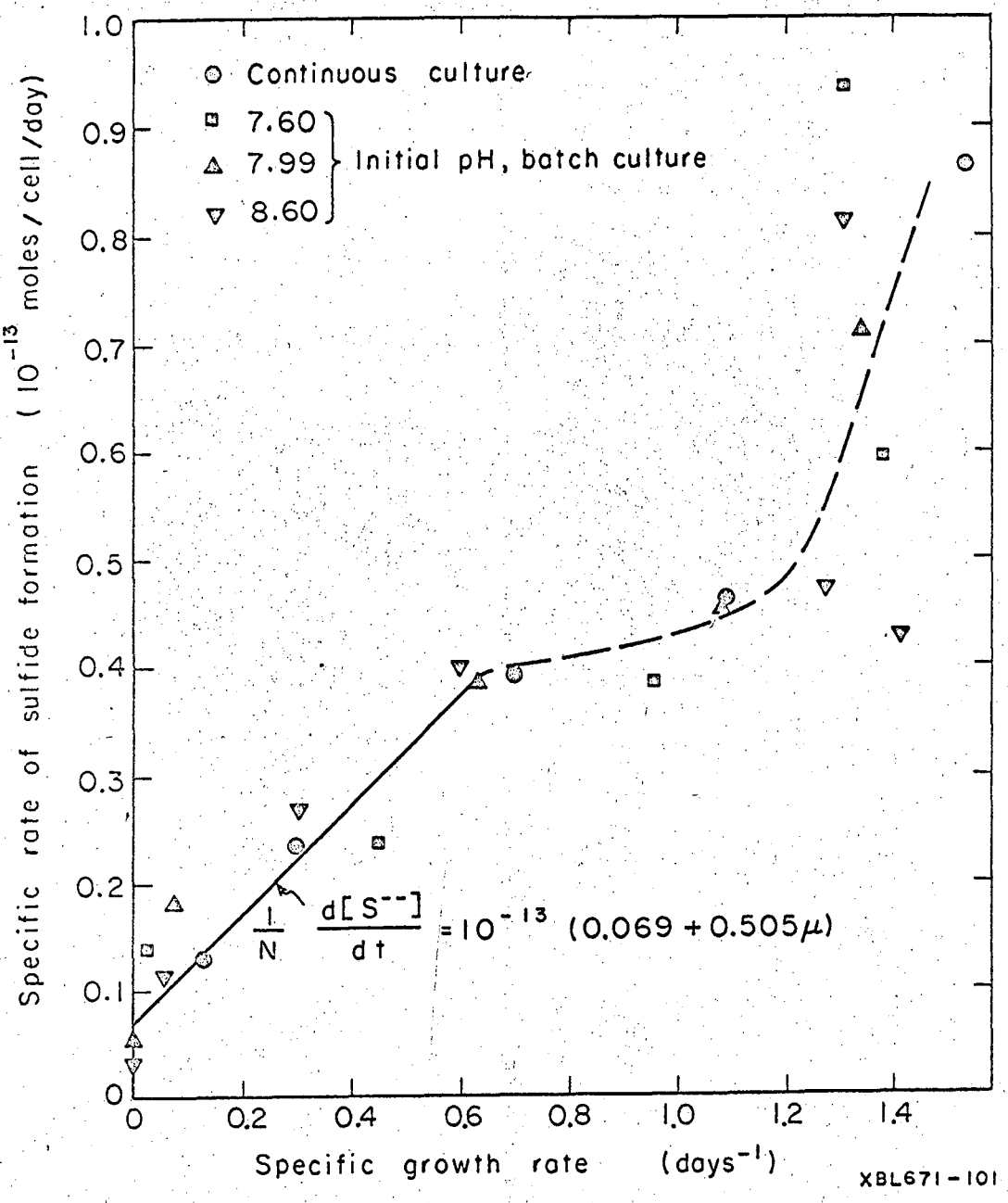

Fig. 44. Specific rate of sulfide formation versus specific growth rate.

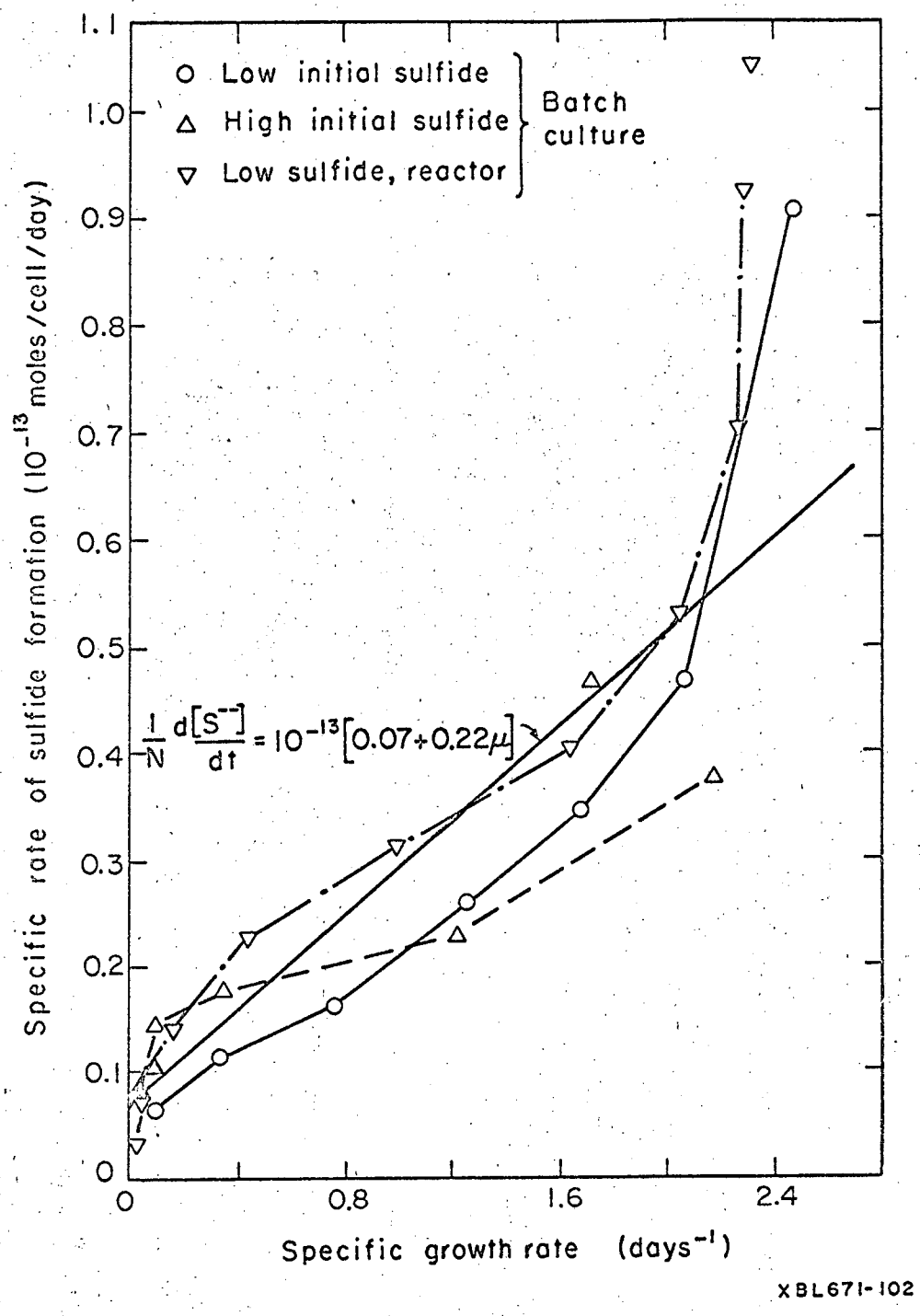

Fig. 45. Specific rate of sulfide formation versus specific growth rate.

does not appear to be adequate to correlate data at high specific growth rates, as discussed previously. Figure 46 is an idealization of the data of Figs. 44 and 45. The straight dotted line is predicted by Eq. (20) and the curved solid line represents typical observed data. The results may be interpreted as being due to several factors. Partial uncoupling of energy production, and cell division lead to the rapid rise in the data at high specific growth rates, corresponding to the early phases of exponential growth. For these systems energy production per organism is assumed to be directly proportional to the specific rate of sulfide production. As specific growth rates decrease, the average cell size becomes smaller and maintainence energy requirements become more significant in comparison to biosynthetic energy requirements. These assumptions are supported by examination of the relationship between the specific rate of sulfide production per dry mass of cells and specific growth rate as shown in Fig. 47. Assuming the energy production to be related to specific rate of sulfide production region 2 of Fig. 47 represents a constant energy consumption per dry cell mass. At higher specific growth rates (region 3) energy consumption per cell increases in a manner which suggests that energy uncoupling takes place, i.e., that more energy is being produced by the cell than is required for normal growth and maintainence. The Luedeking-Piret model thus appears to be an over-simplification of the cellular processes occurring at high specific growth rates for these organisms.

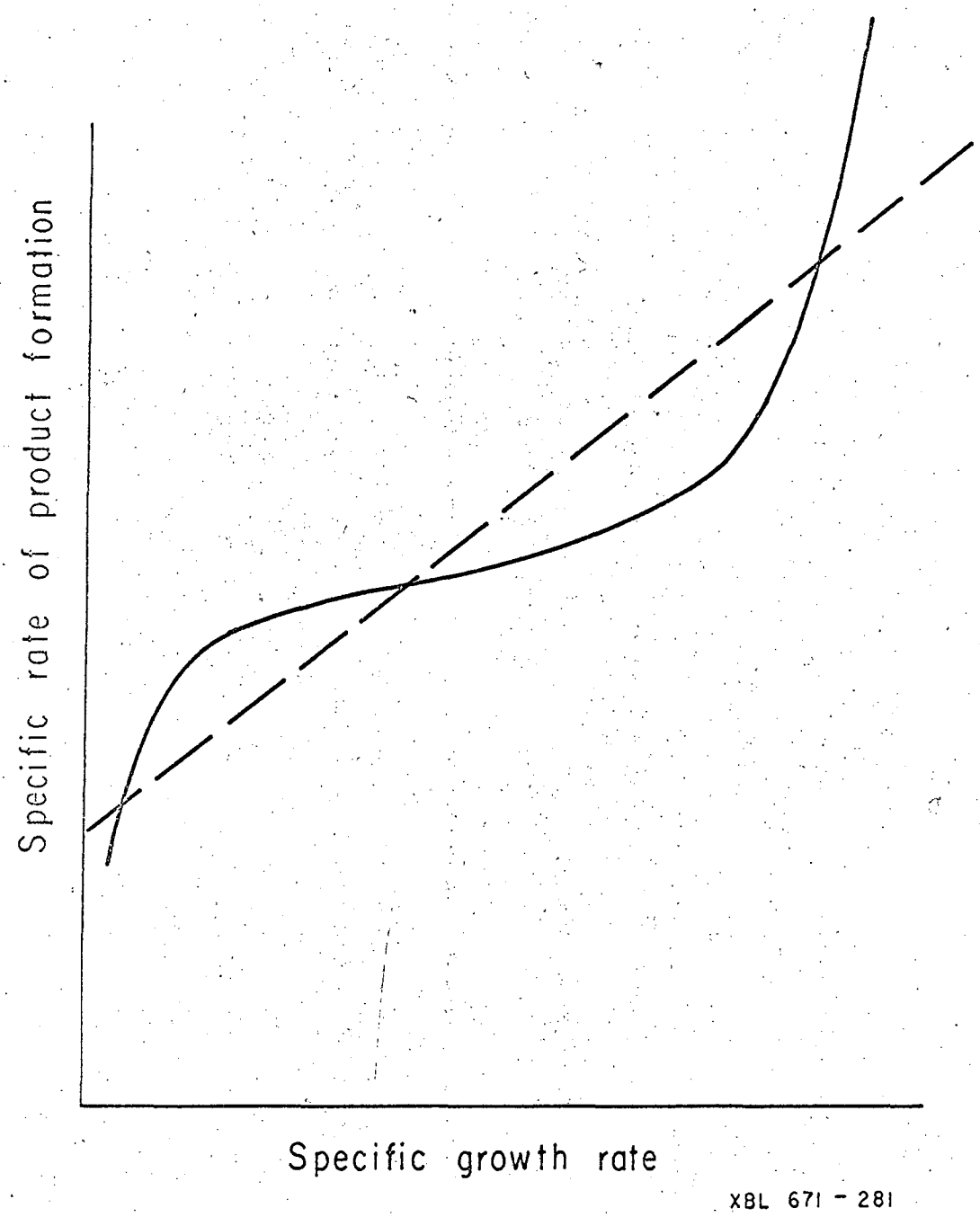

Fig. 46. Idealized plot of specific rate of sulfide production versus specific growth rate.

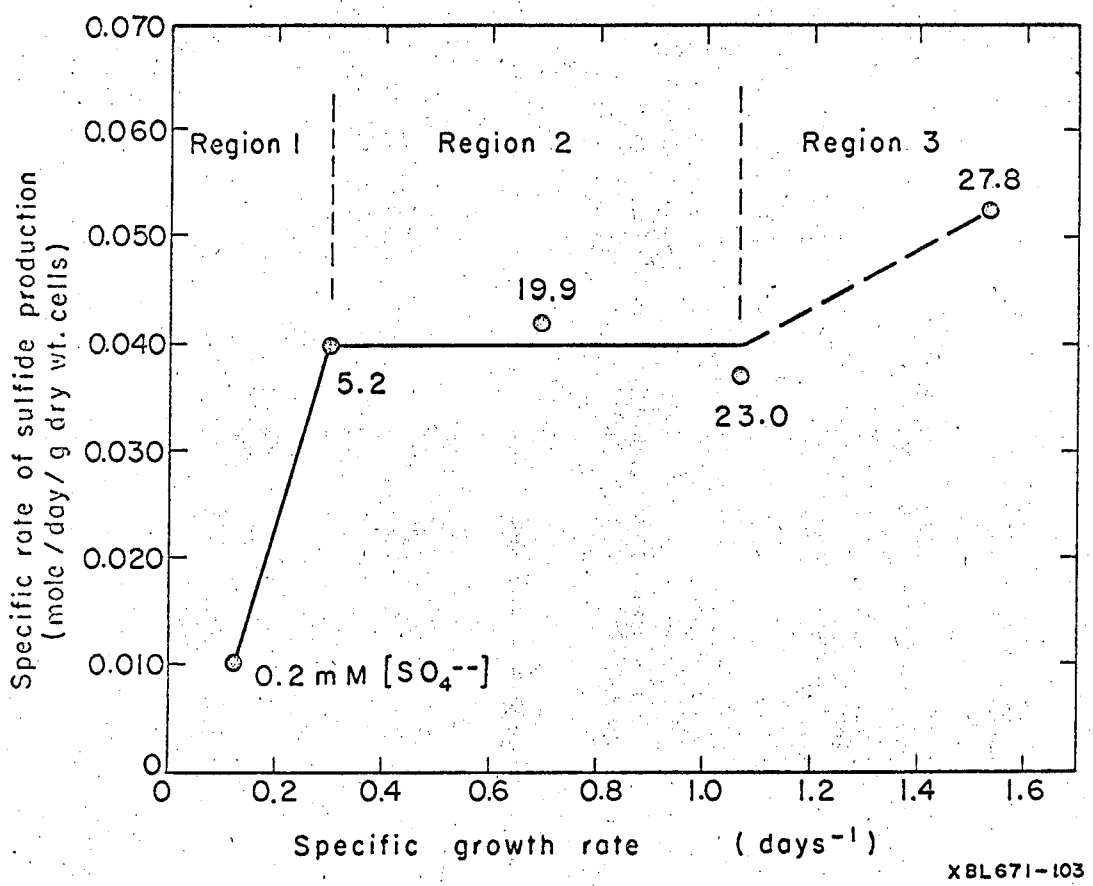

Fig. 47. Specific rate of sulfide formation (per dry cell mass) versus specific growth rate.

NOMENCLATURE

A	= surface area of reactor in contact with culture, cm^2
D	= dilution rate, $days^{-1}$
E	= fermentation efficiency
$F(t)$	= polynomial in time
(H_2S)	= sulfide concentration, moles/liter
k	= sticking coefficient
μ	= specific growth rate, $days^{-1}$
N	= number of bacteria per liter
η	= number of suspended cells in reactor
η_T	= total number of cells in reactor
P	= product concentration, moles/liter
(SO_4^{--})	= sulfate concentration, moles/liter
t	= time, days
V	= volume of culture in reactor, ml
y	= dependent variable
a,α,β,C,k,K	= constants

Subscripts

a	= apparent
B	= batch growth phase
m	= maximum
o	= initial, end of lag phase
T	= total
w	= on wall; wash-out phase

Subscripts

*	= at beginning of wash-out

APPENDIX I

CLASSIFICATION OF THE SULFATE-REDUCING BACTERIA

The salt-tolerant sulfate-reducing bacteria isolated by Leban and Wilke from San Franciso Bay was used throughout this work.[5] They identified the organism as Desulfovibrio aestaurii and discussed its characteristics.[5] Littlewood and Postgate have studied the sodium chloride tolerance of a variety of fresh-water and salt-water sulfate-reducing bacteria of the genus Desulfovibrio and have proposed that the species distinction between D. desulfuricans and D. aestuarii be removed because no well-defined level of tolerance for sodium chloride existed between fresh-water and salt-water varieties studied.[26] While the strain isolated here showed a high tolerance for sodium chloride equaled only by one of the strains studied by Littlewood and Postgate (the strain was Canet 41), the organism should be classified as Desulfovibrio desulfuricans to be consistent with their proposal that the species D. aestaurii be eliminated. However, more recent work on the base composition of the DNA of 30 strains of sulfate-reducing bacteria has shown that the organisms currently classified under the genus D. desulfuricans fall into three separate and well-defined groups, indicating a need for revision of the current method of classification of sulfate-reducing bacteria.[27] In spite of the present uncertainty in the taxonomy of sulfate-reducing bacteria, we will refer to this strain as Desulfovibrio desulfuricans.

APPENDIX II

METHODS

A. Preparation of the Media

All the ingredients of a particular culture medium, except $FeCl_3$ and $FeSO_4(NH_4)_2SO_4 \cdot 6H_2O$, were dissolved in an appropriate amount of distilled water. The solution was then sterilized in a steam-autoclave at 17 psig for twenty to thirty minutes. After cooling, which was normally done in the sterilizer itself, the pH and redox potential of the solution were measured with a Beckman Zeromatic pH Meter. From 0.5 to 0.8 g/liter of $Na_2S \cdot 9H_2O$ were then added to obtain a pH of 8.0 to 8.2 and a redox potential of -100 to -120 mV. Sometimes it was necessary to add from 0.05 to 0.2 g/liter of ascorbic acid. The ascorbic acid lowered the pH without raising the redox potential. Such a medium contained from 0.001 to 0.003 moles per liter of H_2S. The medium was then filtered to remove any precipitate formed during sterilization, and a trace of $FeSO_4)_2SO_4 \cdot 6H_2O$ or $FeCl_3$ was added. All the work described was done under sterile conditions.

The prepared medium was stored in sterile, completely full, glass-stoppered, Pyrex reagent bottles of various sizes. All of the growth experiments were done in 60 ml bottles.

B. Composition of the Media

The compositions of all the media mentioned in the report, in which they are referred to only by their letters, are given below:

The values given are for one liter of medium after dilution; distilled water was used in each case.

1. Medium A

	Weight (grams)
K_2HPO_4	0.5
NH_4Cl	1.0
$CaSO_4$	1.0
$MgSO_4 \cdot 7H_2O$	2.0
Sodium lactate (60% syrup)	6.0
$FeSO_4(NH_4)_2SO_4 \cdot 6H_2O$	trace
NaCl	100.0

Some variations of Medium A used as enrichment media also contained 3% NaCl and 13% NaCl.

2. Medium B

	Weight (grams)
K_2HPO_4	0.5
NH_4Cl	1.0
$MgSO_4 \cdot 7H_2O$	2.0
Na_2SO_4	18.25
$CaCl_2 \cdot 2H_2O$	0.1
Sodium lactate (60% syrup)	21.0
$CaCO_3$	1.0
$FeSO_4(NH_4)_2SO_4 \cdot 6H_2O$	trace
NaCl	10.1

3. Medium C

	Weight (grams)
K_2HPO_4	0.5
NH_4Cl	1.0
$CaSO_4$	1.0
$MgSO_4 \cdot 7H_2O$	2.0
Sodium lactate (60% syrup)	6.0
$FeCl_3 4H_2O$	trace
Na_2SO_4	1.5
NaCl	100.0

4. Medium D

	Weight (grams)
K_2HPO_4	0.5
NH_4Cl	1.0
$CaSO_4 \cdot 2H_2O$	1.4
$MgSO_4 \cdot 7H_2O$	2.0
$FeCl_2 \cdot 4H_2O$	trace
$FeSO_4 \cdot (NH_4)_2SO_4 \cdot 6H_2O$	trace
Sodium lactate (60% syrup)	6.0
Peptone	1.0
Yeast extract	1.0
NaCl	100.0

5. Medium E

	Weight (grams)
K_2HPO_4	0.5
NH_4Cl	1.0
$MgSO_4 \cdot 7H_2O$	2.0
Na_2SO_4	1.0
$CaCl_2 \cdot 2H_2O$	0.1
$FeCl_2 \cdot 4H_2O$	trace
Sodium lactate (60% syrup)	6.0
Peptone	1.0
Yeast extract	1.0
NaCl	100.0

6. Medium F

Same composition as Medium E, except no peptone and yeast extract.

7. Medium G

Same compositon as Medium E, but no $MgSO_4$ and Na_2SO_4, and 40 grams sodium lactate instead of 6 grams.

8. MacPherson's Medium

	Weight (grams)
Lactic acid	9.01
KH_2PO_4	0.340
$CaCl_2$	0.056
$MgSO_4 \cdot 7H_2O$	0.0616
Na_2SO_4	4.26
NH_4Cl	0.535
Yeast extract	1.0
Sodium chloride	100.0
$FeSO_4 \cdot 7H_2O$	0.007
$Na_2S \cdot 9H_2O$	0.240

9. Medium M	Weight (grams)
Lactic acid	7.66
$CaCl_2$	0.111
$MgSO_4 \cdot 7H_2O$	0.123
Yeast extract	2.5

The other components of MacPherson's Medium are present in the same concentrations in Medium M.

10. Yeast Dextrose Agar Medium	Weight (grams)
KH_2PO_4	1.0
$MgSO_4 \cdot 7H_2O$	0.5
Dextrose	20.0
Yeast extract	5.0
Agar	2.0

11. N.I.H. Thioglycollate Broth	Weight (grams)
Yeast extract	5.0
Casitone	15.0
Dextrose	1.0
Sodium chloride	2.5
ℓ-cystine	0.05
Thioglycollic acid	0.3 ml
Agar	0.75 g

C. Chemical Methods

In the determination of sulfide, a measured quantity of culture medium, usually 10 ml, was added to 5 ml of 0.1 normal iodine solution in a 50 ml Erlenmeyer flask. We added 5 ml of 10% acetic acid and the mixture was allowed to stand for about two minutes.. The excess iodine was then back titrated with 0.1 normal thiosulfate solution, using starch as an indicator.

If the solution to be analyzed contained substances other than sulfide capable of reacting with iodine, two samples were analyzed. The first sample was analyzed in the manner described above. The second sample was first boiled for a few minutes with 5 ml of one normal sulfuric acid, cooled, then reacted with iodine and back titrated with thiosulfate in the same way as the first sample. Boiling the sample with sulfuric acid drove out sulfide before the addition of iodine. By subtracting the iodine consumed in the second sample from the iodine consumed in the first one, the iodine that reacted with sulfide only was obtained.

Sulfate was determined by precipitation as barium sulfate, followed by disgestion, ignition, and weighing of the precipitate.

Hydrogen ion activity was determined with a Beckman Zeromatic pH meter equipped with glass and calomel reference electrodes (manufactured by Beckman Instruments, Inc., of Fullerton, California).

D. Total Counts

Cell concentrations were commonly determined by conventional optical counting techniques using a Petroff-Hausser counting chamber with an improved Neubauer ruling (manufactured by C. A. Hausser and Son of Philadelphia, Pa., U.S.A.). The same counting chamber was used throughout the work and the precautions suggested by Norris and Powell[28] and by Cook and Lund[29] were followed, short of measuring the chamber depth. In counts on successive slides of the same sample gave a standard deviation of 11.9%. In measurements during kinetic experiments, three successive slides were prepared and counted to minimize the random error.

E. Dry Weights

Dry weight measurements were made by passing a measured volume of culture, usually 30 to 50 ml, through weighed cellulose acetate filters with an average pore size of .45 μ (manufactured by Millipore Filter Corporation, Bedford, Massachusetts, U.S.A.). The filter and collected organisms were then dried at 95°C for 48 hrs and weighed again. As a control, a similar procedure was followed with a second filter pad and the filtered culture fluid. The dry weight of organisms present in the sample was calculated as the weight increase of the experimental filter pad less the weight increase of the control filter pad. A precipitate of ferrous sulfide was present during all measurements but calculations show that it could not contribute more than 1% to the dry weight of the organisms at the cell concentrations studied. Unfortunately, the precipitate did prevent meaningful optical density measurements or dry weight measurements at low cell concentrations.

F. Culture Purity

Cultures were periodically checked for purity following the procedures recommended by Postgate.[30] Additional precautions included aerobic plating on yeast dextrose agar and medium E to test for facultative anaerobes and anaerobic stabbing into N.I.H. Thioglycollate broth to test for clostridia.

G. Electron Microscopy

1. Preparation of Support

Thin films of carbon were prepared by depositing graphite on glass slides 25 × 74 × 1 mm that had been chemically cleaned, rinsed with a dilute detergent solution, and air-dried. The deposition was accomplished by using two graphite rods as electrodes in an electric arc in a bell jar to a pressure below one micron of mercury. The tips of the graphite electrodes in contact with the arc evaporated and condensed on striking the walls of the bell jar. The specially-prepared glass slides were placed about 150 mm below the arc on the base of the bell jar and thus a portion of the evaporated carbon condensed on the slides. After a darkening of the slide surfaces had been obtained, the arc was shut off and the slides were removed from the apparatus. The carbon film on each slide was then cut into small squares about 2 to 3 mm on a side using a scalpel and the squares of carbon floated off the slide onto the surface of a large bowl of water. Each floating square was then picked-up with a circular copper grid (3 mm diameter, 200 mesh, Ernest F. Fullam, Inc., Schenectady, N. Y.) in such a manner that each square of carbon film lay unwrinkled on the grid, covering the maximum possible number of holes of the grid. Capture of the films with the grids was accomplished more easily if the grids were first dipped in ethanol just prior to manipulation.

The carbon films on the grids were allowed to dry in a dust free petri dish and then examined with a low magnification light microscope to be usre that the film had remained intact during the manipulations. The carbon film covering opening in the grid is relatively transparent to electrons and thus serves well as a support for the electron microscopy of small particles such as latex beads or bacteria.

2. Preparation of Cells

The cell suspension to be photographed was centrifuged and washed in a filtered 0.4% sucrose solution and the concentration adjusted to give a slightly turbid suspension. A drop of the cell suspension was put on the surface of the grid-mounted carbon film and allowed to remain there for 10 sec, during which some of the cells settled. After that time, the bulk of the residual liquid was drawn off by touching the edge of the grid with the edge of a tissue. A drop of 2% solution of phosphotungstate buffered to pH 7 was then added to the grid before it dried; the phosphotungstate was removed in the same manner as the first drop after 30 sec contact with the grid. The grid was allowed to dry in air.

3. Microscopy

The grids were mounted in a Hitachi HU-11A electron microscope and photographs were made at magnifications of 8,000x and 11,000x.

APPENDIX III

TABLES OF SUPPLEMENTARY DATA

Table I. Batch growth in MacPherson's medium.

Time (days)	Optical count (cells/ml)	Sulfide concentration (mM/liter)
0	0.36×10^7	1.1
1.91	3.95×10^7	2.6
2.94	7.85×10^7	7.2
3.94	13.20×10^7	12.9
5.01	9.30×10^7	16.7
5.93	10.20×10^7	19.1

Table II. Batch growth in MacPherson's medium, initial concentration of potassium phosphate reduced by one half.

Time (days)	Optical count (cells/ml)	Sulfide concentration (mM/liter)
0	0.36×10^7	1.1
1.94	4.60×10^7	2.2
3.01	9.20×10^7	6.4
4.03	10.60×10^7	13.0
5.07	9.40×10^7	15.8
5.93	11.70×10^7	18.4
7.01	12.20×10^7	20.3

Table III. Batch growth in MacPherson's medium, initial concentration of ammonioum chloride reduced by one half.

Time (days)	Optical count (cells/ml)	Sulfide concentration (mM/liter)
0	0.36×10^7	1.1
2.17	4.20×10^7	2.3
3.15	9.70×10^7	7.9
4.17	14.10×10^7	14.5
5.20	8.70×10^7	16.9
6.87	10.10×10^7	19.5
7.90	8.70×10^7	22.2

Table IV. Batch growth in MacPherson's medium, initial concentration of ferrous sulfate reduced by one half.

Time (days)	Optical count (cells/ml)	Sulfide concentration (mM/liter)
0	$.36 \quad 10^7$	1.1
2.20	$5.67 \quad 10^7$	3.0
3.18	$8.80 \quad 10^7$	7.6
4.25	$11.20 \quad 10^7$	14.6
5.20	$9.00 \quad 10^7$	16.3
6.87	$8.00 \quad 10^7$	20.1
7.90	$7.70 \quad 10^7$	22.2

Table V. Batch growth in MacPherson's medium, initial concentration of calcium chloride reduced by one half.

Time (days)	Optical count (cells/ml)	Sulfide concentration (mM/liter)
0	0.36×10^7	1.13
1.93	3.07×10^7	1.90
3.00	5.67×10^7	5.00
4.00	8.90×10^7	9.40
5.06	9.80×10^7	13.50
5.93	9.50×10^7	16.10
7.01	11.20×10^7	18.50

Table VI. Batch growth in MacPherson's medium, initial concentration of magnesium sulfate reduced by one half.

Time (days)	Optical count (cells/ml)	Sulfide concentration (mM/liter)
0	$.36 \times 10^7$	1.1
2.18	3.70×10^7	2.0
3.17	4.07×10^7	5.7
4.18	10.30×10^7	12.1
5.20	7.00×10^7	14.6
6.87	12.50×10^7	19.1
7.90	8.80×10^7	20.3

Table VII. Batch growth in MacPherson's medium, initial concentration of sodium sulfate reduced by one half.

Time (days)	Optical count (cells/ml)	Sulfide concentration (mM/liter)
0	0.36×10^7	1.1
1.95	2.60×10^7	2.2
3.02	8.30×10^7	7.5
4.03	10.60×10^7	13.0
5.08	7.90×10^7	14.6
5.93	9.00×10^7	15.2
7.01	9.80×10^7	15.9

Table VIII. Batch growth in MacPherson's medium, initial lactic acid concentration reduced by one half.

Time (days)	Optical count (cells/ml)	Sulfide concentration (mM/liter)
0	0.36×10^7	1.1
1.93	5.80×10^7	3.8
2.92	-	8.1
3.03	15.60×10^7	-
3.92	-	14.1
4.08	13.10×10^7	-
5.01	14.30×10^7	18.3
5.93	11.40×10^7	20.1
7.01	15.10×10^7	20.9

Table IX. Batch growth in MacPherson's medium, initial concentration of yeast extract reduced by one half.

Time (days)	Optical count (cells/ml)	Sulfide concentration (mM/liter)
0	0.36×10^7	0.9
2.19	1.85×10^7	2.6
3.17	6.30×10^7	5.0
4.24	4.65×10^7	9.9
5.20	4.70×10^7	10.7
6.87	4.40×10^7	13.7
7.90	4.25×10^7	15.4

Table X. Batch growth in MacPherson's medium with no yeast extract present.

Time (days)	Optical count (cells/ml)	Sulfide concentration (mM/liter)
0	0.36×10^7	0.5
2.21	0.15×10^7	0.7
5.20	0.10×10^7	0.6
7.90	0.125×10^7	0.6

Table XII. Batch growth in modified MacPherson's medium.

Time (days)	Optical count (cells/ml)	Sulfide concentration (mM/liter)
0	$.21 \times 10^7$	.5
.93	$.11 \times 10^7$	-
1.35	$.44 \times 10^7$	-
2.25	2.70×10^7	1.9
3.18	9.67×10^7	6.6
4.24	12.90×10^7	12.0
6.16	12.04×10^7	18.2
7.20	-	20.3
8.12	12.10×10^7	21.0
10.16	-	22.6
12.24	-	23.0
14.12	-	24.1
16.08	-	24.1
26.20	-	23.9

Table XIII. Batch growth in modified MacPherson's medium, 100 mM lactic acid.

Time (days)	Optical count (cells/ml)	Sulfide concentration (mM/liter)
0	$.21 \times 10^7$	0.4
1.20	$.32 \times 10^7$	-
2.17	3.07×10^7	2.0
3.11	9.71×10^7	6.1
4.16	13.90×10^7	11.1
6.31	14.80×10^7	17.9
7.20	-	20.1
8.95	9.26×10^7	21.4
10.16	-	22.5
12.24	-	23.4
14.12	-	23.7
16.08	-	24.5
26.20	-	25.6

Table XIV. Batch growth in modified MacPherson's medium, .2% (w/v) yeast extract.

Time (days)	Optical count (cells/ml)	Sulfide concentration (mM/liter)
0	$.21 \times 10^7$	.4
.97	$.40 \times 10^7$	-
1.39	$.94 \times 10^7$	-
2.29	3.72×10^7	2.8
3.20	22.10×10^7	9.8
4.25	37.30×10^7	17.5
6.17	19.95×10^7	23.4
7.20	-	24.8
8.13	18.20×10^7	25.3
10.16	-	26.5
12.24	-	26.8
14.12	-	27.5
16.08	-	27.6
26.20	-	27.6

Table XV. Batch growth in modified MacPherson's medium, .3% (w/v) yeast extract.

Time (days)	Optical count (cells/ml)	Sulfide concentration (mM/liter)
0	$.21 \times 10^7$	.3
1.02	$.140 \times 10^7$	-
1.95	1.42×10^7	.2
2.97	8.29×10^7	4.4
3.97	26.30×10^7	13.0
6.25	26.50×10^7	25.8
7.20	-	27.0
8.25	23.40×10^7	27.6
10.16	-	28.4
12.24	-	28.5
14.12	-	28.7
16.08	-	28.6
26.20	-	32.0

Table XVI. Batch growth in modified MacPherson's medium, .5% (w/v) yeast extract.

Time (days)	Optical count (cells/ml)	Sulfide concentration (mM/liter)
0	$.21 \times 10^7$	.3
1.10	$.16 \times 10^7$	-
2.02	2.19×10^7	-
2.99	5.04×10^7	-
4.00	8.92×10^7	5.0
6.24	26.20×10^7	18.0
7.20	-	23.8
8.26	22.60×10^7	25.8
10.16	-	27.8
11.08	21.50×10^7	27.4
14.12	-	28.6
16.08	-	28.6
26.20	-	28.8

Table XVIII. Batch growth in modified MacPherson's medium, 1.0% (w/v) yeast extract.

Time (days)	Optical count (cells/ml)	Sulfide concentration (mM/liter)
0	$.21 \times 10^7$	.3
1.17	$.50 \times 10^7$	-
2.10	$.92 \times 10^7$	-
3.09	1.88×10^7	-
4.15	3.47×10^7	1.8
6.30	28.90×10^7	13.5
7.20	-	27.2
8.94	41.50×10^7	30.8
10.16	-	31.9
11.08	40.30×10^7	31.8
14.12	-	31.7
16.08	-	31.4
26.20	-	31.7

Table XX. Batch growth in medium M, initial pH = 7.60.

Time (days)	Optical count (cells/ml)	Sulfide concentration (mM/liter)	pH
0	$.10 \times 10^7$	9.7	7.60
2.04	$.24 \times 10^7$	-	-
3.87	$.24 \times 10^7$	10.8	7.40
5.94	$.67 \times 10^7$	-	-
7.69	-	13.8	-
7.75	6.55×10^7	-	-
8.67	17.10×10^7	21.8	-
10.06	25.40×10^7	25.4	-
11.96	28.20×10^7	31.0	6.73
14.03	27.20×10^7	32.3	-
17.98	-	33.3	-

Table XXI. Batch growth in medium M, initial pH = 7.99

Time (days)	Optical count (cells/ml)	Sulfide concentration (mM/liter)	pH (pH units)
0	$.10 \times 10^7$	9.7	7.99
2.04	$.18 \times 10^7$	-	-
3.87	$.29 \times 10^7$	10.0	7.69
5.93	1.53×10^7	-	-
7.69	-	18.1	-
7.79	15.90×10^7	-	-
8.66	-	26.8	-
8.79	21.70×10^7	-	-
10.09	22.20×10^7	30.7	-
11.98	27.70×10^7	31.9	6.90
14.05	25.60×10^7	32.4	-
17.98	-	33.0	-

Table XXII. Batch growth in medium M, initial pH = 8.60.

Time (days)	Optical count (cells/ml)	Sulfide concentration (mM/liter)	pH (pH units)
0	$.10 \times 10^7$	9.7	8.60
2.04	$.18 \times 10^7$	-	-
3.87	$.13 \times 10^7$	10.9	8.10
5.94	$.73 \times 10^7$	-	-
7.73	9.53×10^7	14.4	-
8.66	-	23.4	-
8.77	18.80×10^7	-	-
10.09	22.40×10^7	30.0	-
11.97	27.70×10^7	32.8	7.00
14.04	28.80×10^7	33.9	-
17.98	-	34.5	-

APPENDIX IV

DERIVATION OF WALL GROWTH EQUATIONS

For a perfectly-mix continuous stirred-tank reactor, the following material balance applies:

Accumulation = Input + Generation - Output

$$V \frac{dN}{dt} = F N_i + V \mu N + A \mu N_w - F N \qquad (23)$$

where V = reactor volume

F = feed rate to reactor

A = wall area in contact with reactor culture

N = cell concentration solution

N_i = cell concentration in feed (assumed zero)

μ = specific growth rate (assumed same on wall as in suspension)

N_w = cell concentration on walls per unit wall area

$= k N$

Substituting and rearranging Eq. (23),

$$\frac{dN}{dt} = (\mu + \frac{A\mu k}{V} - D)N$$

where D = dilution rate

$= F/V$

k = sticking coefficient

separating variables and integrating

$$\ln N = \ln N_o + (\mu + \frac{Ak\mu}{V} - D)t$$

$$= \ln N_o + (\mu_a - D)t$$

where μ_a = apparent specific growth rate of culture during washout

$= \mu(1 + Ak/V)$

and $$k = (V/A)(\mu_a/\mu - 1) \qquad (24)$$

In the maximum growth rate experiment, $\mu_a = 2.81$ days^{-1} (measured from washout data), $\mu = 2.03$ days^{-1} (measured from batch growth data, V = 2.4 liters, and A = 1200 cm^2. Substituting into Eq. (24)

$$k = (2400/1200)((2.81/2.03) - 1)$$
$$= 0.77 \text{ cm}$$
$$= \frac{\text{cells/unit wall area}}{\text{cells/unit volume of culture}}$$

At the maximum concentration in the reactor, N = 4.13×10^7 cells/ml

$$N_w = k\,N$$
$$= 0.77 \times 4.13 \times 10^7$$
$$= 3.2 \times 10^7 \text{ cells/cm}^2$$

$$\text{and Area/cell} = \frac{10^8 \text{ microns}^2/\text{cm}^2}{3.2 \times 10^7 \text{ cells/cm}^2}$$
$$= 3.2 \text{ square microns}$$

From photomicrographs, typical dimentions of the cell are .6 microns by 4 microns = 2.4 square microns/cell. Thus this model of wall growth predicts wall coverage of about 75% by cells at suspension concentrations corresponding to the maximum observed during the washout experiment.

REFERENCES

1. John R. Postgate, Recent Advances in the Study of the Sulfate-Reducing Bacteria, Bact. Rev. 29, 425 (1965).
2. J. R. Postgate, The Chemical Physiology of the Sulfate-Reducing Bacteria, Producers Monthly 22, 12 (1958).
3. C. E. ZoBell, Ecology of Sulfate-Reducing Bacteria, Producers Monthly 22, 12 (1958).
4. J. R. Postgate, Some Problems in the Field of Bacterial Sulphate Reduction (private communication).
5. M. Leban and C. R. Wilke, Lawrence Radiation Laboratory Report UCRL-10966, 1963).
6. J. R. Postgate, Economic Activities of Sulfate-Reducing Bacteria, Progress in Industrial Microbiol. 2, 48 (1960).
7. Rhona MacPherson and J. D. A. Miller, Nutritional Studies on Desulfovibrio desulfuricans using Chemically Defined Media, J. Gen. Microbiol. 31, 365 (1963).
8. L. O. Zwillenberg, Electron Microscopic Gram-negative and Gram-positive Bacteria Embedded in Phosphotungstate, Antonie van Leewuenhoek 30, 154 (1964).
9. John Postgate, Sulfate Reduction by Bacteria, Ann. Rev. Microbiol. 13, 505 (1959).
10. C. W. Cotman and D. M. Smith, J. Sci. Instr. 41, 561 (1964).
11. L. Michaelis and M. L. Menten, Biochem. Zeitschr. 49, 333 (1913).
12. L. P. Miller, Tolerance of Sulfate-Reducing Bacteria to Hydrogen Sulfide, Contrib. Boyce Thompson Inst. 16, 73 (1950).
13. D. E. Contois, J. Gen. Microbiol. 21, 40 (1959).
14. W. D. Maxon (The Upjohn Company, Kalamazoo, Michigan), personal communication (1966).
15. R. J. Munson and B. A. Bridges, J. Gen. Microbiol. 37, 411 (1964).
16. Dennis Herbert, The Chemical Composition of Micro-organisms as a Function of their Environment in Microbiol Reaction to Environment, 11th Symposium of the Society for General Microbiology held at the Royal Institution, London, April 1961. (Cambridge University Press, 1961), p. 391.

17. M. Schaechter, O. Maaløe, and N. O. Kjeldgaard, J. Gen. Microbial. 19, 592 (1958).

18. R. E. Ecker and M. Schaechter, Ann. N. Y. Acad. Sci. 102, 549 (1963).

19. R. K. Finn, J. Ferm. Technol. 44, 305 (1966).

20. Cyril Hinshelwood, The Chemical Kinetics of the Bacterial Cell (The Clarendon Press, Oxford, 1964).

21. A. T. Reid, Bull. Math. Biophys. 14, 313 (1952).

22. P. F. Verhulst, Mem. Acad. Roy. Bruxelles 18, 1 (1844); 20, 1 (1846).

23. R. Pearl and L. J. Reed, Proc. Natl. Acad. Sci. 6, 275 (1920); Scientific Monthly, 194 (1921).

24. R. Luedeking and E. L. Piret, Transient and Steady States in Continuous Fermentation, J. Biochem. Microbiol. Technol. Eng. 1, 4 (1959).

25. R. Luedeking and E. L. Piret, Kinetic Study of the Lactic Acid Fermentation Batch Process at Controlled pH, J. Biochem. Microbiol. Technol. Eng. 1, 393 (1959).

26. D. Littlewood and J. R. Postgate, Sodium Chloride and the Growth of Desulfovibrio desulfuricans, J. Gen. Microbiol. 17, 2 (1957).

27. Grady F. Saunders, L. Leon Campbell, and John R. Postgate, Base Composition of DNA of Sulfate-reducing Bacteria Deduced from Buoyant Density Measurements on $CsCl_2$, J. Bact. 87, 1073 (1964).

28. K. P. Norris and E. O. Powell, J. Roy. Microscopical Soc. 80, 107 (1961).

29. A. M. Cook and B. M. Lund, J. Gen. Microbiol. 29, 97 (1962).

30. J. R. Postgate, J. Gen. Microbiol. 9, 440 (1953).

31. M. Leban, V. H. Edwards, and C. R. Wilke, "Sulfate Reduction by Bacteria", J. Ferm. Technol. 44, 334 (1966).

PART III: ELECTRONIC SIZING AND COUNTING OF BACTERIA

I. INTRODUCTION

Among the most crucial variables in bacterial kinetics is the cell concentration. Also of importance is the distribution of properties among individuals in the cell population. One such property is the size distribution, which one might expect to have a strong influence on kinetics. Both the cell concentration and the distribution of cell size in a culture can be measured rapidly and accurately with the system to be described here. The technique was originated by W. H. Coulter.[1] The method consists of drawing a measured volume of a dilute suspension of particles in an electrolyte through a small hole in a dielectric material. The electrical resistance of the hole or aperture is increased each time a particle is drawn through the hole. The electrical resistance change is seen as a current change when the voltage across the hole is kept constant. The maximum pulse-amplitude is roughly proportional to the volume of the particles generating the pulse. The current pulses are electronically amplified, analyzed and sorted according to size. The system is shown in Fig. 1. The preamplifier and amplifier magnify and shape the pulses generated in the aperture by particle passage. The pulses are displayed on an oscilloscope to be sure that the aperture is not plugged. The amplified pulses are sent to a pulse-height analyzer that sorts the pulses according to amplitude and remembers pulses of different sizes in its 128 memory channels. The resulting size distribution can be displayed on an osiclloscope, an x-y recorder, and electric typewriter-paper tape punch.

Part III of the dissertation will first review the literature on electronic sizing and counting. Next, the counting system and its calibration with suspensions of small plastic spheres will be described. Then the system will be evaluated as a technique for counting and sizing bacterial cells. Finally, the results will be discussed in light of a theory of the electrical conductivity of bacterial cells and its implication.

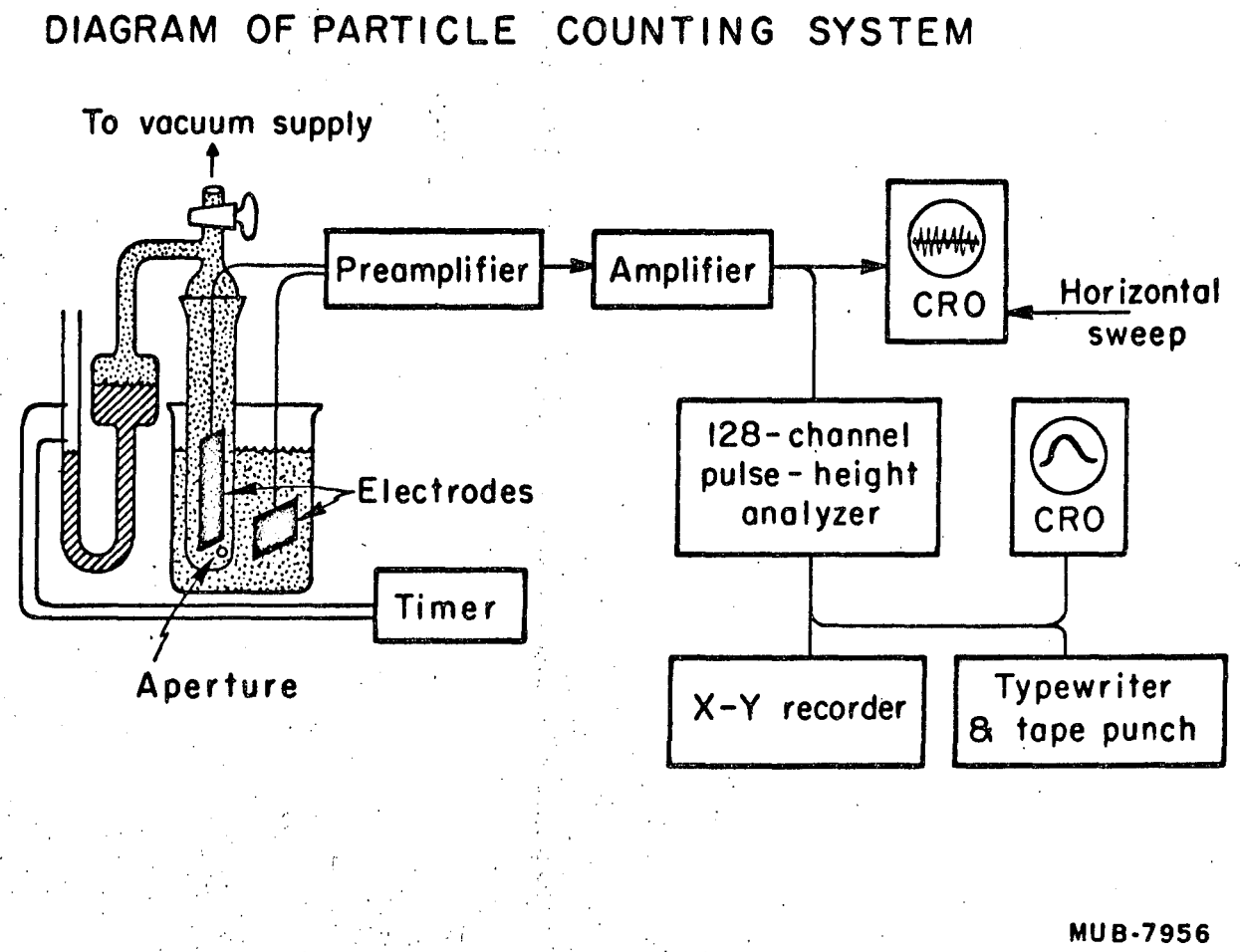

Fig. 1. Schematic diagram of sizing and counting system.

II. LITERATURE REVIEW

A comprehensive literature survey was made of the theory of electronic sizing and counting of small particles and of its application to the sizing and counting of bacteria. The theory will be discussed first, followed by a discussion of the application of the technique to bacteria.

A. Theory of Electronic Sizing and Counting of Particles

1. Response to Particle Size

By making several assumptions, Kubitschek derived the following equation:[2]

$$\frac{\Delta R}{R} = -\frac{v}{V}\frac{\Delta\rho}{\rho_2}\left(1 - \frac{a}{A}\frac{\Delta\rho}{\bar{\rho}_2}\right)^{-1} \qquad (1)$$

where R = electrical resistance of aperture in the absence of any particles,

$\Delta\rho = \bar{\rho}_2 - \rho_1$

$\bar{\rho}_2$ = resistivity of the particle,

ρ_1 = resistivity of electrolyte,

A = cross-sectional area of aperture,

V = volume of aperture,

v = volume of particle, and

a = cross-sectional area of particle.

Equation (1) is based on the following assumptions:

1. The greatest cross-section of the particle, a, is much smaller than A, and the particle is shorter than the aperture depth.
2. The particles are right circular cylinders of volume v.

When $\bar{\rho}_2 \gg \rho_1$ the change in resistance with respect to volume is linear to one percent for right cylinders with diameters less than ten percent of the aperture diameter.

Recently, Gregg and Steidley have advanced the theory of sizing by a theoretical and experimental examination of the effect of particle shape and orientation on the system response.[3] They showed that for spheres small relative to the aperture, the resistance change in the aperture was

$$\Delta R = \frac{3}{2} \rho_1 \, L\beta/A \tag{2}$$

where L = aperture length,

$\beta = 4\pi r_2^3/3LA$, and

r_2 = radius of the sphere.

For particle sizes not negligible with respect to the aperture, they showed that the following equation applied to spheres:

$$\frac{\pi \Delta R}{\rho_1} = \frac{3}{r_2} \left[\frac{\tan^{-1}[K(1 - K^2)^{-1/2}]}{(1 - K^2)^{1/2}} - K \right] \tag{3}$$

where $K = r_1/r_2$,

r_1 = radius of sphere, and

r_2 = radius of aperture.

For small K, Eq. (3) reduces to Eq. (2). For long thin rods, end effects are negligible and Eq. (3) applies except that the right-hand side of the equation must be multiplied by 2/3.

For discs passing through the aperture with their axes of circular symmetry parallel to the axis of the aperture, the signal is approximately three times that for a sphere of equivalent volume because of the sharp edges of the disc. For a disk passing through the orifice with faces parallel to the axis of the aperture, Eq. (4) applies.

$$\Delta R = \frac{3}{2} \rho_1 \delta/\pi^2 \, r_2^4 \tag{4}$$

where δ = particle volume.

All equations were tested by experiments using two model orifices and model particles of various shapes. One model orifice was short compared to its diameter and the other model was long compared to its diameter, thus allowing study of both extremes in orifice construction.

Gregg and Steidley further showed that membrane capacities could be neglected. An equivalent circuit of the orifice-electrode system was analyzed to show that resistance changes could be converted current pulses that were independent of solution conductivity through the use of a constant current source and a zero input impedance amplifier.

In more recent work, the performance of an actual sizing and counting system has been studied by the same group.[4] They suggest that particle dimensions be limited to one third or less of the diameter of the orifice. Increased count rates where shown to shift the measured size distribution toward longer particle sizes due to increased coincident passage of particles through the aperture. System response was shown to be almost independent of electrolyte conductivity except at lower values. Most important of their findings was the result that electronic volumes averaged about 20% lower than optically measured volumes in the case of mammalian cells and 40% lower when pollen suspensions were analyzed. They suggested that bulging of the mammalian cells while resting on the slide during optical sizing could cause erroneously large values for optically determined volumes. The rough, wrinkled surface of pollen particles was proposed as a reason for their low elctronic volume. As pointed out be Adams et al., this behavior is an advantage in the electrical measurement of the volume of particles of irregular shape.

2. Coincidence Effects

(a) Primary effects. The primary effect of coincident passage of particles through the aperture is loss of total count. Mattern, Brackett and Olson were the first to treat this effect.[5] They pointed out that coincident passage of two particles would produce a single pulse of variable amplitude, depending on whether the particles passed

through the aperture close together or far apart. They proposed that a Poisson distribution would describe the distribution of single and multiple passages to particles. They derived the following equation to describe the ratio of instrument count to actual count:

$$\frac{n}{N} = \frac{1 - P_o}{1 - P_o + (P_2 + 2P_3 + \ldots + (n - 1)P_n + \ldots} \qquad (5)$$

where n = instrument count,

N = actual count

$P_o = e^{-m}$ = probability of no cells in critical volume,

m = average number of particles per unit critical volume of the aperture,

$P_1 = me^{-m}$ = probability of one cell in critical volume, and

$P_n = \frac{m^n}{n!} e^{-m}$ = probability of n cells in critical volume.

It can be seen that the variable m will be a function of the aperture size, coincident passage limiting the maximum allowable cell concentration for a given coincidence level and aperture volume.

As pointed out by Harvey and Marr, differentiation of the pulses instead of measurement of pulse amplitude will reduce coincidence effects by shortening pulse lengths.[6] They showed that with differentiation and integration of pulses from a 30-micron-diameter aperture allowed accurate counts between concentrations of 10^4 to 2×10^6 particles per ml. This is in agreement with a calculation based on an equation proposed by Adams et al. which predicts a 2% level of coincidence at a particle concentration of 4×10^6 particles/ml[4] for a 30-micron aperture.

(b). Secondary effects. Secondary effects of particle coincidence result from the skewing of the distribution caused by several smaller particles being counted as a single larger particle. As mentioned earlier, Adams et al. showed that increased count rates caused size distribution to be shifted toward larger sizes because of coincident passage of particles. Harvey and Marr showed that the size distribution obtained by

by analysis of undifferentiated pulses was broadened at higher count rates. They proposed that coincidence of the particles with other particles in the aperture led to the broadening.[5] However, they found that the mode of the distribution did not change with count rate, contrary to the findings of Adams et al. It is our opinion that broadening of the distribution like that observed by Harvey and Marr were due at least partly to coincident occurrence of noise pulses (both positive and negative) with particle passage through the aperture, increased count rates giving rise to increased noise levels. If such results were to be entirely due to coincident passage of particles, the mode of the distribution should have been shifted and counts at size levels below the mode should be reduced while counts above the mode increased. On the contrary, their results showed broadening on both sides of the mode, requiring that some of the particle-generated pulses be combined with negative pulses. Overshoot of particle-generated pulses to negative values occurs, possibly in sufficient amounts to cause the observed broadening of the distribution. The observation that integration of the pulses before pulse-height analysis led to more narrow distribution is consistent with our proposed explanation, because such integration would smooth out high frequency noise.

Mathematical analyses of coincidence effects have been made in attempts to reduce this source of error.[7,8]

3. New Developments in Technique

Recently, three extensions of the technique of Coulter counting have been made.

Fulwyler has used Coulter counting to sort biological cells by volume.[9] The new technique consists of electronically measuring the volume of particles, isolating each particle in a drop, and placing an electric charge on each drop according to the sensed particle volume. The charged droplets then enter an electrostatic field that deflects the drops into collection vessels. Drops with higher charges are deflected to a greater extent by the electrostatic field and fall into collection

vessels different from those that the drops with smaller charges fall into. Using this technique, human erythrocytes were separated from mouse erythrocytes.

A technique for improving the resolution of the Coulter counter based on pulse-shaping prior to pulse-height analysis was begun in the laboratory of Dr. Donald Glaser.[10] Recently, Harvey and Marr made systematic studies to determine optimal degrees of differentiation and integration of pulses prior to analysis.[6] Pulse-shaping is used with this work and will be discussed later.

A third important advance in the technique of Coulter counting has been made by Spielman and Goren.[11] They have introduced a technique called hydrodynamic focussing. The technique consists of feeding the suspension to be analyzed into the Coulter aperture along a single streamline, as shown in Fig. 2. The Coulter aperture is immersed in a particle-free electrolyte and the suspension to be analyzed passes through a small hole in a sample vessel and through the Coulter aperture, which is adjacent to the hole in the sample vessel. Because all particles pass along the same streamline, the trajectory of the particles through the aperture is no longer a variable because all particles have the same trajectory. Hydrodynamic focussing gives roughly the same improvement of resolution as is obtained by pulse shaping. It has the advantage that much more justification is required for an empirical technique such as pulse shaping. It has the disadvantages that a larger volume of concentrated particles is required and that concentration measurements are not possible with the focussing method.

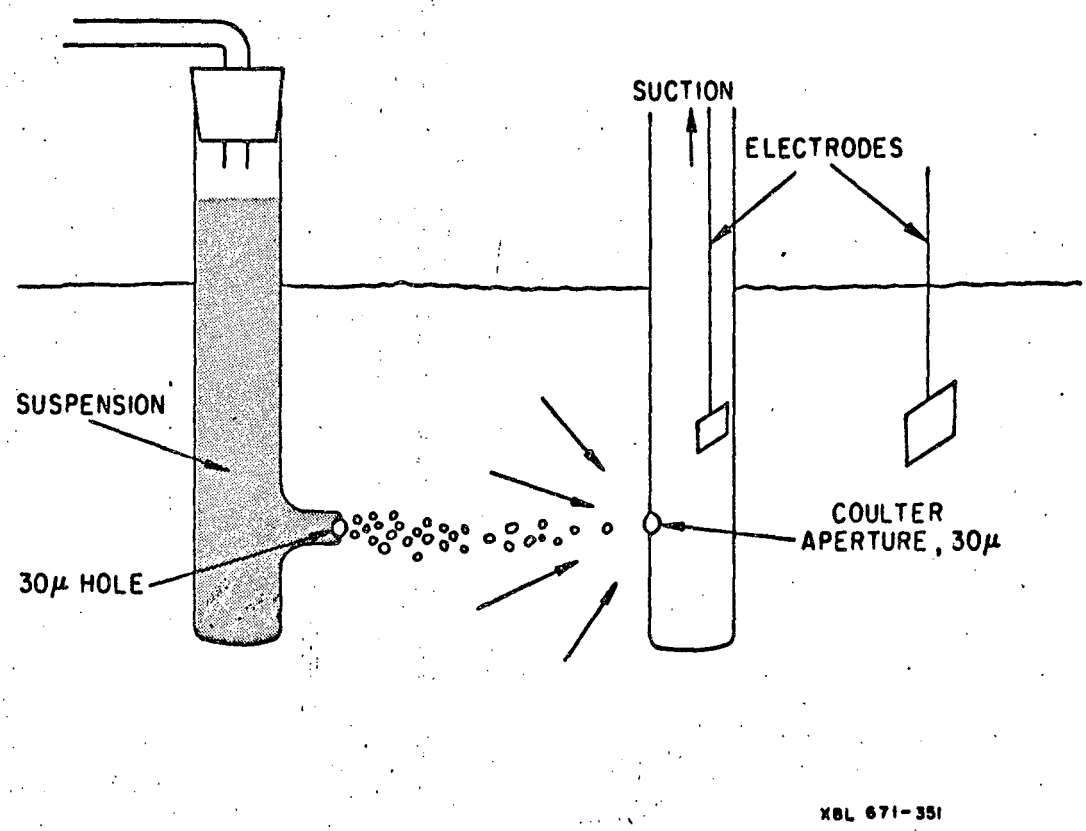

Fig. 2. Diagram of improved particle sizing using hydrodynamic focussing.

B. Sizing and Counting of Bacteria

Kubitschek pioneered the use of a pulse-height analyzer and small-diameter aperture to sizing and counting of bacteria.[2] He measured the size distributions of Escherichia coli cells and Bacillus megaterium spores, using apertures as small as 10 microns in diameter.

Swanton and co-workers compared optical counts, viable counts, and Coulter counts and obtained only fair agreement.[12] They also found that the aperture voltage affected the electronic pulse pattern of line cells but not latex beads or dead cells.

The same group pursued the effect of aperture voltage on viable bacteria, called the emf effect, and showed that during certain phases of growth, the electronic size of cells decreased with increases in aperture voltage. They also found a correlation between plate count and emf effect. Plate counts were consistently lower than electronic counts during growth phases when the emf effect appeared and that the reverse was true when emf sensitivity was not observed. Emf sensitivity was usually greatest before the onset of exponential growth.

Toennies et al. used a Coulter counter to show that the electronic volume of Streptococcus faecalis decreased by 50% over a period of five generation times of exponential growth. Microscopic observation showed that much decrease in the chain length. Harvey and Marr compared the distribution of lengths of E. coli obtained by electron microscopy with the electronic size distribution.[6] By shifting coordinates so that means of the two populations were superimposed, they obtained a chi-square value of the differences of 9.786 with 14 degrees of freedom, which is equivalent to a probability of 0.778 that the observed values were due to chance.

Lark and Lark used the Coulter counter in a study of cell wall synthesis, volume, and ability to concentrate free amino acids during the division cycle.[15] They reported finding little or no change in cell volume until just before cell division, at which point it increased sharply. Their results can be partly explained as the effects of changing

from a long rod into two smaller rods with the accompanying change in electronic sizing due to the shape effects discussed earlier. Increase in cell diameter may also be a factor in the observed results. Lark and Lark found that addition of formaldehyde causes some cells in a population to divide. They measured hemocrit volumes and compared them to electronic volumes, finding that electronic volumes were less than half hemocrit volumes. Lark and Lark proposed that this was due to intercellular water in the hemocrit measurement, but that explanation does not seem adequate to explain such large differences. As will be shown later, electronic sizes are systematically less than optical sizes.

Allison et al. used the Coulter counts in a study into the effects of chloramphenicol.[16] They found that total counts continued to increase somewhat after the addition of chloramphenicol to E. coli cultures in exponential growth. Viable count increased slightly but then began to decrease after about one generation time. Cell conductivity was changed by the addition of chloramphenicol, but not to the point of lysis of the cell membrane; treated cells appeared to be larger than untreated cells.

Ecker and Schoechter correlated the specific growth rate of cells with the volume measured electronically. Agreement was very good for carbon limited cultures, larger cells having higher specific growth rates.

Coulter counting has recently been applied by Knisely and Throop to the determination of lytic activity of the antibiotic lysostaphin, which lyses Staphylococcus aureus in all growth phases. The method was found to be suitable and an improvement over the turbidity method formerly used. They also showed that 30% of unfixed cells died after 10 minutes in a McIlvaine buffer. Lysis was found to follow first-order kinetics.

III. DETERMINATION OF THE SIZE DISTRIBUTION OF POLYSTYRENE BEAD VOLUME STANDARDS

A method of calibrating the electronic sizing and counting system developed in our laboratory was needed. Particles of latex and pollen have been used as standards in other laboratories.[19,20,21,22] The polyvinyl toluene and polystyrene latex particles manufactured and provided by the Dow Chemical Company (Midland, Michigan) were chosen to fill our need for the following reasons: They are

(1) Very uniform in size and shape,

(2) Nonreactive and stable for long periods in the counting medium used, and

(3) Commonly used by other workers as standards.

To determine the size distribution accurately, photographs were made of approximately 450 polystyrene latex particles from a sample of Dow Chemical's Run No. LS-464-E, using a Hitachi Hu-11A electron microscope. The average diameter of 1.305 microns quoted by Dow Chemical for the sample was assumed to be correct. The diameter of the photograph of each sphere was measured with a traveling microscope and the results were analyzed to estimate the distribution of particle sizes and the statistical parameters of the distribution. Figure 3 outlines the steps in the determination of the size distribution from the sample.

A. Methods*

1. Sample Preparation

Carbon films mounted on 3.0 mm diameter copper grids were used as supports for electron microscopy of the latex beads. Preparation of the carbon films and the transfer of the films to the copper grids are described in Appendix I.

---

*All electron microscopy was done with the aid of Mr. Larry Ernst of the Inorganic Materials Research Division of the Lawrence Radiation Laboratory.

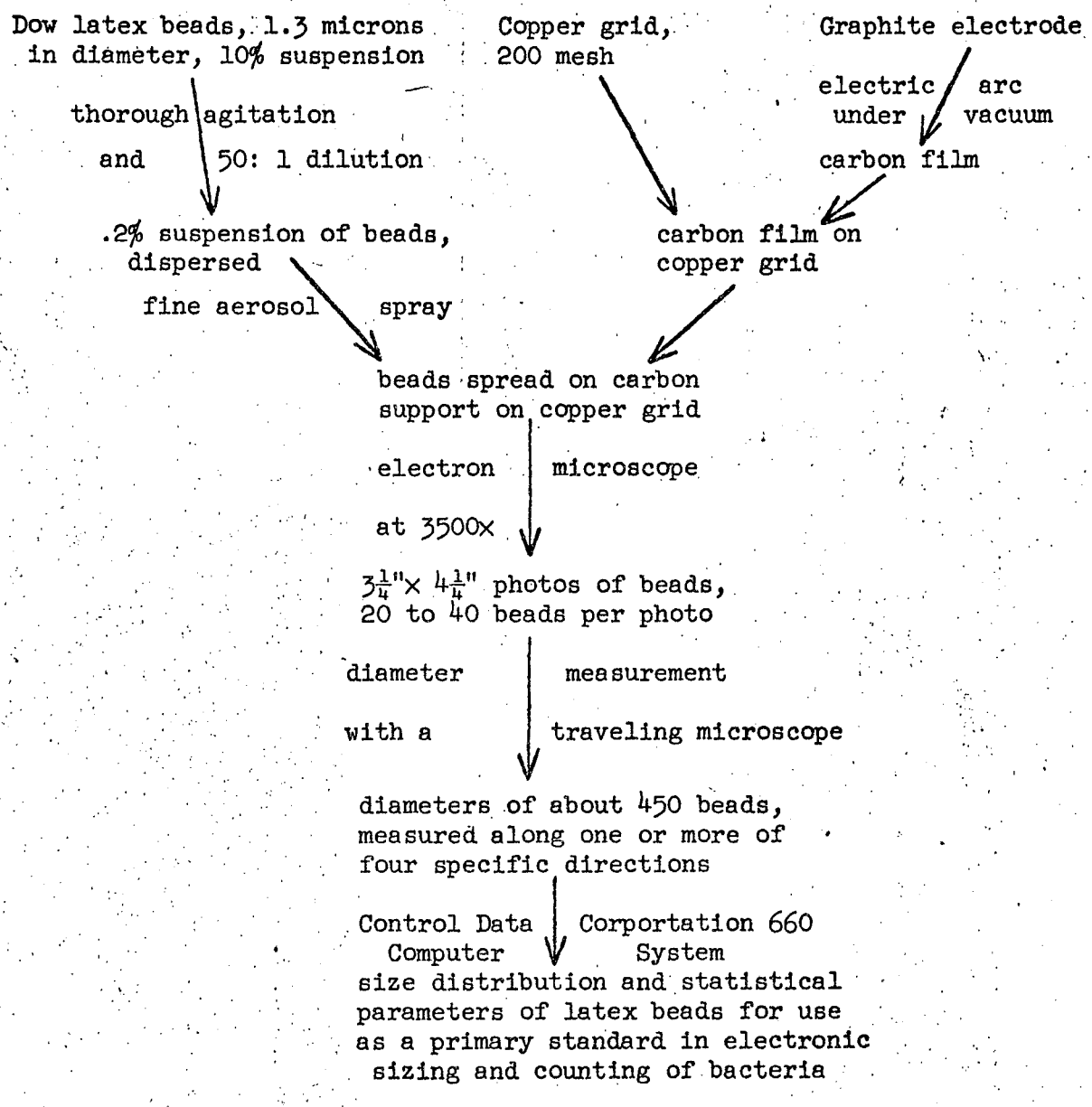

Fig. 3. Outline of the steps in the determination of the size distribution.

The latex beads have a tendency to stick together, which makes the measurement of their diameters more difficult and less accurate. To disperse the beads for photography, the commerical product, which contained about 10% beads in a liquid suspension, was diluted fifty-fold with distilled water and shaken for 5 minutes in a vibrating mixer. The suspension of beads was then sprayed onto the carbon support in the form of a very fine aerosol using a DeVilbiss No. 40 Glass Nebulizer (The DeVilbiss Company, Somerset, Pa.). Repeated sprayings were necessary to achieve the desired concentration on the carbon supports. The sprayed grids were examined with a light microscope after each spraying to determine whether further spraying was required. Even with the precautions just described, the latex particles still had a tendency to agglomerate somewhat, and the addition of various surface-active agents and organic solvents did not appear to improve dispersion.

2. Photography and Diameter Measurement

Seventeen groups of between 20 and 40 beads per groups were photographed at magnifications of about 3500x with a Hitachi Hu-11a electron microscope (accelerating voltage = 50 keV, pole piece #3, V), using current on intermediate lens = 39 ma and 3 1/4" x 4 1/4" contrast grade lantern slides (Eastman Kodak Company, Rochester, New York). The photographs are reproduced in Figs. 4, 5, 6, and 7. The images of the beads on the photographs were about 4.5 cm in diameter. Note that most particles in the photographs are spherical and of a uniform size.

The diameters of the photographic images of the particles were measured using a traveling microscope (David W. Mann Co., Lincoln, Mass.) that was equipped with a stage micrometer (Bausch & Lomb Incorporated, Rochester, New York) and was accurate to ± 1 micron, and an analog-digital converter (Datex Corporation, Monrovia, Calif.). Gear errors were reduced by bringing the cross-hair reticle in the eyepiece into coincidence with the image of the particle boundaries from the same direction for both sides of the particle. Repetitive measurements

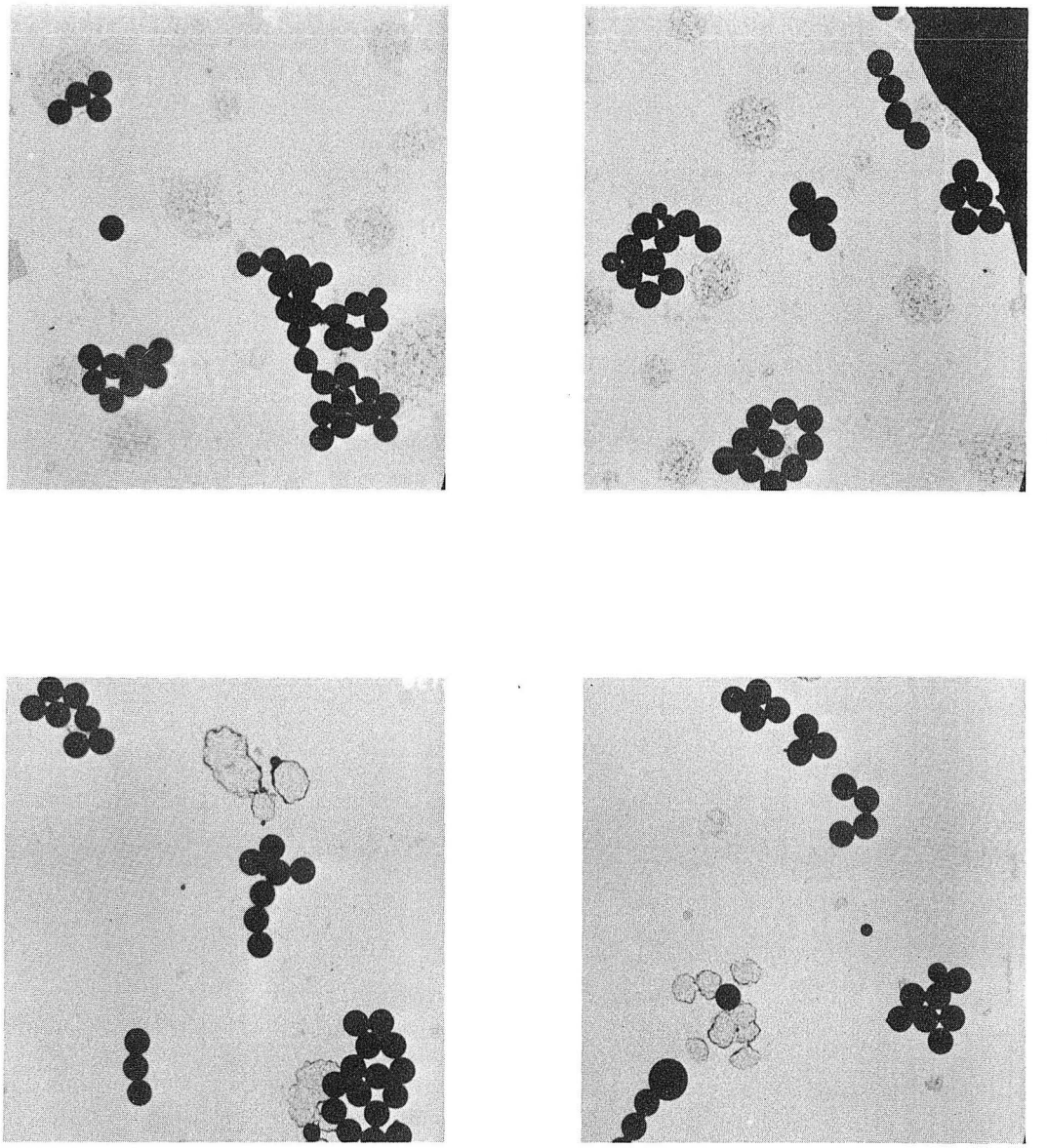

XBB 671-396

Fig. 4. Photographs of polystyrene beads made by electron microscopy.

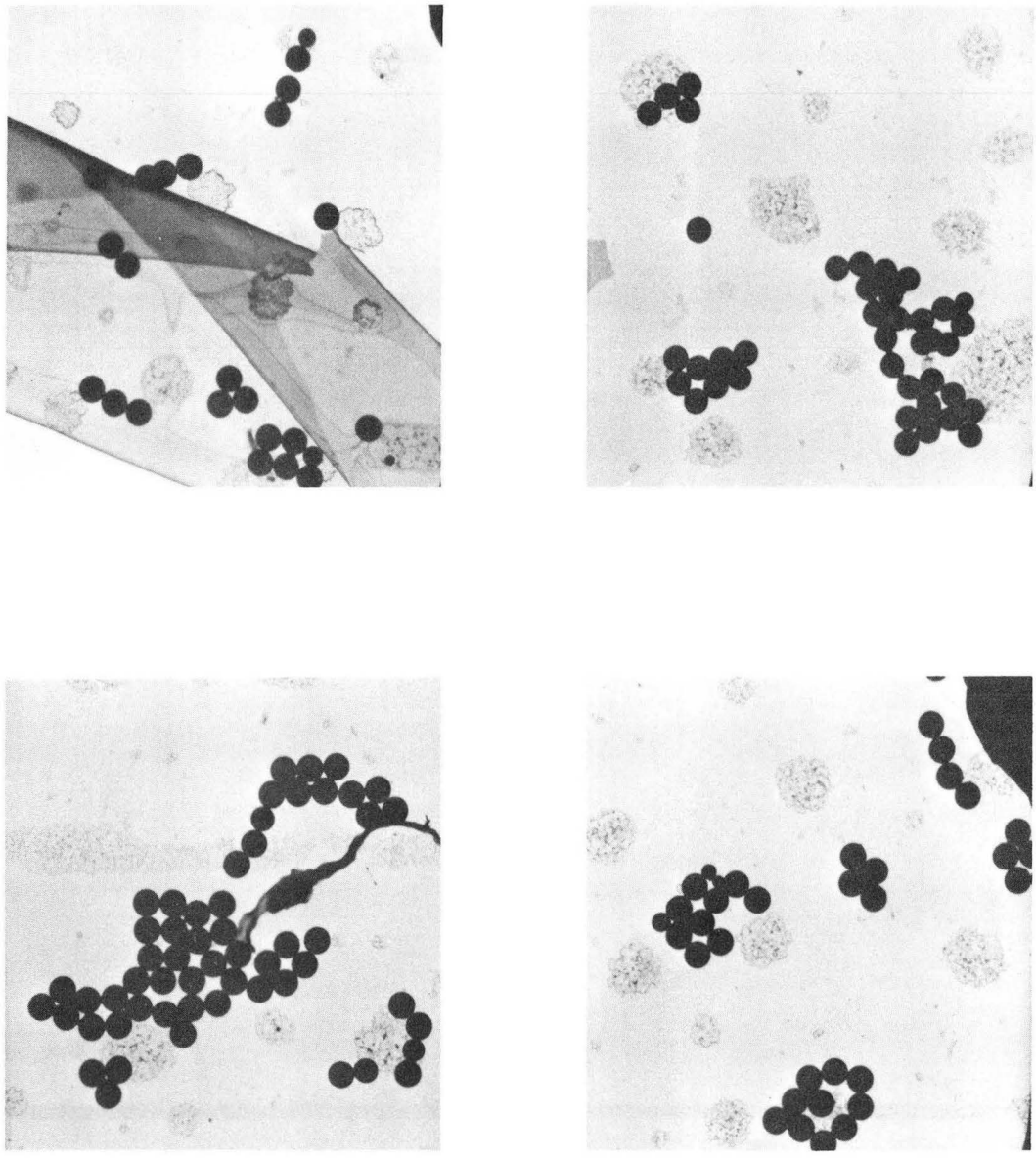

XBB 671-397

Fig. 5. Photographs of polystyrene beads made by electron microscopy.

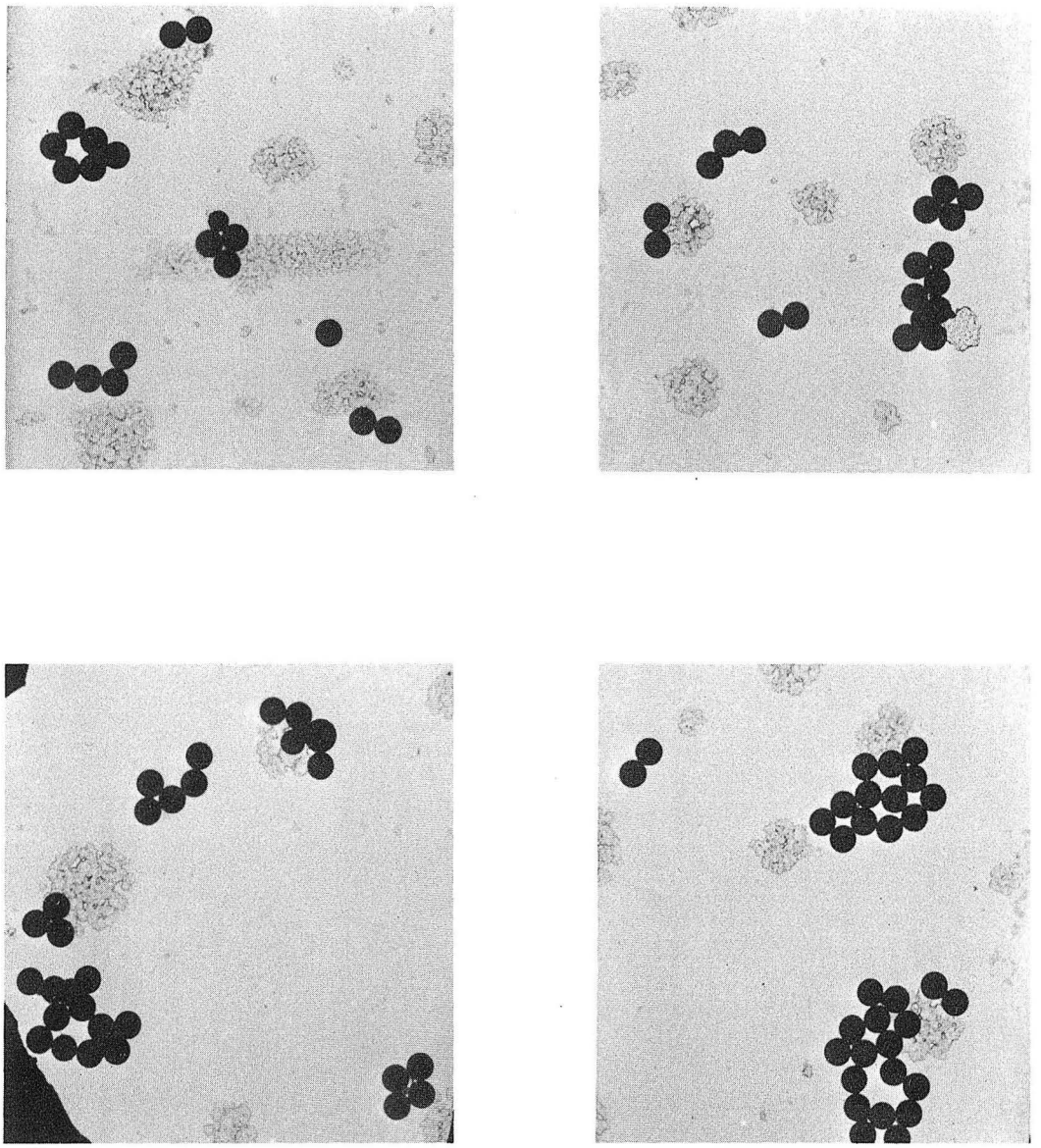

XBB 671-398

Fig. 6. Photographs of polystyrene beads made by electron microscopy.

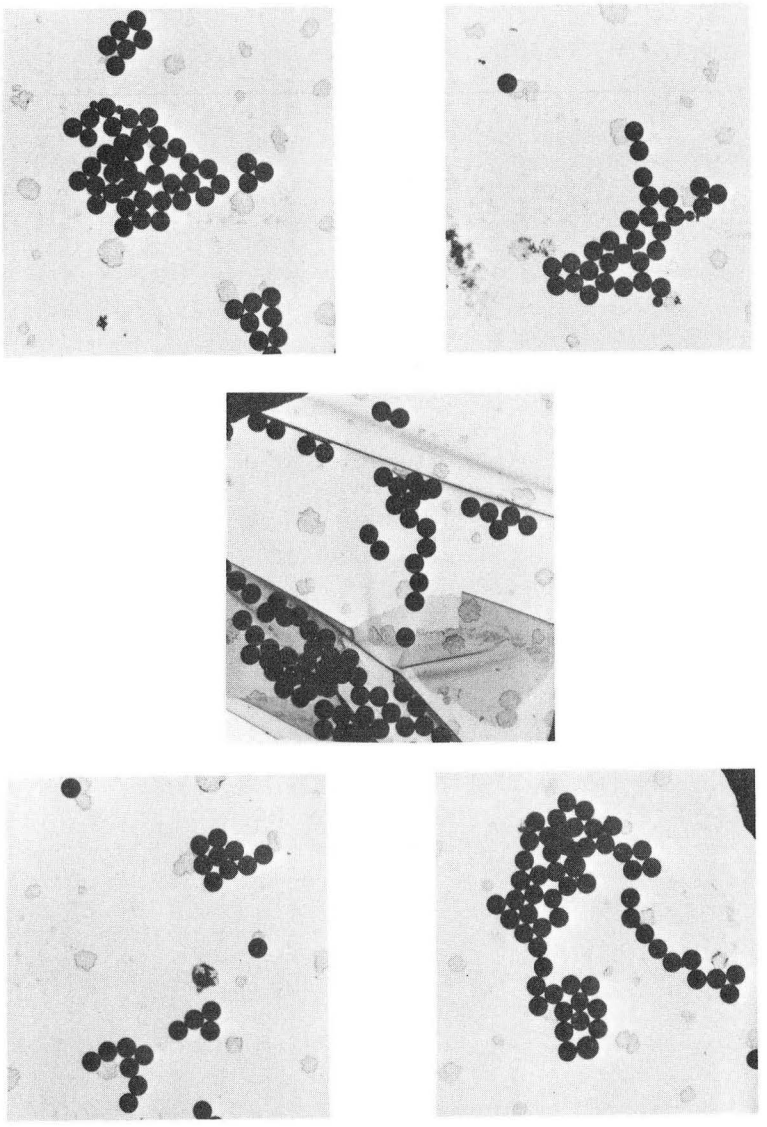

XBB 671-399

Fig. 7. Photographs of polystyrene beads made by electron microscopy.

with the traveling microscope discussed in Appendix II had a standard deviation of 3.45 microns, or about .08% of the diameter of the images of the particles. The accuracy of the traveling microscope was thus more than adequate for the measurement of the diameters of the particle images.

B. Results

1. Astigmatism

Although the electron microscope was cleaned and adjusted to eliminate astigmatism just before use, the extremely narrow range of diameters made a correction for astigmatism necessary. To make corrections for astigmatism possible, the diameter of each particle was measured only along one or more of the four axes shown in Fig. 8. Correction factors for astigmatism were estimated by comparing the average of the diameters measured in the X-direction on several groups of particles with the average of diameters measured in the other three directions for the same groups of particles. Statistically significant differences in magnification were found to occur between the four different axes, with a maximum difference of 1.3% between the X and YA directions. The calculations are discussed in Appendix III. The diameters measured in each direction were then corrected for the observed astigmatism as follows. The diameters in the YA-direction were arbitrarily assumed to be unaffected by astigmatism, and diameters observed in the other three directions were multiplied by the ratio of the averaged diameters in the YA-direction (for a test group) to the averaged diameters in the other direction (for the same group of particles). The following equations summarize the method used to correct for astigmatism:

$$D_{YA}(\text{corrected}) = D_{YA}(\text{observed})$$

$$D_X(\text{corrected}) = D_X(\text{observed} \times (\bar{D}_{YA}/\bar{D}_X)$$

$$D_{YB}(\text{corrected}) = D_{YB}(\text{observed} \times (\bar{D}_{YA}/\bar{D}_{YB})$$

$$D_Z(\text{corrected}) = D_Z(\text{observed}) \times (\bar{D}_{YA}/\bar{D}_Z)$$

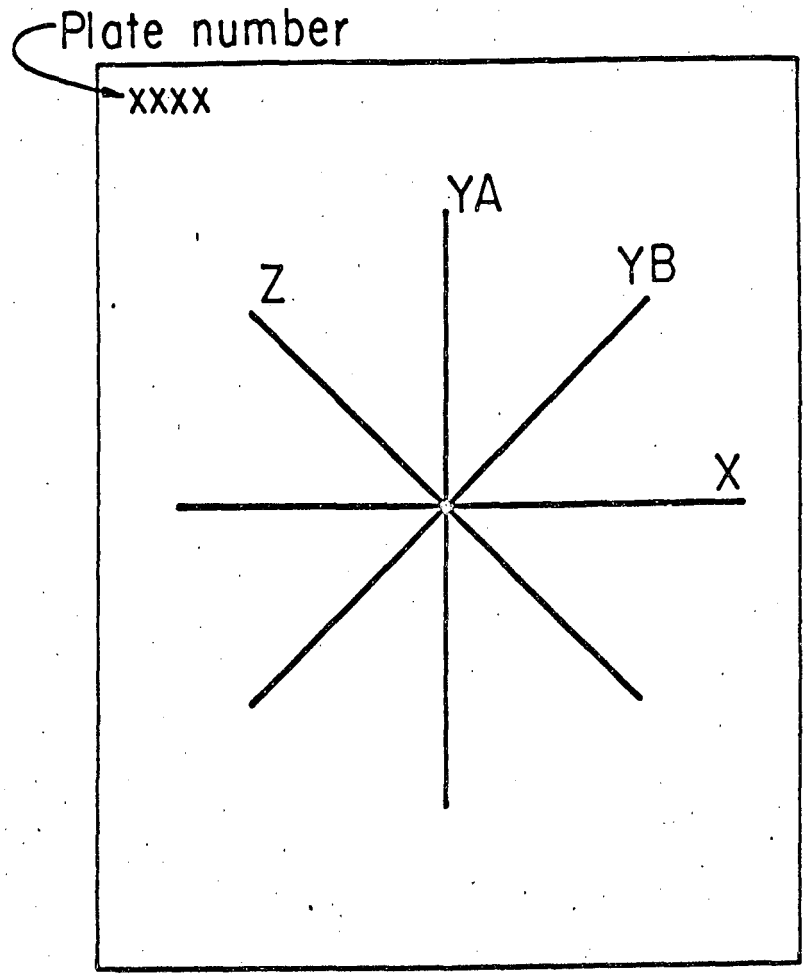

XBL 671-283

Fig. 8. Orientations of the four axes for diameter measurements with respect to each photographic plate.

where D_i (observed) = observed diameter in i-direction of a given particle,

D_i(corrected) = diameter of same particle in i-direction corrected for astigmatism, and

$\bar{D}_{YA}/\bar{D}_i$ = astigmatism correction factors (listed in Table V).

2. Computer Program

The analysis of the particle diameters was done using Control Data Corporation 6600 computer system. Figure 9 is an outline of the program of operations that were performed on the data with the computer. Appendix IV lists the actual program, which was written in the Chippewa version of the Fortran coding language.

The program calculates the diameters and volumes for each particle, correcting for the effects of astigmatism as outlined in the preceding section and for variations in magnification from photo to photo as will be discussed in the next section. Diameters are also adjusted so that the mean diameter of the population is equal to 1.305 microns.

The statistical parameters of particle diameters defined in Table I are also computed for the particle volumes on each photograph. Volume parameters are identified in the program with the corresponding letter or letters assigned to diameter parameters, except that a "V" is added, e.g., UV(I) = mean volume of the particles on the Ith photo, VV(I) = variance of the volumes of the particles on the Ith photo, etc. A similar set of statistical parameters is computed for the combined data of all groups analyzed for both particle diameters and particle volumes. Overall parameters are denoted by the symbols UT = grand weighted mean of particle diameters, UTV = grand weighted mean of particle volumes, VT = grand weighted variance of particle diameters, etc.

The program also sorts the particle sizes into 500 different groups according to diameter by intervals of .01 microns ranging from 0 to 5 microns in diameter. The number of particles found in each of the 500 groups is then printed. A similar histogram of the distribution of particle volumes is computed for intervals .01 cubic microns wide and printed.

```
READ NUMBER OF PHOTOS

READ FOR EACH PHOTO
     IDENTIFICATION NUMBER
     NUMBER OF PARTICLES
     MAGNIFICATION FACTOR
     FOR EACH PARTICLE
        Number of Diameters measured
        Diameter coordinates

DO FOR EACH PHOTO
     SET STATISTICAL PARAMETERS EQUAL TO ZERO INITIALLY
     DO FOR EACH PARTICLE
        Calculate diameters from coordinates
        Correct diameters for astigmatism
        Compute average diameters
     COMPUTE APPARENT MAGNIFICATION FACTOR(MEAN-ESTIMATED)
     DO FOR EACH PARTICLE
        Correct average diameter for magnification error
        Compute average volume
        Prepare histograms of average diameters and average volumes
     COMPUTE STATISTICAL PARAMETERS

DO FOR EACH PHOTO
     WRITE IDENTIFICATION NUMBER
     DO FOR EACH PARTICLE
        Write diameters in four different directions, average diameter
        and average volume
     WRITE STATISTICAL PARAMETERS

WRITE HISTOGRAM OF DIAMETERS

WRITE HISTOGRAM OF VOLUMES

COMPUTE FREQUENCY DIAGRAMS OF DIAMETER AND VOLUME

WRITE FREQUENCY DIAGRAMS OF DIAMETER AND VOLUME

COMPUTE STATISTICAL PARAMETERS FOR COMBINED DATA OF ALL PHOTOS

WRITE OVERALL STATISTICAL PARAMETERS
```

Fig. 9. Outline of computer program for analysis of particle diameter data.

Table I. Statistical parameters calculated for the particle diameters on each photograph

Name	Symbol in computer program	Definition
mean diameter	U(I)	weighted average of diameters of particles on Ith photograph
variance of diameters	V(I)	weighted average of squares of deviations of average particle diameters from U(I) for the Ith photo
standard deviation of diameters	S(I)	square root of V(I)
momental skewness	A3(I)/2	one half the weighted average of the cubes of the deviations of average particle diameters from U(I), divided by S(I) cubed
kurtosis	(A4(I)-3)/2	see definition of A4(I)
---	A4(I)	weighted average of the difference between the average particle diameters and U(I), raised to the fourth power, divided by V(I) squared

Both histograms are normalized by dividing each value by the total number of particles analyzed and the two resulting frequency diagrams are then printed.

C. Discussion

The magnification of the electron microscope could be estimated within an accuracy of only about 10%, making a check of the average diameter of 1.305 microns given by the supplier impossible. It was thus assumed in the calculations that the figure was correct. With this assumption, the apparent magnification factors were calculated independently for each photograph (denoted as DIAMETER FACTOR in Tables II and III). Large, statistically non-random variations in magnification appeared to occur as shown by the graph (Fig. 10) of apparent magnification versus photograph. The apparent magnification factors are plotted in the same order that the photographs were taken, and a fairly regular variation in the mangnification factors can be observed. There are three or more sources of this systematic error. The changes in magnification between photographs were caused, at least in part, by the adjustments made on the microscope to keep the specimen in focus. We were not aware of this source of error when the photographs were taken and did not record the fine adjustments in the microscope that could have been used in conjunction with a calibration experiment to calculate magnification factors on each photo. The second likely source of variation in magnification is the shift in intensity of illumination of the screen to lower values for photography after focusing. A third possible source of error, variation in magnification as a function of position of the sample in the electron microscope, could also be contributing to the observed variation between photos. Variation in the size of the photographs themselves during processing is unlikely since glass photographic plates were used rather than film.

Table II. Comparison of different methods of estimating magnification factors

Method of estimation	Standard deviation of diameters (microns)	Nature of histogram of combined data
Data supplied by manufacturer	0.0158	not available
Mean-estimated, very large and very small data removed	0.01493	good, smooth
Assumed same for all photos	0.04041	poor, ragged
Estimated from smoothed curve of Fig. 7	0.03295	fair, somewhat ragged
Mean-estimated except for photos 1, 2, 3, 6, which were adjusted towards normal values by two standard deviations	0.01892	fair, somewhat ragged
Last 5 photos, same factor for each photo	0.01326	fair
Last 5 photos, mean-estimated factors	0.01093	fair-to-good

Table III. Comparison of statistical parameters of distributions with and without consideration of unusually small and large particles

Parameter	Without unusual data	All data analyzed
mean diameter (microns)	1.305	1.28988
mean volume (cubic microns)	1.1641	1.14611
standard deviation of diameters (microns)	0.01493	0.11227
standard deviation of volumes (cubic microns)	0.039599	0.24735
momental skewness of diameters (dimensionless)	-0.3826	-2.0748
momental skewness of volumes (dimensionless)	-0.31345	-2.7299
kurtosis of diameters (dimensionless)	1.326	19.375
kurtosis of volumes (dimensionless)	1.150	45.321

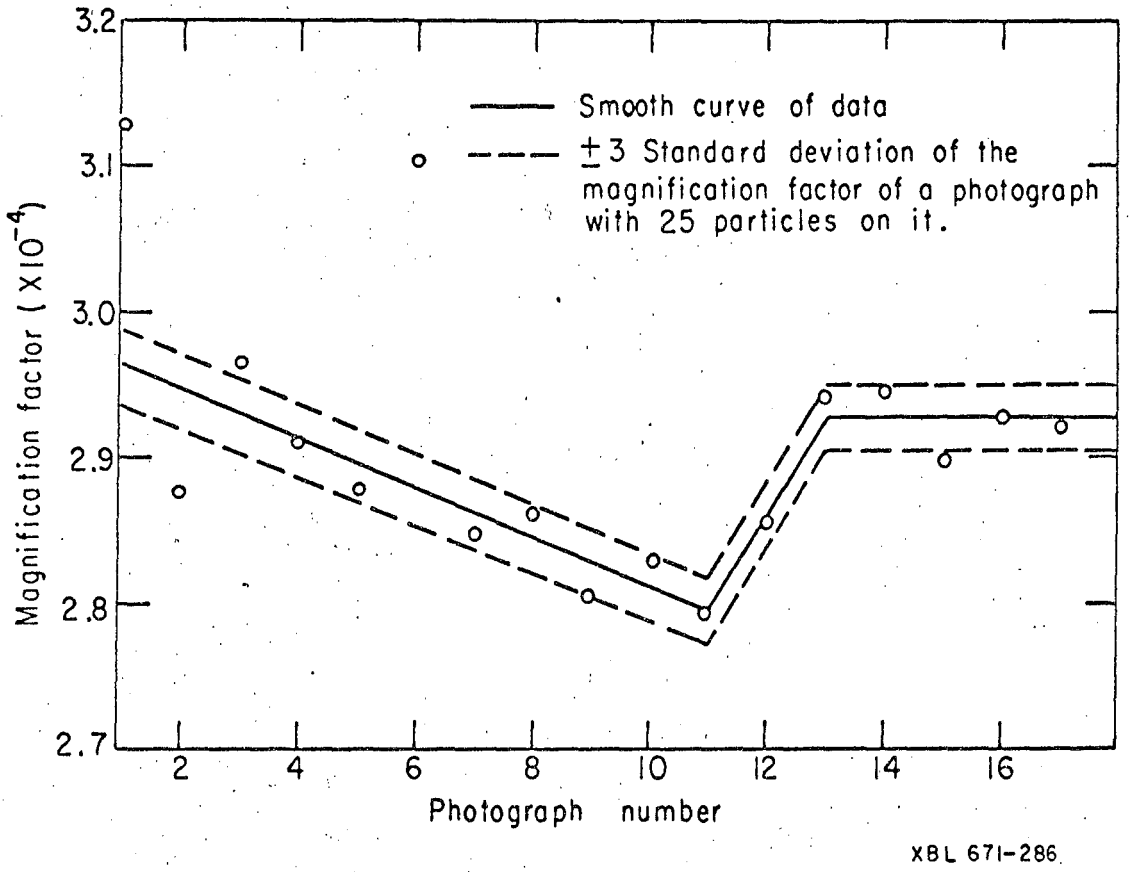

Fig. 10. Magnification factors versus photograph number.

Combination of the data from the different photographs required that fairly accurate estimates of the unknown and varying magnifications be available for each photo has the inherent limitation that the mean diameter of the particles on a given photograph is not likely to be exactly equal to the true mean diameter of the population. When the number of particles per photograph is large enough, and when there is no systematic variation of magnification for different points on the same photo, the means for the photos will normally be distributed about the true mean. The standard deviation of the mean diameters of the photos about the true mean can be estimated from the following formula:

$$s_m = \sigma_p / \sqrt{n}$$

where s_m = standard deviation of the sample mean,

σ_p = square root of the variance of the population, and

n = number of particles on each photograph.

Because each photograph contained between 20 and 37 measurable particles, the assumption of a normal distribution of sample means is fairly accurate and it can be seen that the potential deviation of the calculated size distribution could be dispersed from the true size distribution by roughly $1/\sqrt{25}$, or 20%, and would probably tend to be misshapen somewhat.

To see if a more narrow distribution could be obtained by estimating the magnification for each photograph in other ways, several other approaches were tried. They included the following:

(1) Estimation by assuming that the sources of variation in magnification caused a continuous variation in magnification factors with photographic order, represented by the smoothed curve through the data in Fig. 10.

(2) Assumption of the same magnification for each photograph.

(3) Assumption of the mean-estimated (the method of setting average diameters on each photo equal to 1.305 microns) magnification factors, except for those showing very wide deviations from the majority.

Adjustment of unusual mean-estimated magnification factors toward the majority value by two standard deviation of their respective means.

(4) Analysis of only the last five photos, assuming a constant magnification factor.

(5) Analysis of only the last five photos, using mean-estimated magnification factors.

Table II shows that none of these alternatives improved the overall character of the observed size distribution beyond that originally obtained using mean-estimated magnification factors throughout. The fourth and fifth methods did reduce the standard deviation, but gave distributions of irregular shape compared to the results obtained with the original method of using mean-estimation magnification factors. Certainly not all alternatives were exhausted, and use of a method such as variation of the magnification factors to minimize the value of chi-squared between different photos would probably lead to a significant increase of narrowness of the true distribution, but the difficulty of additional manipulations of the data is not felt to be justified by the return. The final distributions chosen are shown in Figs. 11 and 12, the first being a frequency diagram of diameter and the second a frequency diagram of particle volume. They were calculated by combining all data (including unusually small or large particles) using mean-estimated mangification factors. Statistical parameters for these distributions and for the same magnification factors with particles of unusual sizes removed are compared in Table III. The results are given in complete form for these two cases in Tables XXXXI and XXXXII of the Appendix.

Comparison of the value of the standard deviation of diameters (with unusual particles removed) shown in Table III is 0.0149 microns. This is in good agreement with the value of 0.0158 microns obtained on the same system by the supplier, Dow Chemical Company. This agreement and the relative smoothness of the size distributions in Figs. 11 and 12 is felt to be partial confirmation of our belief that the measured distribution is reaonably close to the true distribution.

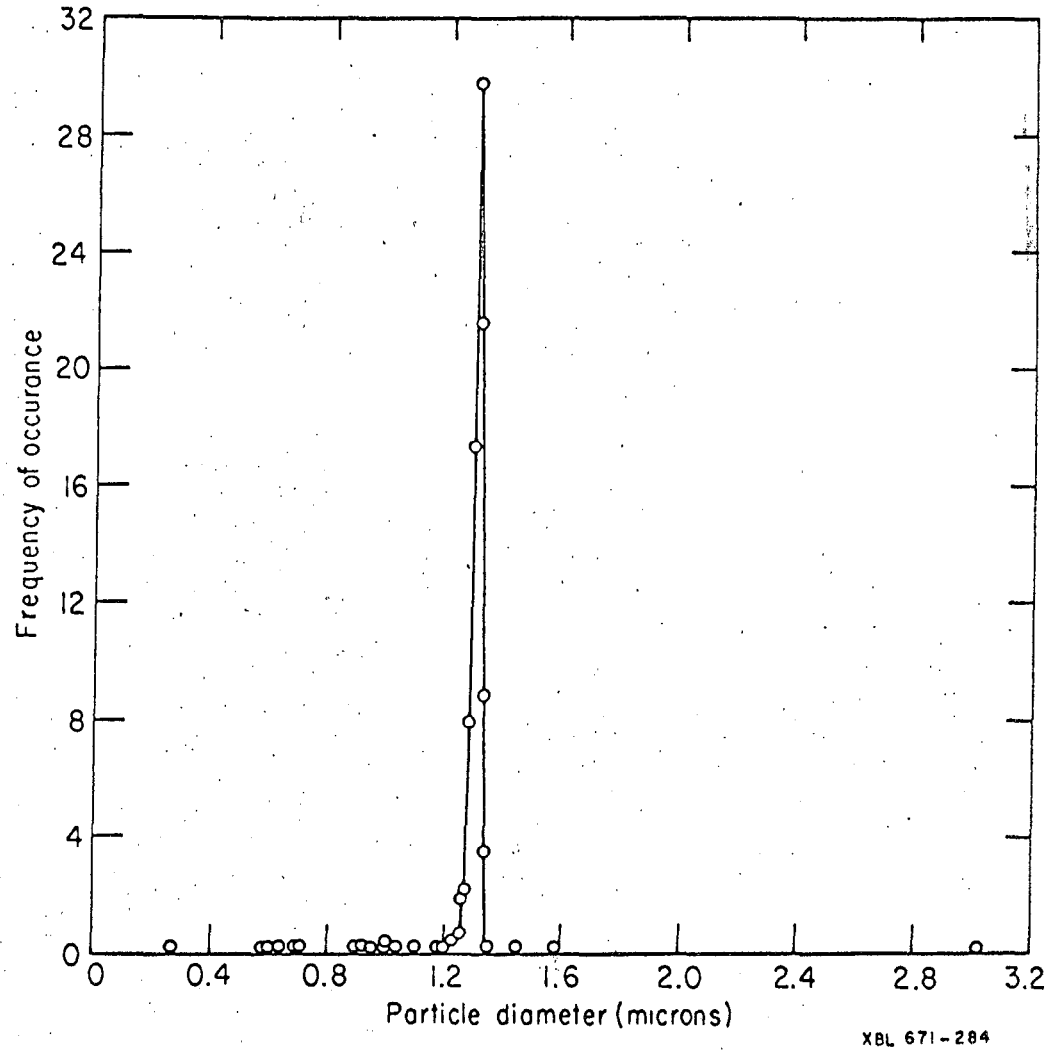

Fig. 11. Frequency diagram of particle diameters.

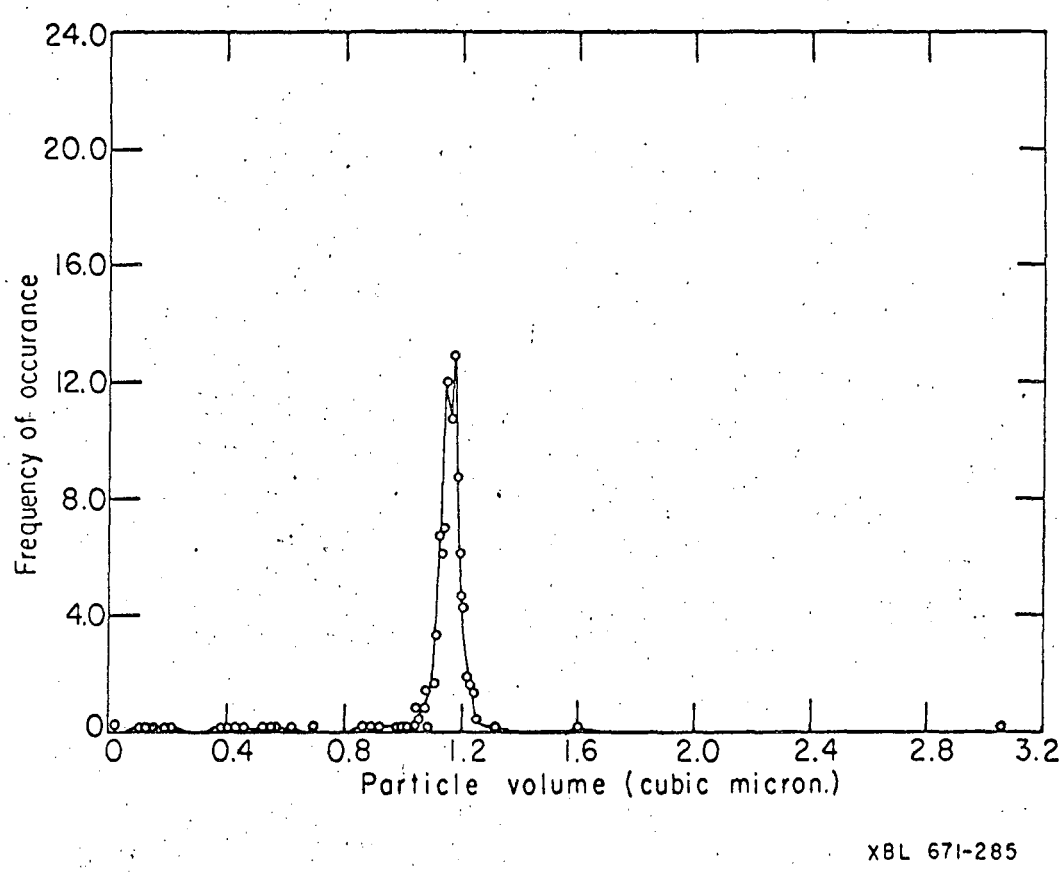

Fig. 12. Frequency diagram of particle volumes.

D. Conclusions

Photographs of about 450 latex spheres have been obtained with an electron microscope and the images of the spheres measured with a traveling microscope. The data have been analyzed and a reasonable estimate of the true size distribution and its statistical parameters has been made from the analysis that is in good agreement with values obtained by the manufacturer.

It is suggested that in the future, lower magnifications be used, so that all particles to be analyzed will be on a single photograph, eliminating the need to consider variations in magnification between photographs.

IV. SYSTEM CALIBRATION

In this section, the physical and electrical properties of the aperture are reported. The linearity of the response of the electronics and of the entire system is demonstrated over a wide range of variables. Reproducibility of the system is examined. Finally, the effects of pulse shaping are examined and optimal settings are chosen on the basis of resolution.

A. Characteristics of the Aperture

1. Physical Characteristics

Dimensions and appearance of the aperture were determined using a phase contrast microscope having a calibrated fine focus adjustment for depth measurements. The aperture was examined with an oil immersion objective and photographed at a magnification of about 720×. Diameters were measured from the photographs and computed by comparison to a photograph of a stage micrometer made at the same magnification. The diameter was found to be 32.1 microns at the outer surface of the aperture. In appearance, the aperture seems to be a right circular cylinder with slightly beveled edges at either end of the aperture. The average length was measured as 29.5 microns.

2. Electrical Characteristics

The conductivity of the electrolyte was varied, and both electrolyte conductivity and the reciprocal of the aperture resistance were measured. The results are shown in Fig. 13 and Table IV. The slight nonlinearity of the curve may be due to an electrode resistivity.

The effect of aperture voltage on aperture resistance was also tested. A circuit diagram is given in Fig. 14. As can be seen, what we call aperture voltage is actually the electrical potential across the aperture and a 34 kohm resistor in series with it. For the sake of convenience, we shall always refer to aperture voltage as defined in Fig. 14. Aperture voltage was varied from 0.65 volts to 150 volts and aperture currents were measured..

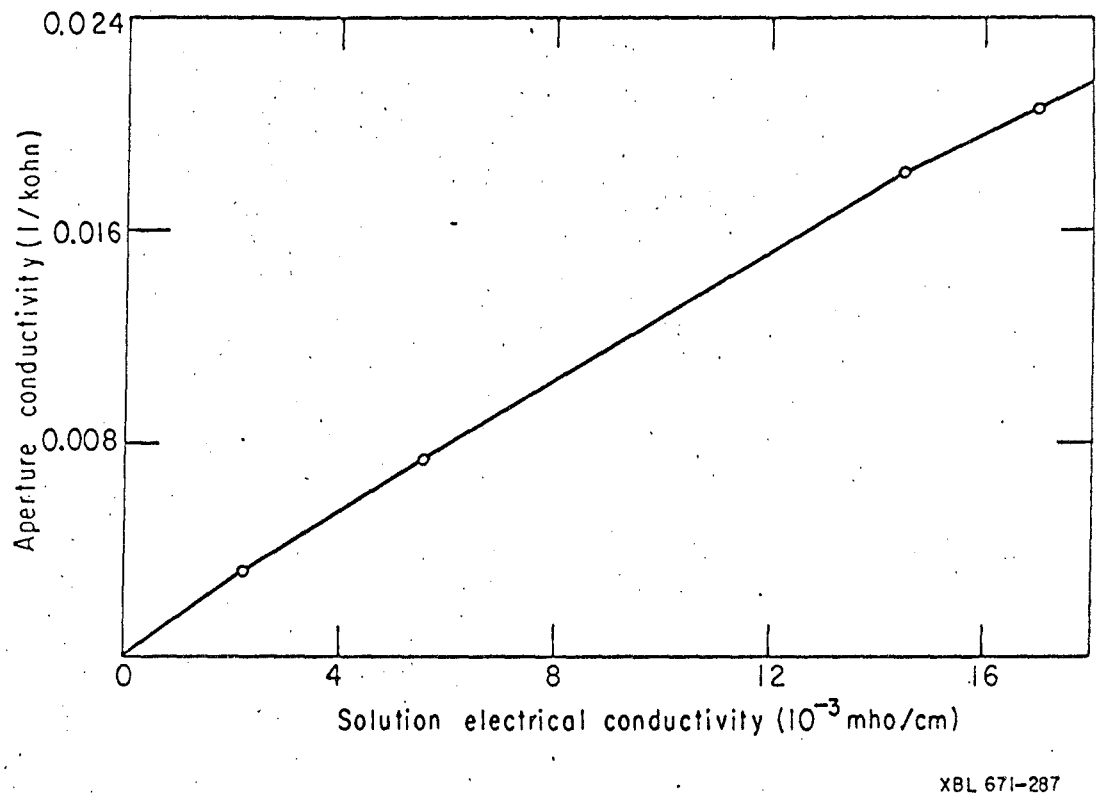

Fig. 13. Aperture conductivity versus solution conductivity.

Table IV. Effect of Solution Conductivity on Aperture Conductivity

Electrolyte Identification	Reciprocal of Aperture Resistance ($kohms^{-1}$)	Conductivity of Electrolyte (10^{-3} mho/cm)
1	.0286	> 17.9
2	.0206	17.0
3	.0182	14.6
4	.00741	5.5
5	.00318	2.18

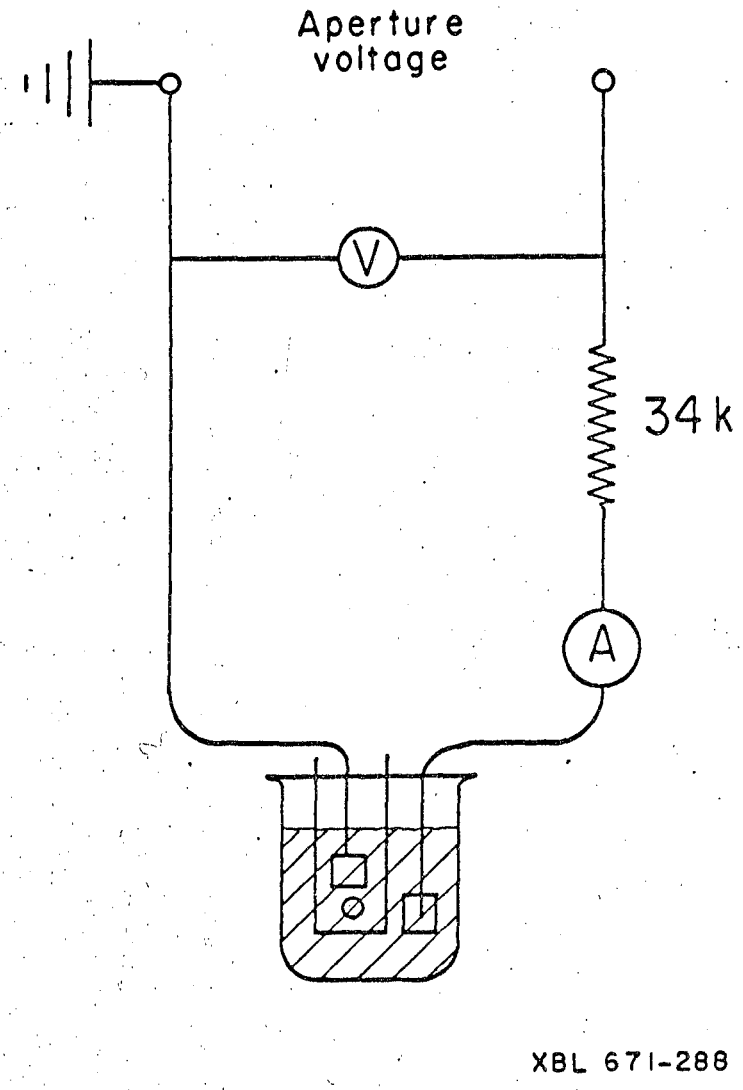

Fig. 14. Circuit diagram of aperture.

The results are shown in Table V. The first entry in the table is a voltage of 0.65 volts with no resulting current. This is due to polarization of the electrodes. Aperture current is plotted versus voltage in Fig. 15. Deviations from the expected linear relationship is evident at voltages above 60 volts. Deviations at higher voltage are due to heating in the aperture, leading to a higher electrical conductivity in the aperture. If heating is indeed responsible, the decrease in the overall aperture resistance should be directly proportional to the overall power input to the aperture. Figure 14 shows a circuit diagram for the aperture system under study.

From the circuit in Fig. 14 and from the value of polarization voltage, the following equations can be derived.

$$\text{Overall Aperture Resistance} = \frac{V - .65}{I} - 34\ K$$

$$\text{Overall Aperture} = (V - .65)I - (34)I^2$$

$$\text{Decrease in Overall Aperture Resistance} = \lim_{I \to 0} (R) - R$$

$$= R_o - R$$

$$= - \Delta R$$

Values for these variables are shown in Table V. The erratic values of the aperture resistance at aperture voltages below 20 volts are due to inaccuracy in the measurement of current and voltage at small values. Power input is plotted versus the decrease in aperture resistance in Fig. 16. The correlation is very strong, confirming that changes in aperture resistance are due to heating in the aperture. At an aperture voltage of 150 volts, the decrease of aperture resistance is 19%, suggesting a mean temperature change of roughly 10°C. Thus the temperature rise of the fluid passing through the aperture would be of the order of 20°C. Such a high temperature rise might strongly affect the electronic size of cells passing through the aperture by affecting their electrical properties, but the residence time of particles in the aperture is short

Table V. Effect of Aperture Voltage on Aperture Current

Aperture Voltage (volts)	Aperture Current (milliamps)	Overall Aperture Resistance (kilohms)	ΔR (kilohms)	Overall Aperture Power (watts)
0.65 (extrapolated)	0	-	-	-
1	0.0053	32.0	-	-
2	0.0161	49.9	-	-
3	0.0250	60.0	-	-
5	0.0491	54.6	-	-
10	0.121	43.3	-	-
20	0.225	52.0	0	0.00263
30	0.341	52.1	-0.1	0.00706
40	0.464	50.8	-1.2	0.01094
50	0.568	51.4	-0.6	0.0149
60	0.700	50.8	-1.2	0.0248
70	0.832	49.4	-2.6	0.0342
80	0.955	49.1	-2.9	0.0448
90	1.092	47.8	-4.2	0.0571
100	1.24	46.1	-5.9	0.0709
110	1.36	46.4	-5.6	0.0858
120	1.53	44.0	-8.0	0.1030
130	1.66	43.9	-7.9	0.1209
140	1.80	43.4	-8.6	0.1406
150	1.96	42.2	-9.8	0.1621

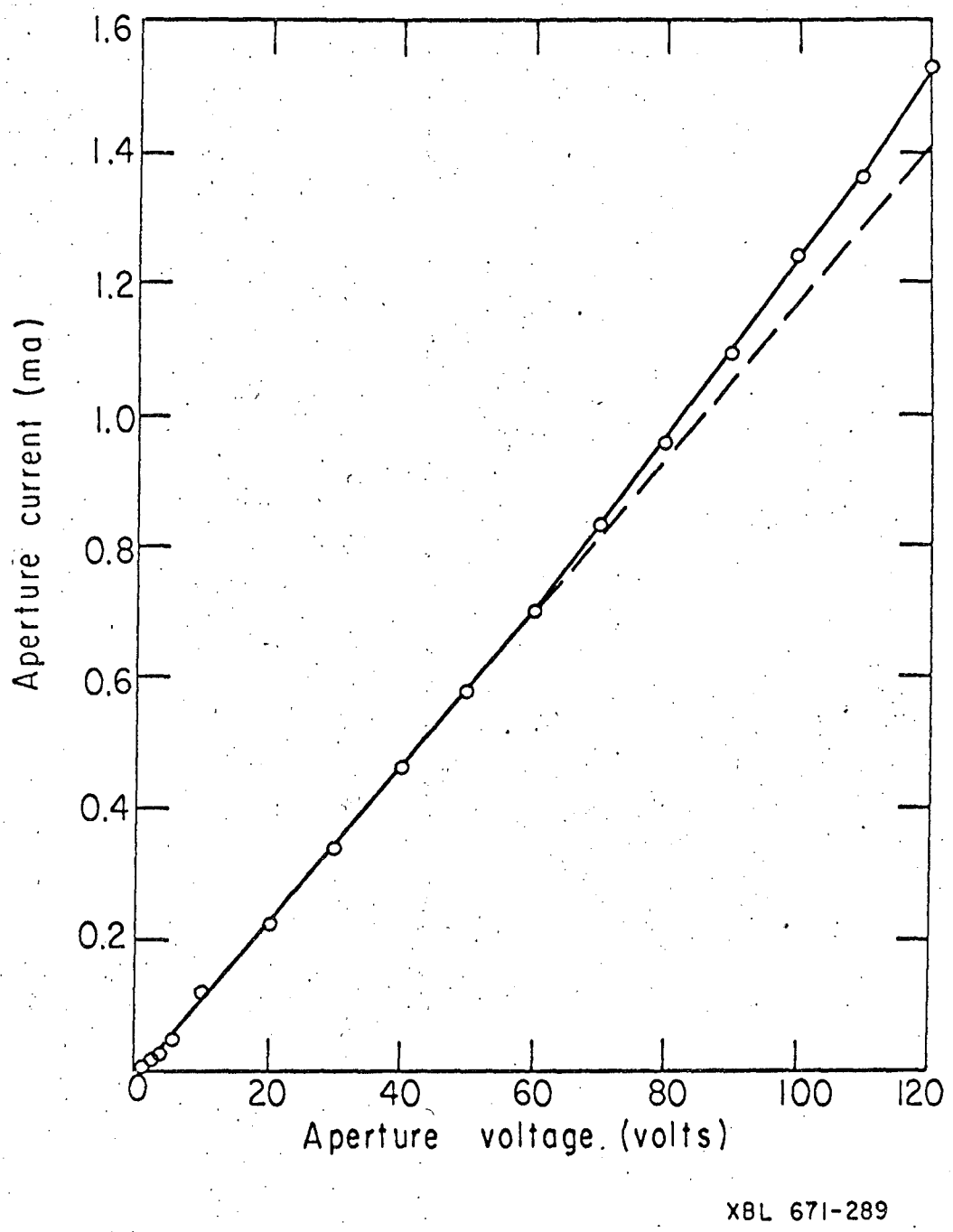

Fig. 15. Aperture current versus aperture voltage.

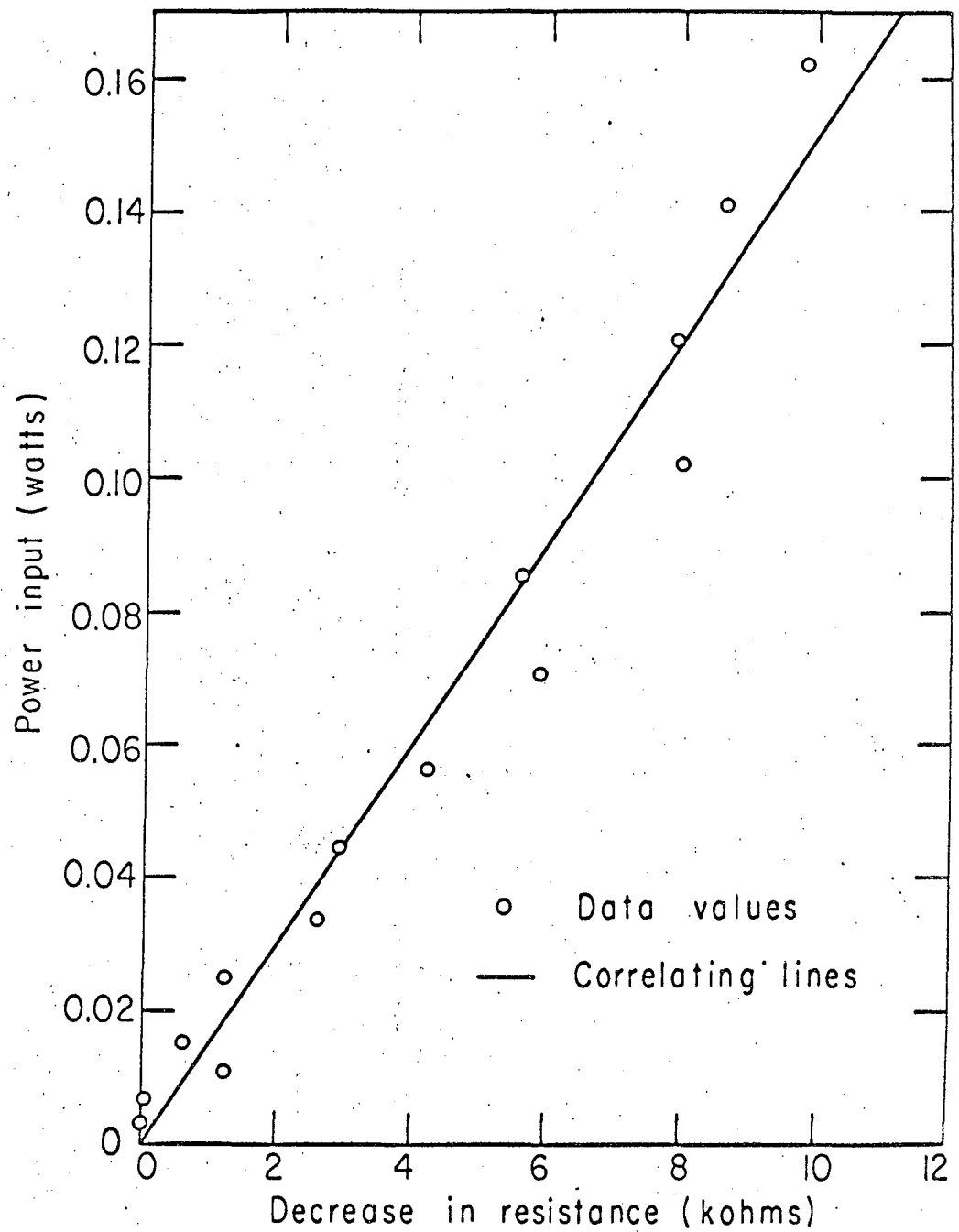

XBL 671-290

Fig. 16. Power input versus decrease in aperture resistance.

so the change would have to be rapid. Also, heating in the aperture could increase the flow rate through the aperture by lowering the viscosity of the electrolyte. Such a change would increase the total count. As will be discussed later, increased counts (by about 10% when the aperture voltage was increased from 24 volts to 96 volts) followed increased aperture voltages in the case of plastic beads, but total counts of bacteria remained constant. It is possible that a fraction of the bacteria were lysed at higher aperture voltages, offsetting the increase in flow rate.

Temperature would be less likely to affect inert particles such as polystyrene beads. The overall conductivity change itself should not greatly affect the sizing capabilities of the system because of the reasons given by Gregg and Steidley, provided that a current sensitive low input impedance preamplifier is used.[3]

However, heating in the aperture could be expected to give slight improvement of resolution because it would promote plug flow by heating regions of low flow rates more, thus decreasing viscosity and leading to an increased flow rate there. As will be shown later, resolution was improved by higher aperture voltages; the standard deviations of both beads and cells being decreased. Also, because the electronics unavoidably integrate the pulses to a certain extent, the higher conductivities in the regions of longer residence times tend to give pulse areas more nearly equal to areas of pulses from particles passing through rapidly. Thus the integrated pulses seen by the electronics are more nearly equal for particles of the same size. The main disadvantages of the increased aperture voltages are that boiling in the aperture is a more common occurrence and that the electronic sizes of bacteria are reduced, as will be discussed later.

B. Characteristics of Electronics

Referring to Fig. 1, it will be noted that electrical pulses caused by passage of particles are first amplified in the preamplifier and then shaped and further amplified by the amplifier before sorting and counting by the pulse-height analyzer. The aperture voltage is applied with a modified Lawrence Radiation Laboratory Slim Gem Power Supply, Model 4V9804 (not shown in Fig. 1). The preamplifier is an EC 1000 low-noise Lawrence Radiation Laboratory 198 system charge sensitive preamplifier (number 11X 2950 P-1). The amplifier is a Tranlamp (number 15X-4845). The pulse height analyzer is a 128-channel analyzer (manufactured by Nuclear Data, Inc., Palatine, Ill.), Model 110. A Nuclear Data Model 410 cathode-ray oscilloscope is used to display the memory of the analyzer. The analyzer also drives an X-Y recorder (Model 2D-2, Mosely Autograf, Pasadena, Calif.) and an electric typewriter paper tape punch (Model 33, Teletype Corporation, Skokie, Ill.). The output of the analyzer is a graph of the number of counts per channel versus channel. The output may be displayed as a picture on the cathode ray oscilloscope, a graph plotted by the X-Y recorder, as a typed listing of the number of counts in each channel, or as a punched record on a piece of paper computer tape.

Because the height of the pulses generated by the passage of particles through the aperture is directly related to particle volume, it is desirable that the electronic system used to analyze the pulses give a linear response to pulse amplitude. The linearity of the counting system was tested using a pulse generator. The generator can generate pulses of a variety of shapes and amplitudes. The effect of pulse shape was tested by varying test pulse amplitudes while keeping rise and fall times constant. Two types of test pulses were used. Short pulses had rise times of 0.05 μsec and decay times of 2.5 μsec; long pulses had rise times of 1 μsec and decay times of 50 μsec.

These two types of test pulses were fed to the preamplifier through a 1.5 pF capacitor test input while changing settings of the amplifier such as gain, differentiation, and integration. The results of these experiments are shown in Table VI. Overall gain [channels/(input volt × nominal amplifier gain)] of the system was strongly dependent on pulse shape, but linear for a wide range of amplitudes when the pulse rise and fall times were kept constant. The longer pulse gave a consistently higher gain. Pulse shaping in the form of differentiation and integration consistently decreased the apparent gain (amplitude of output pulse divided by amplitude of input pulse). PHA gain [channel/(output pulse amplitude)] was a function of both pulse length and the degree of pulse shaping. Some of these features are shown in Fig. 17, which is a graph of pulse height analyzer channel versus relative input pulse amplitude for no pulse shaping (integration = 0.05 μsec, differentiation = 5000 μsec) and for some pulse shaping (integration = 1.0 μsec, differentiation = 2.0 μsec). The long pulses always show a higher gain. Also, pulse length affected the results more strongly in the case of no pulse shaping. As can be seen from Table VI, the gain for the case of no shaping is significantly greater than for the case with shaping. The difference does not appear as great because the amplitude of the input pulses was adjusted to obtain nearly full-scale readings on the pulse height analyzer. Nonlinearity observed in the highest datum of the short pulse, pulse shaped case is due to exceeding the linear range of the pulse generator. The linearity in the rest of the data is apparent.

Table VI. Test of linearity of electronics

A=Nominal Gain Coarse	Fine	Pulse Length	Diff. (μs)	Int. (μs)	Noise (input volts)	Apparent Gain output volts / input volts	PHA Gain channels / output volts	Overall Gain channels / input volts / A
100	10	short	1	1	0.015	28.6	9.35	2.68
100	10	long	1	1	0.010	40.9	13.5	5.52
100	0	short	2.0	0.5	0.0164	23.5	11.7	2.74
100	0	long	2.0	0.5	0.009	35.8	13.8	5.08
100	0	short	2.0	1.0	0.022	18.2	11.3	2.06
100	0	long	2.0	1.0	0.011	30.2	14.5	4.36
100	0.	short	5.0	1.0	0.028	17.8	13.8	2.46
100	0	long	5.0	1.0	0.013	31.5	15.0	4.71
100	0	short	5.0	2.0	0.022	17.0	13.8	1.66
100	0	long	5.0	2.0	0.016	26.4	14.7	3.89
100	0	short	5.0	5.0	0.049	7.5	13.1	1.02
100	0	long	5.0	5.0	0.030	17.8	15.1	2.68
200	0	short	1.0	5.0	0.043	6.2	14.7	0.46
200	0	long	1.0	5.0	0.026	15.0	15.5	1.16
50	0	short	5000.	0.024	17.6	11.6	4.07	
50	0	long	5000.	0.05	0.019	21.6	14.3	6.13

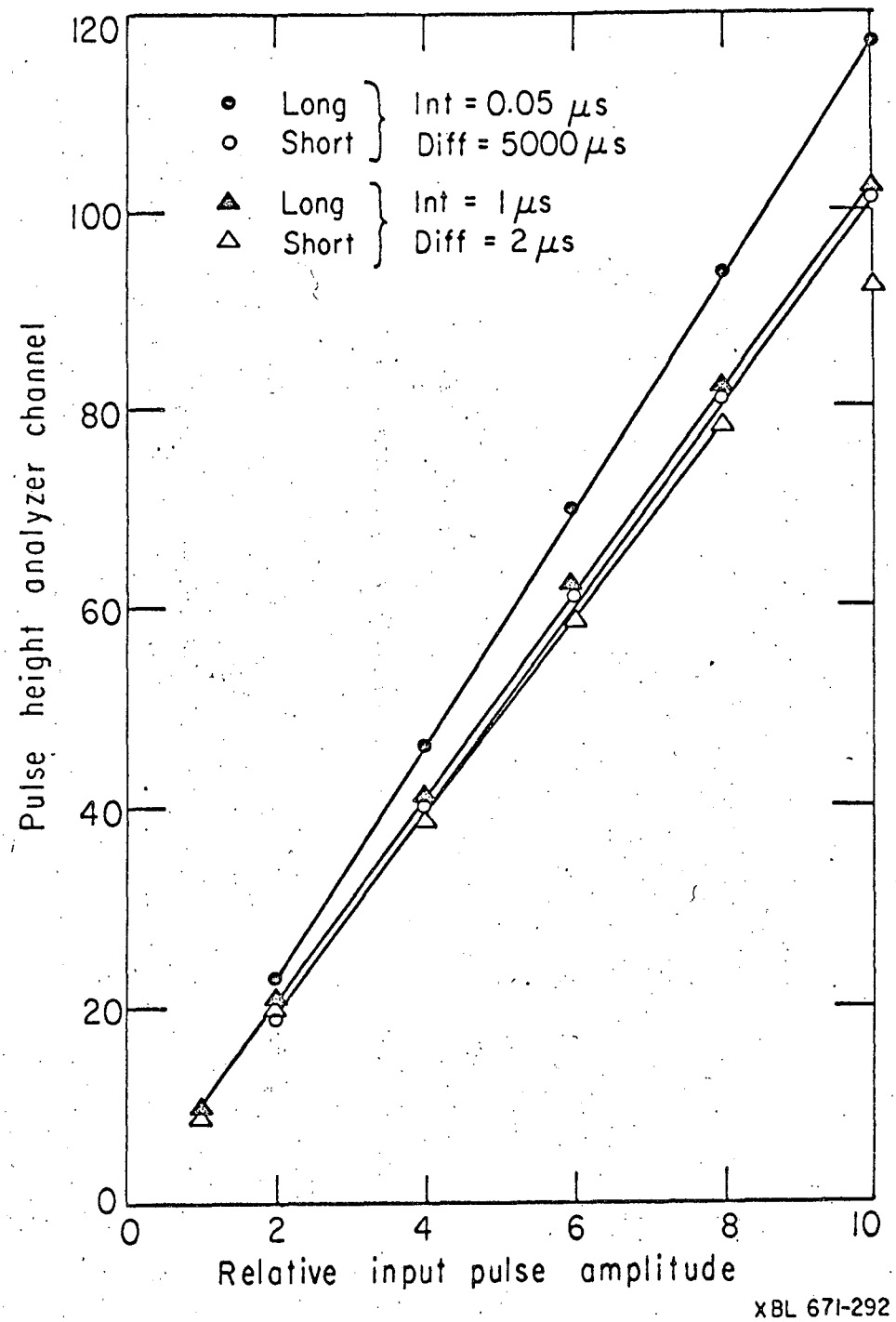

Fig. 17. Pulse height analyzer channel versus relative input pulse amplitude.

C. Linearity of Response to Particle Sizes

The first test of linearity was made by analysis of particle pulses by the simultaneous variation of aperture voltage and amplifier gain so that the product of these two variables remained constant. The results are shown in Tables VII, VIII, and IX and in Fig. 18. Table VII summarizes the results. Aperture resistance was calculated by the method used earlier. Variation in aperture resistance caused an increase in aperture current so that the product of aperture current and amplifier gain was not constant. Thus, when two of the distributions (gains of 200 and 50) were compared in Fig. 18, they did not superimpose directly on top of one another, the distribution at the higher voltage being slightly shifted toward larger apparent size. It is also evident that the higher aperture current led to better resolution, giving more narrow peaks. Saturation of the preamplifier occurred above channel 45 in the case of high gain. Multiple peaks are due to coincident passage through the aperture of two or more particles. Tables VIII and IX list the pulse height analysis distributions obtained at aperture voltages of 100 and 25, respectively. Note that the first number printed in each table is the length of time spent analyzing pulses in ten thousandths of a minute. Other numbers represent counts per channel accumulated during the counting period.

Another means of testing linearity consisted of noting the channel number at which singlet, doublet, triplet, and quadruplet peaks occurred as the amplifier gain was varied. Table X lists the peak positions obtained, and Fig. 19 shows the results as pulse-height analysis channel versus amplifier gain. Linearity is demonstrated in two senses in Fig. 19. First, a straight line is obtained for each degree of multiplets. Secondly, the slopes of the lines are proportional to the number of particles in the multiplet.

From these results, the linearity of the response is established.

Table VII. Linearity test by simultaneous variation of aperture current and amplifier gain.

Gain	DC Voltage (volts)	Aperture Current (milliamps)	Aperture Resistance (kohms)	1st Peak (channel number)	2nd Peak (channel number)
400	12.5	0.15	49.3	8 1/2	18
200	25.0	0.31	46.7	10	20
100	50.0	0.64	44.1	11	21
50	100.0	1.39	38.0	10^{+}	20

Table VIII. Pulse height analysis of 1.305 μ polystyrene beads.

Aperture current = 1.39 milliamps,
Gain = 50, counts per channel by channel*

010000	000000	000016	000571	001484	002059	002375	002891
006665	017832	024173	020169	013390	008139	004867	003609
003145	003551	006068	009093	009565	008488	007206	005235
003387	002671	002506	002907	003565	003930	004387	004846
004495	004131	003650	003207	002758	002415	002306	002477
002709	003024	003122	003141	003104	003135	003466	003912
004587	005221	005204	005065	004707	004343	004115	003901
003618	003134	002193	001081	000433	000165	000102	000092
000080	000054	000076	000044	000067	000062	000052	000035
000041	000036	000025	000027	000014	000014	000018	000017
000022	000022	000007	000013	000010	000006	000011	000010
000006	000005	000004	000011	000006	000004	000003	000007
000004	000006	000003	000004	000000	000005	000001	000006
000004	000000	000002	000005	000003	000004	000001	000001
000000	000002	000004	000001	000002	000002	000001	000003
000001	000002	000000	000002	000000	000000	000001	000000

*Counts per channel are listed by channel, left to right, top to bottom, beginning with channel 1 and ending with channel 128.

Table IX. Pulse height analysis of 1.305 μ polystyrene beads.

Aperture current = .31 milliamps,
Gain = 200, counts per channel by channel*

010000	000000	000002	000150	000730	002053	004654	006202
009481	015261	018166	015817	012585	009940	007185	005268
004031	004537	006135	007668	008139	007600	006197	005021
003968	003524	003328	003117	003357	003716	003906	003981
003988	003745	003458	003019	002618	002307	002277	002418
002435	002592	002709	002484	002427	002157	002060	001666
001574	001432	001458	001406	001516	001482	001598	001535
001424	001438	001234	001179	001082	000994	000942	000918
001003	000951	000887	000818	000889	000844	000829	000742
000754	000768	000730	000669	000662	000588	000553	000557
000574	000521	000511	000488	000477	000472	000528	000459
000439	000422	000421	000404	000346	000370	000357	000353
000350	000320	000340	000316	000294	000261	000278	000280
000316	000274	000249	000280	000265	000226	000235	000229
000212	000234	000211	000197	000221	000174	000198	000164
000194	000190	000171	000160	000154	000157	000145	000149

*Counts per channel are listed by channel, left to right, top to bottom, beginning with channel 1 and ending with channel 128.

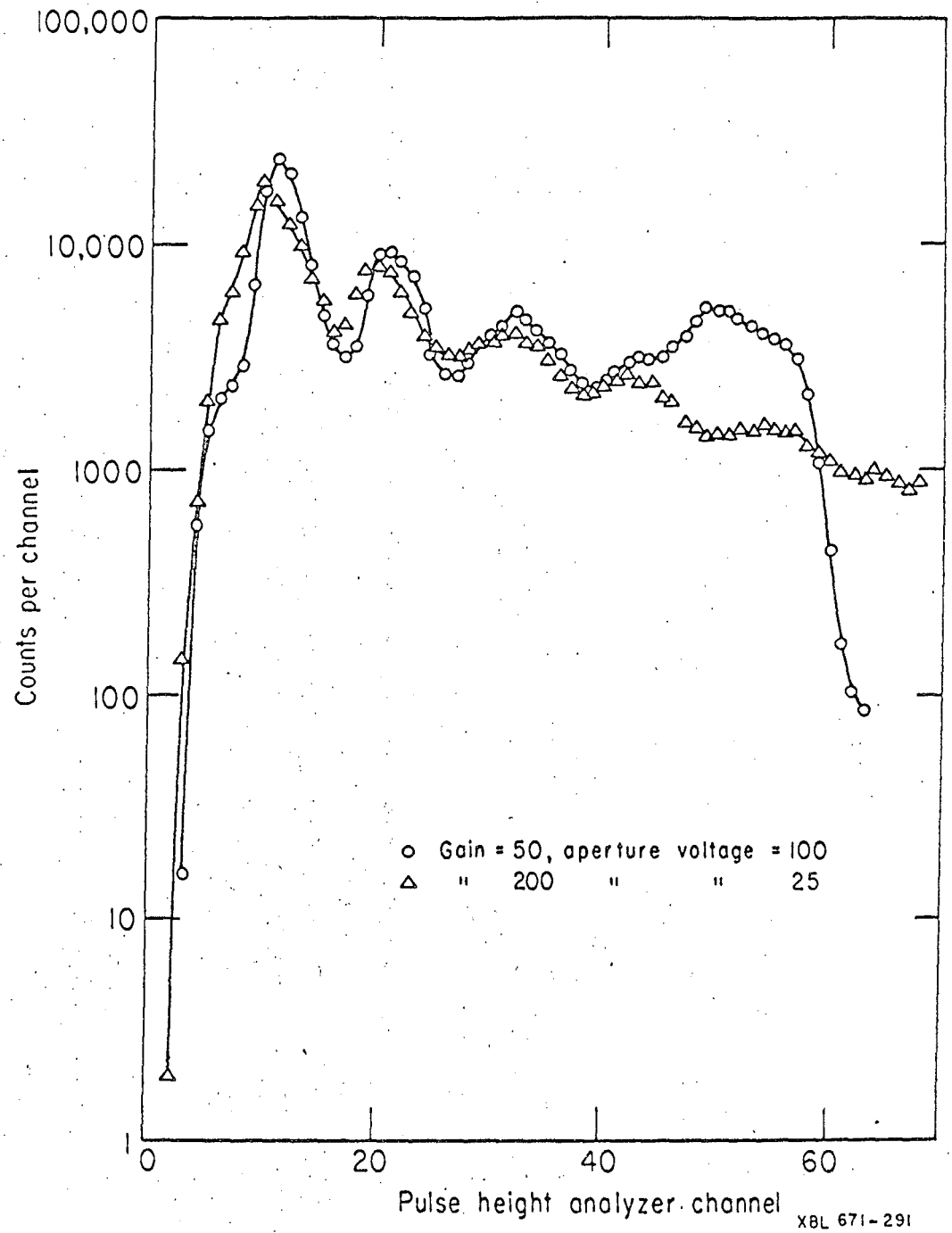

Fig. 18. Linearity test by simultaneous variation of aperture current and amplifier gain.

Table X. Linearity check by variation of gain.

1.305 micron beads
Differentiation = 1 μsec
Integration = 5 μsec

Amplifier Gain	Singlet Peak (channel)	Doublet Peak (channel)	Triplet Peak (channel)	Quadruplet Peak (channel)
25	2-1/4	4-3/4	7	9-1/2
50	7	12-1/2	17-1/2	23
100	9	18	27-1/2	37
200	20-1/2	38-1/2	58-1/2	75-1/2
400	43-1/2	78-1/2	-	-

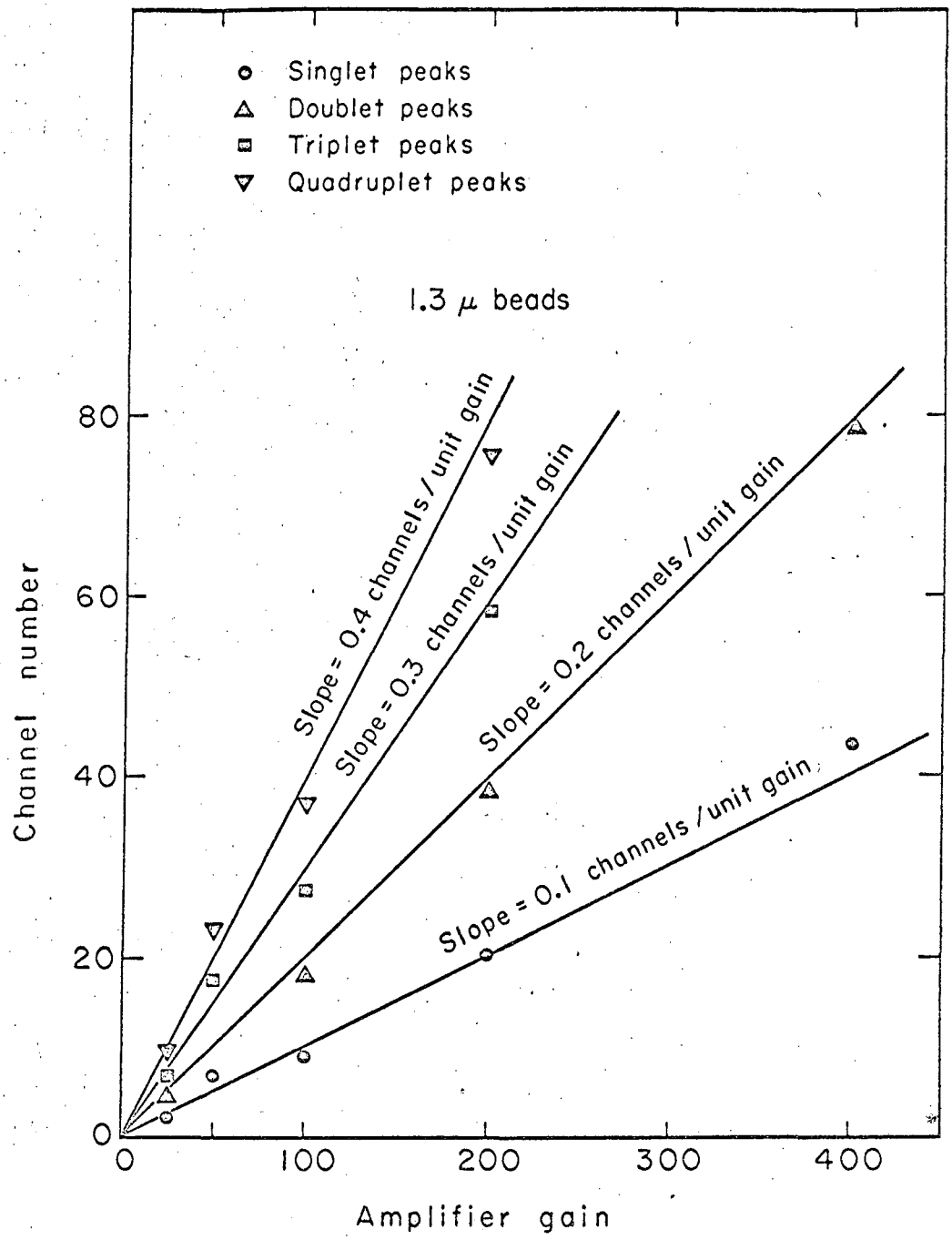

MUB-12525

Fig. 19. Channel number versus amplifier gain for single and multiplet peaks of 1.305 μ beads.

D. Effect of Pulse-Shaping on Resolution

As mentioned earlier, improved resolution in electronic sizing results from shaping the particle-generated pulses using differentiation and integration. Harvey and Marr have published results of pulse-shaping on the sizing of plastic beads (of the same type used in our work).[6] Using different electronics from ours, they found that the optimal time constants in pulse-shaping were 0.8 μsec first differentiation and integration and 3.2 μsec for the second differentiation. The setting of the first differentiation was found to have the greatest effect on the resolution. They concluded that pulse shaping reduced coincidence by shortening the pulse length. Because we are using a different amplifier and preamplifer, we undertook a brief study of the effects of varying differentiation and integration. A double-barreled approach was used. Photographs were taken of an oscilloscope monitoring the shaped pulses to see the effect of pulse shaping. At the same time, the pulses were sorted using the pulse-height analyzer to obtain a size distribution. Table XI summarizes the results of oscilloscope monitoring of the effect of pulse shaping on pulses from 2.051 μ polyvinyltoluene beads. As can be seen from Table XI, the linear pulses (differentiation = 5000 μsec and integration = .05 μsec) were the longest of all pulses, while setting of integration = 1 μsec = differentiation gave the shortest pulse duration. At settings of integration less than 2 μsec, pulses were somewhat ragged due to high frequency noise. Rise times were most uniform at the two following settings: differentiation = 2 μsec, integration = 5 μsec and differentiation = 5 μsec and integration = 2 μsec. Rise times at differentiation = 1 μsec = integration seemed to be overcorrected and the pulses were somewhat ragged. Results of pulse height analysis were in agreement with the information obtained from the oscilloscope traces, as can be seen in Fig. 20. Two size distributions of 2.051 μ diameter beads are shown in Fig. 20. One distribution was obtained with linear setting on the amplifier (differentiation = 5000 μsec, integration = .05 μsec) and the other using optimal shaping settings (differentiation = 2 μsec, integration = 5 μsec). Note that two peaks exist on the singlet peak for

Table XI. Effects of pulse shaping, 2.051 μ spheres.

Differentiation (μsec)	Integration (μsec)	Gain		Rise Time (μsec)		Duration (μsec)	
		Coarse,	Fine	Min.	Max.	Min.	Max.
5000	0.05	8,	2.90	7	15	17	27
5	0.05	16,	3.0	5	8	12	18
2	0.01	25,	3.0	5	7	9	17
2	5	50,	3.0	6	8	12	16
5	2	16,	0	7	8	13	18
5	5	16,	0	6	9	10	15
1	1	25,	0	3	7	6	12

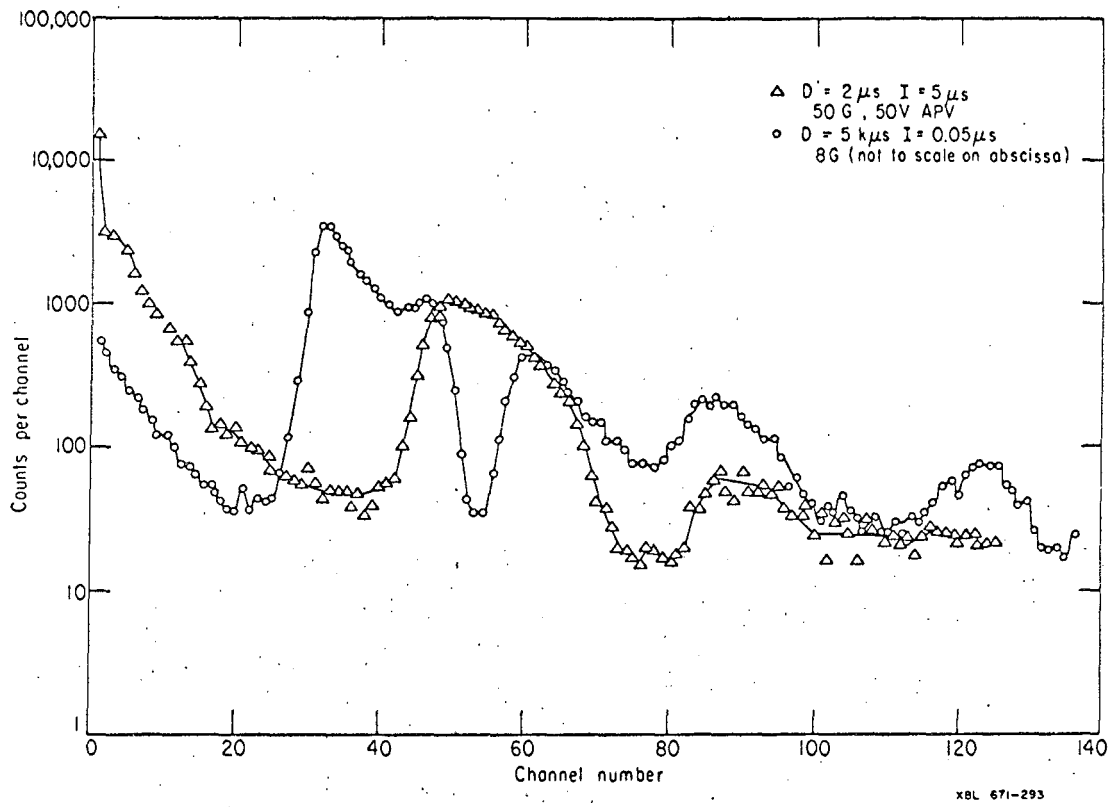

Fig. 20. Pulse height analysis of 2.051 micron beads, with and without pulse-shaping.

the unshaped case, while the second smaller peak has been eliminated on the singlet peak with pulse-shaping. The reason for the second peak on the singlet peak is not clear. Resolution using pulse shaping does not appear to be improved very much over the unshaped effect.

Another feature of the distributions shown is that the doublet peak falls at less than twice the abscissa as the singlet peak. Similarly, the triplet peak falls at an abscissa less than three times that of the singlet peak. This may be the result of several factors. First, the diameter of the 2.051 μ particles considered here are appreciable with respect to the diameter of the aperture, which means the limits of linearity may be broached on multiplets. Secondly, a shape effect could be responsible for the results. However, Gregg and Steidley showed that at aspect ratios greater than one, right circular cylinders passing through the aperture with center of circular symmetry parallel to that of the aperture gave larger resistance changes than those observed with spheres of equal volume.[3] Thus shape effects would act in the opposite direction from that observed. With settings of 1 μsec on both pulse-shaping parameters, the multiplet peaks are linearly related to one another, but much resolution is lost. If the effect is one of particle size, smaller spheres should improve linearity in the multiplet positions. Figure 21 shows three pulse-height analysis distributions obtained with 1.305 μ diameter polystyrene spheres with and without shaping of pulses. Again, settings of differentiation = 2 μsec, integration = 5 μsec clearly give the best resolution for single particles but settings of differentiation = integration = 1 μsec give better overall resolution. Furthermore, multiplets are now integral multiples of the mode of the singlet peak, except for the triplet peak. Resolution at other settings of differentiation and integration are not greatly different from the optimal settings, as shown by the distribution obtained at values of 1 μsec for both shaping parameters. Harvey and Marr proposed coincidence of pulses was the major reason for spreading of the distribution, but the decreased resolution at shorter pulse lengths (e.g., differentiation = integration = 1 μsec) is evidence that coincidence is not the only factor affecting resolution.

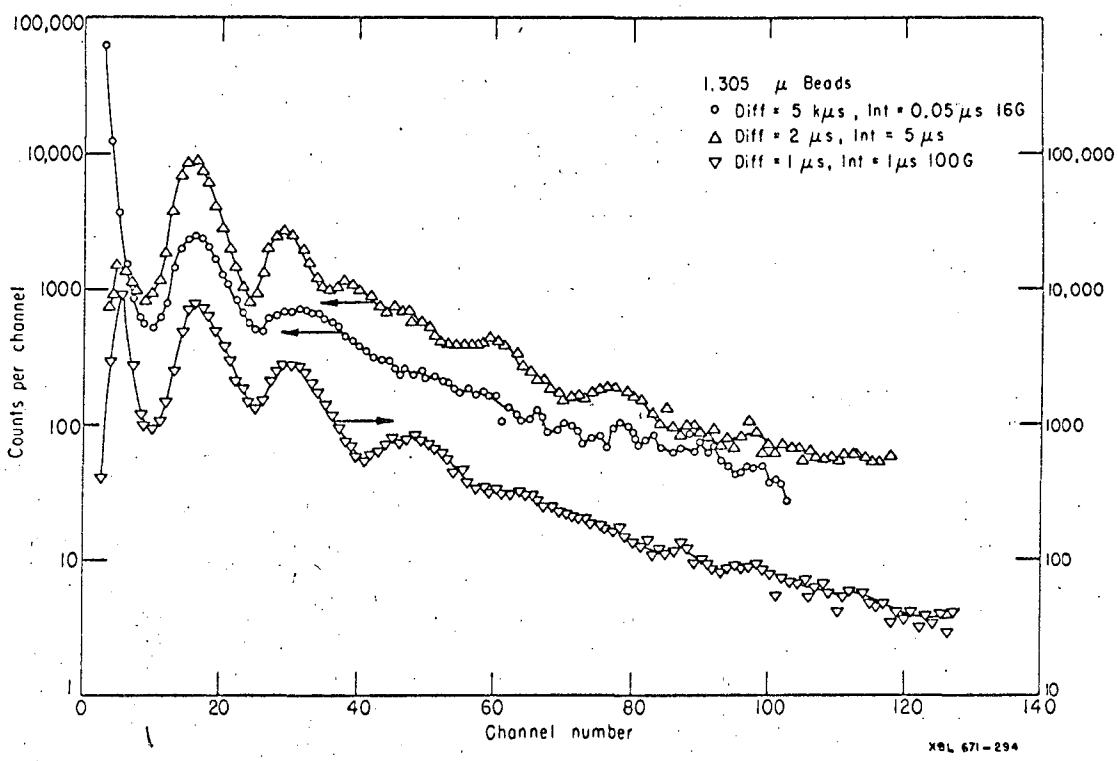

Fig. 21. Pulse height analysis of 1.305 micron beads, with and without pulse-shaping.

Now that optimal settings of pulse shaping have been determined, it is of interest to compare the results obtained using electronic sizing with the values measured by electron microscopy. Such a comparison is made in Fig. 22. It is immediately apparent that even using optimal settings, resolution by electronic sizing is limited. Also, the electron microscope measurements indicate a strong negative skewness while the electronic sizing results show a weak positive skewness. Combination of pulse-shaping with the hydrodynamic focussing technique of Spielman and Goren should lead to better resolution.

E. Effects of Other Variables on Counting System Response

1. Effect of Particle Conductivity

In addition to the 1.305 μ diameter polystyrene beads, Dow Chemical Company supplied us with 2.051 μ diameter polyvinyl toluene beads. If the conductivities are the same, the relative responses of the sizing system to the two types of beads should be proportional to their volumes. To a good approximation, that ratio will be given by the ratio of the mean diameters cubed. With that assumption, a ratio of 3.88 is obtained as the expected ratio. Table XII summarizes the results of an experiment to determine whether this requirement for linearity was met. At three different gains, the modes of the singlet and doublet peaks were measured from distributions obtained electronically. Then ratios were calculated and compared to the expected value of 3.88. As can be seen in the table, the 1.305 μ beads (polystyrene) gave a consistently lower response than did the 2.051 μ beads (polyvinyl toluene), obtaining ratios as high as 5.38. It should be noted that measurement of the mode is not highly accurate nor is it necessarily representative of mean values.

Other workers have observed similar results; they proposed that the difference was due to different surface electrical conductivity of the two types of beads.

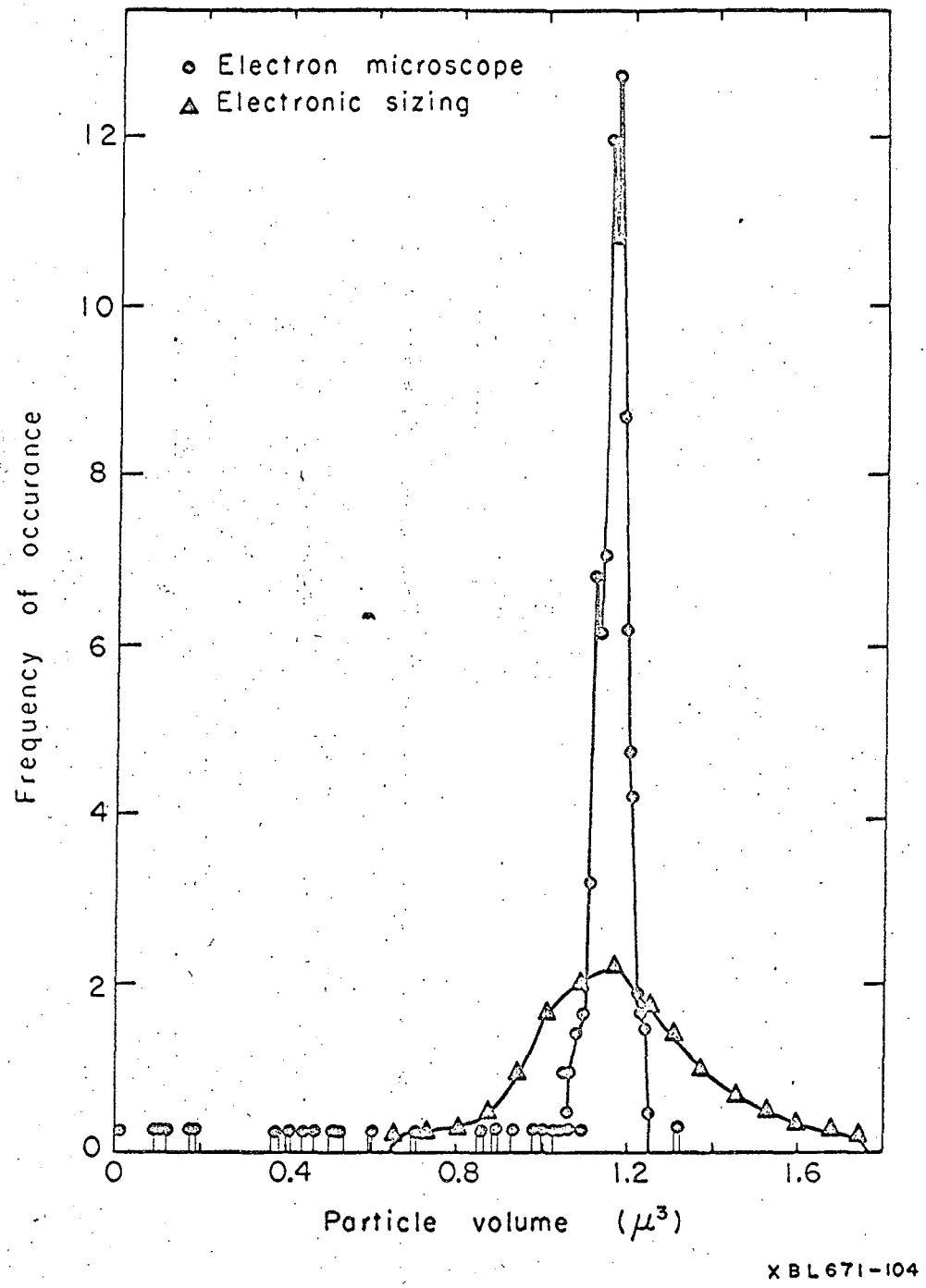

Fig. 22. Comparison of size distribution obtained electronically with size distribution obtained by electron microscopy.

Table XII. Response of sizing and counting system to different types of beads, mixture of 1.305 μ and 2.051 μ beads.

Particle	Gain	Singlet (channel)	Singlets Ratio	Doublet (channel)	Doublets Ratio
Polystyrene, 1.305 μ	16.0	4	5.38	9	4.45
Polyvinyl toluene, 2.051 μ	16.0	21.5		40	
Polystyrene, 1.305 μ	25.0	10	4.60	21	4.10
Polyvinyl toluene, 2.051 μ	25.0	46		86	
Polystyrene 1.305 μ	50.0	23	3.98	42-1/2	-
Polyvinyl toluene, 2.051 μ	50.0	91.5		-	

To test for an effect of bead conductivity in a more rigorous fashion, a comparison was made of 58 size distributions measured on 2.051 μ beads with 73 distributions measured on 1.305 μ beads. The distributions were obtained during measurements on bacteria, as will be discussed later. Table XIII summarizes the results for six different experiments. Overall volume factors were calculated as the product of the volume factor required to convert pulse-height analysis channel number to the known volume in cubic microns, times the amplifier gain, times the aperture voltage. The overall volume factor thus has units of (cubic microns × unit amplifier gain × aperture volt)/(channel number). The factor converts volumes measured as channel number at unit aperture voltage and unit amplifier gain settings to cubic microns. Thus the overall volume factor may be directly related to the response of the system to particles and should not vary from one particle size to another. Volume factors were systematically lower for 2.051 μ beads than for 1.305 μ beads by an average factor of 6.3%, showing a higher apparent bead size and thus a lower bead conductivity. This is in agreement with the results discussed earlier in this section where the response of the polyvinyl toluene beads was greater than that of the polystyrene beads. However, an error in the original measurements of bead diameters of only 2% could give the same result, so difference in bead electrical conductivity is not the only possible explanation. Further evidence that error in measuring bead diameters is responsible for the observed differences comes from the results of Harvey and Marr, who found a linear response to bead size over a range from 0.2 to 20 cubic microns[6] using beads from the same source.

2. Reproducibility

The reproducibility of the measurement of total count and of average particle size should be known because they are limitations on the results. As was seen in Table XIII, overall volume factors varied between experiments even when bead size was constant. Variation between experiments could be explained, for example, as variations in the

Table XIII. Effect of bead type on overall volume factor.

Experiment	Date	Particle Size (cubic microns)	Number of Distributions Analyzed	Overall Volume Factor
Counting #2	6/27/66	2.051	20	355.2
Counting #3	7/1/66	"	20	367.0
Centrifugation	7/8/66	"	15	374.4
Sizing	7/9/66	"	3	374.4[a]
Sizing	7/9/66	1.305	14	390.8
Time	7/12/66	"	29	377.3
Counting #4	7/14/66	"	30	397.3[b]

[a]Mean overall volume factor, 2.051 μ beads = 365.2

[b]Mean overall volume factor, 1.305 μ beads = 388.3

electrical conductivity of the electrolyte due to changes in electrolyte temperature or electrolyte concentration. It is because of those sources of variation that a distribution is measured on the plastic beads under conditions identical with those during measurement of each experimental size distribution. By studying the variation of volume factors and total counts measured on a given day on a given sample at constant electrolyte composition and constant bead size, one can measure reproducibility. Measurements of volume factors (factors required to convert channel number scale to cubic micron scale, distinct from overall volume factor) made during counting experiment #3 on 2.051 μ beads are shown in Table XIV separated according to aperture voltage and gain. Aperture voltage does not appear to affect the volume factor. An overall standard deviation of .0069 was observed, corresponding to a value of 4.5% of the mean volume factor.

To estimate the expected error of total electronic counts, the counts of the first 17 distributions on the bead solution standard of the Time Experiment were averaged and the standard deviation was calculated. An average count of 2.51×10^5 particles/ml was obtained with a standard deviation of 1.163×10^4 particles/ml, corresponding to 4.6% of the average concentration. Errors in both electronic sizing and electronic counting are thus of the order of 5%.

3. Effect of Aperture Voltage

As shown in the previous section (Table XIV), aperture voltage does not affect volume factors, aperture resistance changes showing no effect on volume factors. However, standard deviations of measured size distributions are decreased by shifting to higher voltages, as can be seen from Table XV. Those data show a 26% decrease in standard deviation of volumes when measured at an aperture potential of 96 volts instead of a potential of 24 volts. Values of kurtosis and momental skewness also varied strongly with aperture potential. Aperture emf does not affect total counts of plastic beads.

Table XIV. Volume factors obtained in counting experiment #3.

Volume Factors	
Aperture Voltage = 24 volts,[a] Gain = 100	Aperture Voltage = 96 volts,[b] Gain = 25
.147	.162
.158	.166
.152	.152
.159	.150
.153	.148
.151	.144
.153	.141
.153	.145
.156	.164
.157	
.157	

[a]Average volume factor (24 V) = 0.154

[b]Average volume factor (96 V) = 0.152

Overall standard deviation = .0069
Overall standard deviation = 4.5%

Table XV. Effect of aperture voltage on standard deviation of volume distributions of plastic beads.

Standard Deviations, cubic microns	
Aperture Voltage = 24 V	Aperture Voltage = 96 V
.82	.60
.64	.61
.85	.60
.61	.52
.60	.58
.68	.58
.64	.43
.75	.54
.72	.56
Av. .70 cubic microns	Av. .56 cubic microns
.70/.56 = 1.26	

(Data from counting experiment #3).

V. MEASUREMENTS OF BACTERIAL CELLS

Preparation for measurements of bacterial cells has been discussed in the foregoing sections. After an introduction and literature review, measurement of the size distribution of plastic beads and their use in calibration of the instrument was described. Because the resolution of the system was found to be limited in the case of the plastic beads, the same limitation can be expected in the case of bacteria. Shape effects, which were also discussed in earlier sections, should also play a role because rod-shaped bacteria will be used in this section. The first subject discussed in this section will deal with methods used in culture of the organisms and in computerized analysis of the results. The ability of the system to measure total particle concentrations will then be compared with other methods. Finally, the ability of the system to measure the size of bacteria will be discussed in light of a theory of the electrical conductivity of the bacterial cell.

A. Methods

1. Organism and Cultivation

The coliform bacterium *Escherichia coli* B, strain Hershey, was used throughout this work. It had been obtained from the culture collection of the Department of Bacteriology, University of California, Berkeley. Stock cultures of the organism were stored at 10°C on nutrient agar slants (3g/ℓ peptone, 15g/ℓ agar). During experiments, a daily subculture was used to maintain a fresh culture ready for use. Batch culture in nutrient broth (same composition as nutrient agar except no agar present) was used exclusively as a growth medium. Overnight cultures were used as inocula. Inocula were usually 0.5%, giving an initial concentration of about 10^6 cells/ml. Cultures were usually grown in a 2-liter glass and Teflon reactor that was mixed by magnetic stirring and sparged with nitogen gas to remove oxygen. The reactor was kept submerged in a 30°C water bath except during sampling. Occasionally, when only a small culture volume was required, cultures were grown in 40 ml culture tubes in a 30°C incubator.

2. Measurements of Cell Concentration

For counting, cells were either washed and diluted or directly diluted into a formaldehyde-buffer-saline solution of the following composition: NaCl, 9g/ℓ; K_2HPO_4, 1.141 g/ℓ; KH_2PO_4, 0.680 g/ℓ; 37% formaldehyde solution, 2 ml/ℓ. Without formaldehyde, the cells disintegrated much more quickly in the buffer solution, being practically transparent to the sizing and counting system within an hour after dilution in buffer. With the addition of formaldehyde, the cells remained intact for at least 7 hours.

Viable counts were made using the conventional dilution technique. Nutrient medium diluted 1:10 in distilled water and sterilized was used as a diluting agent and diluted samples were plated in triplicate and counted on nutrient agar. Optical counts were made using a Petroff-Hauser counting chamber. As has been pointed out by Norris and Powell, large variation in chamber depths occur.[23] To avoid that difficulty, the chamber depth was measured for each slide counted. Depth measurements were made with a calibrated fine-focus wheel on the microscope, and total counts were corrected accordingly. Formaldehyde was added at a concentration of 0.2% to culture samples taken for optical count and optical density measurements. Optical counts were measured directly on the culture samples, but optical density measurements were made on wahsed cell suspensions.

Optical density measurements were made using a Coleman Model 9 nephlo-colorimeter (Coleman Instruments, Inc., Maywood, Ill.) acting as a nephlometer with 19 × 100 mm cuvettes. Readings were converted into Coleman Nephlos units of turbidity using a set of standard tubes of known turbidity.

3. Data Analysis

Electronic sizing and counting data were analyzed using several computer programs. To take into account the effects of day-to-day variations in system variables (e.g., room temperature or concentration of diluting solution) a measurement of the size distribution of a cell

suspension was accompanied by a size distribution measurement on a suspension of plastic spheres of known diameter at identical settings of all variables. The main computer program, called BUGSIZE, first reads the distribution measured on the plastic beads and then reads the distribution measured on the cells. The distribution on the plastic beads is analyzed first and the gain of the electronics system is determined from the known mean diameter of the beads. Then the cell size distribution and parameters are calculated in terms of cubic microns on the basis of the gain measurement of the spheres. Corrections for background noise, live counting time and aperture flow rate are made to convert the distributions into particles per channel per ml values. The program does not attempt to correct for the shape of the cells. Both size distributions obtained and the parameters calculated from them are printed out. The program plots the uncorrected and final corrected distributions for the standard size particles and then does the same for uncorrected and corrected experimental distribution. After all sets of data have been analyzed, the data are summarized in a table.

Inspection of plotted distributions was used to estimate points where the distribution should be truncated during calculations of total count, average size, etc. In the case of the beads that were being used as standards, the singlet peak was truncated on both sides. Distributions obtained with bacteria were truncated only on the lower side. These truncations were necessary because subtraction of background noise was not completely effective in removing background. Once channel numbers for the truncation were known, they were read in along with the other data and the results were recalculated in the truncated distributions.

In order to correct for background noise using the main program, it was convenient to first fit an equation to the appropriate background noise distribution (collected at conditions and settings identical with those used in measuring the experimental distribution). An equation of the form

$$A = \text{noise per channel per ml}$$
$$= \alpha_1 e^{-\beta_1 N} + \alpha_2 e^{-\beta_2 N}$$

where N = channel number and α,β are constants, was chosen because a semilogarithmic plot of noise distribution appeared to asymptotically approach straight lines at low and high channel numbers. This can be seen in Fig. 23. One could attribute the low channel, high level, and steep slope portion of the background distribution to electronic noise and the values at higher channels to particles in the solution.

Also shown in Fig. 23 is the locus of an equation of the following form:

$$A = 694.2 \exp(-.04354\ N) + 4346.6 \exp(-.4198N)$$

The equation was fitted to the data using a program called NOISE using the nonlinear least squares technique discussed in the first chapter of this thesis. Like the BUGSIZE program, the NOISE program is written in the Chippewa dialect of the FORTRAN computer language. Before fitting the equation, the data are corrected to per ml values. A listing of NOISE is given in Appendix V.

Referring back to Fig. 23, it should be noted that while agreement between the equation and the background noise data is good at low and intermediate channel numbers, agreement is poor at higher channel numbers. Addition of a third term might improve agreement in that region, but it is not necessary because the area of greatest interest and of the highest noise is at low and intermediate channel numbers.

The results shown in Fig. 23 are typical. Coefficients obtained from background measurements are summarized in Table XVI. For values of aperture voltage and amplifer gain different from those shown in Table XVI, estimates were made by hand calculations. As can be seen, coefficients varied from run to run, even during immediate duplication. This

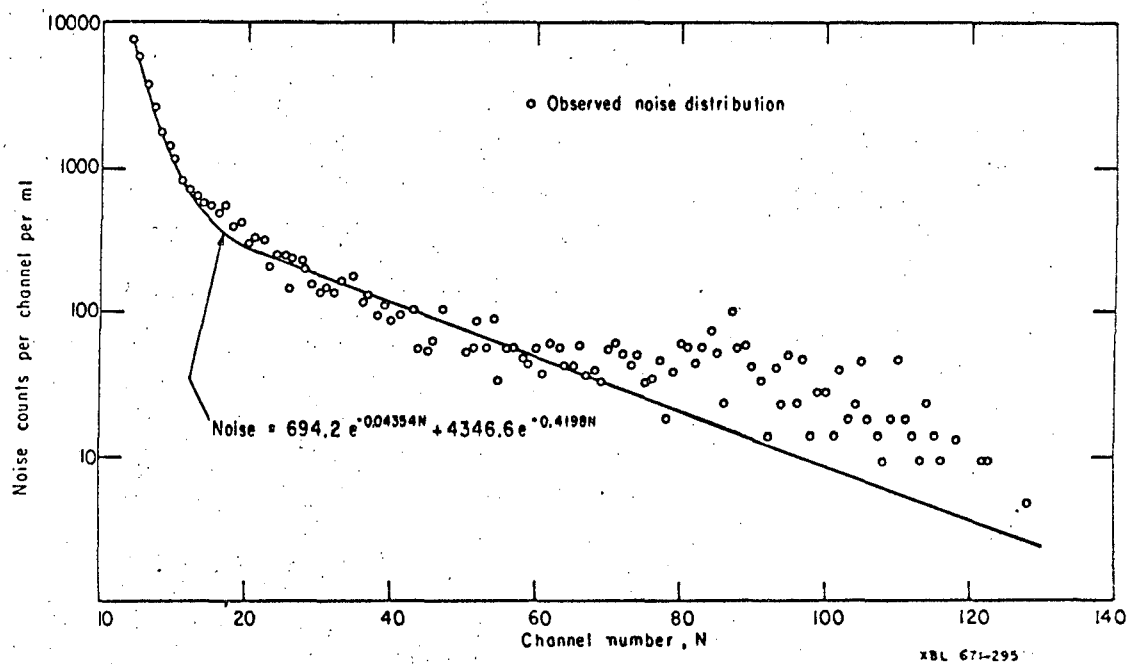

Fig. 23. Distribution of background noise.

Table XVI. Coefficients in background noise equation.

Experiment	Aperture Voltage (volts)	Gain	α_1	β_1	α_2	β_2
Counting #3	24	100	356.2	-.04947	3.634×10^6	-1.393
Time	120	50	694.3	-.04354	4.347×10^4	- .4198
"	"	"	689.4	-.04636	4.276×10^4	- .4629
"	60	100	2385.4	-.1004	5.184×10^6	-1.305
"	"	100	2027.9	-.08366	1.223×10^7	-1.473
"	30	200	652.1	-.05018	5.987×10^7	- .9434
"	"	"	768.6	-.0535	4.403×10^7	- .9054
Osmotic	120	100	2107.6	-.07660	2.338×10^6	- .6774
"	"	"	1991.4	-.07982	1.451×10^6	- .6434

result demonstrates the need for truncation of distributions. An alternative to fitting equations would be direct electronic subtraction of background noise from each distribution while in the pulse-height analyzer memory. The drawback to that technique is that it takes too much time for analysis of rapidly decaying samples of bacteria. The scatter in the results is also increased by such a procedure. BUGSIZE and NOISE are given in Appendix V, along with a definition of variables and program outline for both programs.

B. Electronic Counting of Bacteria

This section will compare classical bacteriological measurements of cell concentration with the electronic method under study. Three batch culture experiments were performed with *E. coli*. Samples were taken at about hourly intervals and each sample was analyzed for viable count, optical count, optical density, and electronic count and size distribution. Dry weight and packed cell volumes were not measured because at the low cell concentrations, very large samples would be required.

A summary of the results of the three batch culture experiments is shown in Tables XVII to XXV. Electronic parameters were usually averages of about 5 distributions. Because each datum represented several distributions requiring several pages to print out the results, it is not possible to present all that information here. A distribution from counting experiment #4 is shown in Table XXVI.

Figure 24 shows cell concentration versus time for several methods used in counting experiment #3. Results of counting experiments #2 and #4 were similar, optical counts tending to be higher, and electronic counts tending to agree with plate counts. In the next four figures, data from all three counting experiments are pooled. Figure 25 shows the fair agreement between optical count and electronic count, with optical count usually larger than electronic count. Figure 26 shows much better agreement between plate counts and electronic counts. Comparisons of electronic variables with turbidity are presented in Figs. 27 and 28.

Table XVII. Conditions of electronic counting analysis, counting experiment #2.

Set	Sample	Time	Dilution	Aperture Voltage (volts)	Gain	Diff. (μsec)	Int. (μsec)
1	1	2 min	none	24	100	1	1
2	"	"	"	48	50	"	"
3	"	"	"	"	"	"	"
4	"	"	"	96	25	"	"
5	"	"	"	"	"	"	"
6	2	1 hr 25 min	1:2	24	100	"	"
7	"	"	"	"	"	"	"
8	"	"	"	96	25	"	"
9	"	"	"	"	"	"	"
10	3	2 hr 40 min	1:10.5	24	100	"	"
11	"	"	"	"	"	"	"
12	"	"	"	96	25	"	"
13	"	"	"	"	"	"	"
14	4	4 hr 45 min	1:100	24	100	"	"
15	"	"	"	"	"	"	"
16	"	"	"	96	25	"	"
17	"	"	"	"	"	"	"
18	5	5 hr 35 min	"	24	100	"	"
19	"	"	"	"	"	"	"
20	"	"	"	"	"	"	"
21	"	"	"	"	"	"	"
22	6	6 hr 55 min	1:100	24	100	"	"
23	"	"	"	48	50	"	"
24	"	"	"	"	"	"	"
25	"	"	"	96	25	"	"
26	"	"	"	"	"	"	"
27	Test Data						

Table XVIII. Summary of results, Counting Experiment #2

SUMMARY OF CALCULATED RESULTS, ALL DISTRIBUTIONS

	PARTICLES/ML	VOLUME PERCENT	AVE.VOL.(MU**3)	VOLUME FACTOR	STD.DEV.(MU**3)	SKEWNESS	KURTOSIS
NSET =	1						
BEADS	7.2288101E+04	3.2830975E-05	4.5415845E+00	1.5889553E-01	5.7389925E-01	7.6601918E-02	-3.0761726E-01
CELLS	1.1129283E+06	1.6198722E-04	1.4555045E+00	1.5889553E-01	1.8923169E+00	2.4150656E+00	1.5874256E+01
NSET =	2						
BEADS	1.0111403E+05	4.5978844E-05	4.5472270E+00	1.4760532E-01	6.4911717E-01	3.3739208E-01	-9.3734652E-02
CELLS	8.0164642E+05	1.4021893E-04	1.7491369E+00	1.4760532E-01	1.9251598E+00	2.0156091E+00	9.6213004E+00
NSET =	3						
BEADS	1.0111403E+05	4.5978844E-05	4.5472270E+00	1.4760532E-01	6.4911717E-01	3.3739208E-01	-9.3734652E-02
CELLS	7.3922407E+05	1.7106069E-04	2.3143574E+00	1.4760532E-01	2.2414010E+00	1.5678549E+00	5.6775735E+00
NSET =	4						
BEADS	1.1188228E+05	5.0852389E-05	4.5451690E+00	1.4902139E-01	6.0797302E-01	-3.1880180E-02	-1.9522942E-01
CELLS	8.1142150E+05	1.5021832E-04	1.8512982E+00	1.4902139E-01	1.4868019E+00	1.1417287E+00	3.2463973E+00
NSET =	5						
BEADS	1.1484109E+05	5.2189111E-05	4.5444632E+00	1.4649621E-01	6.0806903E-01	1.1344948E-01	-4.2439257E-01
CELLS	8.2454203E+05	1.5277630E-04	1.8528625E+00	1.4649621E-01	1.4540915E+00	1.1357008E+00	3.1702200E+00
NSET =	6						
BEADS	1.3631071E+05	6.2204452E-05	4.5634311E+00	1.4875615E-01	8.0273528E-01	2.5146932E-01	-1.3393757E-01
CELLS	1.3840321E+06	4.0402236E-04	2.9191690E+00	1.4875615E-01	1.8501043E+00	1.5933190E+00	7.9071787E+00
NSET =	7						
BEADS	1.3631071E+05	6.2204452E-05	4.5634311E+00	1.4875615E-01	8.0273528E-01	2.5146932E-01	-1.3393757E-01
CELLS	1.2018722E+06	3.5868410E-04	2.9843780E+00	1.4875615E-01	1.8156332E+00	1.5337969E+00	7.6548387E+00
NSET =	8						
BEADS	1.0857834E+05	4.9313630E-05	4.5417567E+00	1.4358837E-01	5.7349972E-01	4.1024616E-02	-3.8590803E-01
CELLS	1.2056714E+06	2.6828770E-04	2.2252141E+00	1.4358837E-01	1.2598307E+00	9.6478488E-01	3.5465806E+00
NSET =	9						
BEADS	1.0554525E+05	4.7924297E-05	4.5405398E+00	1.4246944E-01	5.5862082E-01	4.3057128E-03	-3.4229545E-01
CELLS	1.2917858E+06	3.1246352E-04	2.4188494E+00	1.4246944E-01	1.2526510E+00	7.1776369E-01	1.3180751E+00
NSET =	10						
BEADS	8.9925037E+04	4.0954222E-05	4.5542625E+00	1.5039300E-01	7.2692496E-01	3.9607173E-01	-1.4915241E-02
CELLS	1.1198879E+05	3.5049609E-05	3.1297426E+00	1.5039300E-01	1.8868450E+00	1.0670104E+00	3.7883955E+00
NSET =	11						
BEADS	8.9925037E+04	4.0954222E-05	4.5542625E+00	1.5039300E-01	7.2692496E-01	3.9607173E-01	-1.4915241E-02
CELLS	3.1056014E+05	9.0574561E-05	2.9164902E+00	1.5039300E-01	1.6499795E+00	1.4592945E+00	7.6437249E+00
NSET =	12						
BEADS	1.0455406E+05	4.7511763E-05	4.5442293E+00	1.4171955E-01	6.0283716E-01	5.9881590E-02	-4.0500248E-01
CELLS	1.5246972E+06	2.3627303E-04	1.5496391E+00	1.4171955E-01	8.3010519E-01	1.1947034E+00	5.4165445E+00
NSET =	13						
BEADS	1.0172594E+05	4.6206892E-05	4.5422919E+00	1.4864019E-01	5.8231224E-01	9.6159330E-02	-4.2878820E-01
CELLS	1.5282973E+06	2.4557262E-04	1.6068380E+00	1.4864019E-01	8.6299488E-01	1.1891244E+00	5.3559055E+00
NSET =	14						
BEADS	8.1560312E+04	3.7140897E-05	4.5537954E+00	1.7684511E-01	7.0398022E-01	1.2693560E-01	-7.8630629E-02
CELLS	7.4661137E+05	1.6070258E-04	2.0186875E+00	1.7684511E-01	1.1297575E+00	1.6255698E+00	1.5801541E+01
NSET =	15						
BEADS	8.1560312E+04	3.7140897E-05	4.5537954E+00	1.7684511E-01	7.0398022E-01	1.2693560E-01	-7.8630629E-02
CELLS	7.3928242E+05	1.5024045E-04	2.0322470E+00	1.7684511E-01	1.1207124E+00	1.4595419E+00	1.2552337E+01
NSET =	16						
BEADS	9.8846508E+04	4.4906268E-05	4.5430303E+00	1.4132583E-01	5.9058139E-01	8.8585007E-02	-4.2983337E-01
CELLS	7.3806920E+05	1.2370564E-04	1.6760710E+00	1.4132583E-01	8.2387237E-01	8.7287431E-01	3.3912701E+00
NSET =	17						
BEADS	8.5502655E+04	3.8821207E-05	4.5403510E+00	1.4832837E-01	5.5158519E-01	-8.3378031E-02	-2.6647945E-01
CELLS	7.4971253E+05	1.3107128E-04	1.7482872E+00	1.4832837E-01	8.5611405E-01	8.3323602E-01	2.5246893E+00
NSET =	18						
BEADS	8.5947913E+04	3.9184926E-05	4.5591481E+00	1.4713342E-01	7.6893420E-01	3.1856375E-01	-8.0798910E-02
CELLS	8.0237132E+05	1.4069511E-04	1.7534912E+00	1.4713342E-01	1.1508380E+00	1.8224311E+00	1.4201038E+01
NSET =	19						

BEADS	8.3430276E+04	3.8026699E-05	4.5575619E+00	1.4977679E-01	7.5393230E-01	3.0410462E-01	-9.9915894E-02
CELLS	7.8765435E+05	1.4698279E-04	1.8660823E+00	1.4977679E-01	1.2037939E+00	1.9188199E+00	1.5219152E+01
NSET = 20							
BEADS	8.7933896E+04	3.9964226E-05	4.5448033E+00	1.3922476E-01	6.0287555E-01	-7.1978116E-02	-3.2676805E-01
CELLS	6.2026315E+05	1.0899965E-04	1.7573130E+00	1.3922476E-01	9.5368401E-01	8.3256950E-01	2.6150442E+00
NSET = 21							
BEADS	8.8536109E+04	4.0172862E-05	4.5376551E+00	1.4431363E-01	5.1926895E-01	7.4698867E-03	-3.7576557E-01
CELLS	8.0287458E+05	1.4425960E-04	1.7967843E+00	1.4431363E-01	9.9184575E-01	8.9625526E-01	2.7206758E+00
NSET = 22							
BEADS	8.0133386E+04	3.6479351E-05	4.5623286E+00	1.5784432E-01	6.9216350E-01	1.5525421E-01	-1.7526553E-01
CELLS	8.3535218E+05	1.9416210E-04	2.3243143E+00	1.5784432E-01	1.6508910E+00	1.6946560E+00	9.4469029E+00
NSET = 23							
BEADS	8.0091356E+04	3.6385635E-05	4.5430165E+00	1.4617592E-01	5.9259162E-01	1.4687765E-01	-3.1493257E-01
CELLS	9.2622576E+05	1.9286606E-04	2.0822792E+00	1.4617592E-01	1.6227206E+00	1.5931171E+00	7.9851527E+00
NSET = 24							
BEADS	8.0091356E+04	3.6385635E-05	4.5430165E+00	1.4617592E-01	5.9259162E-01	1.4687765E-01	-3.1493257E-01
CELLS	3.7628277E+05	1.0102493E-04	2.6848142E+00	1.4617592E-01	1.8244578E+00	1.0782421E+00	3.6129614E+00
NSET = 25							
BEADS	9.3419848E+04	4.2430423E-05	4.5419067E+00	1.4307049E-01	5.7291540E-01	-1.1937404E-02	-3.3616934E-01
CELLS	9.0808700E+05	1.7877237E-04	1.9685700E+00	1.4307049E-01	1.2711413E+00	8.3780013E-01	2.0327787E+00
NSET = 26							
BEADS	2.2900080E+05	1.1796595E-04	5.1513337E+00	1.6646974E-01	2.5282011E+00	-2.4800844E-01	-4.3909367E-01
CELLS	9.4004471E+05	2.1683691E-04	2.3065659E+00	1.6646974E-01	1.4935000E+00	8.2148328E-01	1.7612688E+00
Test Data NSET = 27							
BEADS	2.6000000E+01	1.0959463E-08	4.2151779E+00	4.1670960E-01	5.7004012E-01	-5.9210460E-02	-1.1198488E-01
CELLS	2.6000000E+01	1.0959463E-08	4.2151779E+00	4.1670960E-01	5.7004012E-01	-5.9210460E-02	-1.1198488E-01

Table XIX. Results of counting experiment #2.

Sample	Viable Count (cells/ml)	Optical Count (cells/ml)	Optical Density (Nephlos units)	Electronic Count (cells/ml)	Electronic Volume Percent
1 (inoculum)	-	9.08×10^7		-	-
2	7.50×10^5 (10 min)	8.00×10^5 (2 min)	15.4 (2 min)	7.43×10^7 (2 min)	1.53×10^{-4}
3	2.54×10^6 (1 hr 30 min)	4.12×10^6 (1 hr 25 min)	17.8 (1 hr 25 min)	2.50×10^6 (1 hr 25 min)	6.71×10^{-4}
4	1.81×10^7 (2 hr 45 min)	1.012×10^7 (2 hr 40 min)	30.6 (2 hr 40 min)	1.60×10^7	2.529×10^{-3}
5	1.06×10^8 (4 hr 50 min)	4.90×10^7 (4 hr 45 min)	132.1 (4 hr 45 min)	7.43×10^7 (4 hr 50 min)	.0126
6	5.89×10^7 (5 hr 40 min)	2.72×10^7 (5 hr 35 min)	159.8 (5 hr 35 min)	7.95×10^7 (5 hr 35 min)	.0144
7	6.11×10^7 (7 hr 2 min)	3.18×10^7 (6 hr 55 min)	170.2 (6 hr 55 min)	9.02×10^7 (6 hr 55 min)	.0196

Table XX. Conditions of electronic counting analysis, counting experiment #3.

Set	Sample	Time	Dilution	Aperture Voltage (volts)	Gain	Diff. (μsec)	Int. (μsec)
1	1	5 min	1:1	24	100	1	1
2	"	"	1:2	24	100	"	"
3	"	"	1:2	96	25	"	"
4	2	63 min	1:4	24	100	"	"
5	"	"	"	"	"	"	"
6	"	"	"	96	25	"	"
7	"	"	"	"	"	"	"
8	3	2 hr 12 min	1:10	24	100	"	"
9	"	"	"	"	"	"	"
10	"	"	"	96	25	"	"
11	"	"	"	"	"	"	"
12	4	3 hr 15 min	1:51	24	100	"	"
13	"	"	"	"	"	"	"
14	"	"	"	96	25	"	"
15	"	"	"	"	"	"	"
16	5	4 hr 25 min	1:151	24	100	"	"
17	"	"	"	"	"	"	"
18	"	"	"	96	25	"	"
19	"	"	"	"	"	"	"
20	6	5 hr 35 min	1:151	24	100	"	"
21	"	"	"	"	"	"	"
22	"	"	"	96	25	"	"
23	"	"	"	"	"	"	"
24	7	7 hr	1:151	24	100	"	"
25	"	"	"	"	"	"	"
26	"	"	"	96	25	"	"
27	"	"	"	"	"	"	"
28	"	"	"	24	100	"	"

Table XXI. Summary of results,
counting experiment #3

SUMMARY OF CALCULATED RESULTS, ALL DISTRIBUTIONS

	PARTICLES/ML	VOLUME PERCENT	AVE.VOL.(MU**3)	VOLUME FACTOR	STD.DEV.(MU**3)	SKEWNESS	KURTOSIS
NSET =	1						
BEADS	1.3477659E+05	6.1514770E-05	4.5642029E+00	1.4728054E-01	8.2189003E-01	4.0924429E-01	7.6785660E-02
CELLS	5.9730549E+05	1.3640651E-04	2.2836976E+00	1.4728054E-01	1.8500297E+00	2.1503707E+00	1.2715790E+01
NSET =	2						
BEADS	1.3477659E+05	6.1514770E-05	4.5642029E+00	1.4728054E-01	8.2189003E-01	4.0924429E-01	7.6785660E-02
CELLS	2.9777460E+05	7.0079190E-05	2.3534308E+00	1.4728054E-01	1.9708492E+00	2.0513431E+00	1.1271003E+01
NSET =	3						
BEADS	8.3818390E+04	3.8091683E-05	4.5445496E+00	1.6156187E-01	6.0357166E-01	5.0724383E-03	-3.2886017E-01
CELLS	3.3966070E+05	7.0791228E-05	2.0841749E+00	1.6156187E-01	1.3815170E+00	1.1595438E+00	3.5383774E+00
NSET =	4						
BEADS	8.4332714E+04	3.8343879E-05	4.5467384E+00	1.5756172E-01	6.4039227E-01	2.7478697E-01	-1.2506937E-01
CELLS	3.1287733E+05	1.1775681E-04	3.7636734E+00	1.5756172E-01	2.1445689E+00	1.0959523E+00	4.1112137E+00
NSET =	5						
BEADS	8.4332714E+04	3.8343879E-05	4.5467384E+00	1.5756172E-01	6.4039227E-01	2.7478697E-01	-1.2506937E-01
CELLS	2.9121471E+05	1.1060952E-04	3.7982121E+00	1.5756172E-01	2.0809067E+00	1.1410924E+00	4.6724439E+00
NSET =	6						
BEADS	9.3469625E+04	4.2475637E-05	4.5443252E+00	1.6605916E-01	6.0665335E-01	1.2683566E-01	-3.1044673E-01
CELLS	3.1733356E+05	1.0633904E-04	3.3510177E+00	1.6605916E-01	1.5478629E+00	4.4362676E-01	2.4837020E-01
NSET =	7						
BEADS	9.3469625E+04	4.2475637E-05	4.5443252E+00	1.6605916E-01	6.0665335E-01	1.2683566E-01	-3.1044673E-01
CELLS	3.1826684E+05	1.0563673E-04	3.3191247E+00	1.6605916E-01	1.5730196E+00	4.5995096E-01	3.5613893E-01
NSET =	8						
BEADS	9.0540240E+04	4.1356828E-05	4.5677842E+00	1.5242503E-01	8.5160861E-01	4.0140314E-01	1.5385985E-01
CELLS	2.5370668E+05	6.3896719E-05	2.5185273E+00	1.5242503E-01	1.4686311E+00	1.2748260E+00	5.7313938E+00
NSET =	9						
BEADS	8.0302178E+04	3.6497264E-05	4.5449906E+00	1.5887964E-01	6.1498224E-01	1.6706492E-01	-6.1485472E-02
CELLS	9.2863088E+05	1.8967130E-04	2.0424832E+00	1.5887964E-01	1.3094438E+00	1.8811609E+00	1.3721156E+01
NSET =	10						
BEADS	8.8564630E+04	4.0249023E-05	4.5445933E+00	1.5205896E-01	5.9939986E-01	-8.0368832E-02	-1.5326358E-01
CELLS	8.9771977E+05	1.7016875E-04	1.8955664E+00	1.5205896E-01	1.0011431E+00	9.9460567E-01	3.2758451E+00
NSET =	11						
BEADS	8.3582051E+04	3.7932241E-05	4.5383238E+00	1.4977339E-01	5.2221272E-01	-2.0694993E-01	-6.8954234E-02
CELLS	7.5988605E+05	1.5413152E-04	2.0283504E+00	1.4977339E-01	1.0224845E+00	8.4430001E-01	2.1908106E+00
NSET =	12						
BEADS	7.6571920E+04	3.4790913E-05	4.5435603E+00	1.5315574E-01	6.0063437E-01	1.9148512E-01	-2.2022224E-01
CELLS	6.5687475E+05	1.3090450E-04	1.9928380E+00	1.5315574E-01	1.1336124E+00	1.9735060E+00	1.6644597E+01
NSET =	13						
BEADS	8.0694180E+04	3.6721105E-05	4.5506510E+00	1.5049772E-01	6.8445590E-01	3.1220367E-01	-7.2089216E-02
CELLS	5.4470369E+05	1.1611518E-04	2.1317128E+00	1.5049772E-01	1.2047215E+00	2.1488624E+00	1.8511921E+01
NSET =	14						
BEADS	9.0558775E+04	4.1137785E-05	4.5426614E+00	1.4775510E-01	5.8228062E-01	5.5194406E-03	-3.2014992E-01
CELLS	5.5208903E+05	1.1046708E-04	2.0008925E+00	1.4775510E-01	9.0014324E-01	9.7153742E-01	3.4397835E+00
NSET =	15						
BEADS	9.0558775E+04	4.1137785E-05	4.5426614E+00	1.4775510E-01	5.8228062E-01	5.5194406E-03	-3.2014992E-01
CELLS	5.3760648E+05	1.0739704E-04	1.9976888E+00	1.4775510E-01	9.1498344E-01	9.8538613E-01	4.1106353E+00
NSET =	16						
BEADS	7.9266601E+04	3.6040531E-05	4.5467487E+00	1.5335077E-01	6.3634252E-01	2.0166679E-01	-8.6884430E-02
CELLS	3.8984919E+05	7.7880555E-05	1.9977098E+00	1.5335077E-01	1.1285229E+00	1.9325693E+00	1.8557432E+01
NSET =	17						
BEADS	7.9266601E+04	3.6040531E-05	4.5467487E+00	1.5335077E-01	6.3634252E-01	2.0166679E-01	-8.6884430E-02
CELLS	3.8921495E+05	7.7367530E-05	1.9877857E+00	1.5335077E-01	1.1785167E+00	1.8392225E+00	1.6289062E+01
NSET =	18						
BEADS	7.7868785E+04	3.5280227E-05	4.5307278E+00	1.4352901E-01	4.2600091E-01	1.1813519E-01	-5.2279570E-01
CELLS	3.9887787E+05	7.2048658E-05	1.8062837E+00	1.4352901E-01	8.9119600E-01	8.6186719E-01	2.8950376E+00
NSET =	19						

BEADS	9.9886225E+04	4.5385112E-05	4.5436808E+00	1.4121306E-01	5.9737559E-01	7.3483903E-02	-4.3242175E-01
CELLS	3.9777250E+05	6.8921565E-05	1.7326881E+00	1.4121306E-01	8.7441688E-01	8.6557117E-01	2.9271539E+03
NSET = 20							
BEADS	8.4289592E+04	3.8410341E-05	4.5569495E+00	1.5336734E-01	7.4713279E-01	3.0650446E-01	-7.8436700E-02
CELLS	5.4653185E+05	1.1312354E-04	2.0698435E+00	1.5336734E-01	1.0909141E+00	1.3437829E+00	9.9225351E+03
NSET = 21							
BEADS	8.4289592E+04	3.8410341E-05	4.5569495E+00	1.5336734E-01	7.4713279E-01	3.0650446E-01	-7.8436700E-02
CELLS	3.3951012E+09	6.9631593E-01	2.0509430E+00	1.5336734E-01	1.1838635E+00	1.7469329E+00	1.4233398E+01
NSET = 22							
BEADS	8.7119139E+04	3.9545269E-05	4.5392171E+00	1.4548497E-01	5.4304518E-01	4.4938530E-02	-4.1230040E-01
CELLS	2.1670046E+05	4.4995023E-05	2.0763695E+00	1.4548497E-01	9.3582369E-01	6.9984654E-01	1.4447666E+03
NSET = 23							
BEADS	8.7119139E+04	3.9545269E-05	4.5392171E+00	1.4548497E-01	5.4304518E-01	4.4938530E-02	-4.1230040E-01
CELLS	5.6514162E+05	1.1592781E-04	2.0513055E+00	1.4548497E-01	9.6443719E-01	7.3672867E-01	2.3050008E+00
NSET = 24							
BEADS	8.0513344E+04	3.6666245E-05	4.5540581E+00	1.5557411E-01	7.2034484E-01	3.3011766E-01	-4.9503495E-02
CELLS	6.8867608E+05	1.4901548E-04	2.1637964E+00	1.5557411E-01	1.1932667E+00	1.4470875E+00	1.0568254E+01
NSET = 25							
BEADS	8.2075020E+04	3.7420380E-05	4.5592898E+00	1.5692649E-01	7.6112883E-01	2.1904283E-01	3.3110719E-02
CELLS	6.7611099E+05	1.4813153E-04	2.1909353E+00	1.5692649E-01	1.2717778E+00	1.5782140E+00	1.2337375E+01
NSET = 26							
BEADS	8.4378141E+04	3.8328292E-05	4.5424433E+00	1.6445181E-01	5.6872300E-01	-2.4455096E-01	-4.1308946E-02
CELLS	6.7728135E+05	1.5908770E-04	2.3489160E+00	1.6445181E-01	1.1398624E+00	6.8340179E-01	1.5841952E+03
NSET = 27							
BEADS	8.4378141E+04	3.8328292E-05	4.5424433E+00	1.6445181E-01	5.6872300E-01	-2.4455096E-01	-4.1308946E-02
CELLS	6.7891369E+05	1.5159457E-04	2.2328989E+00	1.6445181E-01	1.0985725E+00	6.3554245E-01	1.4243511E+03
NSET = 28							
BEADS	7.7620631E+04	3.5311253E-05	4.5492097E+00	1.5728160E-01	6.6291266E-01	1.9771141E-01	-1.7132455E-01
CELLS	6.5031043E+05	1.4134473E-04	2.1734961E+00	1.5728160E-01	1.2394813E+00	1.6659854E+00	1.3441191E+01

Table XXII. Results of counting experiment #3.

Sample	Viable Count (cells/ml)	Optical Count (cells/ml)	Optical Density (Nephlos units)	Electronic Count (cells/ml	Electronic Volume Percent
1 (inoculum)	1.17×10^8	-	-	-	-
2	6.8×10^5 (5 min)	1.04×10^6 (0 min)	18.9 @1:½ (5 min) 9.6 @1:1	6.24×10^5 (5 min)	1.39×10^{-4}
3	1.49×10^6 (58 min)	2.46×10^6 (58 min)	21.9 @1:½ (1 hr 3 min) 9.9 @1:1	1.24×10^6	4.40×10^{-4}
4	1.08×10^7 (2 hr 5 min)	1.69×10^7 (2 hr 2 min)	48.5 @1:½ (2 hr 12 min) 19.7 @1:1	8.62×10^6 (2 hr 12 min)	1.71×10^{-3}
5	2.70×10^6 (3 hr 10 min)	4.70×10^7 (3 hr 15 min)	111.6 @1:½ (3 hr 15 min) 50.2 @1:1	2.92×10^7 (3 hr 15 min)	.00597
6	-	7.18×10^7 (4 hr 15 min)	107.4 @1:1 (4 hr 25 min) 51.3 @1:2	5.95×10^7 (4 hr 25 min)	.0112
7	8.00×10^7 (5 hr 25 min)	1.10×10^8 (5 hr 35 min)	147.2 @1:1 (5 hr 35 min) 70.5 @1:2	8.40×10^7 (5 hr 35 min)	.0173
8	8.10×10^7 (6 hr 55 min)	1.51×10^8 (6 hr 55 min)	97.1 @1:2 (7 hr) 46.2 @1:3	1.018×10^8 (7 hr)	.0226

Table XXIII. Conditions of electronic counting analysis, counting experiment #4.

Set	Sample	Time	Dilution	Aperture Voltage (volts)	Gain	Diff. (μsec)	Int. (μsec)
1	1 (inoculum)	0	1:2000	30	200	1	1
2	"	"	"	"	"	"	"
3	"	"	"	60	100	"	"
4	"	"	"	"	"	"	"
5	2	1 hr 3 min	1:10	"	"	"	"
6	"	"	"	120	50	"	"
7	"	"	"	"	"	"	"
8	"	"	"	30	200	"	"
9	"	"	"	"	"	"	"
10*	"	"	"	60	100	"	"
11	3	2 hr	1:15	30	200	"	"
12	"	"	"	"	"	"	"
13	"	"	"	60	100	"	"
14	"	"	"	"	"	"	"
15	"	"	"	120	50	"	"
16	"	"	"	"	"	"	"
17	"	"	"	30	200	"	"
18	"	"	"	"	"	"	"
19*	"	2 hr	1:15	60	100	"	"
20	4	3 hr	1:101	30	200	"	"
21	"	"	"	"	"	"	"
22	"	"	"	60	100	"	"
23	"	"	"	"	"	"	"
24	"	"	"	120	50	"	"
25	"	"	"	"	"	"	"
26	5	4 hr 5 min	1:101	30	200	"	"
27	"	"	"	"	"	"	"
28	"	"	"	"	"	"	"

* 2.05 micron spheres mixed with cell sample to establish the electrical conductivity of the sample solution.

Table XXIII (continued)

Set	Sample	Time	Dilution	Aperture Voltage (volts)	Gain	Diff. (μsec)	Int. (μsec)
29	5	4 hr 5 min	1:101	60	100	1	1
30	"	"	"	60	100	"	"
31	"	"	"	120	50	"	"
32	"	"	"	"	"	"	"
33	6	5 hr 5 min	1:201	30	200	"	"
34	"	"	"	"	"	"	"
35	"	"	"	60	100	"	"
36	"	"	"	"	"	"	"
37	"	"	"	120	50	"	"
38	"	"	"	"	"	"	"
39	"	"	"	"	"	"	"
40	7	5 hr 56 min	"	30	200	"	"
41	"	"	"	"	"	"	"
42	"	"	"	"	"	"	"
43	"	"	"	60	100	"	"
44	"	"	"	"	"	"	"
45	"	"	"	120	50	"	"
46	"	"	"	"	"	"	"
47	8	6 hr 56 min	1:301	30	200	"	"
48	"	"	"	"	"	"	"
49	"	"	"	60	100	"	"
50	"	"	"	"	"	"	"
51	"	"	"	120	50	"	"
52	"	"	"	"	"	"	"

Table XXIV. Summary of results,
counting experiment #4

SUMMARY OF CALCULATED RESULTS,ALL DISTRIBUTIONS

	PARTICLES/ML	VOLUME PERCENT	AVE.VOL.(MU**3)	VOLUME FACTOR	STD.DEV.(MU**3)	SKEWNESS	KURTOSIS
NSET =	1						
BEADS	7.6188862E+05	8.9907774E-05	1.1800645E+00	6.2263022E-02	2.4100389E-01	1.3173124E-01	-3.9067369E-01
CELLS	5.2204195E+04	1.2064516E-05	2.3110243E+00	6.2263022E-02	9.8594758E-01	5.2351525E-01	1.4645695E+00
NSET =	2						
BEADS	7.6188862E+05	8.9907774E-05	1.1800645E+00	6.2268022E-02	2.4100389E-01	1.3173124E-01	-3.9067369E-01
CELLS	4.9743715E+04	1.1577675E-05	2.3475577E+00	6.2263022E-02	9.5131250E-01	6.6525178E-01	1.5259379E+00
NSET =	3						
BEADS	6.5740142E+05	7.7444293E-05	1.1780366E+00	6.2637527E-02	2.2547552E-01	1.5133856E-01	-1.9469530E-01
CELLS	5.4769104E+04	1.2109909E-05	2.2110839E+00	6.2537527E-02	9.7927592E-01	8.2899041E-01	2.3159238E+00
NSET =	4						
BEADS	7.7400343E+05	9.1339582E-05	1.1800927E+00	6.2880485E-02	2.3983767E-01	1.0013162E-01	-2.7648562E-01
CELLS	5.9550853E+04	2.1503215E-05	3.0917255E+00	6.2880485E-02	1.3037273E+00	5.3734949E-01	4.9004932E-01
NSET =	5						
BEADS	7.7400343E+05	9.1339582E-05	1.1800927E+00	6.2880485E-02	2.3983757E-01	1.0013152E-01	-2.7648562E-01
CELLS	1.5066295E+05	3.9363436E-05	2.6126832E+00	6.2880485E-02	1.1928513E+00	6.9103621E-01	1.1745638E+00
NSET =	6						
BEADS	7.7486996E+05	9.1112816E-05	1.1758466E+00	6.1983776E-02	2.0809596E-01	1.8590349E-01	-9.8826177E-02
CELLS	1.5571297E+05	3.3608074E-05	2.1583349E+00	6.1983775E-02	1.0965606E+00	4.8573230E-01	3.0798402E-01
NSET =	7						
BEADS	7.7486996E+05	9.1112816E-05	1.1758465E+00	6.1983776E-02	2.0809596E-01	1.8590349E-01	-9.8826177E-02
CELLS	1.4861388E+05	3.4118747E-05	2.2957982E+00	6.1983776E-02	1.0851355E+00	5.4854910E-01	3.7413086E-01
NSET =	8						
BEADS	1.0494948E+06	1.2358936E-04	1.1776052E+00	6.8149950E-02	2.2701984E-01	3.2920312E-01	-2.5383912E-01
CELLS	5.4262341E+05	7.4988039E-05	1.3819404E+00	6.8149950E-02	1.2477133E+00	1.1592392E+00	2.7711712E+00
NSET =	9						
BEADS	1.0494948E+06	1.2358936E-04	1.1776052E+00	6.8149950E-02	2.2701984E-01	3.2920812E-01	-2.5383912E-01
CELLS	3.5822575E+05	6.0065342E-05	1.6767453E+00	5.8149950E-02	1.3910763E+00	8.6569316E-01	1.4391069E+00
NSET =	10						
BEADS	6.5740142E+05	7.7444293E-05	1.1780366E+00	6.2537527E-02	2.2547552E-01	1.5133856E-01	-1.9469530E-01
CELLS	2.3121728E+05	8.7745144E-05	3.7949216E+00	6.2537527E-02	1.7189915E+00	3.2375197E-01	-2.2678517E-01
NSET =	11						
BEADS	4.6067819E+05	5.4557638E-05	1.1842896E+00	6.9218223E-02	2.6460899E-01	6.3387715E-03	-2.1814506E-01
CELLS	6.2638717E+05	1.4770474E-04	2.3561647E+00	6.9218223E-02	1.0357186E+00	9.0592441E-01	2.5823702E+00
NSET =	12						
BEADS	4.6067819E+05	5.4557638E-05	1.1842896E+00	6.9218223E-02	2.6460899E-01	6.3387715E-03	-2.1814506E-01
CELLS	6.0253171E+05	1.4759913E-04	2.4513087E+00	6.9218223E-02	1.0299260E+00	8.9937914E-01	2.4227492E+00
NSET =	13						
BEADS	4.5539067E+05	5.3722957E-05	1.1797114E+00	6.8937164E-02	2.3757933E-01	1.4321154E-01	-1.0889794E-01
CELLS	6.4294170E+05	1.5274085E-04	2.3756562E+00	6.8937164E-02	9.8132719E-01	8.6232697E-01	2.4327056E+00
NSET =	14						
BEADS	4.5539067E+05	5.3722957E-05	1.1797114E+00	6.8937164E-02	2.3757933E-01	1.4321154E-01	-1.0889794E-01
CELLS	6.3844288E+05	1.5051325E-04	2.3575053E+00	6.8937164E-02	9.7769612E-01	8.6763759E-01	2.4572217E+00
NSET =	15						
BEADS	3.9970776E+05	4.6914100E-05	1.1737100E+00	6.4631850E-02	1.8975210E-01	2.1615612E-01	-2.1111628E-01
CELLS	6.4542207E+05	1.2812012E-04	1.9850595E+00	6.4631850E-02	8.7084116E-01	7.8043797E-01	1.4254759E+00
NSET =	16						
BEADS	3.9970776E+05	4.6914100E-05	1.1737100E+00	6.4631850E-02	1.8975210E-01	2.1615612E-01	-2.1111628E-01
CELLS	6.4269090E+05	1.2773034E-04	1.9874381E+00	6.4631850E-02	8.7345952E-01	7.8705794E-01	1.4267203E+00
NSET =	17						
BEADS	4.2424096E+05	5.0043851E-05	1.1796091E+00	6.6926629E-02	2.3914055E-01	1.7797546E-01	-4.1863697E-01
CELLS	6.3195728E+05	1.4745452E-04	2.3335598E+00	6.6926629E-02	1.0318515E+00	8.5396382E-01	2.2077350E+00
NSET =	18						
BEADS	4.2424096E+05	5.0043851E-05	1.1796091E+00	6.6926629E-02	2.3914055E-01	1.7797545E-01	-4.1863697E-01
CELLS	5.9021659E+05	1.4282017E-04	2.4197925E+00	6.6926629E-02	1.0484279E+00	8.3430585E-01	2.1072024E+00
NSET =	19						

BEADS	4.5539067E+05	5.3722957E-05	1.1797114E+00	6.8937154E-02	2.3757933E-01	1.4321164E-01	-1.0389794E-01
CELLS	7.2079250E+05	2.0892652E-04	2.8985664E+00	6.8937164E-02	1.5425430E+00	7.5844783E-01	9.7651561E-01
NSET = 20							
BEADS	4.5758740E+05	5.4045181E-05	1.1810398E+00	6.5699665E-02	2.4833475E-01	1.3623464E-01	-3.3047526E-01
CELLS	3.4257425E+05	6.7343278E-05	1.9658309E+00	6.5699665E-02	9.3336103E-01	6.8251661E-01	1.8711138E+00
NSET = 21							
BEADS	4.5758740E+05	5.4045181E-05	1.1810398E+00	6.5699665E-02	2.4833475E-01	1.3623464E-01	-3.3047526E-01
CELLS	3.1564571E+05	6.6386939E-05	2.1190511E+00	6.5699665E-02	9.0164373E-01	8.6989677E-01	2.5325258E+00
NSET = 22							
BEADS	4.3995462E+05	5.1812690E-05	1.1776826E+00	6.7950216E-02	2.2310583E-01	1.7349251E-01	-1.4794820E-01
CELLS	3.1787622E+05	6.9123234E-05	2.1745321E+00	6.7950216E-02	9.0742029E-01	9.8329332E-01	2.5317984E+00
NSET = 23							
BEADS	4.3995462E+05	5.1812690E-05	1.1776826E+00	6.7950216E-02	2.2310583E-01	1.7349251E-01	-1.4794820E-01
CELLS	3.2084303E+05	7.1304944E-05	2.2130949E+00	6.7950216E-02	9.5096468E-01	8.7553913E-01	2.3885143E+00
NSET = 24							
BEADS	4.2643973E+05	5.0159845E-05	1.1762470E+00	6.5705487E-02	2.1401859E-01	2.8958060E-01	-9.8698433E-02
CELLS	3.2109603E+05	6.1110318E-05	1.9031789E+00	6.5705487E-02	8.3334424E-01	9.2609227E-01	2.2893308E+00
NSET = 25							
BEADS	4.2643973E+05	5.0159845E-05	1.1762470E+00	6.5705487E-02	2.1401859E-01	2.8958060E-01	-9.8698433E-02
CELLS	3.1323995E+05	6.1786672E-05	1.9725029E+00	6.5705487E-02	8.5044573E-01	8.9277539E-01	2.3735113E+00
NSET = 26							
BEADS	3.6560872E+05	4.3074021E-05	1.1781453E+00	6.9828404E-02	2.2557019E-01	1.1753131E-01	-2.3141498E-01
CELLS	4.9503624E+05	1.0925843E-04	2.2073805E+00	6.9828404E-02	9.4697766E-01	8.4579550E-01	2.4255503E+00
NSET = 27							
BEADS	3.6560872E+05	4.3074021E-05	1.1781453E+00	6.9828404E-02	2.2557019E-01	1.1753131E-01	-2.3141498E-01
CELLS	5.0057522E+05	1.0649893E-04	2.1275311E+00	6.9828404E-02	9.4426188E-01	8.8801161E-01	2.6350614E+00
NSET = 28							
BEADS	3.6560872E+05	4.3074021E-05	1.1781453E+00	6.9828404E-02	2.2557019E-01	1.1753131E-01	-2.3141498E-01
CELLS	5.1605336E+05	1.0683047E-04	2.0701559E+00	6.9828404E-02	9.3722808E-01	9.3719971E-01	2.9268755E+00
NSET = 29							
BEADS	3.4632819E+05	4.1151445E-05	1.1882210E+00	6.8879100E-02	2.8015541E-01	-9.5144181E-02	1.9194302E-01
CELLS	5.1695828E+05	1.1228735E-04	2.1725076E+00	6.8879100E-02	9.5573053E-01	8.0831272E-01	2.3295852E+00
NSET = 30							
BEADS	3.4632819E+05	4.1151445E-05	1.1882210E+00	6.8879100E-02	2.8015541E-01	-9.5144181E-02	1.9194302E-01
CELLS	5.3023653E+05	1.1514195E-04	2.1715205E+00	6.8879100E-02	9.6486501E-01	8.3286718E-01	2.1728053E+00
NSET = 31							
BEADS	4.1055465E+05	4.8243336E-05	1.1750783E+00	6.4538931E-02	2.0302886E-01	2.5904155E-01	-1.0742325E-01
CELLS	5.3541702E+05	1.0597650E-04	1.9793254E+00	6.4533931E-02	8.4544401E-01	7.9756499E-01	1.6428323E+00
NSET = 32							
BEADS	4.1055465E+05	4.8243386E-05	1.1750783E+00	6.4538931E-02	2.0302886E-01	2.5904155E-01	-1.0742325E-01
CELLS	5.2221393E+05	1.0584050E-04	2.0267671E+00	6.4533931E-02	8.7233804E-01	7.3133653E-01	1.5059995E+00
NSET = 33							
BEADS	4.1146359E+05	4.8529350E-05	1.1794324E+00	6.4514907E-02	2.3727814E-01	1.6655383E-01	-3.6821737E-01
CELLS	3.1980597E+05	6.4703830E-05	2.0232233E+00	6.4514907E-02	8.7413051E-01	8.6819857E-01	2.5941733E+00
NSET = 34							
BEADS	4.1146359E+05	4.8529350E-05	1.1794324E+00	6.4514907E-02	2.3727814E-01	1.6655383E-01	-3.6821737E-01
CELLS	3.1508277E+05	6.5423759E-05	2.0763391E+00	6.4514907E-02	9.0699340E-01	8.8511246E-01	2.6973985E+00
NSET = 35							
BEADS	4.1471326E+05	4.8753532E-05	1.1755962E+00	6.7878771E-02	2.0370349E-01	7.1620905E-02	-1.7178341E-01
CELLS	3.2813205E+05	7.1173769E-05	2.1590589E+00	6.7878771E-02	9.3787032E-01	8.4618536E-01	2.4073921E+00
NSET = 36							
BEADS	4.1471326E+05	4.8753532E-05	1.1755962E+00	6.7878771E-02	2.0370349E-01	7.1620906E-02	-1.7178341E-01
CELLS	3.2973550E+05	7.1213257E-05	2.1662782E+00	6.7878771E-02	9.3007617E-01	8.5601153E-01	2.5524067E+00
NSET = 37							
BEADS	4.0976846E+05	4.8187858E-05	1.1759777E+00	6.5046511E-02	2.1132831E-01	2.7387677E-01	-1.1046358E-01
CELLS	3.2374751E+05	6.6562958E-05	2.0560145E+00	6.5046511E-02	8.4943351E-01	7.5368525E-01	1.5835179E+00
NSET = 38							
BEADS	4.0976846E+05	4.8187858E-05	1.1759777E+00	6.5046511E-02	2.1132831E-01	2.7387677E-01	-1.1046358E-01
CELLS	3.3003157E+05	6.8189471E-05	2.0661499E+00	6.5046511E-02	8.4446163E-01	7.4555208E-01	1.5572573E+00
NSET = 39							
BEADS	4.1707812E+05	4.9226011E-05	1.1802588E+00	7.0047052E-02	2.4072498E-01	8.4242324E-02	-3.1352153E-01
CELLS	2.4845333E+05	5.9210555E-05	2.3831551E+00	7.0047052E-02	9.7561171E-01	8.6446931E-01	2.4213568E+00

NSET = 40							
BEADS	4.1707812E+05	4.9226011E-05	1.1802588E+00	7.0047052E-02	2.4072498E-01	8.4242324E-02	-3.1352153E-01
CELLS	2.4535469E+05	5.8333187E-05	2.3775044E+00	7.0047052E-02	9.5458013E-01	8.7664552E-01	2.4706244E+00
NSET = 41							
BEADS	4.1707812E+05	4.9226011E-05	1.1802588E+00	7.0047052E-02	2.4072498E-01	8.4242324E-02	-3.1352153E-01
CELLS	2.5925635E+05	5.7920977E-05	2.2341199E+00	7.0047052E-02	9.6431652E-01	9.0493789E-01	2.7453007E+00
NSET = 42							
BEADS	3.6622841E+05	4.3153619E-05	1.1783253E+00	6.9894250E-02	2.2672236E-01	1.0994759E-01	-2.2332298E-01
CELLS	2.6087798E+05	5.8585143E-05	2.2495529E+00	6.9894250E-02	9.7605983E-01	8.5239299E-01	2.3908616E+00
NSET = 43							
BEADS	4.1098535E+05	4.8400953E-05	1.1776806E+00	6.6802723E-02	2.2265930E-01	1.8829876E-01	8.1620378E-02
CELLS	2.5999549E+05	6.0146024E-05	2.3095025E+00	6.6802723E-02	9.8613008E-01	8.2235387E-01	2.2189778E+00
NSET = 44							
BEADS	4.1098535E+05	4.8400953E-05	1.1776806E+00	6.6802723E-02	2.2265930E-01	1.8829876E-01	8.1620378E-02
CELLS	2.6012139E+05	6.0123711E-05	2.3113713E+00	6.6802723E-02	9.8511157E-01	7.9643496E-01	2.0231978E+00
NSET = 45							
BEADS	3.9230864E+05	4.6107324E-05	1.1752319E+00	6.4435211E-02	2.0392390E-01	2.2689253E-01	-4.3629398E-02
CELLS	2.7082944E+05	5.9433173E-05	2.1944871E+00	6.4435211E-02	9.2884150E-01	7.3770030E-01	1.4998571E+00
NSET = 46							
BEADS	3.9230864E+05	4.6107324E-05	1.1752319E+00	6.4435211E-02	2.0392390E-01	2.2689253E-01	-4.3629398E-02
CELLS	2.6720618E+05	5.8992903E-05	2.2077671E+00	6.4435211E-02	9.1658191E-01	7.3423475E-01	1.5059150E+00
NSET = 47							
BEADS	3.7932590E+05	4.4752846E-05	1.1797994E+00	6.8984357E-02	2.3798975E-01	9.0095341E-02	-4.1776058E-01
CELLS	2.3902817E+05	5.5250748E-05	2.3114743E+00	6.8984357E-02	9.8216122E-01	7.3310817E-01	1.7781478E+00
NSET = 48							
BEADS	3.7932590E+05	4.4752846E-05	1.1797994E+00	6.8984357E-02	2.3798975E-01	9.0095341E-02	-4.1776058E-01
CELLS	2.3786960E+05	5.4897028E-05	2.3078623E+00	6.8984357E-02	9.8942001E-01	7.7450595E-01	2.0146621E+00
NSET = 49							
BEADS	4.2360230E+05	5.0070796E-05	1.1820237E+00	6.6646069E-02	2.5210330E-01	7.5790015E-02	-1.8554358E-01
CELLS	2.1735293E+05	5.4463136E-05	2.5057489E+00	6.6646069E-02	1.0813421E+00	7.5095199E-01	1.7033209E+00
NSET = 50							
BEADS	4.2360230E+05	5.0070796E-05	1.1820237E+00	6.6646069E-02	2.5210330E-01	7.5790015E-02	-1.8554358E-01
CELLS	1.9881325E+05	5.0800759E-05	2.5551999E+00	6.6646069E-02	1.1091703E+00	6.8938769E-01	1.3644258E+00
NSET = 51							
BEADS	3.9222696E+05	4.6129253E-05	1.1760857E+00	6.4187794E-02	2.1042947E-01	1.8638051E-01	-1.9036175E-01
CELLS	1.9272603E+05	4.7909382E-05	2.4858802E+00	6.4187794E-02	1.0062513E+00	5.9833351E-01	9.0813970E-01
NSET = 52							
BEADS	3.9222696E+05	4.6129253E-05	1.1760857E+00	6.4187794E-02	2.1042947E-01	1.8638051E-01	-1.9036175E-01
CELLS	1.9157518E+05	4.7793039E-05	2.4947302E+00	6.4187794E-02	1.0089928E+00	6.2467539E-01	1.3055895E+00

Table XXV. Results of counting experiment #4.

Sample	Viable Count (cells/ml)	Optical Count (cells/ml)	Optical Density (Nephlos units)	Electronic Count (cells/ml)	Electronic Volume Percent
1	1.18×10^8 (0 hr)	-	-	1.045×10^8 (0 hr)	.239
2	1.45×10^6 (57 min)	2.30×10^6 (52 min)	4.3 (52 min)	1.517×10^6 (52 min)	3.57×10^{-4}
3	9.15×10^6 (2 hr 8 min)	1.38×10^7 (2 hr 5 min)	20.4 (2 hr 5 min)	9.49×10^6 (2 hr 5 min)	.00215
4	3.00×10^7 (3 hr 11 min)	4.52×10^7 (3 hr 6 min)	62.7 (3 hr 6 min)	3.25×10^7 (3 hr 6 min)	.00668
5	4.82×10^7 (4 hr 7 min)	6.58×10^7 (4 hr 3 min)	106.6 (4 hr 3 min)	5.22×10^7 (4 hr 3 min)	.01099
6	5.93×10^7 (5 hr 10 min)	7.86×10^7 (5 hr 5 min)	91.9 (5 hr 5 min)	6.49×10^7 (5 hr 5 min)	.0136
7	5.07×10^7 (5 hr 55 min)	8.16×10^7 (5 hr 56 min)	115.4 (5 hr 56 min)	5.20×10^7 (5 hr 56 min)	.0119
8	4.89×10^7 (6 hr 52 min)	7.38×10^7 (6 hr 52 min)	141.1 (6 hr 52 min)	3.36×10^7 (6 hr 52 min)	.0156

Table XXVI. Typical distribution, counting experiment #4

THIS IS DATA SET 6
COUNTING EXPERIMENT 4,7/14/66,E.COLI B,HERSHEY IN BATCH CULTURE
1ST,SAMPLED 1HR 3MIN AFTER INOC.,ANALYSED 3MIN LATER,1/10 DILUTION

1.305 μ spheres, Aperture voltage= 120V, Gain=50,Vacuum=8.0in
FLOW = .210700 ML/MIN COR. FACTOR = 5.017003E+01

LIVE COUNTING TIME = 946.0000 /10000 MINUTES

OBSERVED PULSE-HEIGHT ANALYSIS DISTRIBUTION

0	0	1	74	199	295	255	281	240	235
169	175	182	411	1013	1831	2053	1958	1691	1447
1177	988	687	591	467	377	345	362	482	648
733	786	708	664	614	557	485	474	376	312
293	266	228	204	216	228	232	262	264	264
255	271	260	222	246	257	224	238	249	221
197	201	182	156	164	155	155	131	148	138
144	168	143	134	154	161	181	166	200	162
172	191	209	181	190	182	197	162	143	150
132	122	130	158	124	129	130	132	124	103
107	112	94	86	96	94	70	80	62	41
21	22	10	9	9	7	6	7	6	3
1	8	1	4	0	1	3			

TOTAL PARTICLE CONCENTRATION = 7.7486996E+05 /ML PERCENT BY VOLUME PARTICLES = 9.1112816E-05
MEAN PARTICLE VOLUME = 1.1758466E+00 CUBIC MICRONS VOL. FACTOR = 6.1983776E-02
VARIANCE OF VOLUME = 4.3303928E-02 STANDARD DEVIATION = 2.0809576E-01 CUBIC MICRONS
MOMENTAL SKEWNESS = 1.8590349E-01 KURTOSIS =-9.8826177E-02
MEAN PARTICLE DIAMETER = 1.3050003E+00 MICRONS DIAMETER FACTOR = 4.9101327E-01
VARIANCE OF DIAMETER = 5.9333152E-03 STANDARD DEVIATION = 7.7023016E-02 MICRONS
MOMENTAL SKEWNESS = 2.8790519E-02 KURTOSIS =-6.6993553E-02

DISTRIBUTION AFTER CORRECTION FOR NOISE AND VOLUME

0.	0.	0.	0.	5.94756E+03
1.19871E+04	1.07910E+04	1.25347E+04	1.09385E+04	1.09307E+04
7.78492E+03	8.20018E+03	8.63172E+03	2.01785E+04	5.04237E+04
9.14956E+04	1.02659E+05	9.79144E+04	8.45371E+04	7.23113E+04
5.87795E+04	4.93102E+04	3.42208E+04	2.94155E+04	2.32048E+04
1.85993E+04	1.71032E+04	1.79649E+04	2.39938E+04	3.23301E+04
3.66022E+04	3.92686E+04	3.53624E+04	3.31616E+04	3.06596E+04
2.73061E+04	2.41997E+04	2.36535E+04	1.87423E+04	1.55366E+04
1.45883E+04	1.32385E+04	1.13356E+04	1.01348E+04	1.07430E+04
1.13491E+04	1.15536E+04	1.30623E+04	1.31652E+04	1.31695E+04
1.27212E+04	1.35270E+04	1.29781E+04	1.10744E+04	1.22812E+04
1.28357E+04	1.11825E+04	1.18873E+04	1.24414E+04	1.10388E+04
9.83691E+03	1.00395E+04	9.08816E+03	7.78556E+03	8.18866E+03
7.73880E+03	7.74040E+03	6.53786E+03	7.39221E+03	6.89192E+03
7.19428E+03	8.39955E+03	7.14663E+03	6.53628E+03	7.70081E+03
8.05308E+03	9.05752E+03	8.30596E+03	1.00127E+04	8.10713E+03
8.60970E+03	9.56377E+03	1.04676E+04	9.06363E+03	9.51589E+03
9.11523E+03	9.86845E+03	8.11314E+03	7.16052E+03	7.51230E+03
6.60980E+03	6.10854E+03	6.51051E+03	7.91577E+03	6.21046E+03
6.46176E+03	6.51237E+03	6.61312E+03	5.21216E+03	5.15897E+03
5.35001E+03	5.61121E+03	4.70848E+03	4.30744E+03	4.80945E+03
4.20770E+03	3.50550E+03	4.00757E+03	3.10477E+03	2.05144E+03

1.04928E+03	1.09857E+03	4.96849E+02	4.46886E+02	4.47083E+02
3.46933E+02	2.96944E+02	3.47238E+02	2.97234E+02	1.46933E+02
4.67455E+01	3.98092E+02	4.70311E+01	1.97675E+02	0.
4.74155E+01	1.47873E+02			

E.COLI B,APERTURE VOLTAGE=120V,GAIN=50,VACUUM=8.0IN
FLOW = .210700 ML/MIN COR. FACTOR = 1.019567E+01

LIVE COUNTING TIME = 4655.0000 /10000 MINUTES

OBSERVED PULSE-HEIGHT ANALYSIS DISTRIBUTION

1	2	194	464	461	376	298	232	225	189
191	185	204	186	227	262	306	326	353	415
495	515	498	535	559	529	533	530	485	494
440	406	374	345	331	292	283	246	229	217
178	209	194	180	164	196	148	145	191	128
139	133	128	138	139	124	130	111	105	99
92	104	125	99	101	93	93	67	82	73
58	69	82	50	43	49	50	40	49	35
26	21	33	29	19	22	16	15	10	11
19	8	15	5	5	6	6	3	3	4
0	3	5	1	1	5	2	1	0	1
2	1	1	0	0	0	0	0	0	0
0	0	0	0	0	0	0			

TOTAL PARTICLE CONCENTRATION = 1.5571297E+05 /ML PERCENT BY VOLUME PARTICLES = 3.3608074E-05
MEAN PARTICLE VOLUME = 2.1583349E+00 CUBIC MICRONS VOL. FACTOR = 6.1983776E-02
VARIANCE OF VOLUME = 1.2024452E+00 STANDARD DEVIATION = 1.0965606E+00 CUBIC MICRONS
MOMENTAL SKEWNESS = 4.8573230E-01 KURTOSIS = 3.0798402E-01
MEAN PARTICLE DIAMETER = 1.5584245E+00 MICRONS DIAMETER FACTOR = 4.9101327E-01
VARIANCE OF DIAMETER = 7.1661119E-02 STANDARD DEVIATION = 2.6769595E-01 MICRONS
MOMENTAL SKEWNESS = 5.5858356E-02 KURTOSIS =-4.5021549E-02

DISTRIBUTION AFTER CORRECTION FOR NOISE AND VOLUME

0.	0.	0.	0.	6.63931E+02
1.02049E+03	1.03593E+03	9.02344E+02	1.19158E+03	1.06769E+03
1.25355E+03	1.30653E+03	1.58070E+03	1.45592E+03	1.91588E+03
2.33551E+03	2.78008E+03	3.00530E+03	3.29863E+03	3.94651E+03
4.77623E+03	4.99295E+03	4.83144E+03	5.21971E+03	5.47478E+03
5.17872E+03	5.22881E+03	5.20708E+03	4.75672E+03	4.85654E+03
4.31358E+03	3.97439E+03	3.65517E+03	3.36624E+03	3.22995E+03
2.73654E+03	2.75264E+03	2.38106E+03	2.21315E+03	2.09598E+03
1.70331E+03	2.02413E+03	1.87575E+03	1.73736E+03	1.57840E+03
1.90865E+03	1.42308E+03	1.39615E+03	1.86856E+03	1.22968E+03
1.34535E+03	1.29695E+03	1.23891E+03	1.34369E+03	1.35658E+03
1.20623E+03	1.26937E+03	1.07852E+03	1.01962E+03	9.60612E+02
8.91320E+02	1.01566E+03	1.23167E+03	9.68406E+02	9.90543E+02
9.10648E+02	9.12248E+02	6.48692E+02	8.03094E+02	7.12737E+02
5.61146E+02	6.64389E+02	8.09361E+02	4.83279E+02	4.13038E+02
4.75293E+02	4.86524E+02	3.85558E+02	4.78268E+02	3.36437E+02
2.45546E+02	1.95400E+02	3.18545E+02	2.78526E+02	1.77300E+02
2.08596E+02	1.48082E+02	1.38527E+02	8.81627E+01	9.89461E+01
1.81074E+02	6.94605E+01	1.41346E+02	3.98830E+01	4.03557E+01
5.10039E+01	5.14372E+01	2.12651E+01	2.16622E+01	3.22382E+01
0.	2.27551E+01	4.34801E+01	3.01688E+00	3.32274E+00
4.43982E+01	1.40916E+01	4.16432E+00	0.	4.66731E+00

1.50985E+01	5.12836E+00	5.34425E+00	0.	0.
0.	0.	0.	0.	0.
0.	0.	0.	0.	0.
0.	0.			

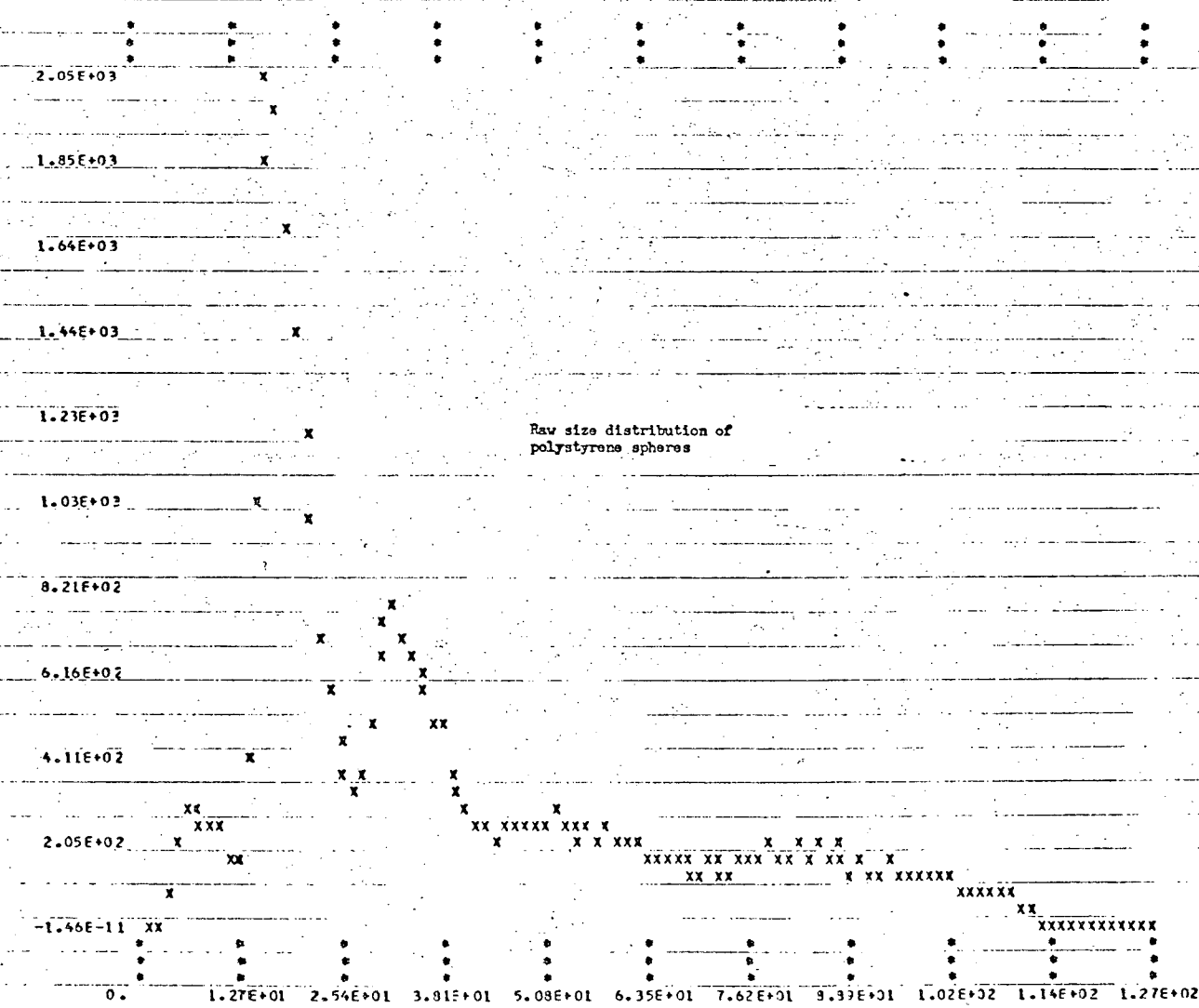

Raw size distribution of polystyrene spheres

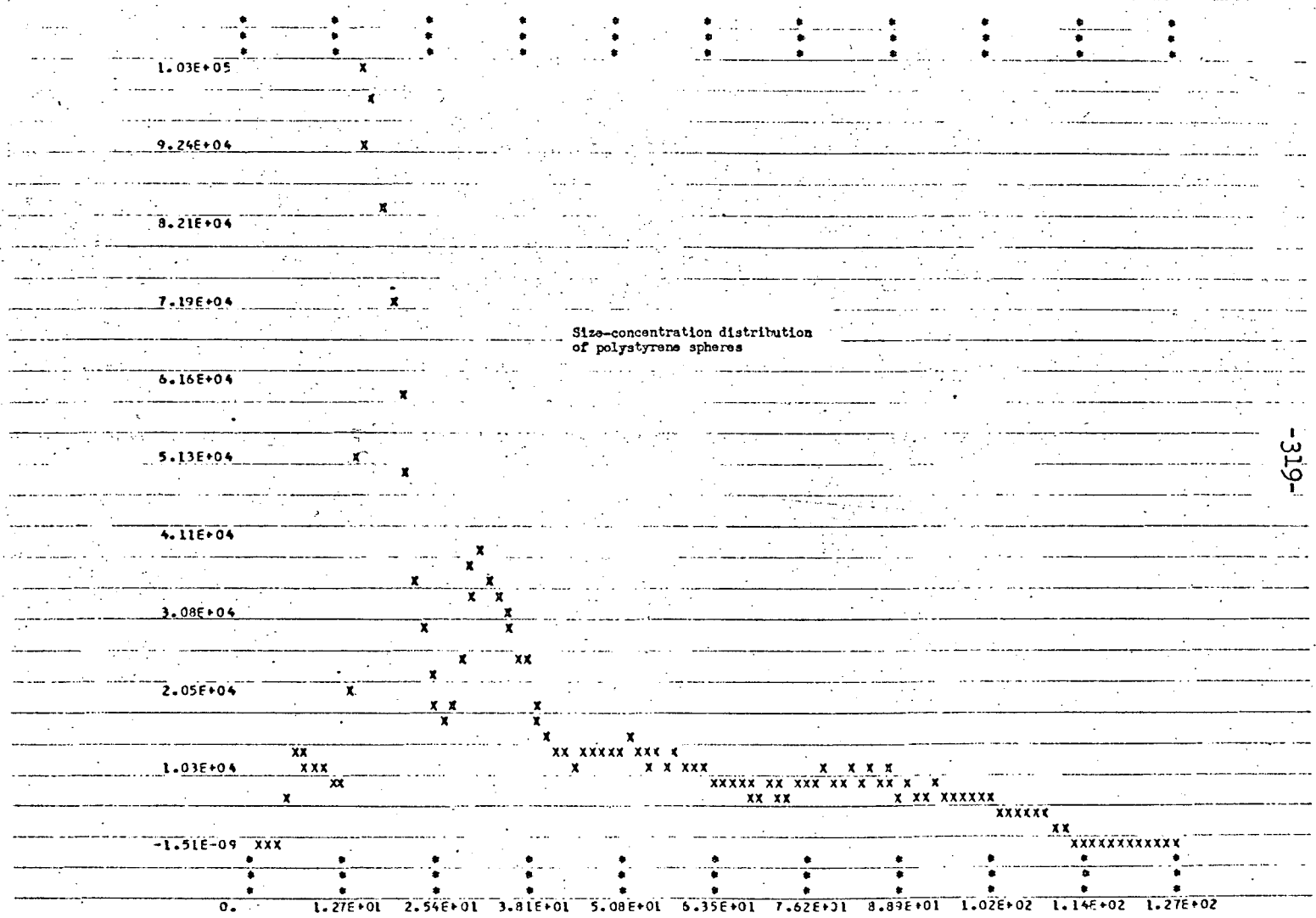

Size-concentration distribution of polystyrene spheres

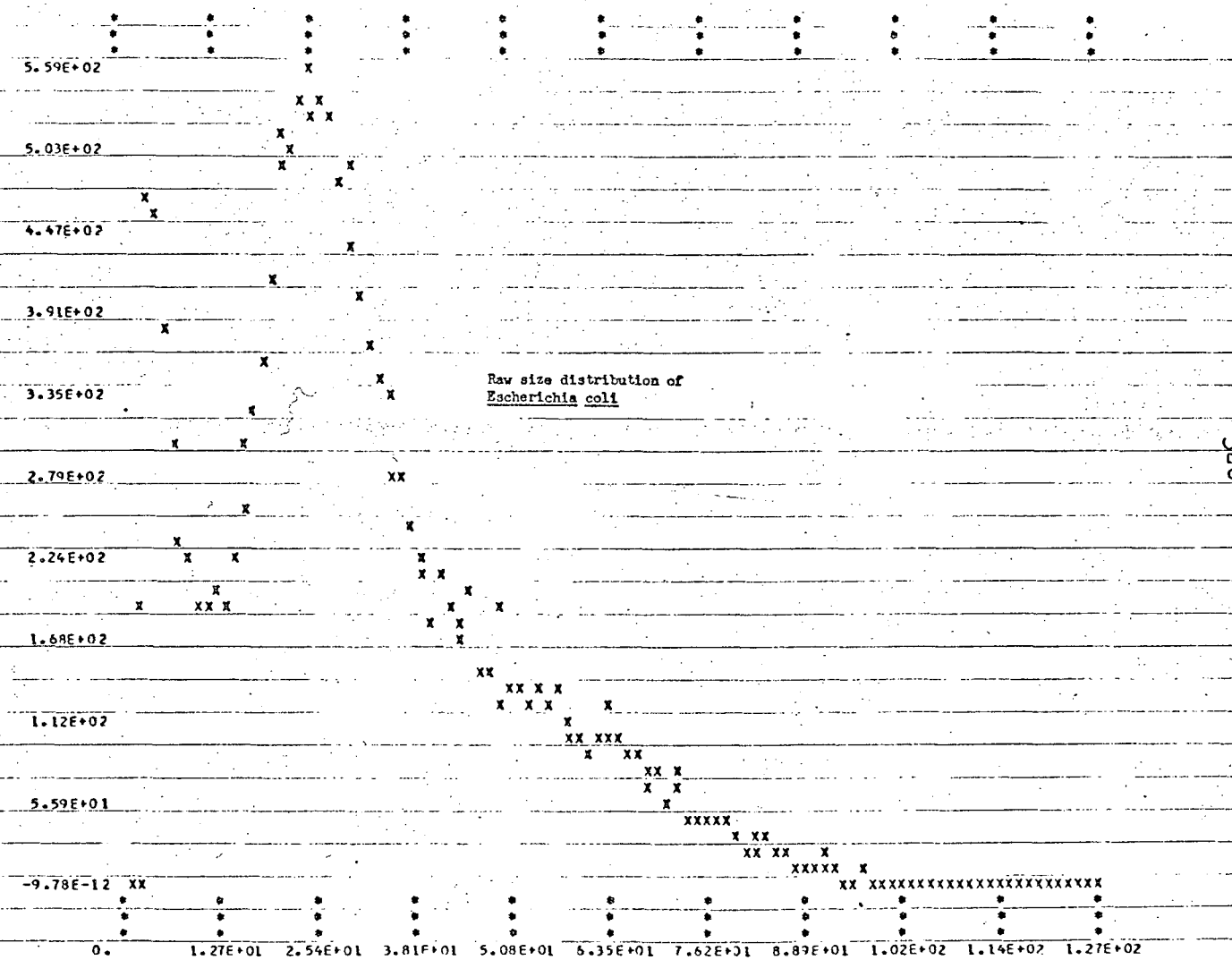

Raw size distribution of
Escherichia coli

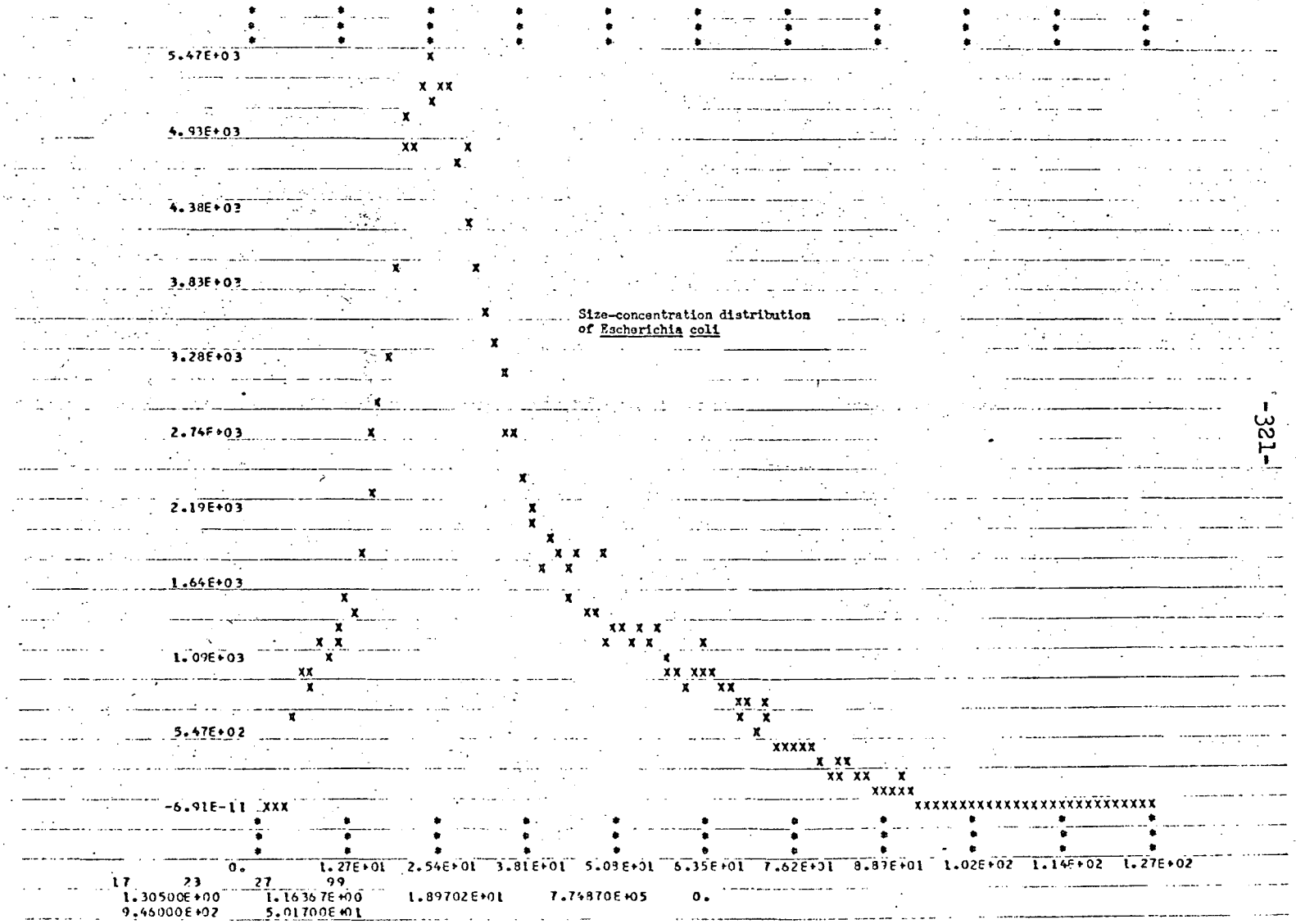

Size-concentration distribution of *Escherichia coli*

```
NMINOS =  11 NMINCE =  13
    6.94249E+02    -4.35400E-02    4.34656E+04    -4.19790E-01
    6.94249E+02    -4.35400E-02    4.34656E+04    -4.19790E-01
```

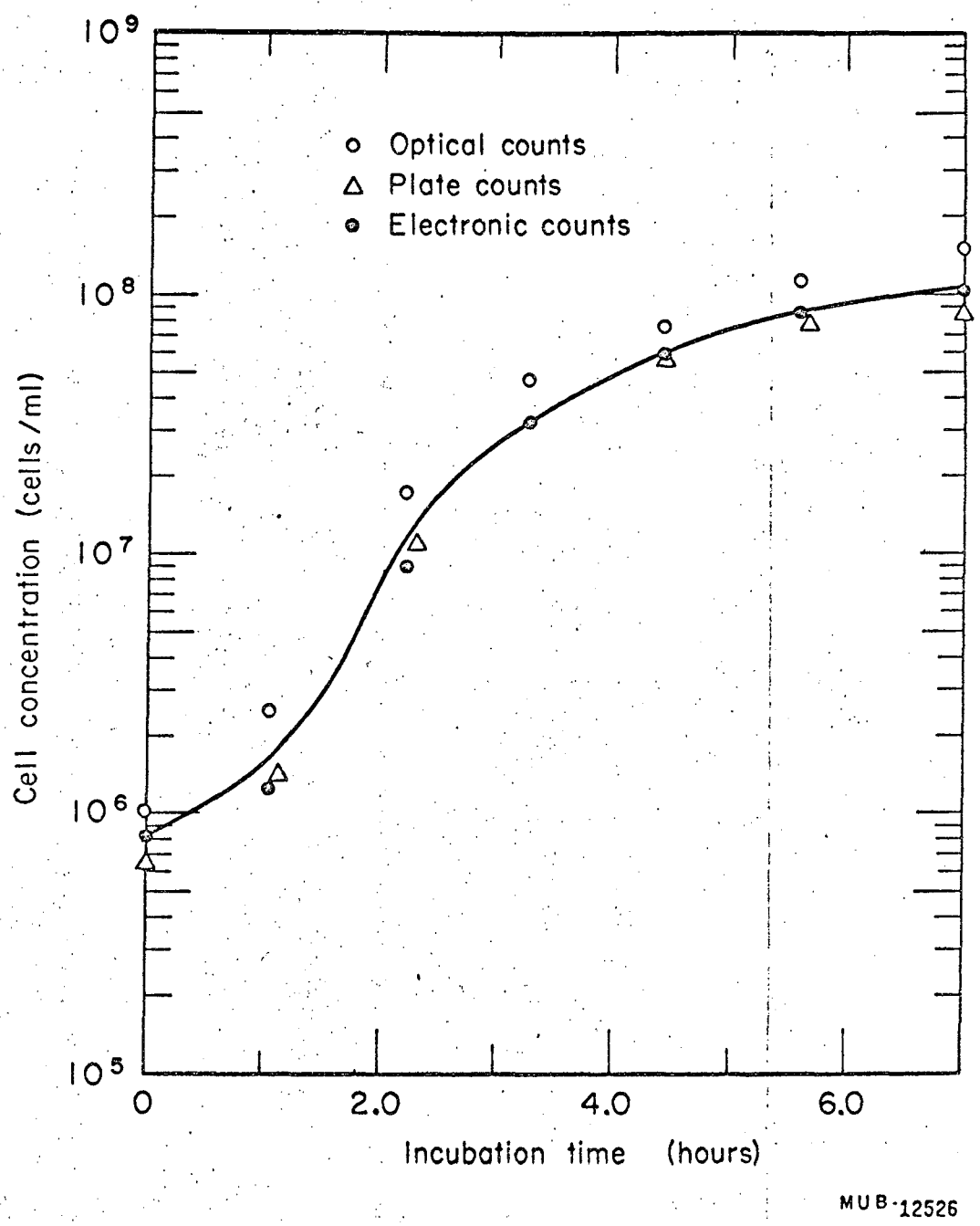

Fig. 24. Cell concentration versus incubation time, counting experiment #3.

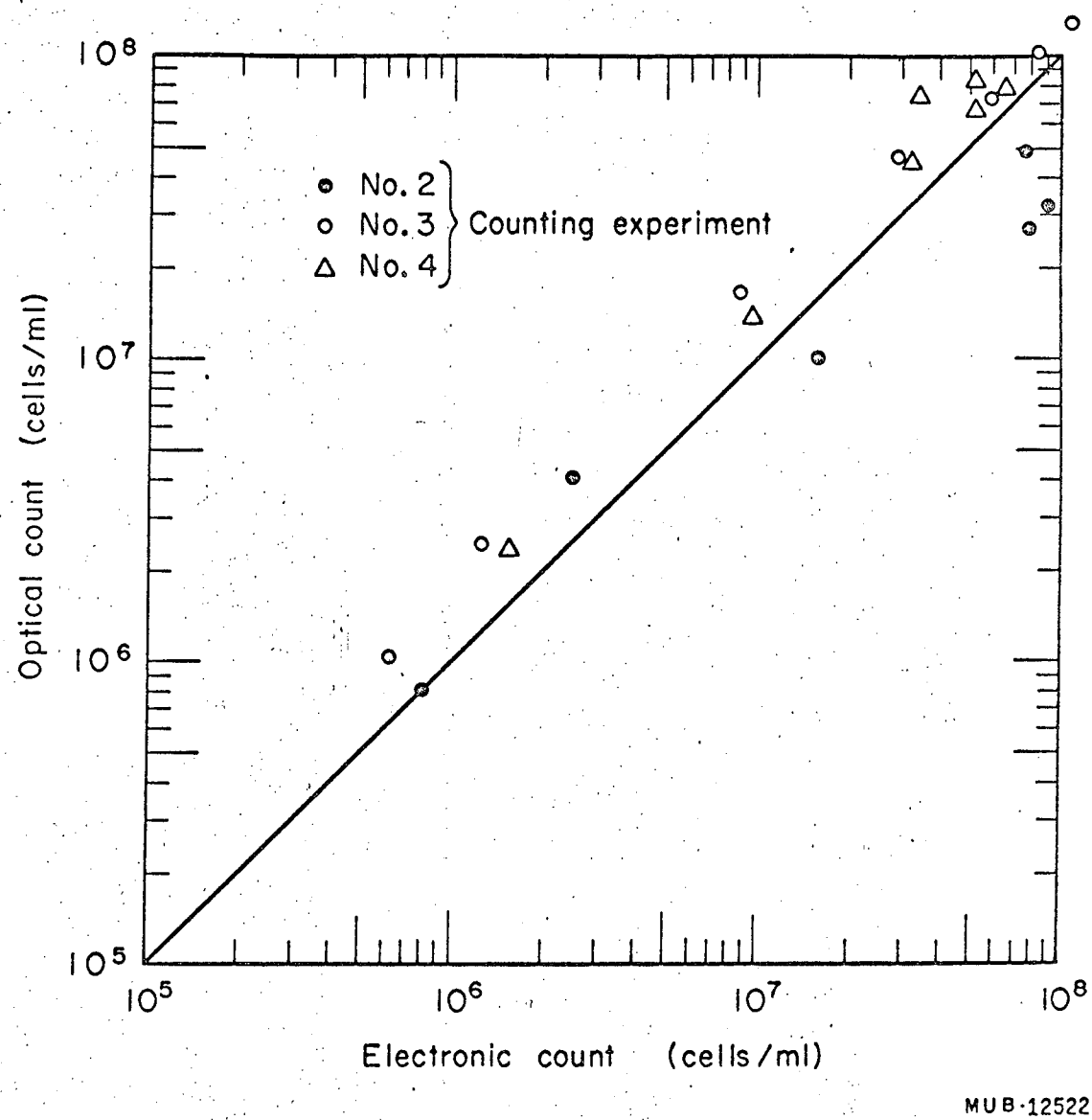

Fig. 25. Optical count versus electronic count.

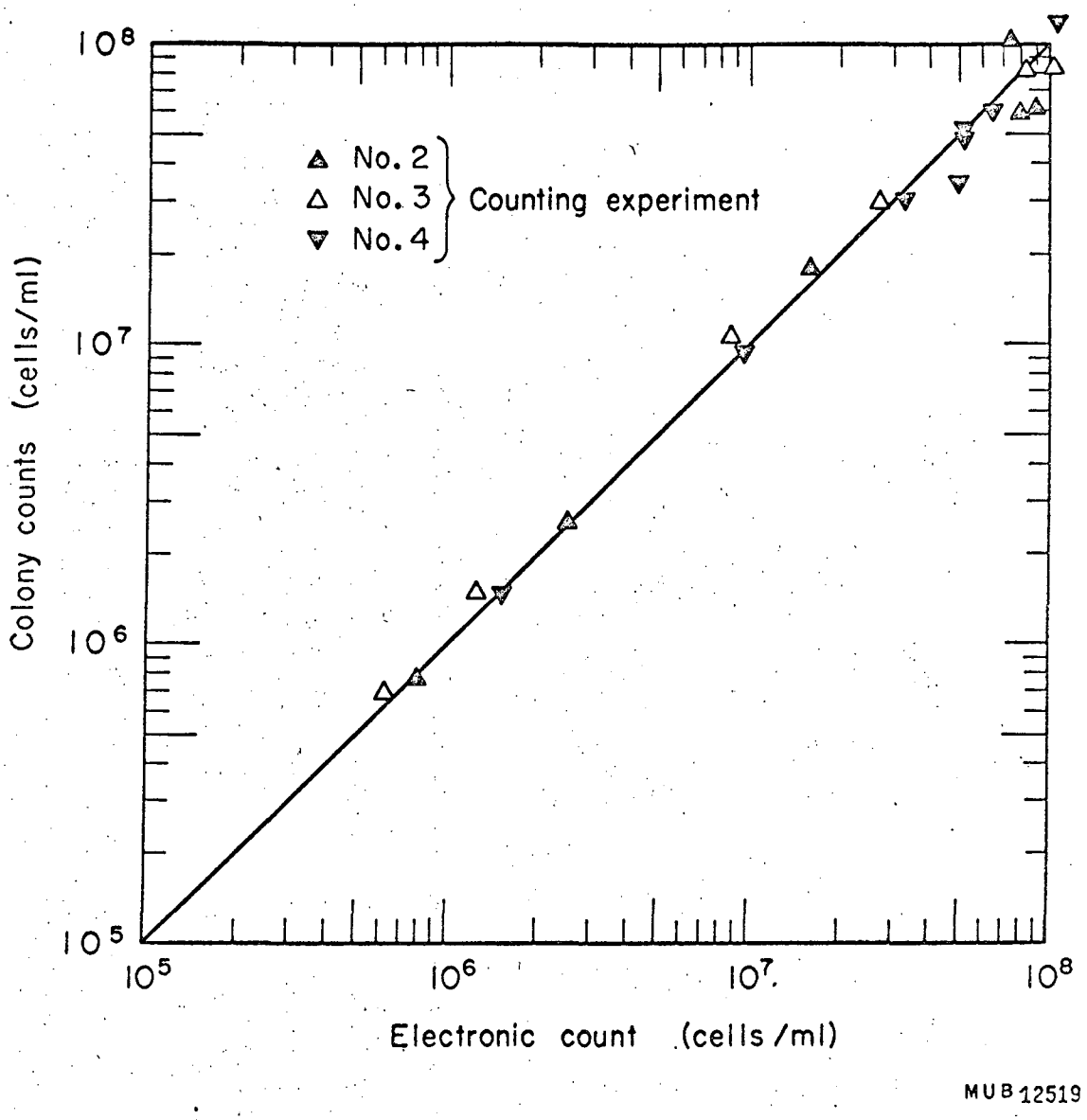

Fig. 26. Plate count versus electronic count.

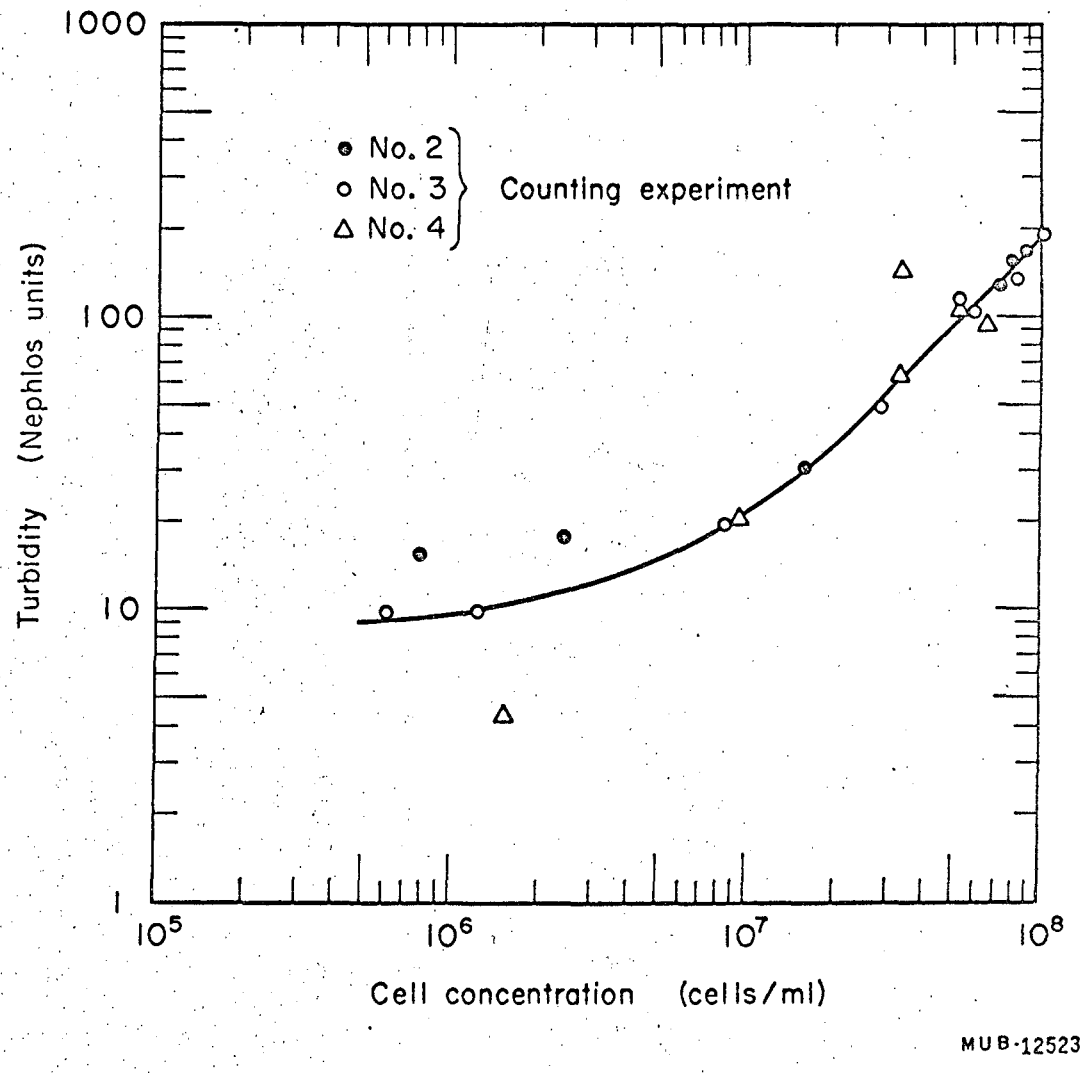

Fig. 27. Turbidity versus electronic count.

Figure 27 compares turbidity with electronic count. All but four points correlated very well. In Fig. 28, a plot of turbidity versus cell concentration in percent by volume cells (electronic) shows a somewhat more scattered correlation.

From the preceding, it is clear that electronic counting gives consistent results, which show good agreement with two classical means of measuring cell concentration and shows fair agreement with a third.

Aperture voltage did not affect total counts in counting experiments #2 and #3.

C. Electronic Sizing of Bacteria

This section discusses some aspects of the accuracy of electronic sizing of bacteria. A theory of the electrical conductivity of bacterial cells is proposed and discussed in relation to experimental results.

1. Model for the Electrical Conductivity of the Bacterial Cell

Working with suspensions of bacteria in electrolytes, Carstensen et al. proposed a model for the electrical conductivity of bacteria.[24] Their model postulates that the bacterial cell is an electrically non-conducting core with a conductive shell. The core corresponds to the portion of the cell within and including the cell membrane, while the shell models the cell wall. The cell wall is permeable to low molecular weight compounds and ions and thus has a reasonably high electrical conductivity. The cell membrane, on the other hand, forms a barrier to the passage of electric current. Carstensen et al. combined the theory with measurements of the electrical conductivity of suspensions of bacteria. Our results, discussed here, partly confirm the validity of the model by the independent method of electronic sizing.

Slight modification of their model to include the effect of aperture voltage is required to explain some of our results.

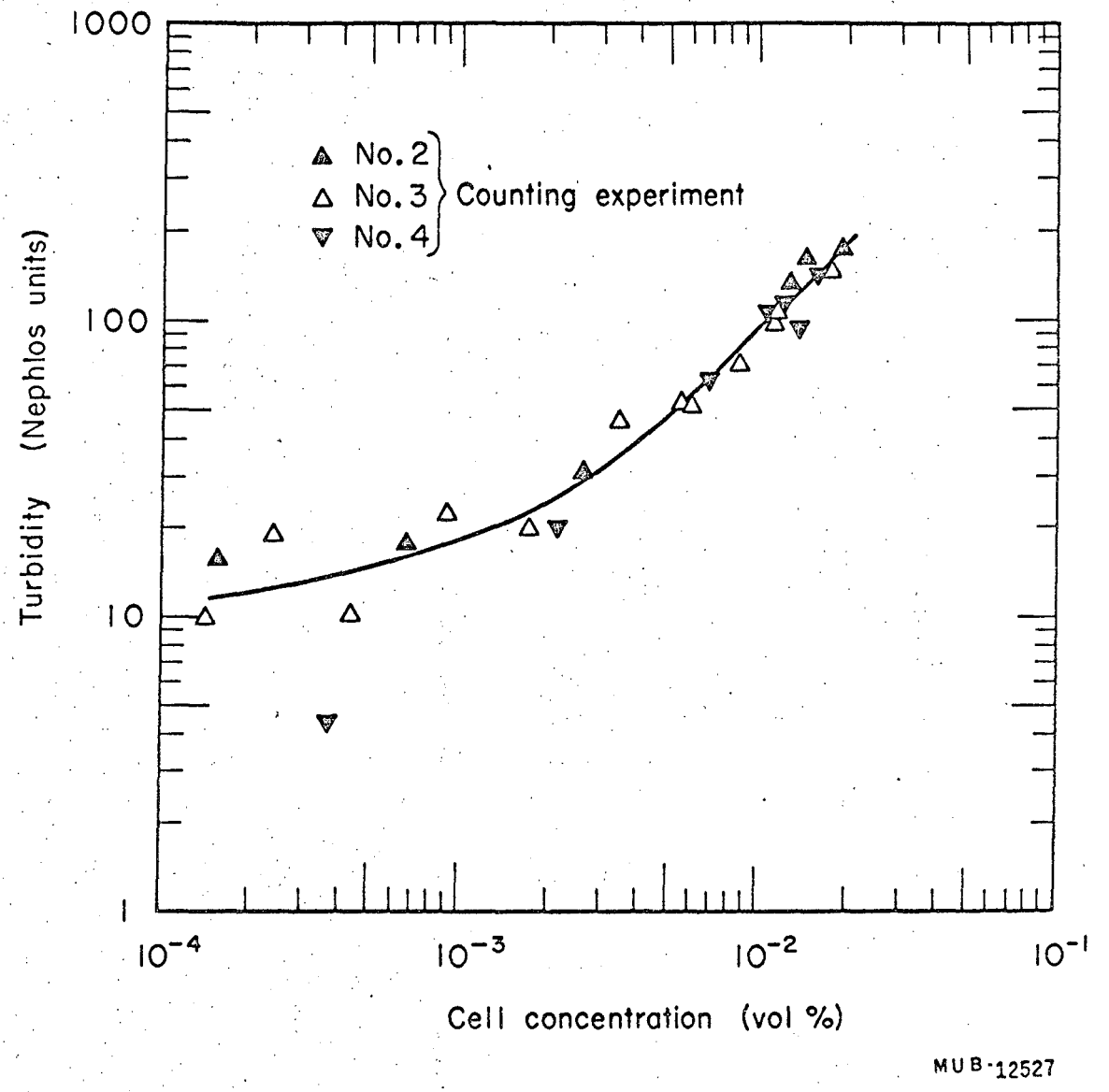

Fig. 28. Turbidity versus electronically determined percent by volume cells.

2. Experimental Results

Microscopic polystyrene or polyvinyl toluene beads of known sizes were used to calibrate the counting system for sizing. A size distribution of the beads was measured using the counting system, and the gain of the system was established from comparison of the measured electronic size of particles and the known size of the particles.

If results are in accord with the theory of Carstensen et al., the electronic volume will be consistently lower than the mean cell volume measured optically.

An experiment was designed to test for this effect through all phases of culture growth and also to test for the effect of heat-killing cells on their electronic sizing properties. Periodically, samples were taken from a batch culture of *E. coli* B. Samples were analyzed electronically. Photomicrographs were also made of the cells for optical sizing of the cells. The results of the experiment, called the Sizing Experiment, are listed in Tables XXVII, XXVIII, and XXIX. Two important results are evident in the data of Table XXIX. First, the electronic size of formalin-fixed cells is much smaller than the optical size of the cells. Thus the results are consistent with the proposed theory. Secondly, the heat-killed cells are the same size as normal formalin-fixed cells in both electronic and optical volume determinations. However, reference to Table XXVIII shows that in the second sample (exponential phase cells, 2 hr 20 min after inoculation) the electronic count for heat-killed cells is 20 times smaller than the total count on corresponding formalin-fixed cells. This result can be explained by the proposed theory as lysis and disruption of the cell membrane by the heat killing, thus making the cell transparent to the electronic counting system. The optical size of the cells remains the same. Less effect of heat killing was observed on the 54-min sample, where the heat-killed cells registered one fourth the count of formalin-fixed cells. Reduction of the count by heat killing was not observed in the other samples and the phenomenon thus appears to be strongest on cells in the exponential growth phase. Comparison of optical size distribution for heat-killed and normal formalin-fixed cells

Table XXVII. Sizing experiment (7/9/66)

Set	Sample	Time	Dilution	Aperture Voltage (volts)	Gain	Diff. (μsec)	Int. (μsec)
1	Inoc.	0	1:000	24	100	1	1
2	"	"	"	"	"	1	1
3	"	"	"	24	100	2	2
4	"	"	"	96	25	1	1
5	"	"	"	"	"	"	"
6	"	"	"	"	"	2	2
7	"	"	"	"	"	"	"
8*	1	30 min	none	24	100	1	1
9	1	"	"	"	"	2	2
10	"	"	"	96	25	"	"
11*	"	"	"	156	25	"	"
12*	"	"	"	"	"	"	"
13*	", HK	"	"	96	25	1	1
14*	", HK	"	"	24	200	"	"
15	2	2 hr 20 min	1:10	"	"	"	"
16	"	"	"	"	"	"	"
17	"	"	"	"	100	2	2
18	"	"	"	"	"	"	"
19	"	"	"	100	50	1	1
20	"	"	"	"	"	"	"
21	"	"	"	"	"	"	"
22	"	"	"	200	25	"	"
23	", HK	"	"	100	50	"	"
24	", HK	"	"	50	"	2	2
25	", HK	"	"	100	50	1	1
26	", HK	"	"	200	25	"	"
27	3	4 hr 22 min	1:100	100	50	"	"

Table XXVII (continued)

Set	Sample	Time	Dilution	Aperture Voltage (volts)	Gain	Diff. (μsec)	Int. (μsec)
28	"	"	"	50	"	2	2
29	"	"	"	50	100	1	1
30	"	"	"	50	50	2	2
31	", HK	"	"	"	"	"	"
32	3, HK	4 hr 22 min	1:100	50	100	1	1
33	"	"	"	100	50	"	"
34	4	5 hr 10 min	1:200	50	100	"	"
35	"	"	"	50	50	2	2
36	"	"	"	50	100	1	1
37	"	"	"	50 (100)‡	100 (50)‡	"	"
38	"	"	"	"	50	"	"
39	", HK	"	"	"	"	"	"
40	", HK	"	"	50	100	"	"
41	", HK	"	"	96 (50)‡	25 (50)‡	2	2
42	5	6 hr 15 min	"	50	100	1	1
43	"	"	"	50	50	2	2
44	"	"	"	50	100	1	1
45	"	"	"	100	50	"	"
46	"	"	"	96	25	2	2
47	"	"	"	200	25	1	1
48	"	"	"	50	100	"	"

*Bad size distributions, not included in calculations.

‡Numbers in parentheses indicate instrument settings for cell size distributions if different from bead size distributions.

Table XXVIII. Summary of results sizing experiment

SUMMARY OF CALCULATED RESULTS,ALL DISTRIBUTIONS

	PARTICLES/ML	VOLUME PERCENT	AVE.VOL.(MU**3)	VOLUME FACTOR	STD.DEV.(MU**3)	SKEWNESS	KURTOSIS
NSET =	1						
BEADS	1.4489731E+05	6.6906510E-05	4.5545450E+00	1.5711951E-01	7.1916869E-01	2.1966800E-01	-1.5819433E-01
CELLS	5.6082242E+04	9.1334996E-06	1.6285903E+00	1.5711951E-01	1.4570577E+00	3.4592398E+00	3.1610999E+01
NSET =	2						
BEADS	1.4689731E+05	6.6906510E-05	4.5546450E+00	1.5711961E-01	7.1916869E-01	2.1966800E-01	-1.5819483E-01
CELLS	5.4878474E+04	9.9762742E-06	1.8179848E+00	1.5711961E-01	1.6972684E+00	3.0938007E+00	2.4712832E+01
NSET =	3						
BEADS	1.5281330E+05	6.9598956E-05	4.5545090E+00	9.7633662E-02	7.1659703E-01	2.0430061E-01	-1.3216158E-01
CELLS	5.1634403E+04	1.0161500E-05	1.9679708E+00	9.7533552E-02	1.2724485E+00	1.8571124E+00	9.7301355E+00
NSET =	4						
BEADS	1.5101672E+05	6.8610007E-05	4.5432060E+00	1.5349290E-01	5.8324494E-01	-1.1586037E-01	-2.8335433E-01
CELLS	4.7419090E+04	9.0284086E-06	1.9039607E+00	1.5349290E-01	1.3064982E+00	1.1532541E+00	3.1207045E+00
NSET =	5						
BEADS	1.5101672E+05	6.8610007E-05	4.5432060E+00	1.5349290E-01	5.8324494E-01	-1.1586037E-01	-2.8335433E-01
CELLS	6.9091735E+04	1.1574149E-05	1.6751858E+00	1.5349290E-01	1.3733730E+00	1.3873813E+00	5.3247531E+00
NSET =	6						
BEADS	1.4812154E+05	6.7141714E-05	4.5328797E+00	9.8211524E-02	4.4933995E-01	-2.5444610E-01	-1.6140516E-01
CELLS	6.5217061E+04	1.2710072E-05	1.9488876E+00	9.8211524E-02	1.3785949E+00	9.9478368E-01	2.2812926E+00
NSET =	7						
BEADS	1.4812154E+05	6.7141714E-05	4.5328797E+00	9.8211524E-02	4.4933995E-01	-2.5444610E-01	-1.6140516E-01
CELLS	7.1498552E+04	1.4128293E-05	1.9763250E+00	9.8211524E-02	1.3740968E+00	8.9989172E-01	1.3873355E+00
NSET =	8						
BEADS	1.3532824E+05	6.1602194E-05	4.5520576E+00	1.5806571E-01	6.8424781E-01	5.5441948E-02	-2.9644151E-01
CELLS	3.8280817E+05	1.3114446E-04	3.4258532E+00	1.5806571E-01	2.6992967E+00	1.5584012E+00	5.7954652E+00
NSET =	9						
BEADS	1.4335365E+05	6.5297662E-05	4.5550050E+00	9.6535663E-02	7.1998572E-01	1.7353178E-01	-2.2464142E-01
CELLS	6.3943502E+05	1.5500579E-04	2.4241054E+00	9.6535663E-02	1.7269695E+00	1.1075765E+00	3.1924113E+00
NSET =	10						
BEADS	2.2520379E+06	2.6702359E-04	1.1856976E+00	9.8392947E-02	2.7722595E-01	1.0810374E-01	-2.2963144E-01
CELLS	5.3614090E+05	1.4675273E-04	2.7372045E+00	9.8392947E-02	1.4241385E+00	5.4073226E-01	9.5314054E-01
NSET =	11						
BEADS	2.1281681E+06	2.5149808E-04	1.1817585E+00	5.9449801E-02	2.5216710E-01	1.2285759E-01	-2.5217310E-01
CELLS	6.7331918E+05	1.3741191E-04	2.0408138E+00	5.9449801E-02	9.4996849E-01	4.1176954E-01	1.6173654E-01
NSET =	12						
BEADS	2.1281681E+06	2.5149808E-04	1.1817585E+00	5.9449801E-02	2.5216710E-01	1.2285759E-01	-2.5217310E-01
CELLS	6.6644341E+05	8.4548759E-05	1.2685562E+00	5.9449801E-02	7.0350837E-01	6.7139083E-01	1.2888434E+00
NSET =	13						
BEADS	1.5101672E+05	6.8610007E-05	4.5432060E+00	1.5349290E-01	5.8324494E-01	-1.1586037E-01	-2.8335433E-01
CELLS	7.0280415E+05	2.3358223E-04	3.3235750E+00	1.5349290E-01	1.6978326E+00	6.8358415E-01	1.0410479E+00
NSET =	14						
BEADS	3.4157645E+05	4.0288059E-05	1.1794741E+00	8.0528043E-02	2.3819044E-01	1.8353435E-01	-3.9182268E-01
CELLS	1.5424844E+05	2.2221541E-05	1.4405331E+00	8.0528043E-02	3.8502253E-01	2.1108961E+00	2.9222235E+01
NSET =	15						
BEADS	3.4157645E+05	4.0288059E-05	1.1794741E+00	8.0528043E-02	2.3819044E-01	1.8353435E-01	-3.9182268E-01
CELLS	9.5381104E+05	2.4207856E-04	2.5380138E+00	8.0528043E-02	1.1299398E+00	8.4240089E-01	2.4588480E+00
NSET =	16						
BEADS	3.4157645E+05	4.0288059E-05	1.1794741E+00	8.0528043E-02	2.3819044E-01	1.8353435E-01	-3.9182268E-01
CELLS	9.5948373E+05	2.4509189E-04	2.5544143E+00	8.0528043E-02	1.1274197E+00	8.6997842E-01	2.5543857E+00
NSET =	17						
BEADS	3.7258995E+04	4.4023758E-06	1.1815605E+00	6.0774591E-02	2.5099325E-01	1.0811888E-01	-3.8019587E-01
CELLS	8.5911884E+05	1.3978462E-04	1.6270696E+00	6.0774591E-02	7.1649487E-01	1.2123285E+00	5.1964098E+00
NSET =	18						
BEADS	3.7258995E+04	4.4023758E-06	1.1815605E+00	6.0774591E-02	2.5099325E-01	1.0811888E-01	-3.8019587E-01
CELLS	8.6692623E+05	1.3603251E-04	1.5691359E+00	6.0774591E-02	7.1469154E-01	1.2354957E+00	5.4401448E+00
NSET =	19						

BEADS	3.4329985E+05	4.0426089E-05	1.1775737E+00	7.8871745E-02	2.2200162E-01	1.9568620E-01	5.8508592E-02
CELLS	9.2426383E+05	2.1456827E-04	2.3213045E+00	7.8871745E-02	1.3223959E+00	8.7439171E-01	2.1455197E+00
NSET = 20							
BEADS	3.5009420E+05	4.1185243E-05	1.1764046E+00	7.7728463E-02	2.1291563E-01	2.0326662E-01	4.1363234E-03
CELLS	9.3988211E+05	1.7196945E-04	1.8295917E+00	7.7728463E-02	7.9291984E-01	6.5935280E-01	9.1301501E-01
NSET = 21							
BEADS	3.5009420E+05	4.1185243E-05	1.1764046E+00	7.7728463E-02	2.1291563E-01	2.0326662E-01	4.1363234E-03
CELLS	9.5555396E+05	2.1772270E-04	2.2784972E+00	7.7728453E-02	1.3135910E+00	8.4047494E-01	1.9941732E+00
NSET = 22							
BEADS	3.3721111E+05	3.9776909E-05	1.1795848E+00	8.0038118E-02	2.3483538E-01	8.6236555E-02	-1.4912087E-01
CELLS	9.9033073E+05	1.8950616E-04	1.9135644E+00	8.0038113E-02	7.9019006E-01	4.5480088E-01	2.6930501E-01
NSET = 23							
BEADS	3.7806656E+05	4.4482552E-05	1.1765799E+00	7.7215674E-02	2.1533130E-01	2.2476064E-01	-1.2082639E-01
CELLS	5.1305840E+04	1.1070696E-05	2.1577848E+00	7.7215674E-02	1.4116030E+00	1.0111965E+00	2.0925552E+00
NSET = 24							
BEADS	3.2771635E+05	3.8968692E-05	1.1890982E+00	9.9198785E-02	2.9798901E-01	1.0074473E-01	-3.3187680E-01
CELLS	5.0033597E+04	1.0641324E-05	2.1268356E+00	9.9198785E-02	1.2520519E+00	7.9840243E-01	1.0504236E+00
NSET = 25							
BEADS	3.4329985E+05	4.0426089E-05	1.1775737E+00	7.8871745E-02	2.2200162E-01	1.9568620E-01	5.8508592E-02
CELLS	4.9818303E+04	1.0845806E-05	2.1770725E+00	7.8871745E-02	1.4128137E+00	1.0364593E+00	2.2703579E+00
NSET = 26							
BEADS	3.8324692E+05	4.5171799E-05	1.1785605E+00	7.6942499E-02	2.3028700E-01	1.6319907E-01	-1.5755935E-01
CELLS	4.8601300E+04	8.8660365E-06	1.8242385E+00	7.6942499E-02	8.4436277E-01	4.5432102E-01	1.0060283E-01
NSET = 27							
BEADS	3.8272199E+05	4.5125340E-05	1.1790632E+00	7.5546016E-02	2.3540592E-01	2.3352989E-01	-1.1462918E-01
CELLS	5.4165514E+05	9.5530522E-05	1.7635779E+00	7.5546016E-02	7.7212725E-01	9.6937635E-01	3.4465338E+00
NSET = 28							
BEADS	3.1251136E+05	3.7077781E-05	1.1864459E+00	1.0145361E-01	2.8002085E-01	4.4255329E-02	-3.4425532E-01
CELLS	5.5952274E+05	1.0585275E-04	1.8918399E+00	1.0145361E-01	8.7403469E-01	8.1763556E-01	2.1225654E+00
NSET = 29							
BEADS	2.7422537E+05	3.2349510E-05	1.1796688E+00	8.1136661E-02	2.3792876E-01	1.5547391E-01	-1.9121511E-01
CELLS	5.3118515E+05	1.0561095E-04	1.9882134E+00	8.1136661E-02	8.7376905E-01	8.1741601E-01	2.3150974E+00
NSET = 30							
BEADS	3.2771635E+05	3.8968692E-05	1.1890982E+00	9.9198785E-02	2.9798901E-01	1.0074473E-01	-3.3187680E-01
CELLS	2.4090079E+05	5.5676969E-05	2.3111991E+00	9.9198785E-02	1.1912072E+00	1.0867369E+00	4.6713886E+00
NSET = 31							
BEADS	3.2771635E+05	3.8968692E-05	1.1890982E+00	9.9198785E-02	2.9798901E-01	1.0074473E-01	-3.3187680E-01
CELLS	4.8802482E+04	2.0148554E-05	4.1285921E+00	9.9198785E-02	1.8168447E+00	5.8076119E-01	7.8194284E-01
NSET = 32							
BEADS	3.6943608E+05	4.3555280E-05	1.1789666E+00	8.0554293E-02	2.3263138E-01	1.4049232E-01	-2.7168882E-01
CELLS	5.0285764E+05	9.4348536E-05	1.8762474E+00	8.0554293E-02	9.1135580E-01	1.2116762E+00	5.8437255E+00
NSET = 33							
BEADS	3.5228410E+05	4.1468523E-05	1.1771330E+00	7.5297575E-02	2.1597151E-01	7.7708506E-02	-7.7738534E-02
CELLS	4.6414051E+05	8.3227324E-05	1.7931493E+00	7.5297575E-02	8.6912497E-01	1.0478448E+00	3.6881095E+00
NSET = 34							
BEADS	3.6943608E+05	4.3555280E-05	1.1789666E+00	8.0554293E-02	2.3263138E-01	1.4049232E-01	-2.7168882E-01
CELLS	3.5462436E+05	7.0405505E-05	1.9853544E+00	8.0554293E-02	9.9088482E-01	1.0737710E+00	4.6184753E+00
NSET = 35							
BEADS	3.2771635E+05	3.8968692E-05	1.1890982E+00	9.9198786E-02	2.9798901E-01	1.0074473E-01	-3.3187680E-01
CELLS	3.5125673E+05	7.0455040E-05	2.0057990E+00	9.9198785E-02	1.1467853E+00	1.5811989E+00	9.4282610E+00
NSET = 36							
BEADS	4.0103598E+05	4.7433650E-05	1.1827779E+00	7.8953461E-02	2.5820351E-01	9.6224172E-02	-2.4968598E-01
CELLS	3.2332760E+05	6.7721355E-05	2.0945121E+00	7.8953451E-02	9.8544814E-01	9.6327010E-01	3.5600334E+00
NSET = 37							
BEADS	3.4835427E+05	4.1025226E-05	1.1776869E+00	7.6417182E-02	2.1907665E-01	3.8834412E-02	8.4005699E-03
CELLS	3.5982565E+05	7.2950409E-05	2.0273821E+00	7.6417182E-02	9.6943236E-01	8.6806115E-01	2.6018102E+00
NSET = 38							
BEADS	3.6849527E+05	4.3464654E-05	1.1795173E+00	7.8051398E-02	2.3366922E-01	8.2948832E-02	1.3342100E-02
CELLS	3.4778821E+05	5.6198022E-05	1.6158691E+00	7.8051398E-02	7.8612447E-01	6.8216124E-01	1.2538115E+00
NSET = 39							
BEADS	3.6849527E+05	4.3464654E-05	1.1795173E+00	7.8051398E-02	2.3366922E-01	8.2948832E-02	1.3342100E-02
CELLS	3.5786872E+05	6.5302096E-05	1.8247500E+00	7.8051398E-02	9.3634676E-01	1.0448718E+00	3.5855336E+00

NSET = 40							
BEADS	3.4335427E+05	4.1025226E-05	1.1776869E+00	7.6417182E-02	2.1907665E-01	3.8834412E-02	8.4005699E-03
CELLS	3.5445376E+05	6.5159575E-05	1.8383096E+00	7.6417182E-02	9.2462228E-01	1.2244306E+00	5.2178585E+00
NSET = 41							
BEADS	1.4739359E+05	6.6939673E-05	4.5415593E+00	1.0128459E-01	5.5012154E-01	-4.7013435E-01	2.1859453E-01
CELLS	3.9488076E+05	9.0577487E-05	2.2937934E+00	1.0128459E-01	1.2544484E+00	1.1476707E+00	5.0949752E+00
NSET = 42							
BEADS	4.0103598E+05	4.7433650E-05	1.1827779E+00	7.8953461E-02	2.5820351E-01	9.6224172E-02	-2.4968598E-01
CELLS	4.1078820E+05	8.3718205E-05	2.0379895E+00	7.8953461E-02	1.0147118E+00	8.2375106E-01	2.7518289E+00
NSET = 43							
BEADS	3.1251136E+05	3.7077781E-05	1.1864459E+00	1.0145361E-01	2.8002085E-01	4.4255329E-02	-3.4425532E-01
CELLS	4.1696656E+05	8.9673164E-05	2.1505080E+00	1.0145361E-01	1.1829303E+00	1.2930777E+00	7.1378457E+00
NSET = 44							
BEADS	3.6943608E+05	4.3555280E-05	1.1789666E+00	8.0554293E-02	2.3263138E-01	1.4049232E-01	-2.7168892E-01
CELLS	4.2784911E+05	9.2204665E-05	2.1553744E+00	8.0554293E-02	1.0551385E+00	8.0354060E-01	2.7103044E+00
NSET = 45							
BEADS	3.6849527E+05	4.3464654E-05	1.1795173E+00	7.8051398E-02	2.3366922E-01	8.2948832E-02	1.3342133E-02
CELLS	3.9729197E+05	8.4248617E-05	2.1205718E+00	7.8051398E-02	9.8947511E-01	7.4443761E-01	1.9102529E+00
NSET = 46							
BEADS	1.4812154E+05	6.7141714E-05	4.5328797E+00	9.8211524E-02	4.4933995E-01	-2.5444610E-01	-1.6140516E-01
CELLS	4.1153920E+05	8.5265385E-05	2.0718654E+00	9.8211524E-02	9.8550539E-01	5.8888167E-01	9.2355058E-01
NSET = 47							
BEADS	3.3721111E+05	3.9776909E-05	1.1795848E+00	8.0038118E-02	2.3483538E-01	8.6236555E-02	-1.4912087E-01
CELLS	4.1448530E+05	9.0234927E-05	2.1770356E+00	8.0038118E-02	1.0373578E+00	7.8013618E-01	2.1082829E+00
NSET = 48							
BEADS	3.7629383E+05	4.4392961E-05	1.1797419E+00	8.0131223E-02	2.3598896E-01	6.5898524E-02	-2.0909854E-01
CELLS	4.1149540E+05	9.2025524E-05	2.2363582E+00	8.0131223E-02	1.1377258E+00	7.3242982E-01	2.1813476E+00

Table XXIX. Sizing experiment.

Type	Time	Total Cells Measured	Ave. length (microns)	Ave. Width (microns)	Ave. Volume* (cubic (microns)	Ave. Electronic Total Count	Electronic Volume (cubic microns)
Formalin (Inoculum	0	35	5.13	1.19	5.26	5.94×10^7	1.85
Formalin	54 min	39	4.96	1.07	4.13	6.14×10^5	-
Heat Killed		-	-	-	-	1.54×10^5	-
Formalin	2 hr 53 min	70	3.65	1.19	3.63	9.31×10^5	2.08
Heat	3 hr 32 min	79	3.57	1.17	3.42	4.99×10^5	2.07
Formalin	4 hr 51 min	78	2.84	1.17	2.64	5.44×10^7	1.84
Heat	5 hr 22 min	147	3.27	1.19	3.20	4.84×10^7	1.98
Formalin	5 hr 43 min	147	3.22	1.24	3.40	6.94×10^7	1.95
Heat	6 hr 16 min	71	2.94	1.27	3.19	7.38×10^7	1.98
Formalin	6 hr 48 min	86	3.22	1.33	3.85	4.13×10^5	2.14

*Calculated with the equation $V = (\pi D^2/4)(L - D/3)$, L and D measured optically.

is made in Fig. 29, while Fig. 30 compares the corresponding electronic size-concentration distributions. The optical distributions are not greatly different, but a strong constrast can be seen in the electronic distributions due to the reduced count for the heat-killed cells. The reduction in cell count by heat killing is significant because electronic sizing thus offers a single means of detecting cell lysis. Our results are in agreement with the work of Kniseley and Throop, who showed that electronic counting could be used to detect cell lysis caused by the antibiotic lysostaphin.[18] Such a result should prove very useful to workers in the field of sterilization kinetics.

Cell size was found to vary during different phases of batch culture growth. Figure 31 shows how mean cell size varied in a variety of batch culture experiments. Optical sizes were always considerably greater than sizes measured electronically, and they did not reflect the maximum shown by the electronic size at incubation times between one and two hours. Electronic sizes during the lag phase showed a pronounced maximum between one and two hours of incubation, followed by a decrease in mean cell size throughout the exponential phase. The decrease in mean cell size during the exponential phase is similar to results obtained by Toennies et al., who showed that the mean cell volume of Streptococcus faecalis decreased during the exponential due to a decrease in mean cell chain lengths.[14] Reference to Table XXIX shows that decrease in mean chain length is also responsible for the phenomenon observed here. At the onset of the stationary phase, cell size showed a slight increase, returning to a value near that of the inoculum, which was also a stationary-phase culture.

It is significant that the pronounced cell size maximum observed during the lag phase corresponded to the point at which emf sensitivity was also observed. Emf sensitivity is the term given to the dependence of electronically measured cell size on the voltage applied to the aperture. It was discovered by Curby and co-workers.[13] They found that emf sensitivity was present in all four species of bacteria that they studied,

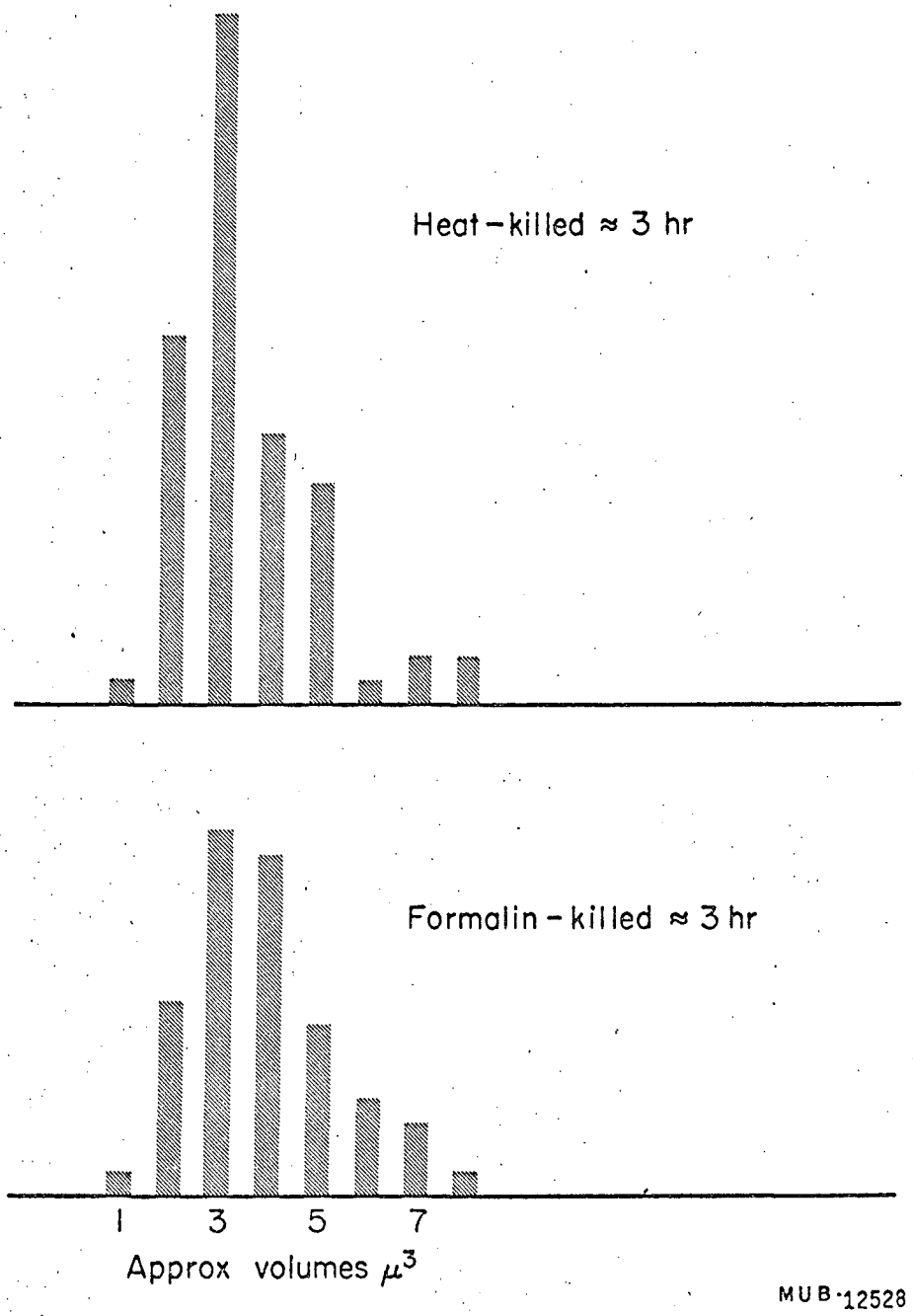

Fig. 29. Comparison of optical size distributions of normal formalin-fixed cells and heat-killed cells.

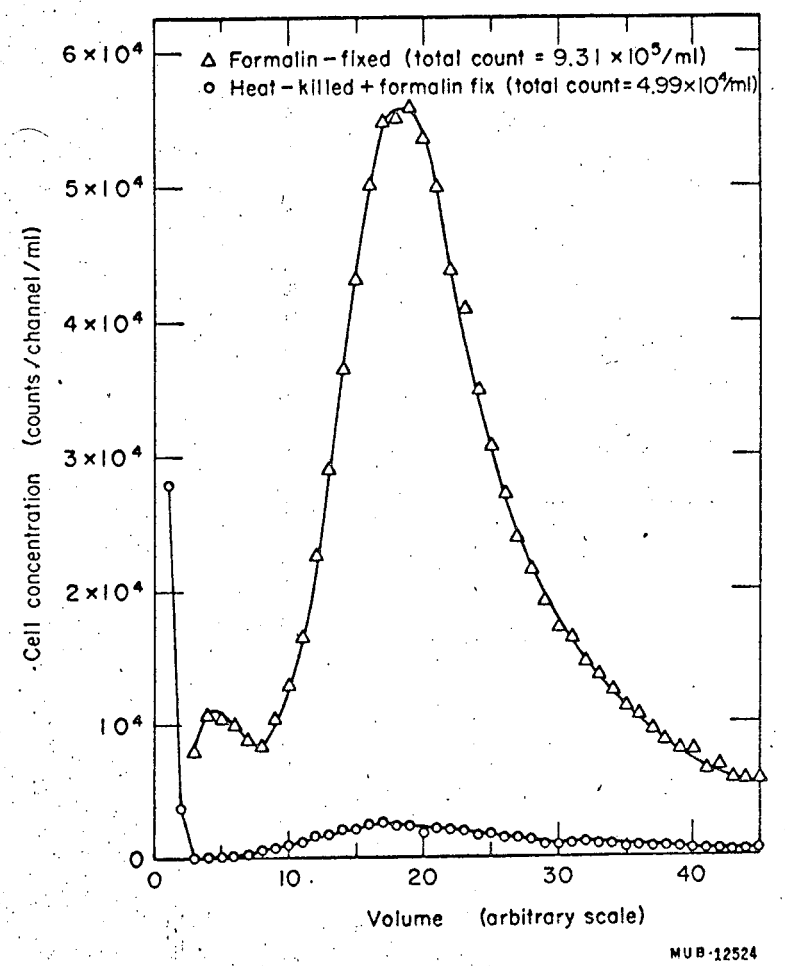

Fig. 30. Comparison of electronic size concentration distributions of heat-killed and normal formalin-fixed cells.

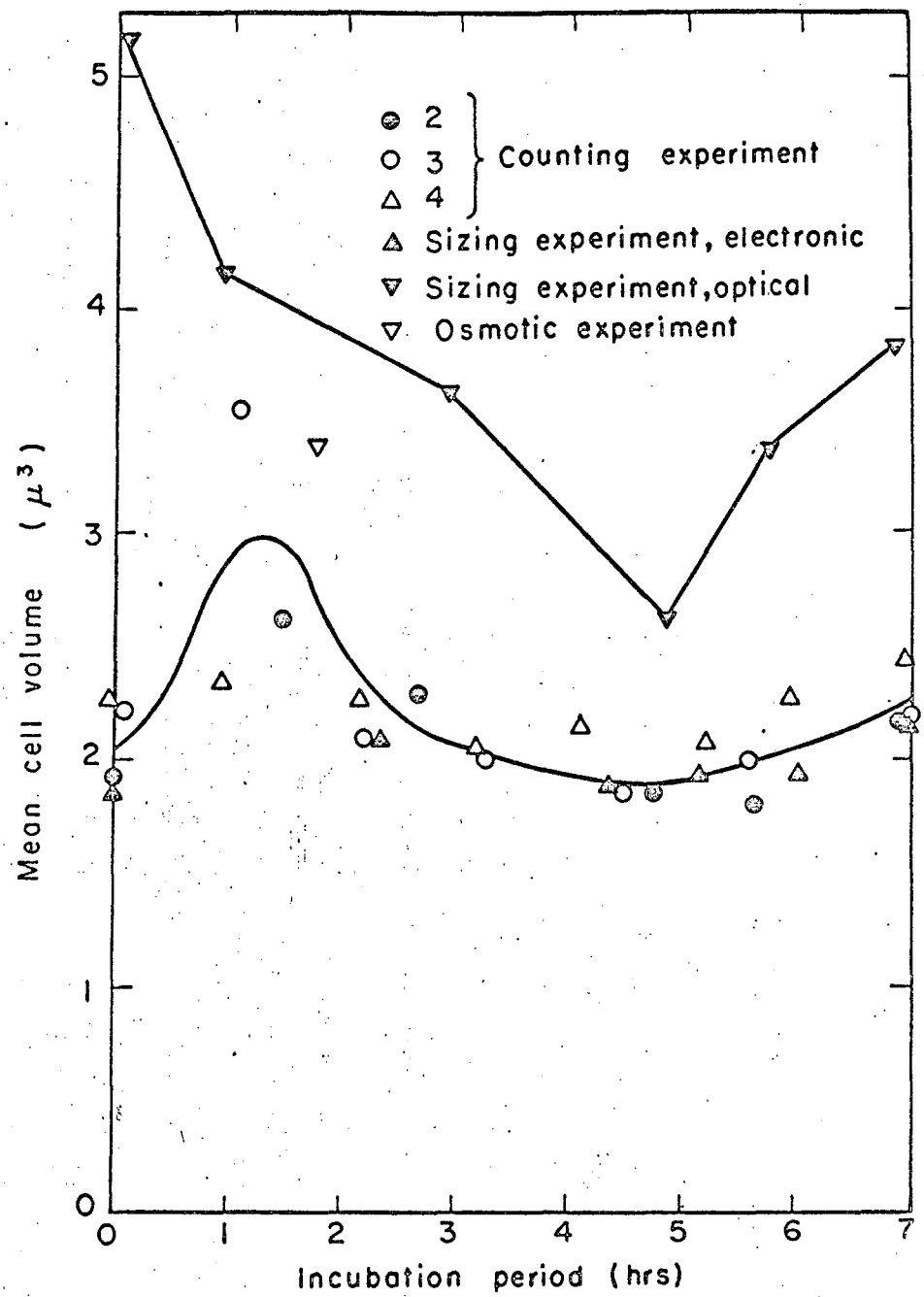

XBL 671-105

Fig. 31. Cell size versus incubation time in several batch cultures.

including E. coli. In some species, emf sensitivity was found to occur in all phases of culture growth, but in other species, including E. coli, emf sensitivity was confined to the lag phase. Curby et al. did not offer an explanation for emf sensitivity.

We have confirmed their results for E. coli, as shown in Fig. 32. The singlet peaks for the polyvinyltoluene spheres were not shifted and had identical modes, neglecting the saturation in the preamplifier observed at high channel numbers at an aperture voltage of 96 volts. Electronic cell size, however, was strongly affected by the aperture voltage, and it can be seen that the mean cell size was decreased considerably by the increased aperture voltage. The hump centered at channel 30 in the cell size distribution measured at 96 volts is again due to saturation in the preamplifier.

Emf sensitivity was found to be reproducible in three separate experiments. Because the electronic size of cells is thus dependent on the voltage applied to the aperture, emf sensitivity raises questions about the accuracy of electronic cell size-concentration distributions. Further investigation of the effect was thus warranted. In making photographs of the cells for optical sizing, it was noted that the cells contained vacuoles during the same phases of batch culture as the occurrence of emf sensitivity. An experiment was performed to obtain more information about emf sensitivity. The experiment, designated as the Osmotic Experiment, was designed to see if the mean electronic cell size was affected by the osmotic pressure of the cell environment. Vacuoles are reportedly osmotically sensitive.[26] Thus a necessary condition for emf sensitivity to be due to vacuoles is that the electronic cell size be osmotically sensitive.

Solution osmotic pressure was varied by adding sucrose to the standard saline buffer solution diluted by one half. The results of the osmotic experiment are shown in Tables XXX and XXXI and in Fig. 33. If the cell or its vacuoles act as an osmometer, the following equations relate the cell volume to the osmotic pressure:

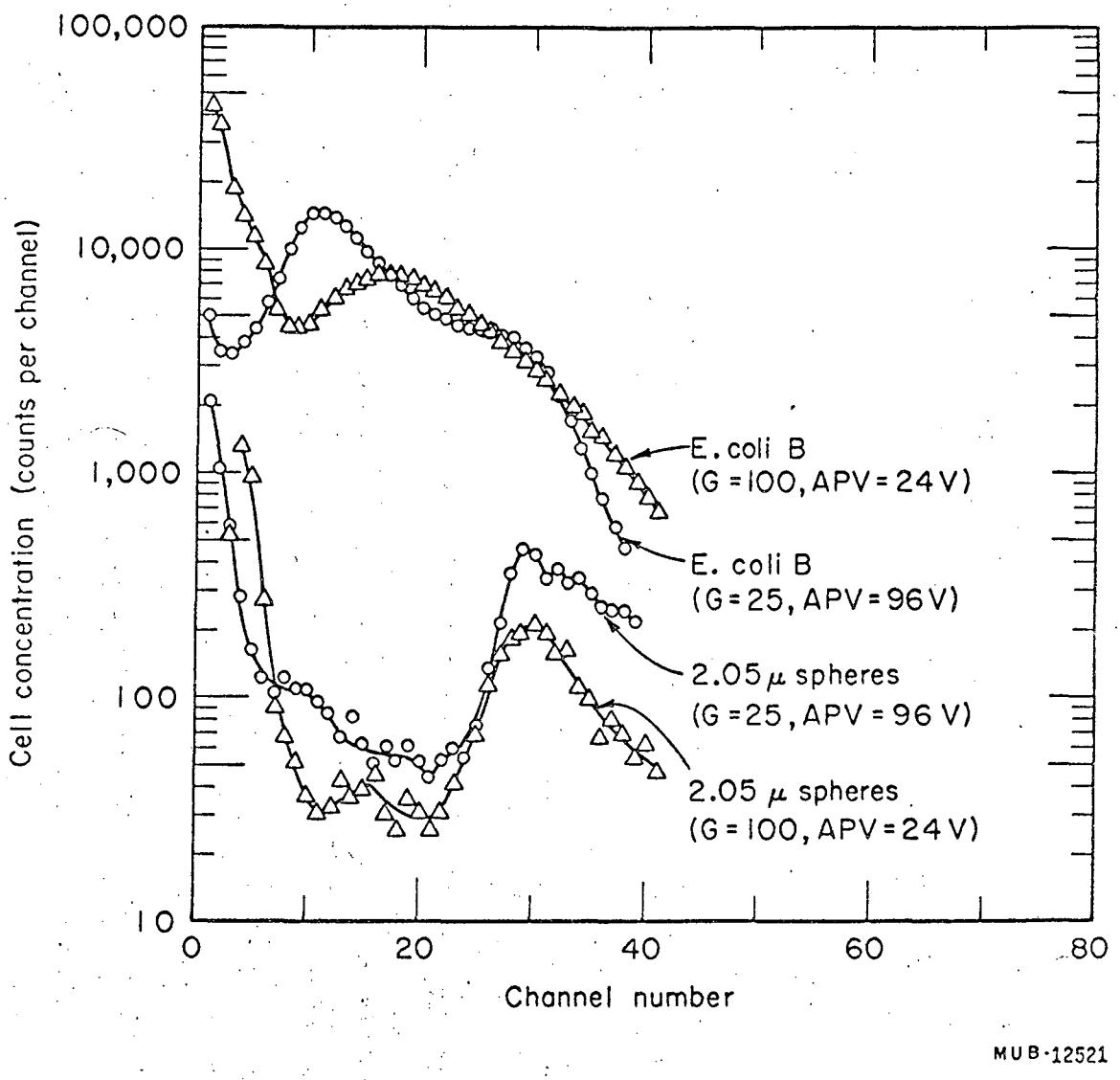

Fig. 32. Particle concentration versus channel number: emf sensitivity.

Table XXX. Conditions of electronic counting and sizing analysis, osmotic experiment.

Set	Osmotic Pressure (atm)	Time since Sampling	Dilution	Aperture Voltage (volts)	Gain	Diff. (μsec)	Int. (μsec)
1	2.0	42 min	1:25	120	50	1	1
2	2.5	-	"	"	"	"	"
3	3.0	-	"	"	"	"	"
4	4.0	-	"	"	"	"	"
5	8.0	-	"	"	"	"	"
6	12.0	-	"	"	"	"	"
7	2.0	1 hr 17 min	"	"	100	"	"
8	3.0	-	"	"	"	"	"
9	4.0	-	"	"	"	"	"
10	8.0	-	"	"	"	"	"
11	12.0	1 hr 51 min	"	"	"	"	"

Table XXXI. Summary of results, osmotic experiment

SUMMARY OF CALCULATED RESULTS, ALL DISTRIBUTIONS

	PARTICLES/ML	VOLUME PERCENT	AVE.VOL.(MU**3)	VOLUME FACTOR	STD.DEV.(MU**3)	SKEWNESS	KURTOSIS
NSET =	1						
BEADS	9.157296CE+04	1.0788737E-05	1.1781575E+00	1.0452627E-01	2.2657113E-01	1.4858397E-01	-2.5099856E-01
CELLS	4.1092127E+04	1.5623333E-05	3.8014708E+00	1.0452627E-01	1.6067875E+00	1.2182441E+00	4.3554141E+00
NSET =	2						
BEADS	1.0220575E+05	1.2044599E-05	1.1784659E+00	1.0372287E-01	2.2809436E-01	1.1515811E-01	-2.6164758E-01
CELLS	3.888482CE+04	1.4263408E-05	3.6681172E+00	1.0372287E-01	1.5556315E+00	1.3598655E+00	4.5330048E+00
NSET =	3						
BEADS	8.8114238E+04	1.0388620E-05	1.1789945E+00	1.0535659E-01	2.3399130E-01	1.8042018E-01	-2.7227138E-01
CELLS	3.7415280E+04	1.3497316E-05	3.6074341E+00	1.0535659E-01	1.4746398E+00	1.3718660E+00	4.8487576E+00
NSET =	4						
BEADS	1.5617872E+05	1.8407544E-05	1.1786205E+00	1.0893269E-01	2.2702038E-01	3.4008739E-02	-2.4416729E-01
CELLS	4.5633880E+04	1.6476587E-05	3.6106041E+00	1.0893269E-01	1.8093525E+00	1.2533095E+00	3.8314842E+00
NSET =	5						
BEADS	1.2935128E+05	1.5279602E-05	1.1812487E+00	1.1385054E-01	2.4946595E-01	1.4644856E-01	-2.6322083E-01
CELLS	4.0559400E+04	1.3810284E-05	3.4049526E+00	1.1385054E-01	1.8925698E+00	1.3682846E+00	4.3245824E+00
NSET =	6						
BEADS	9.3779644E+04	1.1097168E-05	1.1833237E+00	1.2147272E-01	2.6072854E-01	6.0696224E-02	-2.8677425E-01
CELLS	4.1867053E+04	1.2606611E-05	3.0111053E+00	1.2147272E-01	1.8378717E+00	1.5631244E+00	5.7666948E+00
NSET =	7						
BEADS	9.4078884E+04	1.1062350E-05	1.1758589E+00	4.8369352E-02	2.0772397E-01	1.4701038E-01	-2.2679791E-01
CELLS	4.1848689E+04	1.4220647E-05	3.3981106E+00	4.8369352E-02	8.2520495E-01	4.4491362E-01	2.5966748E-01
NSET =	8						
BEADS	9.0091334E+04	1.0596197E-05	1.1761617E+00	4.8930561E-02	2.0752031E-01	2.2064824E-02	-2.2832398E-01
CELLS	4.5908509E+04	1.4175277E-05	3.0877233E+00	4.8930561E-02	8.5940847E-01	5.2957100E-01	5.5095500E-01
NSET =	9						
BEADS	1.7028065E+05	2.0026571E-05	1.1760920E+00	4.9817887E-02	2.0545788E-01	-4.3982363E-02	-1.9044802E-01
CELLS	4.2346883E+04	1.3016549E-05	3.0737916E+00	4.9817887E-02	8.7349241E-01	5.8992873E-01	6.7078968E-01
NSET =	10						
BEADS	1.3184251E+05	1.5525099E-05	1.1775488E+00	5.1200009E-02	2.1980977E-01	6.4707173E-02	-2.9177665E-01
CELLS	4.1953575E+04	1.1238016E-05	2.6786789E+00	5.1200009E-02	9.4698832E-01	7.1791676E-01	1.1437901E+00
NSET =	11						
BEADS	1.0325541E+05	1.2152602E-05	1.1769457E+00	5.6865931E-02	2.1358878E-01	-8.2161094E-03	-3.6189893E-01
CELLS	3.5990374E+04	1.1128970E-05	3.0922074E+00	5.6865931E-02	1.1038046E+00	7.8033870E-01	1.1219284E+00

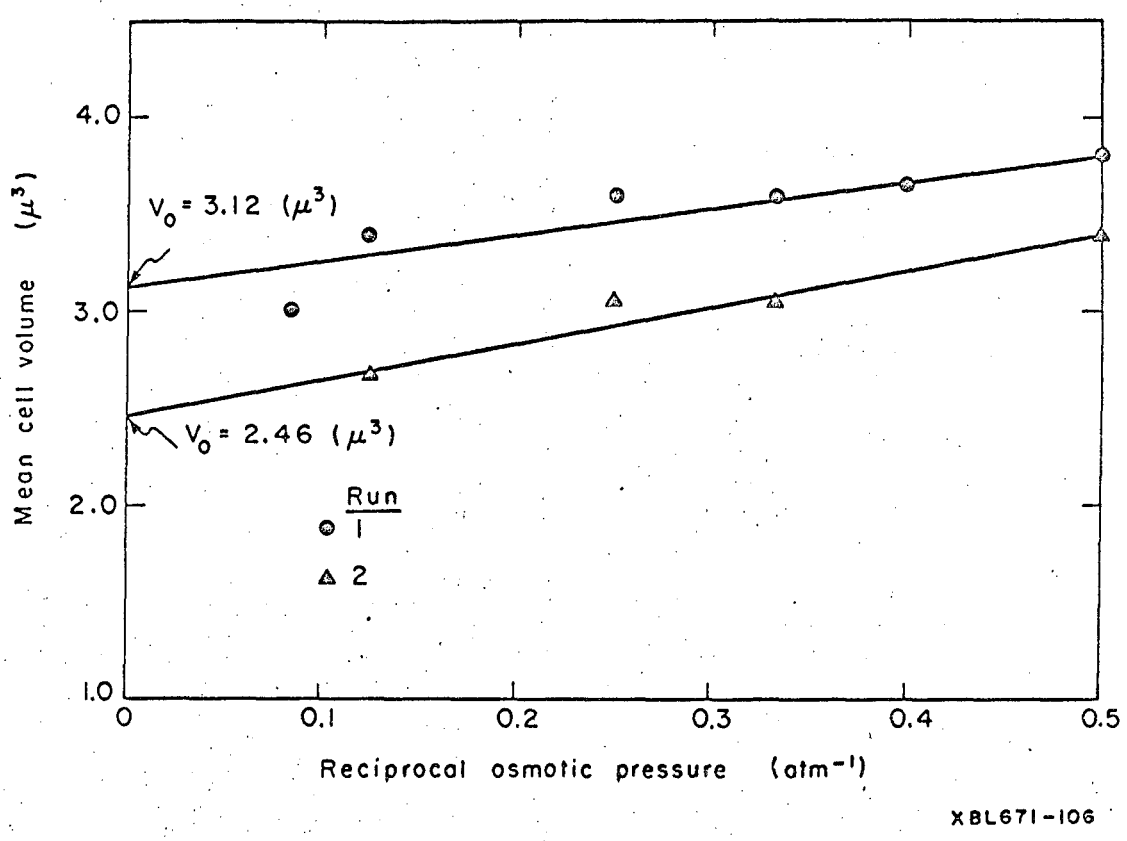

Fig. 33. Mean electronic cell volume versus reciprocal osmotic pressure.

$$\pi(V - V_o) = K$$

$$V = V_o + K/\pi$$

where V = electronic cell volume,

V_o = non-osmotically sensitive volume of the cell,

π = osmotic pressure, and

K = constant.

Thus a graph of volume versus the reciprocal of the osmotic pressure should give a straight line with slope K and V_o as intercept. Figure 33 shows that fair agreement is obtained with the theory, although the second group of data fall below the first group of data due to a shift in time of the mean cell size towards smaller volume. This time shift increases the slopes of Fig. 33, but an osmotic pressure effect can also be definitely seen. Values of the intercepts are much larger than was expected, but the use of a high aperture voltage (120 V) may have already decreased the electronic size of the cells to a point where osmotic effects did not play such a strong role. Another possible source of variation is the fact that the electrolyte (potassium phosphate buffered sodium chloride) was present at half its normal concentration. This could have caused the cells' size to change.

One last experiment, called the Time Experiment, was designed to study emf sensitivity of formalin-fixed cells as a function of how long they had been suspended after sampling. It was important to know the stability of the cells because the time between sampling and electronic sizing and counting often exceeded an hour. The effects of time shifts could be seen in the osmotic experiment. In the time experiment, cells from a 1-3/4 hr culture were suspended in the standard sodium chloride buffer solution containing 0.2% formalin. At intervals, samples were withdrawn and analyzed for optical size and electronic size at three different aperture voltages. The results are shown in Tables XXXII and XXXIII and in Fig. 34. Figure 34 shows that emf sensitivity persisted at

Table XXXII. Time experiment (7/12/66)

Set	Sample	Time	Dilution	Aperture Voltage (volts)	Gain	Diff. (μsec)	Int. (μsec)
1	1½ hr culture	55 min	1:100	30	200	1	1
2	"	"	"	"	"	"	"
3	"	65 min	"	60	100	"	"
4	"	"	"	"	"	"	"
5	"	80 min	"	120	50	"	"
6	"	"	"	"	"	"	"
7	"	2 hr 10 min	"	30	200	"	"
8	"	"	"	"	"	"	"
9	"	2 hr 35 min	"	60	100	"	"
10	"	"	"	"	"	"	"
11	"	2 hr 40 min	"	120	50	"	"
12	"	"	"	"	"	"	"
13	"	2 hr 50 min	"	30	200	"	"
14	"	4 hr 15 min	"	"	"	"	"
15	"	"	"	"	"	"	"
16	"	"	"	60	100	"	"
17	"	"	"	"	"	"	"
18	"	"	"	120	50	"	"
19	"	4 hr 40 min	"	"	"	"	"
20	"	4 hr 50 min	"	30	200	"	"
21	"	4 hr 55 min	"	"	"	"	"
22	"	6 hr 45 min	"	"	"	"	"
23	"	6 hr 55 min	"	"	"	"	"
24	"	7 hr	"	60	100	"	"
25	"	"	"	"	"	"	"
26	"	7 hr 10 min	"	120	50	"	"
27	"	7 hr 15 min	"	"	"	"	"

Table XXXII (continued)

Set	Sample	Time	Dilution	Aperture Voltage (volts)	Gain	Diff. (μsec)	Int. (μsec)
28	1½ hr culture	11 hr 40 min	1:100	30	200	1	1
29	"	11 hr 50 min	"	"	"	"	"
30	"	"	"	60	100	"	"
31	"	12 hr	"	"	"	"	"
32	"	12 hr 10 min	"	120	50	"	"
33	"	"	"	"	"	"	"
34	"	22 hr 50 min	"	30	200	"	"
35	"	"	"	"	"	"	"
36	"	"	"	"	"	"	"
37	"	22 hr 55 min	"	60	100	"	"
38	"	23 hr	"	"	"	"	"
39	"	23 hr 5 min	"	120	50	"	"
40	"	23 hr 10 min	"	"	"	"	"
41	"	29 hr 30 min	"	30	200	"	"
42	"	"	"	"	"	"	"
43	"	"	"	60	100	"	"
44	"	"	"	"	"	"	"
45	"	29 hr 55 min	"	120	50	"	"
46	"	30 hr	"	"	"	"	"

Table XXXIII. Summary of results
time experiment

SUMMARY OF CALCULATED RESULTS,ALL DISTRIBUTIONS

	PARTICLES/ML	VOLUME PERCENT	AVE.VOL.(MU**3)	VOLUME FACTOR	STD.DEV.(MU**3)	SKEWNESS	KURTOSIS
NSET =	1						
BEADS	2.6906746E+05	3.1693238E-05	1.1778919E+00	6.8065037E-02	2.2497959E-01	1.4448363E-01	-4.3592983E-01
CELLS	7.2508052E+04	2.2472439E-05	3.0993026E+00	6.8065037E-02	1.1454683E+00	5.0025426E-01	9.9923311E-01
NSET =	2						
BEADS	2.6906746E+05	3.1693238E-05	1.1778919E+00	6.8065037E-02	2.2497959E-01	1.4448363E-01	-4.3692983E-01
CELLS	8.3893587E+04	2.5981579E-05	3.0969684E+00	6.8065037E-02	1.1793327E+00	5.9442312E-01	9.4767235E-01
NSET =	3						
BEADS	2.6102850E+05	3.0695244E-05	1.1759345E+00	6.2840986E-02	2.0717951E-01	1.0093976E-01	-1.7391831E-01
CELLS	8.8324933E+04	2.2178896E-05	2.5110572E+00	6.2840986E-02	1.0125186E+00	7.1571456E-01	1.5744179E+00
NSET =	4						
BEADS	2.6102850E+05	3.0695244E-05	1.1759345E+00	6.2840986E-02	2.0717951E-01	1.0093976E-01	-1.7391831E-01
CELLS	8.7086538E+04	2.1822832E-05	2.5058789E+00	6.2840986E-02	1.0169229E+00	7.6601360E-01	1.8227635E+00
NSET =	5						
BEADS	2.5517905E+05	2.9959142E-05	1.1740440E+00	6.1957655E-02	1.9194983E-01	1.6469729E-01	-2.2576795E-01
CELLS	8.7699980E+04	1.9284761E-05	2.1989470E+00	6.1967665E-02	9.9331186E-01	5.9431024E-01	9.2730836E-01
NSET =	6						
BEADS	2.6108769E+05	3.0678951E-05	1.1750440E+00	6.1429477E-02	2.0199565E-01	2.1759452E-01	-1.6953495E-01
CELLS	8.8707391E+04	1.9505473E-05	2.1988554E+00	6.1429477E-02	1.0445565E+00	5.2833005E-01	9.1518208E-01
NSET =	7						
BEADS	2.5603862E+05	3.0145160E-05	1.1773677E+00	6.5557625E-02	2.2010966E-01	1.2594881E-01	-3.6529607E-01
CELLS	7.9312588E+04	2.4609423E-05	3.1028396E+00	6.5557625E-02	1.1484896E+00	5.2530003E-01	7.0071525E-01
NSET =	8						
BEADS	2.6573250E+05	3.1347291E-05	1.1796559E+00	6.6626875E-02	2.3616285E-01	7.2708465E-02	-3.4338005E-01
CELLS	7.9893212E+04	2.6107925E-05	3.2678528E+00	6.6626875E-02	1.2120330E+00	4.8839583E-01	5.1857978E-01
NSET =	9						
BEADS	2.5486055E+05	3.0033108E-05	1.1784134E+00	6.4904454E-02	2.2839643E-01	1.4536468E-01	-2.3177118E-01
CELLS	8.3049113E+04	2.2382940E-05	2.6951451E+00	6.4904454E-02	1.0493892E+00	8.2395808E-01	1.8527171E+00
NSET =	10						
BEADS	2.4772277E+05	2.9159787E-05	1.1771137E+00	6.5650094E-02	2.1690410E-01	9.0682936E-02	-2.6786327E-01
CELLS	8.0149645E+04	2.2554679E-05	2.8140710E+00	6.5650094E-02	1.0779105E+00	8.5037995E-01	1.8673613E+00
NSET =	11						
BEADS	2.4128114E+05	2.8329850E-05	1.1741427E+00	6.2866810E-02	1.9363589E-01	2.1015837E-01	-1.7676146E-01
CELLS	8.2622625E+04	1.8037874E-05	2.1831639E+00	6.2866810E-02	1.0358112E+00	5.8428720E-01	1.0494408E+00
NSET =	12						
BEADS	2.4128114E+05	2.8329850E-05	1.1741427E+00	6.2866810E-02	1.9363589E-01	2.1015837E-01	-1.7676146E-01
CELLS	9.1068838E+04	1.9500188E-05	2.1412580E+00	6.2866810E-02	1.0785567E+00	5.7049926E-01	9.8019142E-01
NSET =	13						
BEADS	2.4684689E+05	2.9092729E-05	1.1785739E+00	6.8026236E-02	2.2993253E-01	1.2645792E-01	-4.5177170E-01
CELLS	7.8804019E+04	2.5244386E-05	3.2034389E+00	6.8026235E-02	1.1675329E+00	6.4200598E-01	1.0705332E+00
NSET =	14						
BEADS	2.2159829E+05	2.6038080E-05	1.1750127E+00	6.5909601E-02	2.0109619E-01	1.5603082E-01	-4.5522081E-01
CELLS	7.7308302E+04	2.3323168E-05	3.0169034E+00	6.5909601E-02	1.1455229E+00	5.3901028E-01	7.9372917E-01
NSET =	15						
BEADS	2.2159829E+05	2.6038080E-05	1.1750127E+00	6.5909601E-02	2.0109619E-01	1.5603082E-01	-4.5522081E-01
CELLS	7.9426335E+04	2.4731488E-05	3.1137642E+00	6.5909601E-02	1.1430151E+00	5.6710434E-01	8.3963747E-01
NSET =	16						
BEADS	2.3868292E+05	2.8077098E-05	1.1763346E+00	6.5151482E-02	2.0862665E-01	2.3172444E-02	-1.2436507E-01
CELLS	8.5666066E+04	2.3325581E-05	2.7222140E+00	6.5151482E-02	1.1101699E+00	8.2476496E-01	1.7599030E+00
NSET =	17						
BEADS	2.3868292E+05	2.8077098E-05	1.1763346E+00	6.5151482E-02	2.0862665E-01	2.3172444E-02	-1.2436507E-01
CELLS	8.4776944E+04	2.2452150E-05	2.6484417E+00	6.5151482E-02	1.0997221E+00	7.9663357E-01	1.6967223E+00
NSET =	18						
BEADS	2.4892598E+05	2.9239136E-05	1.1745117E+00	6.1244995E-02	1.9849922E-01	2.4110193E-01	-1.4388952E-01
CELLS	9.6982897E+04	2.0393044E-05	2.1027464E+00	6.1244995E-02	1.1167284E+00	6.8212849E-01	9.8042339E-01
NSET =	19						

BEADS	2.4049749E+05	2.8293386E-05	1.1764524E+00	6.3273078E-02	2.1619462E-01	3.0159445E-01	-1.3785553E-01
CELLS	9.4896441E+04	2.1365813E-05	2.2514872E+00	6.3273078E-02	1.1241371E+00	7.1070672E-01	1.0519534E+00
NSET =	20						
BEADS	2.6491070E+05	3.1297348E-05	1.1814301E+00	6.5254705E-02	2.5122734E-01	1.3698178E-01	-4.2405315E-01
CELLS	8.1712702E+04	2.4426467E-05	2.9893109E+00	6.5254705E-02	1.1881016E+00	5.9149613E-01	8.6100672E-01
NSET =	21						
BEADS	2.6491070E+05	3.1297348E-05	1.1814301E+00	6.5254705E-02	2.5122734E-01	1.3698178E-01	-4.2406316E-01
CELLS	7.3019813E+04	2.2608718E-05	3.0962443E+00	6.5254705E-02	1.1514558E+00	5.5717294E-01	1.0353591E+00
NSET =	22						
BEADS	2.4394302E+05	2.8759146E-05	1.1789288E+00	6.2253763E-02	2.3455800E-01	2.0607464E-01	-3.6645895E-01
CELLS	6.9037362E+04	2.1740708E-05	3.1491220E+00	6.2253763E-02	1.0609884E+00	6.5329087E-01	9.2198917E-01
NSET =	23						
BEADS	2.4394302E+05	2.8759146E-05	1.1789288E+00	6.2253763E-02	2.3455800E-01	2.0607464E-01	-3.6645895E-01
CELLS	7.1568092E+04	2.1992875E-05	3.0730001E+00	6.2253763E-02	1.0903455E+00	6.0591171E-01	8.8736392E-01
NSET =	24						
BEADS	2.4319839E+05	2.8733687E-05	1.1814917E+00	6.2978175E-02	2.5011543E-01	1.0443343E-01	-3.2952834E-01
CELLS	8.3766783E+04	2.1369910E-05	2.5511199E+00	6.2978175E-02	1.0540816E+00	8.5211830E-01	1.9900431E+00
NSET =	25						
BEADS	2.4319839E+05	2.8733687E-05	1.1814917E+00	6.2978175E-02	2.5011543E-01	1.0443343E-01	-3.2952834E-01
CELLS	8.6451898E+04	2.2182283E-05	2.5658527E+00	6.2978175E-02	1.0832262E+00	8.3493878E-01	1.9571195E+00
NSET =	26						
BEADS	1.9446921E+05	2.2867485E-05	1.1758923E+00	6.2310227E-02	2.0611779E-01	6.4738335E-02	-2.0380074E-01
CELLS	9.7595974E+04	2.0310530E-05	2.0810828E+00	6.2310227E-02	1.1137394E+00	7.6339726E-01	1.3409353E+00
NSET =	27						
BEADS	2.1876007E+05	2.5706289E-05	1.1753906E+00	6.1773482E-02	1.9892119E-01	5.3789575E-02	-1.3535054E-01
CELLS	5.5274628E+04	1.1923285E-05	2.1570991E+00	6.1773482E-02	1.0073696E+00	7.0271956E-01	1.1161657E+00
NSET =	28						
BEADS	1.3713459E+06	1.6119575E-04	1.1754566E+00	5.7287645E-02	2.0321782E-01	9.3857318E-02	-2.5919026E-01
CELLS	8.1436617E+04	1.2587400E-05	1.5455683E+00	5.7287645E-02	8.9119055E-01	1.0440085E+00	3.2509691E+00
NSET =	29						
BEADS	1.3713459E+06	1.6119575E-04	1.1754566E+00	5.7287645E-02	2.0321782E-01	9.3857318E-02	-2.5919026E-01
CELLS	5.7881586E+04	9.8416642E-06	1.7003100E+00	5.7287645E-02	9.2343509E-01	9.7252102E-01	2.6554039E+00
NSET =	30						
BEADS	1.1228804E+06	1.3219711E-04	1.1773036E+00	6.3709514E-02	2.1667670E-01	4.1250061E-02	-1.0881590E-01
CELLS	7.9632665E+04	1.3683956E-05	1.7183848E+00	6.3709514E-02	1.0262099E+00	9.5832424E-01	2.8741812E+00
NSET =	31						
BEADS	1.1228804E+06	1.3219711E-04	1.1773036E+00	6.3709514E-02	2.1667670E-01	4.1250061E-02	-1.0881590E-01
CELLS	8.0414560E+04	1.3796251E-05	1.7155409E+00	6.3709514E-02	9.9529515E-01	1.0144793E+00	3.0821033E+00
NSET =	32						
BEADS	1.2380398E+06	1.4560970E-04	1.1761310E+00	6.0036095E-02	2.1200364E-01	2.3900974E-01	-1.8298037E-01
CELLS	8.4024179E+04	1.4223390E-05	1.6927735E+00	6.0036095E-02	9.7054399E-01	9.3670009E-01	2.2488422E+00
NSET =	33						
BEADS	1.3759700E+06	1.6199038E-04	1.1772813E+00	5.9659129E-02	2.1888128E-01	1.3275221E-01	-1.7232652E-01
CELLS	8.9206614E+04	1.4680602E-05	1.6455453E+00	5.9659129E-02	9.8013381E-01	9.2919456E-01	2.1954703E+00
NSET =	34						
BEADS	1.2160580E+06	1.4363326E-04	1.1811382E+00	6.2981648E-02	2.4563526E-01	7.7592893E-02	-2.8494514E-01
CELLS	2.7950655E+04	6.6028761E-06	2.3623332E+00	6.2981648E-02	1.2057440E+00	7.7228293E-01	1.5248093E+00
NSET =	35						
BEADS	1.2160580E+06	1.4363326E-04	1.1811382E+00	6.2981648E-02	2.4563526E-01	7.7592893E-02	-2.8494514E-01
CELLS	7.1865110E+04	1.0286070E-05	1.4313024E+00	6.2981648E-02	8.2025098E-01	1.4349953E+00	6.4073019E+00
NSET =	36						
BEADS	1.2160580E+06	1.4363326E-04	1.1811382E+00	6.2981648E-02	2.4563526E-01	7.7592893E-02	-2.8494514E-01
CELLS	7.6445020E+04	1.1313305E-05	1.4799271E+00	6.2981648E-02	8.7157093E-01	1.3822772E+00	6.0093599E+00
NSET =	37						
BEADS	1.2604732E+06	1.4822028E-04	1.1759098E+00	5.9406971E-02	2.0824663E-01	1.5987425E-01	-1.6081155E-01
CELLS	8.3619390E+04	1.1705377E-05	1.3998400E+00	5.9406971E-02	8.8144073E-01	1.2091026E+00	4.5387752E+00
NSET =	38						
BEADS	1.2604732E+06	1.4822028E-04	1.1759098E+00	5.9406971E-02	2.0824563E-01	1.5987425E-01	-1.6081155E-01
CELLS	8.5166725E+04	1.2340956E-05	1.4490349E+00	5.9406971E-02	9.1230820E-01	1.2272740E+00	4.4329053E+00
NSET =	39						
BEADS	7.3916390E+05	8.7047177E-05	1.1776438E+00	5.6826400E-02	2.2163002E-01	1.1606970E-01	-2.5687074E-01
CELLS	8.4714324E+04	1.2569919E-05	1.4838009E+00	5.6826400E-02	8.8099205E-01	1.1322042E+00	3.3473251E+00

NSET =	40						
BEADS	7.3916390E+05	8.7047177E-05	1.1776438E+00	5.6826400E-02	2.2163002E-01	1.1606970E-01	-2.5587074E-01
CELLS	8.5973194E+04	1.2798576E-05	1.4886705E+00	5.6826400E-02	8.7268021E-01	1.1439638E+00	3.4583887E+00
NSET =	41						
BEADS	1.1220254E+06	1.3229864E-04	1.1791055E+00	6.3827854E-02	2.3098925E-01	3.9804216E-02	-2.8577500E-01
CELLS	7.8135605E+04	1.1066773E-05	1.4535607E+00	6.3827854E-02	8.9795129E-01	1.5691252E+00	7.1023352E+00
NSET =	42						
BEADS	1.1220254E+06	1.3229864E-04	1.1791055E+00	6.3827854E-02	2.3098925E-01	3.9804216E-02	-2.8577500E-01
CELLS	7.8890402E+04	1.1525168E-05	1.4609088E+00	6.3827854E-02	8.7423948E-01	1.4889960E+00	5.5554022E+00
NSET =	43						
BEADS	1.0833656E+06	1.2755874E-04	1.1774302E+00	6.2097952E-02	2.1994802E-01	1.2530258E-01	-1.7265953E-01
CELLS	8.8412044E+04	1.2082706E-05	1.3665358E+00	6.2097952E-02	9.4158520E-01	1.3836354E+00	5.5549737E+00
NSET =	44						
BEADS	1.0833656E+06	1.2755874E-04	1.1774302E+00	6.2097952E-02	2.1994802E-01	1.2530258E-01	-1.7265953E-01
CELLS	9.0212517E+04	1.2373798E-05	1.3715277E+00	6.2097952E-02	9.5185510E-01	1.3688006E+00	5.4579274E+00
NSET =	45						
BEADS	1.0539870E+06	1.2392122E-04	1.1757377E+00	5.9704093E-02	2.0846904E-01	2.3443765E-01	-1.7171536E-01
CELLS	9.0452134E+04	1.3450962E-05	1.4873806E+00	5.9704093E-02	9.5322262E-01	1.1918206E+00	3.6495359E+00
NSET =	46						
BEADS	1.0539870E+06	1.2392122E-04	1.1757377E+00	5.9704093E-02	2.0846904E-01	2.3443765E-01	-1.7171536E-01
CELLS	8.9942539E+04	1.2986091E-05	1.4438209E+00	5.9704093E-02	9.2152792E-01	1.2177252E+00	3.8727534E+00

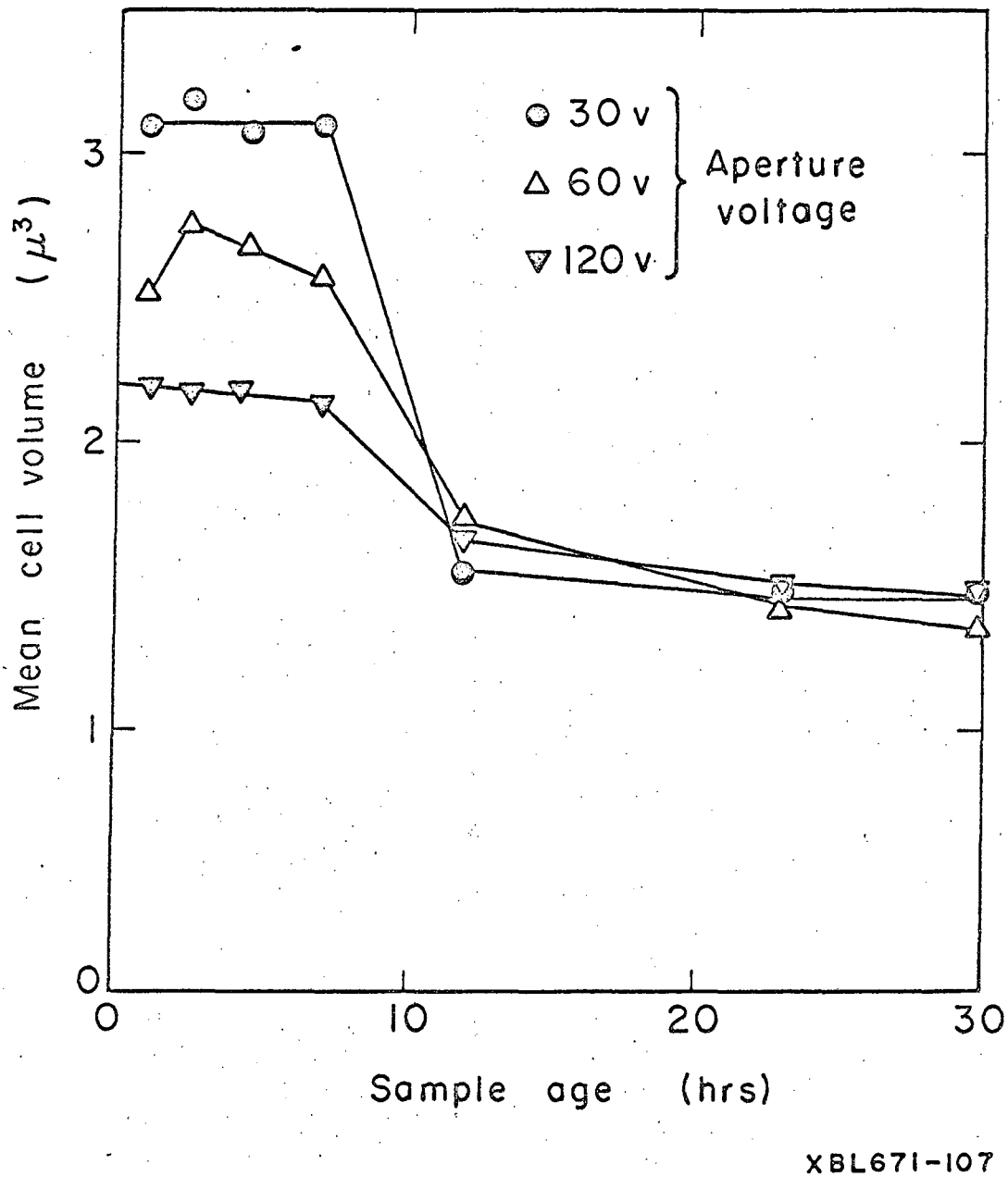

Fig. 34. Mean cell size at different aperture voltages and sample ages, time experiment.

least 7 hrs, with cell size remaining fairly constant. After 7 hrs, the mean cell size dropped sharply down to a mean cell volume of about one and one half cubic microns. From 12 hrs on, no emf sensitivity was detected and mean cell size was independent of aperture voltage. Also, cell volume was nearly constant from 12 hrs onward.

It is our opinion that the rapid decrease in electronic size between 7 and 12 hrs is due to the rupture of membranes in the cell, including vacuolar as well as cytoplasmic membranes. The remaining cell wall and nonsoluble portions such as the ribosomes that remain behind account for the volume observed at times past 12 hrs. Optical volume was constant during the entire experiment and only a slight increase in cell count with time was observed.

3. A modified Model of the Bacterial Cell

As stated earlier, modification of the cell model of Carstensen et al. is required to reconcile with some of our observations. The revised model has the following features:

(1) The cell wall is an electrically conductive shell surrounding the cell membrane and the internal components of the cell. The membrane and cell interior are essentially non-conductive in comparison to the cell wall.

(2) The cell has two types of membranes -- cytoplasmic and vacuolar, the latter appearing in the cell only during the late lag phase and early exponential phase of growth, increasing the length of cells. An increase of cell volume of about 50% is observed during that period, as shown by the sizing and osmotic experiments.

(3) Emf sensitivity is due to rupture by high aperture voltage of the membranes surrounding vacuoles. The effect may show as much as a 50% reduction in cell volume when the aperture voltage is increased from 30 to 120 volts, as shown in the time and sizing experiments.

(4) Cells with disrupted membranes (both cytoplasmic and vacuolar) have a residual cell size due to ribosomes and other content of the cell still held together by the cell wall, as shown by the time experiment.

(5) Heat killing of exponential phase cells lyses the cells, causing the cells to become transparent to electronic sizing, as shown by the sizing experiment.

VI. SUMMARY

Electronic sizing and counting of bacteria is an important technique in microbiology. It is particularly important to the study of bacterial growth kinetics. It was shown here that it also offers a means of studying sterilization kinetics.

An electronic sizing and counting system was built and calibrated using polystyrene beads as standards. An electron microscope study of the beads had established the bead size distribution. Linearity of the system in response to particle size was demonstrated. The size distribution of beads measured electronically was considerably broader than the distribution obtained by electron microscopy.

Electronic counting was compared with the conventional bacteriological techniques of optical counting, measurement of turbidity, and colony counting. Good agreement was found with colony counts and turbidity. Reduction of electronic counts by heat killing occurred with exponential phase cultures.

The aperture voltage was shown to affect the electronic size of cells. The phenomenon appears to be related to vacuole formation in the cells.

A model for the electrical conductivity is proposed and compared with the empirical results.

APPENDIX I

PREPARATION OF CARBON SUPPORTS FOR ELECTRON MICROSCOPY

Thin films of carbon were prepared by depositing graphite onto glass slides 2.5 × 1 × 74 mm that had been chemically cleaned, rinsed with a dilute detergent solution, and air-dried. The deposition was accomplished by using two graphite rods as electrodes in an electric arc in a bell jar. The bell jar was evacuated to a pressure below one micron of mercury. The tips of the graphite electrodes in contact with the arc evaporated and condensed on striking the walls of the bell jar. The specially-prepared glass slides were placed about 150 mm below the arc on the base of the bell jar and thus a portion of the evaporated carbon condensed on the slides. After a darkening of the slide surfaces had been obtained, the arc was shut-off and the slides were removed from the apparatus. The carbon film on each slide was then cut into small squares about 2 to 3 mm on a side using a scalpel and the squares of carbon floated-off the slide onto the surface of a large bowl of water. Each floating square was then picked-up with a circular copper grid (3 mm diameter, 200 mesh, Ernest F. Fullam, Inc., Schenectady, N. Y.) in such a manner that the square of carbon film lay unwrinkled on the grid, covering the maximum possible number of holes of the grid. Capture of the films with the grids was accomplished more easily if the grids were dipped in ethanol just prior to manipulation.

The carbon films on the grids were allowed to dry in a dust-free petri dish and then examined with a low-magnification light microscope to be sure that the film had remained intact during the manipulations.

The carbon film covering openings in the copper grid is relatively transparent to electrons and thus serves well as a support for the electron microscopy of small particles such as latex beads or bacteria.

APPENDIX II

TEST OF THE REPRODUCIBILITY OF THE TRAVELING MICROSCOPE

Repetetive measurements were made on single particles in both the horizontal and the vertical directions to estimate the random error associated with the measurement of the diameters of the photographic images of the particles. Data in the first two columes of Table XXXIV are the coordinates of the opposite sides of the particle; the third column, being the difference of the first two, is thus the diameter of the particle image. The fourth column is the difference of each measurement from the mean of measurements and the last column is the square of that difference. The population standard deviation was estimated for both the data obtained in the horizontal and the vertical directions. A value of 3.42 μ was obtained in the former case and 3.45 μ in the latter case. The mean diameters were 4510.1 μ and 4464.0 μ, respectively. The random error in measurement of the image diameters was thus on the order of .1% of the diameter, which is less than 10% of the standard deviation of the population particle of diameters that from the data, so that the effect of this source of error will not be significant compared to that introduced by magnification errors.

The effects of thermal expansion of the glass plate and/or the measuring screw of the stage micrometer did not contribute significant error to the measurement of image diameter.

Table XXXIV. Reproducibility of the traveling microscope

HORIZONTAL DIRECTION

Lower coordinate (microns)	Upper coordinate (microns)	Diameter (microns)	Deviation (microns)	Deviation Squared (sq. microns)
55316	59830	4514	3.9	15.2
55323	59826	4503	7.1	50.4
55317	59830	4513	2.9	8.4
55320	59827	4507	3.1	9.6
55319	59831	4512	1.9	3.6
55319	59830	4511	0.9	0.8
55322	59831	4509	1.1	1.2
55319	59830	4511	0.9	0.8
55321	59827	4506	4.1	16.8
55320	59835	4515	4.9	24.0
55319	59830	4511	0.9	0.8
55322	59831	4509	1.1	1.2
55322	59828	4506	4.1	16.8
55321	59830	4509	1.1	1.2
55321	59827	4506	4.1	16.8
55320	59827	4507	3.1	9.6
55320	59833	4513	2.9	8.4
55316	59832	4516	5.9	34.8
55321	59833	4512	1.9	3.6
55321	59830	4509	1.1	1.2
55320	59833	4513	2.9	8.4

VERTICAL DIRECTION

Lower coordinate (half microns)	Upper coordinate (half microns)	Diameter ($\frac{1}{2}$micron)	Deviation ($\frac{1}{2}$micron)	Deviation Squared ($\frac{1}{2}$microns sq)
66851	75787	8936	4.0	16.0
66851	75787	8936	4.0	16.0
66861	75783	8922	3.0	9.0
66857	75770	8913	7.5	56.2
66858	75789	8931	1.5	2.3
66861	75787	8926	1.0	1.0
66857	75789	8932	4.0	16.0

APPENDIX III

ESTIMATION OF ASTIGMATISM IN PHOTOGRAPHS

All measurements of particle diameters were made along one of the four axes (X, YA, YB, Z) shown in Fig. 5. By comparing the diameters of a group of particles measured in any two of the four directions, the presence of astigmatism can be detected.

Tables XXXV, XXXVI, and XXXVII show the calculations of the average diameters in the X- and YA-directions, the X- and YB-directions, and the X- and Z-directions respectively. In every case, the average diameters in the directions compared were different from one another. The Student's t test for small samples was applied to calculate the probability that the differences in average diameters in the different directions were caused by random variations. The following formula was used to calculate the value of Student's t for each group of data

$$t_{obs} = \frac{(\bar{D}_X - \bar{D}_i)}{\sigma}\sqrt{n - 1}$$

where $\bar{D}_X$ = mean diameter of particles measured in the X-direction

$\bar{D}_i$ = mean diameter of particles measured in the i-direction

n = number of particles in group analyzed

σ = standard deviation of population (Table 3)

ν = number of degrees of freedom

$= 2(n - 1)$

The calculated values of t_{obs} are shown in Table XXXVIII. Also shown in Table XXXVIII are the probabilities that $t \geq t_{obs}$ would not occur by chance. Clearly, in each case, some systematic error existed, and it is safe to assume that the differences in mean diameters was caused by astigmatism. The astigmatism correction in the YA-direction was arbitrarily set equal to unity and correction factors for the other three directions were calculated with the formula

$$C_i = (\bar{D}_{YA}/\bar{D}_X) \times (\bar{D}_X/\bar{D}_i)$$

Table XXXV.

D_x (microns)	D_{YA} (microns)
4243.	4202.
4343.	4203.
4392.	4195.
4320.	4110.
4551.	4612.
4599.	4609.
4598.	4607.
4513.	4501.
4586.	4513.
4614.	4522.
3348.	3275.
4579.	4525.
4572.	4547.
4536.	4573.

$\bar{D}_x$ = 4413.86 microns

$\bar{D}_{YA}$ = 4356.71 microns

$$\frac{\bar{D}_{YA}}{\bar{D}_x} = .987054$$

Table XXXVI.

D_x (microns)	D_{YB} (microns)
4244.	4175.
4320.	4182.
4551.	4565.
4599.	4583.
4598.	4605.
4586.	4582.
4614.	4490.
4535.	4563.
4536.	4571.
4608.	4587.

$\bar{D}_x$ = 4519.1 microns

$\bar{D}_{YB}$ = 4490.3 microns

$$\frac{\bar{D}_{YB}}{\bar{D}_x} = 0.99363$$

Table XXXVII.

D_x (microns)	D_z (microns)
4150.	4060.
4222.	4194.
4343.	4268.
4337.	4274.
4513.	4521.
4582.	4591.
4404.	4400.

$\bar{D}_x$ = 4363.4 microns

$\bar{D}_z$ = 4329.4 microns

$$\frac{\bar{D}_z}{\bar{D}_x} = .991981$$

Table XXXVIII.

i	n	$\left(\frac{\bar{D}_x}{\bar{D}_i} - 1\right)$	t_{obs}	ν $(= 2(n-1))$	$P_\nu(t<t_{obs})$
Y A	14	.013116	4.09	26	> 99%
Y B	10	.0064138	1.69	18	> 88%
Z	7	.0080842	2.90	12	> 98%

The factors calculated in this way are shown in Table XXXIX. They were used in the computer program described in the test to correct for astigmatism.

Table XXXIX.

Diameter Direction (i)	Correction Factor $(\bar{D}_{YA}/\bar{D}_i)$
X	0.987054
YA	1.000000
YB	0.994485
Z	0.995034

APPENDIX IV

COMPUTER PROGRAM PDDANL AND SELECTED RESULTS

Figure 9 is an outline of the computer program written and used to analyze the particle diameter data. The main program, PDDANL, the subroutine PDHIST, which computes the histogram of diameters, and the subroutine PVHIST, which computes the histogram of volumes, are listed in Table XXXX.

Selected results obtained by analysis of the data are shown in Tables XXXXI and XXXXII. The first set of results was obtained by removing unusually large and unusually small particles from consideration. The factors necessary to correct the mean diameter of each photograph to a value of 1.305 microns under these conditions was assumed to be the best estimate of the magnification in each photograph (these are referred to as mean-estimated magnification factors in the test). Note that in Table XXXXI, MAGNIFICATION FACTOR = DIAMETER FACTOR holds for each photograph. The same magnification factors were used in computing the data shown in Table XXXXII, which differs from the preceding table by the inclusion of very large and small particles that had been excluded from consideration previously. Note the large increase in the statistical parameters of variance, standard deviation, skewness, and kurtosis.

Table XXXX. Program PDDANL

```
PDDANL,1,100,110000.    468001,EDWARDS
RUN(S)
PDDANL.
7
      PROGRAM PDDANL (INPUT,OUTPUT)
C PROGRAM FOR ANALYSIS OF ELECTRON MICROSCOPE MEASUREMENTS OF SMALL
C POLYVINYL-TOLUENE PARTICLES USED AS PRIMARY STANDARDS IN ELECTRONIC
C SIZING AND COUNTING OF BACTERIA
C PROGRAMMED BY VICTOR H. EDWARDS
    1 FORMAT(9I8)
    2 FORMAT(17H WILL USE ASIG IS,L7)
    3 FORMAT(I4,6F10.1/4X,4F10.1)
    4 FORMAT(16H THIS IS GROUP  ,I5,20H NUMBER OF SPHERES =,I5)
    5 FORMAT(53HRESULTS OF STATISTICAL ANALYSIS OF PARTICLE DIAMETERS)
    6 FORMAT(23H PROGRAMMER V.H.EDWARDS/)
    7 FORMAT(28H NUMBER OF GROUPS ANALYSED =,I5/)
    8FORMAT(86H ND   DIAM (X)   DIAM(YA)   DIAM(YB)   DIAM(ZA)   DIAM(Z
     1B)   MEAN DIA(J)   MEAN VOL(J)/)
    9 FORMAT(I3,2X,5(F10.3,1X),2(1X,F11.6))
   100FORMAT(22H NUMBER DIA MEASURED =,I6,11H MEAN DIA =,F12.5,13H DIA F
     1ACTOR =,E12.4)
   11 FORMAT(14H VARIANCE (V)=,E15.7,21H  STANDARD DEVIATION=,F15.7)
   12 FORMAT(11H (M3/S**3)=,F13.6,5X,12H  (M4/S**4)=,F13.6//)
   13 FORMAT(52H STATISTICAL PARAMETERS OF DISTRIBUTION OF DIAMETERS)
   14 FORMAT(50H STATISTICAL PARAMETERS OF DISTRIBUTION OF VOLUMES)
   15 FORMAT(//)
C THIS SECTION OF THE PROGRAM READS THE DATA
      READ 1,NGPS,MX
      DIMENSION FACTOR(20),MV(5,10,10)
      LOGICAL TFAG(17)
      DIMENSION NS(17),U(17),V(17),S(17),L(17),A3(17),A4(17),IDENT(17)
      DIMENSION D(17,37,5),X1(17,37,5),X2(17,37,5),ND(17,37),AD(17,37)
      DIMENSION DEL(17,37),AV(17,37),UV(17),VV(17),SV(17),A3V(17)
      DIMENSION A4V(17),M(5,10,10)
      READ 4,(IDENT(I),NS(I),I=1,NGPS)
      DIMENSION FMAG(20)
  151 FORMAT(6F10.8)
      READ 151,(FMAG(I),I=1,NGPS)
      DO 100 I=1,NGPS
      NIS=NS(I)
      READ 2,TFAG(I)
      READ 3,((ND(I,J),((X1(I,J,K),X2(I,J,K)),K=1,5)),J=1,NIS)
  100 CONTINUE
      DIMENSION CORRECT(5)
      DIMENSION DEFACT(20)
C CORRECT(K) ARE FACTORS TO CORRECT FOR ASTIGMATISM IN THE ELECTRON
C MICROSCOPE, WHILE FMAG(I) ARE USED TO CORRECT MAGNIFICATION ERRORS
      CORRECT(1)=.987054
      CORRECT(2)=1.
      CORRECT(3)=.9933848
      CORRECT(4)=.9950335
      CORRECT(5)=1.
      VSPHERE=3.14159*(1.305**3)/6.
      DO 300 I=1,NGPS
      NIS=NS(I)
      U(I)=0.
```

```
      L(I)=0.
      V(I)=0.
      UV(I)=0.
      VV(I)=0.
C THIS SECTION OF THE PROGRAM COMPUTES AVERAGE DIAMETERS
      DO 200 J=1,NIS
      AD(I,J)=0.
      DO 205 K=1,5
      IF(K-1)201,201,202
  201 D(I,J,K)=(X2(I,J,K)-X1(I,J,K))
      GO TO 205
  202 D(I,J,K)=(X2(I,J,K)-X1(I,J,K))/2.
  205 AD(I,J)=AD(I,J)+D(I,J,K)*CORRECT(K)
      L(I)=L(I)+ND(I,J)
      U(I)=U(I)+AD(I,J)
      AD(I,J)=AD(I,J)/ND(I,J)
  200 CONTINUE
C THIS PART CORRECTS MAG. ERROR AND COMPUTES STATISTICAL PARAMETERS
      U(I)=U(I)/L(I)
      DEFACT(I)=1.305/U(I)
      U(I)=1.305*FMAG(I)/DEFACT(I)
      A3(I)=0.
      A4(I)=0.
      A4V(I)=0.
      A3V(I)=0.
      DO 210 J=1,NIS
      AD(I,J)=AD(I,J)*FMAG(I)
      CALL PDHIST(I,J,AV,AD,NGPS,MX,LOSHOW,IHIGH,M)
      AV(I,J)=.523598*AD(I,J)**3
      CALL PVHIST(I,J,AV,NGPS,MX,LOSHOWV,IHIGHV,MV)
      UV(I)=UV(I)+AV(I,J)*ND(I,J)
  210 CONTINUE
      UV(I)=UV(I)/FLOAT(L(I))
      FACTOR(I)=VSPHERE/UV(I)
      DO 220 J=1,NIS
      V(I)=V(I)+((AD(I,J)-U(I))**2)*ND(I,J)
      A3(I)=A3(I)+((AD(I,J)-U(I))**3)*ND(I,J)
      VV(I)=VV(I)+((AV(I,J)-UV(I))**2)*ND(I,J)
      A3V(I)=A3V(I)+((AV(I,J)-UV(I))**3)*ND(I,J)
      A4V(I)=A4V(I)+((AV(I,J)-UV(I))**4)*ND(I,J)
  220 A4(I)=A4(I)+((AD(I,J)-U(I))**4)*ND(I,J)
      V(I)=V(I)/(L(I)-1)
      S(I)=SQRT(V(I))
      VV(I)=VV(I)/FLOAT(L(I)-1)
      SV(I)=SQRT(VV(I))
      A3(I)=A3(I)/(V(I)*S(I)*L(I))
      A4(I)=A4(I)/(V(I)*V(I)*L(I))
      A3V(I)=A3V(I)/(VV(I)*SV(I)*FLOAT(L(I)))
      A4V(I)=A4V(I)/(VV(I)*VV(I)*FLOAT(L(I)))
      IF(TFAG) GO TO 230
      GO TO 300
  230 DO 239 J=1,NIS
      DEL(I,J)=0.
  239 CONTINUE
  300 CONTINUE
C THIS PART PRINTS OUT THE DIAMETERS,VOLUMES,AND STATISTICAL PARAMETERS
```

```
  240 PRINT 5
      PRINT 6
      PRINT 7,NGPS
      DO 350 I=1,NGPS
      NIS=NS(I)
      PRINT 4444,IDENT(I),NS(I)
 4444 FORMAT(14HPHOTO NUMBER =,I8,22H NUMBER OF PARTICLES =,I6)
      PRINT 152,FMAG(I)
  152 FORMAT(23H MAGNIFICATION FACTOR =,F12.8)
      PRINT 15
      PRINT 8
      PRINT 9,(ND(I,J),(D(I,J,K),K=1,5),AD(I,J),AV(I,J),J=1,NIS)
      PRINT 15
      PRINT 13
      PRINT 10,L(I),U(I),DEFACT(I)
      PRINT 11,V(I),S(I)
      PRINT 12,A3(I),A4(I)
      PRINT 15
      PRINT 14
      PRINT 27,FACTOR(I),UV(I)
  270FORMAT(16H VOLUME FACTOR =,E12.4,14H MEAN VOLUME =,F8.4,14H CUBIC
     1MICRONS)
      PRINT 11,VV(I),SV(I)
      PRINT 12,A3V(I),A4V(I)
  350 CONTINUE
C THIS PART PRINTS OUT THE SIZE DISTRIBUTIONS
   18 FORMAT(6H  K1 =,I5)
   19 FORMAT(45HNUMBER OF PARTICLE DIAMETERS LESS THAN ZERO =,I5)
  20UFORMAT(81H DISTRIBUTION OF PARTICLE DIAMETERS FROM 0 TO 5MICRONS B
     1Y INTERVALS OF .01MICRONS)
   22 FORMAT(10(3X,I5))
   23 FORMAT(45H NUMBER OF PARTICLE DIAMETERS OVER 5MICRONS =,I5)
      PRINT 19,LOSHOW
      PRINT 20
      DO 25 K1=1,5
      PRINT 18,K1
      DO 26 K2=1,10
      PRINT 22,(M(K1,K2,K3),K3=1,10)
   26 CONTINUE
   25 CONTINUE
      PRINT 23,IHIGH
   30 FORMAT(84H DISTRIBUTION OF VOLUMES FROM 0 TO 5 CUBIC MICRONS BY IN
     1TERVALS OF .01 CUBIC MICRONS  )
   31 FORMAT(49H NUMBER OF PARTICLES WITH VOLUME LESS THAN ZERO = ,I5)
   32 FORMAT(60H NUMBER OF PARTICLES WITH VOLUME MORE THAN 5 CUBIC MICRO
     1NS = ,I5)
      PRINT 15
      PRINT 31,LOSHOWV
      PRINT 30
      DO 35 K1=1,5
      PRINT 18,K1
      DO 36 K2=1,10
      PRINT 22,(MV(K1,K2,K3),K3=1,10)
   36 CONTINUE
   35 CONTINUE
      PRINT 32,IHIGHV
```

```
      DIMENSION H(5,10,10),HV(5,10,10)
C THIS PART COMPUTES FREQUENCY DIAGRAMS FOR DIAS AND VOLS AND PRINTS
      NSPHERE=0
      DO 40 I=1,NGPS
      NSPHERE=NSPHERE+NS(I)
   40 CONTINUE
      DO 41 K1=1,5
      DO 41 K2=1,10
      DO 41 K3=1,10
      H(K1,K2,K3)=FLOAT(M(K1,K2,K3))/FLOAT(NSPHERE)
      HV(K1,K2,K3)=FLOAT(MV(K1,K2,K3))/FLOAT(NSPHERE)
   41 CONTINUE
   42 FORMAT(51H FRACTION OF PARTICLES WITH VOLUME LESS THAN ZERO =,F10.
     17)
   43 FORMAT(62H FRACTION OF PARTICLES WITH VOLUME MORE THAN 5 CUBIC MIC
     1RONS =,F10.7)
   49 FORMAT(48H FRACTION OF PARTICLE DIAMETERS LESS THAN ZERO =,F11.8)
   53 FORMAT(47H FRACTION OF PARTICLE DIAMETERS OVER 5MICRONS =,F11.8)
      HLOW=FLOAT(LOSHOW)/FLOAT(NSPHERE)
      HHIGH=FLOAT(IHIGH)/FLOAT(NSPHERE)
      HLOWV=FLOAT(LOSHOWV)/FLOAT(NSPHERE)
      HHIGHV=FLOAT(IHIGHV)/FLOAT(NSPHERE)
      PRINT 49,HLOW
      PRINT 20
      DO 45 K1=1,5
      PRINT 18,K1
      DO 45 K2=1,10
      PRINT 46,(H(K1,K2,K3),K3=1,10)
   45 CONTINUE
      PRINT 53,HHIGH
   46 FORMAT(10(2X,F9.7))
      PRINT 15
      PRINT 42,HLOWV
      PRINT 30
      DO 47 K1=1,5
      PRINT 18,K1
      DO 47 K2=1,10
      PRINT 46,(HV(K1,K2,K3),K3=1,10)
   47 CONTINUE
      PRINT 43,HHIGHV
C THIS LAST PART CALCULATES OVERALL STATISTICAL PARAMETERS AND PRINTSOUT
  101 TLT=0.
      UT=0.
      VT=0.
      FT=0.
      A3T=0.
      A4T=0.
      UTV=0.
      VTV=0.
      FTV=0.
      SUM=0.
      A3TV=0.
      A4TV=0.
      DO 157 I=1,NGPS
      NIS=NS(I)
      DO 156 J=1,NIS
```

```
      UT=UT+AD(I,J)*ND(I,J)
      UTV=UTV+AV(I,J)*ND(I,J)
      TLT=TLT+ND(I,J)
  156 CONTINUE
      FT=FT+DEFACT(I)*FLOAT(L(I))
      FTV=FTV+FACTOR(I)*FLOAT(L(I))
      SUM=SUM+FLOAT(L(I))
  157 CONTINUE
      UT=UT/TLT
      UTV=UTV/TLT
      FT=FT/SUM
      FTV=FTV/SUM
      DO 159 I=1,NGPS
      NIS=NS(I)
      DO 158 J=1,NIS
      DED=AD(I,J)-UT
      DEV=AV(I,J)-UTV
      VT=VT+ND(I,J)*DED**2
      VTV=VTV+ND(I,J)*DEV**2
      A3T=A3T+ND(I,J)*DED**3
      A3TV=A3TV+ND(I,J)*DEV**3
      A4T=A4T+ND(I,J)*DED**4
      A4TV=A4TV+ND(I,J)*DEV**4
  158 CONTINUE
  159 CONTINUE
      VT=VT/(TLT-1.)
      ST=SQRT(VT)
      VTV=VTV/(TLT-1.)
      STV=SQRT(VTV)
      A3T=A3T/(TLT*ST*VT)
      A4T=A4T/(TLT*VT**2)
      A3TV=A3TV/(STV*VTV*TLT)
      A4TV=A4TV/(TLT*VTV**2)
      LTL=TLT
      PRINT 15
  155 FORMAT(42H STATISTICAL PARAMETERS OF COMBINED GROUPS)
      PRINT 155
      PRINT 13
      PRINT 10,LTL,UT,FT
      PRINT 11,VT,ST
      PRINT 12,A3T,A4T
      PRINT 15
      PRINT 14
      PRINT 10,LTL,UTV,FTV
      PRINT 11,VTV,STV
      PRINT 12,A3TV,A4TV
  102 STOP
      END
```

```
      SUBROUTINE PDHIST(I,J,AV,AD,NGPS,MX,LOSHOW,IHIGH,M)
C THIS SUBROUTINE COMPUTES A HISTOGRAM OF DIAMETERS
      DIMENSION AV(17,37),AD(17,37),M(5,10,10)
      IF(I.OR.J.GT.1) GO TO 1004
      LOSHOW= 0.
      IHIGH=0.
      DO 1001 K1=1,5
      DO 1002 K2=1,10
      DO 1003 K3=1,10
      M(K1,K2,K3)=0
 1003 CONTINUE
 1002 CONTINUE
 1001 CONTINUE
 1004 IF(AD(I,J))888,888,887
  887 IF(5.-AD(I,J))777,777,776
  776 K1=0
      K2=0
      K3=0
      ACE1=-1.
      ACE2=-.1
      ACE3=-.01
 1000 ACE1=ACE1+1.
      K1=K1+1
      IF(AD(I,J)  -ACE1) 998,999,1000
  999 K2=1
      K3=1
      GO TO 990
  998 K1=K1-1
      ACE1=ACE1-1.
  997 ACE2=ACE2+.1
      K2=K2+1
      IF(AD(I,J)  -ACE1-ACE2) 996,991,997
  991 K3=1
      GO TO 990
  996 K2=K2-1
      ACE2=ACE2-.1
  995 ACE3=ACE3+.01
      K3=K3+1
      IF(AD(I,J)-ACE1-ACE2-ACE3)994,990,995
  994 K3=K3-1
      ACE3=ACE3-.01
  990 M(K1,K2,K3)=M(K1,K2,K3)+1
      GO TO 666
  888 LOSHOW=LOSHOW+1
      GO TO 666
  777 IHIGH=IHIGH+1
  666 RETURN
      STOP
      END
```

```
      SUBROUTINE PVHIST(I,J,AV,NGPS,MX,LOSHOWV,IHIGHV,MV)
C THIS SUBROUTINE COMPUTES A HISTOGRAM OF VOLUMES
      DIMENSION AV(17,37),MV(5,10,10)
      IF(I.OR.J.GT.1)GO TO 704
      LOSHOWV=0.
      IHIGHV=0.
      DO 701 K1=1,5
      DO 702 K2=1,10
      DO 703 K3=1,10
      MV(K1,K2,K3)=0.
  703 CONTINUE
  702 CONTINUE
  701 CONTINUE
  704 IF(AV(I,J))708,708,707
  707 IF(5.-AV(I,J))607,607,606
  606 K1=0
      K2=0
      K3=0
      ACE1=-1.
      ACE2=-.1
      ACE3=-.01
  600 ACE1=ACE1+1.
      K1=K1+1
      IF(AV(I,J)-ACE1) 598,599,600
  599 K2=1
      K3=1
      GO TO 590
  598 K1=K1-1
      ACE1=ACE1-1.
  597 ACE2=ACE2+.1
      K2=K2+1
      IF(AV(I,J)-ACE1-ACE2)596,591,597
  591 K3=1
      GO TO 590
  596 K2=K2-1
      ACE2=ACE2-.1
  595 ACE3=ACE3+.01
      K3=K3+1
      IF(AV(I,J)-ACE1-ACE2-ACE3)594,590,595
  594 K3=K3-1
  590 MV(K1,K2,K3)=MV(K1,K2,K3)+1
      GO TO 566
  708 LOSHOWV=LOSHOWV+1
      GO TO 566
  607 IHIGHV=IHIGHV+1
  566 RETURN
      STOP
      END
```

Table XXXXI. Size distribution of latex beads with unusual data removed

FRACTION OF PARTICLE DIAMETERS LESS THAN ZERO = 0.
DISTRIBUTION OF PARTICLE DIAMETERS FROM 0 TO 5MICRONS BY INTERVALS OF .01MICRONS

K1 = 1									
0.	0.	0.	0.	0.	0.	0.	0.	0.	0.
0.	0.	0.	0.	0.	0.	0.	0.	0.	0.
0.	0.	0.	0.	0.	0.	0.	0.	0.	0.
0.	0.	0.	0.	0.	0.	0.	0.	0.	0.
0.	0.	0.	0.	0.	0.	0.	0.	0.	0.
0.	0.	0.	0.	0.	0.	0.	0.	0.	0.
0.	0.	0.	0.	0.	0.	0.	0.	0.	0.
0.	0.	0.	0.	0.	0.	0.	0.	0.	0.
0.	0.	0.	0.	0.	0.	0.	0.	0.	0.
0.	0.	0.	0.	0.	0.	0.	0.	0.	0.
0.	0.	0.	0.	0.	0.	0.	0.	0.	0.
K1 = 2									
0.	0.	0.	0.	0.	0.	0.	0.	0.	0.
0.	0.	0.	0.	0.	0.	0.	0.	0.	0.
0.	0.	0.	.0049383	0.	.0074074	.0197531	.0222222	.0839506	.1827160
.3185185	.2271605	.0938272	.0370370	0.	0.	.0024691	0.	0.	0.
0.	0.	0.	0.	0.	0.	0.	0.	0.	0.
0.	0.	0.	0.	0.	0.	0.	0.	0.	0.
0.	0.	0.	0.	0.	0.	0.	0.	0.	0.
0.	0.	0.	0.	0.	0.	0.	0.	0.	0.
0.	0.	0.	0.	0.	0.	0.	0.	0.	0.
0.	0.	0.	0.	0.	0.	0.	0.	0.	0.
0.	0.	0.	0.	0.	0.	0.	0.	0.	0.
K1 = 3									
0.	0.	0.	0.	0.	0.	0.	0.	0.	0.
0.	0.	0.	0.	0.	0.	0.	0.	0.	0.
0.	0.	0.	0.	0.	0.	0.	0.	0.	0.
0.	0.	0.	0.	0.	0.	0.	0.	0.	0.
0.	0.	0.	0.	0.	0.	0.	0.	0.	0.
0.	0.	0.	0.	0.	0.	0.	0.	0.	0.
0.	0.	0.	0.	0.	0.	0.	0.	0.	0.
0.	0.	0.	0.	0.	0.	0.	0.	0.	0.
0.	0.	0.	0.	0.	0.	0.	0.	0.	0.
0.	0.	0.	0.	0.	0.	0.	0.	0.	0.
K1 = 4									
0.	0.	0.	0.	0.	0.	0.	0.	0.	0.
0.	0.	0.	0.	0.	0.	0.	0.	0.	0.
0.	0.	0.	0.	0.	0.	0.	0.	0.	0.
0.	0.	0.	0.	0.	0.	0.	0.	0.	0.
0.	0.	0.	0.	0.	0.	0.	0.	0.	0.
0.	0.	0.	0.	0.	0.	0.	0.	0.	0.
0.	0.	0.	0.	0.	0.	0.	0.	0.	0.
0.	0.	0.	0.	0.	0.	0.	0.	0.	0.
0.	0.	0.	0.	0.	0.	0.	0.	0.	0.
0.	0.	0.	0.	0.	0.	0.	0.	0.	0.
K1 = 5									
0.	0.	0.	0.	0.	0.	0.	0.	0.	0.
0.	0.	0.	0.	0.	0.	0.	0.	0.	0.
0.	0.	0.	0.	0.	0.	0.	0.	0.	0.
0.	0.	0.	0.	0.	0.	0.	0.	0.	0.
0.	0.	0.	0.	0.	0.	0.	0.	0.	0.
0.	0.	0.	0.	0.	0.	0.	0.	0.	0.
0.	0.	0.	0.	0.	0.	0.	0.	0.	0.
0.	0.	0.	0.	0.	0.	0.	0.	0.	0.
0.	0.	0.	0.	0.	0.	0.	0.	0.	0.
0.	0.	0.	0.	0.	0.	0.	0.	0.	0.

FRACTION OF PARTICLE DIAMETERS OVER 5MICRONS = 0.

FRACTION OF PARTICLES WITH VOLUME LESS THAN ZERO = 0.
DISTRIBUTION OF VOLUMES FROM 0 TO 5 CUBIC MICRONS BY INTERVALS OF .01 CUBIC MICRONS

K1 = 1									
0.	0.	0.	0.	0.	0.	0.	0.	0.	0.
0.	0.	0.	0.	0.	0.	0.	0.	0.	0.
0.	0.	0.	0.	0.	0.	0.	0.	0.	0.

0.	0.	0.	0.	0.	0.	0.	0.	0.	0.
0.	0.	0.	0.	0.	0.	0.	0.	0.	0.
0.	0.	0.	0.	0.	0.	0.	0.	0.	0.
0.	0.	0.	0.	0.	0.	0.	0.	0.	0.
0.	0.	0.	0.	0.	0.	0.	0.	0.	0.
0.	0.	0.	0.	0.	0.	0.	0.	0.	0.
0.	0.	0.	0.	0.	0.	0.	0.	.0024691	.0024691

K1 = 2

0.	0.	.0024691	.0024691	.0024691	.0098765	.0049383	.0098765	.0148148	.0024691
.0172840	.0345679	.0716049	.0641975	.0740741	.1259259	.1135802	.1358025	.0913580	.0641975
.0493827	.0444444	.0197531	.0172840	.0148148	.0049383	0.	0.	0.	0.
0.	0.	.0024691	0.	0.	0.	0.	0.	0.	0.
0.	0.	0.	0.	0.	0.	0.	0.	0.	0.
0.	0.	0.	0.	0.	0.	0.	0.	0.	0.
0.	0.	0.	0.	0.	0.	0.	0.	0.	0.
0.	0.	0.	0.	0.	0.	0.	0.	0.	0.
0.	0.	0.	0.	0.	0.	0.	0.	0.	0.
0.	0.	0.	0.	0.	0.	0.	0.	0.	0.
0.	0.	0.	0.	0.	0.	0.	0.	0.	0.

K1 = 3

0.	0.	0.	0.	0.	0.	0.	0.	0.	0.
0.	0.	0.	0.	0.	0.	0.	0.	0.	0.
0.	0.	0.	0.	0.	0.	0.	0.	0.	0.
0.	0.	0.	0.	0.	0.	0.	0.	0.	0.
0.	0.	0.	0.	0.	0.	0.	0.	0.	0.
0.	0.	0.	0.	0.	0.	0.	0.	0.	0.
0.	0.	0.	0.	0.	0.	0.	0.	0.	0.
0.	0.	0.	0.	0.	0.	0.	0.	0.	0.
0.	0.	0.	0.	0.	0.	0.	0.	0.	0.
0.	0.	0.	0.	0.	0.	0.	0.	0.	0.
0.	0.	0.	0.	0.	0.	0.	0.	0.	0.

K1 = 4

0.	0.	0.	0.	0.	0.	0.	0.	0.	0.
0.	0.	0.	0.	0.	0.	0.	0.	0.	0.
0.	0.	0.	0.	0.	0.	0.	0.	0.	0.
0.	0.	0.	0.	0.	0.	0.	0.	0.	0.
0.	0.	0.	0.	0.	0.	0.	0.	0.	0.
0.	0.	0.	0.	0.	0.	0.	0.	0.	0.
0.	0.	0.	0.	0.	0.	0.	0.	0.	0.
0.	0.	0.	0.	0.	0.	0.	0.	0.	0.
0.	0.	0.	0.	0.	0.	0.	0.	0.	0.
0.	0.	0.	0.	0.	0.	0.	0.	0.	0.
0.	0.	0.	0.	0.	0.	0.	0.	0.	0.

K1 = 5

0.	0.	0.	0.	0.	0.	0.	0.	0.	0.
0.	0.	0.	0.	0.	0.	0.	0.	0.	0.
0.	0.	0.	0.	0.	0.	0.	0.	0.	0.
0.	0.	0.	0.	0.	0.	0.	0.	0.	0.
0.	0.	0.	0.	0.	0.	0.	0.	0.	0.
0.	0.	0.	0.	0.	0.	0.	0.	0.	0.
0.	0.	0.	0.	0.	0.	0.	0.	0.	0.
0.	0.	0.	0.	0.	0.	0.	0.	0.	0.
0.	0.	0.	0.	0.	0.	0.	0.	0.	0.
0.	0.	0.	0.	0.	0.	0.	0.	0.	0.
0.	0.	0.	0.	0.	0.	0.	0.	0.	0.

FRACTION OF PARTICLES WITH VOLUME MORE THAN 5 CUBIC MICRONS = 0.

STATISTICAL PARAMETERS OF COMBINED GROUPS
STATISTICAL PARAMETERS OF DISTRIBUTION OF DIAMETERS
NUMBER DIA MEASURED = 585 MEAN DIA = 1.30500 DIA FACTOR = 2.9167E-04
VARIANCE (V)= 2.2278414E-04 STANDARD DEVIATION= 1.4925955E-02
(M3/S**3)= -.765137 (M4/S**4)= 5.652137

STATISTICAL PARAMETERS OF DISTRIBUTION OF VOLUMES
NUMBER DIA MEASURED = 585 MEAN DIA = 1.16413 DIA FACTOR = 9.9961E-01
VARIANCE (V)= 1.5680787E-03 STANDARD DEVIATION= 3.9598974E-02
(M3/S**3)= -.626894 (M4/S**4)= 5.299528

Table XXXXII. Size distribution of latex beads including unusual data

FRACTION OF PARTICLE DIAMETERS LESS THAN ZERO = 0.

DISTRIBUTION OF PARTICLE DIAMETERS FROM 0 TO 5MICRONS BY INTERVALS OF .01MICRONS

K1 = 1									
0.	0.	0.	0.	0.	0.	0.	0.	0.	0.
0.	0.	0.	0.	0.	0.	0.	0.	0.	0.
0.	0.	0.	0.	0.	0.	0.	.0023474	0.	0.
0.	0.	0.	0.	0.	0.	0.	0.	0.	0.
0.	0.	0.	0.	0.	0.	0.	0.	0.	0.
0.	0.	0.	0.	0.	0.	0.	0.	.0023474	0.
.0023474	0.	0.	0.	.0023474	0.	0.	0.	0.	0.
.0023474	.0023474	0.	0.	0.	0.	0.	0.	0.	0.
0.	0.	0.	0.	0.	0.	0.	0.	0.	0.
.0023474	0.	.0023474	0.	.0023474	.0023474	0.	0.	0.	.0023474
K1 = 2									
.0046948	0.	0.	0.	.0023474	0.	0.	0.	0.	0.
.0023474	0.	0.	0.	0.	0.	0.	0.	.0023474	.0023474
.0023474	0.	0.	.0046948	0.	.0070423	.0187793	.0211268	.0798122	.1737089
.3028169	.2159624	.0892019	.0352113	0.	0.	.0023474	0.	0.	0.
0.	0.	0.	0.	0.	.0023474	0.	0.	0.	0.
0.	0.	0.	0.	0.	0.	0.	0.	.0023474	0.
0.	0.	0.	0.	0.	0.	0.	0.	0.	0.
0.	0.	0.	0.	0.	0.	0.	0.	0.	0.
0.	0.	0.	0.	0.	0.	0.	0.	0.	0.
0.	0.	0.	0.	0.	0.	0.	0.	0.	0.
K1 = 3									
0.	.0023474	0.	0.	0.	0.	0.	0.	0.	0.
0.	0.	0.	0.	0.	0.	0.	0.	0.	0.
0.	0.	0.	0.	0.	0.	0.	0.	0.	0.
0.	0.	0.	0.	0.	0.	0.	0.	0.	0.
0.	0.	0.	0.	0.	0.	0.	0.	0.	0.
0.	0.	0.	0.	0.	0.	0.	0.	0.	0.
0.	0.	0.	0.	0.	0.	0.	0.	0.	0.
0.	0.	0.	0.	0.	0.	0.	0.	0.	0.
0.	0.	0.	0.	0.	0.	0.	0.	0.	0.
0.	0.	0.	0.	0.	0.	0.	0.	0.	0.
K1 = 4									
0.	0.	0.	0.	0.	0.	0.	0.	0.	0.
0.	0.	0.	0.	0.	0.	0.	0.	0.	0.
0.	0.	0.	0.	0.	0.	0.	0.	0.	0.
0.	0.	0.	0.	0.	0.	0.	0.	0.	0.
0.	0.	0.	0.	0.	0.	0.	0.	0.	0.
0.	0.	0.	0.	0.	0.	0.	0.	0.	0.
0.	0.	0.	0.	0.	0.	0.	0.	0.	0.
0.	0.	0.	0.	0.	0.	0.	0.	0.	0.
0.	0.	0.	0.	0.	0.	0.	0.	0.	0.
0.	0.	0.	0.	0.	0.	0.	0.	0.	0.
K1 = 5									
0.	0.	0.	0.	0.	0.	0.	0.	0.	0.
0.	0.	0.	0.	0.	0.	0.	0.	0.	0.
0.	0.	0.	0.	0.	0.	0.	0.	0.	0.
0.	0.	0.	0.	0.	0.	0.	0.	0.	0.
0.	0.	0.	0.	0.	0.	0.	0.	0.	0.
0.	0.	0.	0.	0.	0.	0.	0.	0.	0.
0.	0.	0.	0.	0.	0.	0.	0.	0.	0.
0.	0.	0.	0.	0.	0.	0.	0.	0.	0.
0.	0.	0.	0.	0.	0.	0.	0.	0.	0.
0.	0.	0.	0.	0.	0.	0.	0.	0.	0.

FRACTION OF PARTICLE DIAMETERS OVER 5MICRONS = 0.

FRACTION OF PARTICLES WITH VOLUME LESS THAN ZERO = 0.

DISTRIBUTION OF VOLUMES FROM 0 TO 5 CUBIC MICRONS BY INTERVALS OF .01 CUBIC MICRONS

K1 = 1									
0.	.0023474	0.	0.	0.	0.	0.	0.	0.	0.
.0023474	.0023474	0.	.0023474	0.	0.	0.	0.	.0023474	.0023474
0.	0.	0.	0.	0.	0.	0.	0.	0.	0.

0.	0.	0.	0.	0.	0.	0.	0.	.0023474	0.
0.	.0023474	0.	0.	.0023474	0.	.0023474	0.	0.	0.
0.	.0023474	.0023474	.0023474	0.	0.	0.	0.	0.	0.
.0023474	0.	0.	0.	0.	0.	0.	0.	0.	0.
.0023474	0.	0.	0.	0.	0.	0.	0.	0.	0.
0.	0.	0.	0.	0.	0.	.0023474	0.	0.	.0023474
0.	0.	.0023474	0.	0.	0.	0.	0.	.0023474	.0023474

K1 = 2

0.	0.	.0023474	.0023474	.0023474	.0093897	.0046948	.0093897	.0140845	.0023474
.0164319	.0328638	.0680751	.0610329	.0704225	.1197183	.1079812	.1291080	.0868545	.0610329
.0469484	.0422535	.0187793	.0164319	.0140845	.0046948	0.	0.	0.	0.
0.	0.	.0023474	0.	0.	0.	0.	0.	0.	0.
0.	0.	0.	0.	0.	0.	0.	0.	0.	0.
0.	0.	0.	0.	0.	0.	0.	0.	0.	0.
0.	.0023474	0.	0.	0.	0.	0.	0.	0.	0.
0.	0.	0.	0.	0.	0.	0.	0.	0.	0.
0.	0.	0.	0.	0.	0.	0.	0.	0.	0.
0.	0.	0.	0.	0.	0.	0.	0.	0.	0.

K1 = 3

0.	0.	0.	0.	0.	0.	.0023474	0.	0.	0.
0.	0.	0.	0.	0.	0.	0.	0.	0.	0.
0.	0.	0.	0.	0.	0.	0.	0.	0.	0.
0.	0.	0.	0.	0.	0.	0.	0.	0.	0.
0.	0.	0.	0.	0.	0.	0.	0.	0.	0.
0.	0.	0.	0.	0.	0.	0.	0.	0.	0.
0.	0.	0.	0.	0.	0.	0.	0.	0.	0.
0.	0.	0.	0.	0.	0.	0.	0.	0.	0.
0.	0.	0.	0.	0.	0.	0.	0.	0.	0.
0.	0.	0.	0.	0.	0.	0.	0.	0.	0.

K1 = 4

0.	0.	0.	0.	0.	0.	0.	0.	0.	0.
0.	0.	0.	0.	0.	0.	0.	0.	0.	0.
0.	0.	0.	0.	0.	0.	0.	0.	0.	0.
0.	0.	0.	0.	0.	0.	0.	0.	0.	0.
0.	0.	0.	0.	0.	0.	0.	0.	0.	0.
0.	0.	0.	0.	0.	0.	0.	0.	0.	0.
0.	0.	0.	0.	0.	0.	0.	0.	0.	0.
0.	0.	0.	0.	0.	0.	0.	0.	0.	0.
0.	0.	0.	0.	0.	0.	0.	0.	0.	0.
0.	0.	0.	0.	0.	0.	0.	0.	0.	0.

K1 = 5

0.	0.	0.	0.	0.	0.	0.	0.	0.	0.
0.	0.	0.	0.	0.	0.	0.	0.	0.	0.
0.	0.	0.	0.	0.	0.	0.	0.	0.	0.
0.	.0023474	0.	0.	0.	0.	0.	0.	0.	0.
0.	0.	0.	0.	0.	0.	0.	0.	0.	0.
0.	0.	0.	0.	0.	0.	0.	0.	0.	0.
0.	0.	0.	0.	0.	0.	0.	0.	0.	0.
0.	0.	0.	0.	0.	0.	0.	0.	0.	0.
0.	0.	0.	0.	0.	0.	0.	0.	0.	0.
0.	0.	0.	0.	0.	0.	0.	0.	0.	0.

FRACTION OF PARTICLES WITH VOLUME MORE THAN 5 CUBIC MICRONS = 0.

STATISTICAL PARAMETERS OF COMBINED GROUPS
STATISTICAL PARAMETERS OF DISTRIBUTION OF DIAMETERS
NUMBER DIA MEASURED = 614 MEAN DIA = 1.28988 DIA FACTOR = 2.9514E-04
VARIANCE (V)= 1.2604337E-02 STANDARD DEVIATION= 1.1226904E-01
(M3/S**3)= -4.149502 (M4/S**4)= 41.750232

STATISTICAL PARAMETERS OF DISTRIBUTION OF VOLUMES
NUMBER DIA MEASURED = 614 MEAN DIA = 1.14611 DIA FACTOR = 1.0170E+00
VARIANCE (V)= 6.1183063E-02 STANDARD DEVIATION= 2.4735210E-01
(M3/S**3)= 5.459772 (M4/S**4)= 93.641829

APPENDIX V

COMPUTER PROGRAMS BUGSIZE AND NOISE

A. General Remarks

The name BUGSIZE is the name of the computer program used to analyze electronic sizing and counting distributions. A source listing of the program is given in Table XXXXIII. Section B of this appendix outlines the computer program and Sec. C of this appendix lists definitions of the variables and constants used in the program. Program NOISE is listed in Table XXXXIV.

B. Outline of Computer Program Bugsize

DIMENSION Subscripted Variables

READ AND PRINT NSETS

DO THE FOLLOWING CALCULATIONS FOR ALL SETS OF DATA

- Read data for set number = NSET
- Calculate ALIVES and ALIVE
  - (= MS(1) and ME(1); live counting time is stored in the first channel)
- Calculate CORS and CORE
- Shift original standard and experimental distribution
  - back one channel (live time is stored in the first channel prior to the operation)
- Calculate smoothed distributions
  - (S(N,2), E(N,2))
  - from original distribution (MS(N), ME(N))
- Convert original data (MS(N), ME(N)) to floating point
  - (S(N,1), E(N,1))
- Calculate background noise
  - (ANOISE(K,N)) from empirically measured coefficients
- Calculate new distributions (S(N,3) and E(N,3)) by correcting original distribution (S(N,1) and E(N,1)) for flow rate, live counting time, and background noise

Table XXXXIII. Program BUGSIZE

```
      PROGRAM BUGSIZE(INPUT,OUTPUT,TAPE 3=OUTPUT)
C
CCHIPPEWA FORTRAN PROGRAM BUGSIZE
C
CDESIGNED FOR USE IN THE ANALYSIS AND INTERPRETATION OF DATA OBTAINED IN
C
CTHE ELECTRONIC SIZING AND COUNTING OF SUSPENSIONS OF MICROSCOPIC
C
CPARTICLES
C
CPROGRAMMED BY VICTOR H. EDWARDS
C
      ODIMENSION MS(128),ME(128),E(128,3),S(128,3),ANOISE(2,128),
      1STD(10),EXPT(10),X(2,4),AID(20),AM(2,4),TC(2),TPV(2),YMAX(4),
      2YP(128),XP(128),AD(2,4)
    5 FORMAT(25H NUMBER OF SETS OF DATA =,I6)
      READ 5,NSETS
      PRINT 5,NSETS
      DO 9999 NSET=1,NSETS
      READ 3,(AID(I),I=1,20)
      READ 1,DIA
      READ 1,FLOWS,FLOWE
    1 FORMAT(6F10.5)
    3 FORMAT(10A7)
      READ 3,(STD(I),I=1,10)
    4 FORMAT(8(I6,2X))
      READ 4,(MS(N),N=1,128)
      READ 1,(X(1,I),I=1,4)
      READ 2,NMINOS,NMAXS,NMINS,NM
    2 FORMAT(6I10)
      READ 3,(EXPT(I),I=1,10)
      READ 4,(ME(N),N=1,128)
      READ 1,(X(2,I),I=1,4)
      READ 2,NMINOE,NMAXE
C
C        FLOWS IS THE FLOWRATE IN ML/MIN DURING THE STANDARD RUN AND
C
C        FLOWE IS THE FLOWRATE IN ML/MIN DURING THE EXPERIMENTAL RUN
C
C        MS(N) IS THE DISTRIBUTION OBTAINED WITH THE STANDARD AND ME(N)
C
C        IS THE DISTRIBUTION OBTAINED WITH THE UNKNOWN
C
      ALIVES=MS(1)
      ALIVEE=ME(1)
      CCRS=10000./(FLOWS*ALIVES)
      CCRE=10000./(FLOWE*ALIVEE)
      DO 45 N=1,127
      MS(N)=MS(N+1)
      ME(N)=ME(N+1)
   45 CONTINUE
      DO 55 N=2,126
      S(N,2)=FLOAT(MS(N-1)+MS(N+1)+2*MS(N))/4.
      E(N,2)=FLOAT(ME(N-1)+ME(N+1)+2*ME(N))/4.
   55 CONTINUE
      S(1,2)=FLOAT(MS(2)+2*MS(1))/3.
```

```
      S(127,2)=FLOAT(MS(126)+2*MS(127))/3.
      E(1,2)=FLOAT(ME(2)+2*ME(1))/3.
      E(127,2)=FLOAT(ME(126)+2*ME(127))/3.
      DO 85 N=1,127
      S(N,1)=MS(N)
      E(N,1)=ME(N)
   85 CONTINUE
      DO 145 K=1,2
      DO 140 N=1,127
      T=N+1
      ANOISE(K,N)=X(K,1)*EXP(X(K,2)*T)+X(K,3)*EXP(X(K,4)*T)
  140 CONTINUE
  145 CONTINUE
      DO 165 N=1,127
      S(N,3)=S(N,1)*CORS-ANOISE(1,N)
      E(N,3)=E(N,1)*CORE-ANOISE(2,N)
      S(N,3)=AMAX1(S(N,3),0.)
      E(N,3)=AMAX1(E(N,3),0.)
  165 CONTINUE
C
C         THIS SECTION COMPUTES THE MEAN PARTICLE DIAMETER BY DETERMINING
C
C   THE SCALE FACTOR FROM THE STANDARD AND FROM THE DATA CORRECTED
C
C   FOR BACKGROUND NOISE AND COUNTING VOLUME
C
      DO 210 L=1,2
      TC(L)=0.
      TPV(L)=0.
      DO 210 M=1,4
      AD(L,M)=0.
      AM(L,M)=0.
  210 CONTINUE
      IF(NMAXS.GT.0) GO TO 214
      SMAX=0.
      EMAX=0.
      DO 200 N=8,127
      SMAX=AMAX1(SMAX,S(N,2))
      EMAX=AMAX1(EMAX,E(N,2))
      IF(S(N,2).EQ.SMAX)NMAXS=N
      IF(E(N,2).EQ.EMAX)NMAXE=N
  200 CONTINUE
      SMIN=S(NMAXS,2)
      NM=FLOAT(NMAXS)*1.9
      DO 205 N=NMAXS,NM
      SMIN=AMIN1(SMIN,S(N,2))
      IF(SMIN.EQ.S(N,2))NMINS=N
  205 CONTINUE
      SMINO=100000.
      EMINO=100000.
      DO 211 N=1,NMAXS
      SMINO=AMIN1(SMINO,S(N,3))
      IF(SMINO.EQ.S(N,3)) NMINOS=N
  211 CONTINUE
      DO 212 N=1,NMAXE
      EMINO=AMIN1(EMINO,E(N,3))
      IF(EMINO.EQ.E(N,3)) NMINOE=N
```

```
  212 CONTINUE
  214 CONTINUE
C
C         L=1 FOR STANDARD AND L=2 FOR UNKNOWN. M=1 FOR MEAN,=Z FOR VAR.
C
C    =3 FOR THIRD MOMENT, AND =4 FOR FOURTH MOMENT. TC(L)=TOTAL COUNT
C
      NMINOS=MAX0(1,MIN0(NMINOS,127))
      NMINOE=MAX0(1,MIN0(NMINOE,127))
      NMAXS=MAX0(3,MIN0(NMAXS,127))
      NMINS=MAX0(4,MIN0(NMINS,127))
      NMAXE=MAX0(3,MIN0(NMAXE,127))
      NT=0
      DO 215 N=NMINOS,NMINS
      TC(1)=TC(1)+S(N,3)
      NT=NT+1
      AD(1,1)=AD(1,1)+S(N,3)*(FLOAT(N))**(0.33333333)
      AM(1,1)=AM(1,1)+S(N,3)*FLOAT(N)
  215 CONTINUE
      AD(1,1)=AD(1,1)/TC(1)
      AM(1,1)=AM(1,1)/TC(1)
      AVOLS=0.1666666*3.14159*DIA**3
      PRINT 4,NMAXS,NMAXE,NMINS,NM
      PRINT 7,DIA,AVOLS,AM(1,1),TC(1),TPV(1),ALIVES,CORS
      PRINT 213,NMINOS,NMINOE
  213 FORMAT(9H NMINOS =I4,9H NMINOE =,I4)
      PRINT 7,(X(1,I),I=1,4)
      PRINT 7,(X(2,I),I=1,4)
      IF(AD(1,1).LE.0.) FACTS=1.
      IF(AD(1,1).GT.0.)FACTS=0.1666667*3.14159*(DIA/AD(1,1))**3
C
C         FACTS IS THE CORRECTION FACTOR REQUIRED TO CONVERT CHANNEL NO.
C
C  TO VOLUME IN CUBIC MICRONS. AVOLS IS THE MEAN VOLUME OF THE STANDARD
C
C  SINGLETS. TPV(L) IS THE PERCENT BY VOLUME PARTICLES
C
      FACTSD=DIA/AD(1,1)
      DO 220 N=NMINOS,NMINS
      DO 220 M=2,4
      DELD=FACTSD*((FLOAT(N))**(.33333333)-AD(1,1))
      DEL=FACTS*(FLOAT(N)-AM(1,1))
      AM(1,M)=AM(1,M)+S(N,3)*DEL**M
      AD(1,M)=AD(1,M)+S(N,3)*DELD**M
  220 CONTINUE
      AD(1,1)=DIA
      AM(1,1)=AM(1,1)*FACTS
      TPV(1)=(1.0E-10)*AM(1,1)*TC(1)
      DO 225 M=2,4
      AD(1,M)=AD(1,M)/TC(1)
      AM(1,M)=AM(1,M)/TC(1)
  225 CONTINUE
      SSD=SQRT(AD(1,2))
      ASKEWSD=AD(1,3)/(2.*AD(1,2)*SSD)
      AKURTSD=0.5*(AD(1,4)/(AD(1,2)**2)-3.)
      SS=SQRT(AM(1,2))
      ASKEWS=AM(1,3)/(2.*AM(1,2)*SS)
```

```
      AKURTS=.5*(AM(1,4)/(AM(1,2)**2)-3.)
      DO 230 N=NMINOE,127
      AM(2,1)=AM(2,1)+E(N,3)*FLOAT(N)
      AD(2,1)=AD(2,1)+E(N,3)*(FLOAT(N)**(.333333))
      TC(2)=TC(2)+E(N,3)
  230 CONTINUE
      AM(2,1)=AM(2,1)/TC(2)
      AD(2,1)=AD(2,1)/TC(2)
      DO 235 N=NMINOE,127
      DO 235 M=2,4
      DEL=FACTS*(FLOAT(N)-AM(2,1))
      DELD=FACTSD*((FLOAT(N))**(.333333)-AD(2,1))
      AD(2,M)=AD(2,M)+E(N,3)*DELD**M
      AM(2,M)=AM(2,M)+E(N,3)*DEL**M
  235 CONTINUE
      AD(2,1)=AD(2,1)*FACTSD
      AM(2,1)=AM(2,1)*FACTS
      DO 240 M=2,4
      AD(2,M)=AD(2,M)/TC(2)
      AM(2,M)=AM(2,M)/TC(2)
  240 CONTINUE
      TPV(2)=(1.0E-10)*AM(2,1)*TC(2)
      SE=SQRT(AM(2,2))
      SED=SQRT(AD(2,2))
      ASKEWE=AM(2,3)/(2.*SE*AM(2,2))
      AKURTE=.5*(AM(2,4)/(AM(2,2)**2)-3.)
      ASKEWED=AD(2,3)/(2.*SED*AD(2,2))
      AKURTED=.5*(AD(2,4)/(AD(2,2)**2)-3.)
   12 FORMAT(31H TOTAL PARTICLE CONCENTRATION =,E14.7,4H /ML,2X,30H PERC
     1ENT BY VOLUME PARTICLES =,E14.7)
  130FORMAT(23H MEAN PARTICLE VOLUME =,E14.7,14H CUBIC MICRONS,2X,14H V
     1OL. FACTOR =,E14.7)
  140FORMAT(21H VARIANCE OF VOLUME =,E14.7,2X,21H STANDARD DEVIATION =,
     1E14.7,14H CUBIC MICRONS)
   15 FORMAT(20H MOMENTAL SKEWNESS =,E14.7,2X,11H KURTOSIS =E14.7)
  200FORMAT(25H MEAN PARTICLE DIAMETER =,E14.7,8H MICRONS,2X,18H DIAMET
     1ER FACTOR =,E14.7)
  210FORMAT(23H VARIANCE OF DIAMETER =,E14.7,2X,21H STANDARD DEVIATION
     1=,E14.7,8H MICRONS)
      PRINT 11
   11 FORMAT(1H1)
      PRINT 16,NSET
   16 FORMAT(17H THIS IS DATA SET,I6)
      PRINT 3,(AID(I),I=1,20)
      PRINT 8
    8 FORMAT(//)
      PRINT 3,(STD(I),I=1,10)
   10 FORMAT(7H FLOW =,F12.6,7H ML/MIN,2X,14H COR. FACTOR =,E16.6,/)
      PRINT 10,FLOWS,CORS
      PRINT 19,ALIVES
   19 FORMAT(21H LIVE COUNTING TIME =,F10.4,15H /10000 MINUTES)
      PRINT 9
    9 FORMAT(/)
      PRINT 17
   17 FORMAT(44H OBSERVED PULSE-HEIGHT ANALYSIS DISTRIBUTION,/)
      PRINT 6,(MS(N),N=1,127)
    6 FORMAT(10(3X,I7)
```

```
      PRINT 9
      PRINT 12,TC(1),TPV(1)
      PRINT 13,AM(1,1),FACTS
      PRINT 14,AM(1,2),SS
      PRINT 15,ASKEWS,AKURTS
      PRINT 20,AD(1,1),FACTSD
      PRINT 21,AD(1,2),SSD
      PRINT 15,ASKEWSD,AKURTSD
      PRINT 18
   18 FORMAT(/,51H DISTRIBUTION AFTER CORRECTION FOR NOISE AND VOLUME,/)
      PRINT 7,(S(N,3),N=1,127)
    7 FORMAT(5(3X,E13.5))
      PRINT 8
      PRINT 3,(EXPT(I),I=1,10)
      PRINT 10,FLOWE,CORE
      PRINT 19,ALIVEE
      PRINT 9
      PRINT 17
      PRINT 6,(ME(N),N=1,127)
      PRINT 9
      PRINT 12,TC(2),TPV(2)
      PRINT 13,AM(2,1),FACTS
      PRINT 14,AM(2,2),SE
      PRINT 15,ASKEWE,AKURTE
      PRINT 20,AD(2,1),FACTSD
      PRINT 21,AD(2,2),SED
      PRINT 15,ASKEWED,AKURTED
      PRINT 18
      PRINT 7,(E(N,3),N=1,127)
      PRINT 8
C
C       THIS SECTION COMPUTES PLOTTING PARAMETERS AND PLOTS DISTRIBUTIONS
C
C    BOTH BEFORE AND AFTER REMOVAL OF NOISE AND CORRECTION TO /ML VALUES
C
      DO 245 L=1,4
      YMAX(L)=0.
  245 CONTINUE
      DO 250 N=1,127
      YMAX(1)=AMAX1(YMAX(1),S(N,1))
      YMAX(2)=AMAX1(YMAX(2),S(N,3))
      YMAX(3)=AMAX1(YMAX(3),E(N,1))
      YMAX(4)=AMAX1(YMAX(4),E(N,3))
  250 CONTINUE
      YY=1.5*S(NMAXS,1)
      IF(YMAX(1).GT.YY) YMAX(1)=YY
      YY=1.5*S(NMAXS,3)
      IF(YMAX(2).GT.YY) YMAX(2)=YY
      YY=1.5*E(NMAXE,1)
      IF(YMAX(3).GT.YY) YMAX(3)=YY
      YY=1.5*E(NMAXE,3)
      IF(YMAX(4).GT.YY) YMAX(4)=YY
      YMIN=0.
      XMIN=0.
      XMAX=127.
      NUM=127.
      DO 260 L=1,2
```

```
      IF(L.EQ.1)K=1
      IF(L.EQ.2)K=3
      DO 255 N=1,127
      XP(N)=FLOAT(N)
      YP(N)=S(N,K)
      IF(YP(N).GT.YMAX(L)) YP(N)=YMAX(L)
  255 CONTINUE
      YM=YMAX(L)
      CALL PPLT(XP,YP,XMIN,XMAX,YMIN,YM,NUM)
  260 CONTINUE
      DO 270 L=3,4
      IF(L.EQ.3)K=1
      IF(L.EQ.4)K=3
      DO 265 N=1,127
      XP(N)=FLOAT(N)
      YP(N)=E(N,K)
      IF(YP(N).GT.YMAX(L)) YP(N)=YMAX(L)
  265 CONTINUE
      YM=YMAX(L)
      CALL PPLT(XP,YP,XMIN,XMAX,YMIN,YM,NUM)
  270 CONTINUE
C
C        THIS SECTION IS USED TO SUMMARIZE THE DATA
C
C   3 F ALL DISTRIBUTIONS ANALYSED IN THE FORM OF A TABLE
C
      DIMENSION Z(14,80)
      Z(1,NSET)=TC(1)
      Z(8,NSET)=TC(2)
      Z(2,NSET)=TPV(1)
      Z(9,NSET)=TPV(2)
      Z(3,NSET)=AM(1,1)
      Z(10,NSET)=AM(2,1)
      Z(4,NSET)=FACTS
      Z(11,NSET)=FACTS
      Z(5,NSET)=SS
      Z(12,NSET)=SE
      Z(6,NSET)=ASKEWS
      Z(13,NSET)=ASKEWE
      Z(7,NSET)=AKURTS
      Z(14,NSET)=AKURTE
      IF(NSET.LT.NSETS) GO TO 9999
      PRINT 30,(AID(I),I=1,10)
   30 FORMAT(1H1,10A7,/)
      PRINT 31
   31 FORMAT(9X,48H SUMMARY OF CALCULATED RESULTS,ALL DISTRIBUTIONS,//)
      PRINT 32
   32 FORMAT(8X,13H PARTICLES/ML,3X,15H VOLUME PERCENT,2X,16H AVE.VOL.(M
     1U**3),2X,14H VOLUME FACTOR,2X,16H STD.DEV.(MU**3),4X,9H SKEWNESS,9
     2X,9H KURTOSIS,/)
      DO 37 N=1,NSETS
      PRINT 33,N
   33 FORMAT(7H NSET =,I4)
      PRINT 34,(Z(I,N),I=1,7)
   34 FORMAT(6H BEADS,7(2X,E15.7))
      PRINT 35,(Z(I,N),I=8,14)
   35 FORMAT(6H CELLS,7(2X,E15.7))
```

```
   37 CCNTINUE
 9999 CCNTINUE
      STOP
      END
```

```
      SUBROUTINE PPLT (X, Y, XMIN, XMAX, YMIN, YMAX, NUM)

      THIS SUBROUTINE, GIVEN A SET OF N X-Y COORDINATES, WILL PLOT THEM
      ON A 51-101 X-Y GRID, THUS MAKING APPARENT THE CHARACTERISTICS OF
      THE EQUATION FROM WHICH THEY WERE OBTAINED OR REPRESENT

      DIMENSION X(1), Y(1), XGRID(11), YGRID(11), GRID(101)
      DATA BLNK,XXXXX/1H ,1HX/
      T1= (XMAX-XMIN)/10.
      T2 = (YMAX - YMIN) / 10.
      XGRID(1) = XMIN
      YGRID(1) = YMAX
      DO 25 I = 2, 11
      XGRID(I) = XGRID(I - 1) + T1
   25 YGRID(I) = YGRID(I - 1) - T2
      WRITE (3, 35)
   35 FORMAT (1H1)
      DO 40 I = 1, 3
   40 WRITE (3, 45)
   45 FORMAT (20X, 1H*, 10(9X, 1H*))
      L = 1
      M = 1
      DO 65 K = 1, 10
      DO 50 I = 1, 101
   50 GRID(I) = BLNK
      A = FLOAT(M)
      Q = (YMAX * (51. - A) + YMIN * (A - 1.))/ 50.
      DO 53 IL = 1, NUM
      IF (ABS(Q - Y(IL)) - (YMAX - YMIN) / 100.) 41, 53, 53
   41 IXP = 100. * (X(IL) - XMIN) / (XMAX - XMIN) + 1.5
      GRID(IXP) = XXXXX
   53 CONTINUE
      WRITE (3,75) YGRID(L),(GRID(I), I = 1, 101)
      N = M + 1
      M = N + 3
      DO 60 J = N, M
      DO 55 I = 1, 101
   55 GRID(I) = BLNK
      A = FLOAT(J)
      Q = (YMAX * (51. - A) + YMIN * (A - 1.))/ 50.
      IL = 0
  700 IL = IL + 1
      IF (ABS(Q - Y(IL)) - (YMAX - YMIN) / 100.) 46, 57, 57
   46 IXP = 100. * (X(IL) - XMIN) / (XMAX - XMIN) + 1.5
      GRID(IXP) = XXXXX
   57 IF(IL .LT. NUM) GO TO 700
   60 WRITE (3,76)(GRID(I), I = 1, 101)
      M = M + 1
   65 L = L + 1
      DO 66 I = 1, 101
   66 GRID(I) = BLNK
      DO 72 IL = 1, NUM
      IF (ABS(YMIN - Y(IL)) - (YMAX - YMIN) / 100.) 69, 72, 72
   69 IXP = 100. * (X(IL) - XMIN) / (XMAX - XMIN) + 1.5
      GRID(IXP) = XXXXX
```

```
72 CONTINUE
   WRITE (3,75) YGRID(11),(GRID(I), I = 1, 101)
75 FORMAT (10X, 1PE9.2, 1X, 101A1)
76 FORMAT (20X, 101A1)
   DO 80 I = 1, 3
80 WRITE (3, 45)
   WRITE (3,85) (XGRID(I), I = 1, 11)
85 FORMAT (16X, 11(1PE9.2, 1X))
   RETURN
   END
```

Table XXXXIV. Program NOISE

```
      PROGRAM NOISE(INPUT,OUTPUT)
      DIMENSION N(128),AN(128),CC(4),B(128,4),W(128),AID(20)
      DIMENSION AC(128),C(128)
    1 FORMAT(8(I6,2X))
    2 FORMAT(5E16.6)
    3 FORMAT(6F10.4)
    4 FORMAT(6I10)
    5 FORMAT(5(3X,E13.5))
    6 FORMAT(10A7)
    7 FORMAT(1H1,10A7,/,10A7,/)
   80FORMAT(14H IST CHANNEL =,I4,2X,7H FLOW =,F12.6,8H ML/MIN, 2X,14H C
     1OR. FACTOR =,E16.6,/)
    9 FORMAT(53H TABLE OF COUNTS/ML, BY PULSE-HEIGHT ANALYZER CHANNEL,/)
      M=0
      READ 4,MAX
  100 READ 6,(AID(I),I=1,20)
      READ 1,(N(I),I=1,128)
      READ 3,AN1,A1,AN2,A2
      READ 3,FLOW
      READ 4,NINNY
      AN1I=AN1
      AN2I=AN2
      A1I=A1
      A2I=A2
      COR=10000./(FLOW*FLOAT(N(1)))
C
C        THE LOOP DO 30 CONVERTS OBSERVED COUNTS TO COUNTS PER ML BASIS
C   BY DIVIDING BY FLOW THROUGH APERTURE AND LIVE COUNTING TIME
C
      DO 30 I=1,128
      IF(I.LT.NINNY) AN(I)=0.
      IF(I.GE.NINNY) AN(I)=COR*FLOAT(N(I))
      IF(I.GE.NINNY.AND.AN(I).GT.0.) W(I)=1./AN(I)
      IF(AN(I).LE.0.) W(I)=1.
      IF(I.LT.NINNY) W(I)=0.
   30 CONTINUE
      PRINT 7,(AID(J),J=1,20)
      PRINT 8,NINNY,FLOW,COR
      PRINT 9
      PRINT 5,(AN(I),I=1,128)
      PRINT 11,AN1,AN2,A1,A2
      DO 21 I=1,128
      CHNO=I
   20 FORMAT(3E10.3)
   21 CONTINUE
C
C        THE LOOP DO 31 CALCULATES NOISE VALUES IN EACH CHANNEL
C   FROM THE LATEST ESTIMATES OF THE COEFFICIENTS IN THE NOISE EQUATION
C   IT ALSO CALCULATES VALUES FOR AN OVER-DETERMINED SET OF EQUATIONS
C   OF THE FORM B*CC=C, WHERE CC ARE THE COEFFICIENT CORRECTIONS
C
      K=0
   33 DO 31 I=NINNY,128
      F1=A1*FLOAT(I)
      F2=A2*FLOAT(I)
      AC(I)=AN1*EXP(F1)+AN2*EXP(F2)
```

```
      RW=SQRT(W(I))
      L=I+1-NINNY
      C(L)=RW*(AN(I)-AC(I))
      B(L,1)=EXP(F1)*RW
      B(L,2)=EXP(F2)*RW
      B(L,3)= FLOAT(I)*AN1*B(L,1)
      B(L,4)= FLOAT(I)*AN2*B(L,2)
   31 CONTINUE
      NINN=128-NINNY+1
      CALL LSQS(B,CC,C,NINN,4,1,KERR,9)
      IF(KERR.EQ.0) GO TO 32
      PRINT 15
   15 FORMAT(//,20X,36H THE SYSTEM WAS FOUND TO BE SINGULAR)
      DO 40 I=1,NINN
      PRINT 5,(B(I,L),L=1,4),C(I)
   40 CONTINUE
      GO TO 999
   32 PRINT 10, (CC(L),L=1,4)
  100FORMAT(11H DELTA N1 =,E12.5,2X,11H DELTA N2 =,E12.5,2X,/,11H DELTA
     1 A1 =,E12.5,2X,11H DELTA A2 =,E12.5)
     0CHECK=ABS(CC(1)/AN1I)+ABS(CC(2)/AN2I)+ABS(CC(3)/A1I)+ABS(CC(4)/A2I
     1)
      AN1=AN1+CC(1)
      AN2=AN2+CC(2)
      A1=A1+CC(3)
      A2=A2+CC(4)
      K=K+1
      PRINT 11,AN1,AN2,A1,A2
  110FORMAT(5H N1 =,E16.6,3X,5H N2 =,E16.6,3X,5H A1 =,E16.6,3X,5H A2 =,
     1E16.6)
      ERR=0.
      IF(CHECK.GE.5.) GO TO 999
      IF(K.GT.100) GO TO 999
      IF(CHECK .GE. .001) GO TO 33
      CHI=0.
      NDATA=0
      DO 34 I=1,128
      F1=A1*FLOAT(I)
      F2=A2*FLOAT(I)
      AC(I)=AN1*EXP(F1)+AN2*EXP(F2)
      IF(I.LT.NINNY) GO TO 34
      UC=(AC(I)-AN(I))**2
      ERR=ERR+UC
      CHI=CHI+UC*W(I)
      NDATA=NDATA+1
   34 CONTINUE
      IFREE = NDATA-4
      PRINT 13,ERR,CHI,IFREE
  130FORMAT(1H1,23H ERROR SUM OF SQUARES =,E16.6,3X,14H CHI-SQUARED =,
     1E16.6,3X,6H WITH ,I4,2X,19H DEGREES OF FREEDOM,/)
      PRINT 14
   14 FORMAT(44H TABLE OF CALCULATED BACKGROUND NOISE VALUES)
      PRINT 5,(AC(I),I=1,128)
  999 M=M+1
      IF(M.LT.MAX) GO TO 100
      STOP
      END
```

Change negative values of S(N,3) and E(N,3) to zero values

Set initial values of certain variables (TC(L), TPV(L), AD(L,M), AM(L,M) to zero

If not already read in as data, calculate NMAXS, NMAXE, NM, NMINS, NMINOS, and NMINOE

Make values of NMAXS, etc. just calculated fall within realistic limits

Calculate average diameter AD(1,1), average volume AM(1,1), and total concentration of singlets and print out along with NMAXS, etc. and values of coefficients of noise equation

Calculate factor (FACTS) required to convert average volumes from units of channel number to units of cubic microns and similarly calculate FACTSD for correction diameter distribution

Calculate higher moments of standard distribution, in terms of microns or cubic microns. From these calculate SSD, ASKEWSD, etc.

Calculate average diameter AD(2,1), average volume AM(2,1) and total count TC(2) for experimental distribution

Calculate higher moments of experimental distribution. Then calculate SE, SED, ASKEWE, etc.

Print out calculated results first for standard distribution and then for experimental distribution

Determine parameters needed for plotting subroutine, e.g., YMAX(I), XP(N), YP(N)

Plot results of original standard distribution, corrected standard distribution, original experimental distribution, and corrected experimental distribution

Calculate storage parameters Z(J, NSET) for use in summarizing results

If this is not the last data set, i.e., if NSET < NSETS, go on to next set. Otherwise print out table summarizing results

STOP and END

DEFINITION OF VARIABLES IN PROGRAM BUGSIZE

MS(N)	= Value of standard distribution in Nth channel
ME(N)	= Value of experimental distribution in Nth channel
S(N,1)	= MS(N - 1)
E(N,1)	= ME(N - 1)
S(N,2)	= Smoothed value of S(N,1)
E(N,2)	= Smoothed value of Nth value of E(N,1) distribution
S(N,3)	= Value of S(N,1) corrected to per ml values and for noise
E(N,3)	= Value of E(N,1) corrected to per ml value and for noise
ANOISE(1,N)	= Nth value of background noise for standard distribution
ANOISE(2,N)	= Nth value of noise for experimental distribution
STD(I)	= Label for standard distribution
EXPT(I)	= Label for experimental distribution
X(2,I)	= Ith coefficient of experimental background noise equation
AID(I)	= Label for group NSET
AM(L,1)	= Mean volume for standard (L = 1) and experiment (L = 2) distributions
AM(L,M)	= Mth moment about the mean volume (M = 2,3,4) for standard (L = 1) and experimental (L = 2) distributions
TC(L)	= Total concentration of standard singlets (L = 1) and entire experimental distribution (L = 2)
TPV(L)	= Total percent by volume of standard singlets (L = 1) and entire experimental distribution (L = 2)
YMAX(L)	= Maximum value of Lth distribution (L = 1, original standard; L = 2, standard corrected; L = 3, original experimental; L = 4, corrected experimental)
YP(N)	= Nth value of distribution to be plotted
XP(N)	= Abscissa of Nth value of distribution
AD(L,1)	= Mean diameter for standard (L = 1) and experimental (L = 2) distributions
AD(L,M)	= Mth moment about mean diameter (M = 2,3,4) for standard (L = 1) and experimental (L = 2) distributions
NSETS	= Number of data sets

NSET	= Index of data set being analyzed
DIA	= Mean diameter of standard particles
FLOWS	= Flowrate through aperture during measurement of standard distribution, ml/min
FLOWE	= Flowrate through aperture during measurement of experimental distribution, ml/min
NMINOS	= Channel number of lower limit of singlet peak of standard
NMAXS	= Channel number mode of singlet peak of standard
NMINS	= Channel number of upper limit of singlet peak of standard distribution
NMINOE	= Channel number of lower limit of experimental distribution
NMAXE	= Channel number of mode of experimental distribution
ALIVES	= Live counting time spent in accumulation of standard distribution
ALIVEE	= Live counting time spent in accumulation of experimental distribution
CORS	= Factor to correct counts per channel for flowrate and counting time, standard distribution
CORE	= Factor to correct counts per channel for flowrate and counting time, experimental distribution
SMAX,EMAX, SMIN,EMIN, SMINO,EMINO	= Dummy variables for use in determination of NMAXS, NMAXE, etc.
DEL,DELD	= Dummy variables used in calculating higher moments
SSD	= Standard deviation of diameters of standard
SS	= Standard deviation of volumes of standard distribution
SED	= Standard deviation of diameters of experimental distribution
SE	= Standard deviation of volumes of experimental distribution
ASKEWSD, ASKEWS, ASKEWED, ASKEWE	= Momental skewness of standard diameter distribution, standard volume distribution, experimental diameter distribution and experimental volume distribution, respectively.

$$= \frac{1}{2} \frac{\text{third moment about mean}}{(\text{standard deviation})^3}$$

AKURTSD,AKURTS, AKURTED,AKURTE = Kurtosis

$$= \frac{1}{2} \left(\frac{\text{fourth moment}}{(\text{variance})^2} - 3 \right)$$

YY = Dummy variable used to calculate scale on computer plots of distributions

A(K,NSET) = Dummy variables set up to store various calculated variables of all NSETS groups for printout in a summary of results

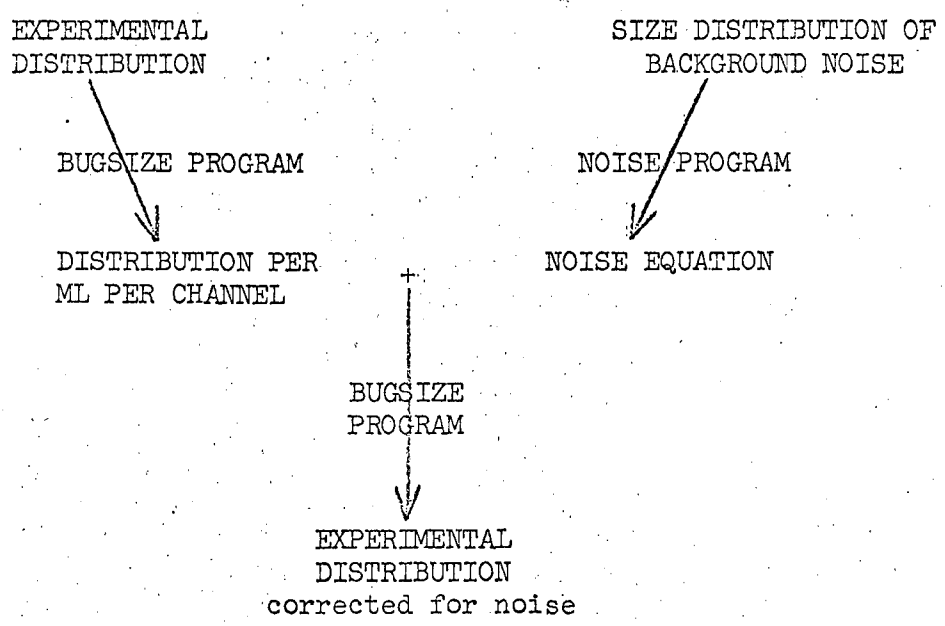
EXPERIMENTAL DISTRIBUTION
SIZE DISTRIBUTION OF BACKGROUND NOISE
BUGSIZE PROGRAM
NOISE PROGRAM
DISTRIBUTION PER ML PER CHANNEL
NOISE EQUATION
+
BUGSIZE PROGRAM
EXPERIMENTAL DISTRIBUTION corrected for noise

GENERAL SUMMARY

For engineers to design processes for the production of bacteria and their products, they need models that relate the rate of production to the important variables of the system. Modeling is difficult because there are many potentially important variables in a culture, and it is necessary to select a few critical variables to make the model mathematically tractable.

To assist in the development of a conceptual view of a bacterial cell culture, various schemes for the classification of pure culture fermentation processes are presented. The development of the modeling of bacterial kinetics is outlined with a literature survey of mathematical models of bacterial kinetics.

A generalized version of the logistic equation is proposed for use in the measurement of rates of growth and metabolism in batch culture, and a computer program to fit the equation to the data is presented. The program is shown to successfully fit both synthetic and real batch kinetic data, including correct prediction of the derivatives of the fitted dependent variables.

To obtain kinetic information for the design of processes using sulfate-reducing bacteria to remove sulfate from sodium chloride solutions, rate studies were made on a strain of sulfate-reducing bacteria able to tolerate high concentrations of sodium chloride. Effects of all components of the growth media on batch culture growth were studied to determine optimal concentrations of each component. A computer was used to fit equations of the type just discussed to the batch data, thus permitting more accurate determination of the metabolic rates.

Mixing, reduced sulfide concentrations, and pH control were shown to increase rates of growth and sulfide production. A continuous culture system was built and used to measure the growth kinetics in continuous culture. Anomalous specific growth rates observed during washout of the continuous reactor system could be explained by postulating wall growth by bacteria. Most batch and all continuous culture data could be correlated by the logistic equation.

Batch culture and continuous culture data were correlated by plotting specific rate of sulfide production versus specific growth rate, but the straight line predicted by the Luedeking-Piret model gave only rough correlation. The data indicates a division into three distinct regions: (1) A region at low specific growth rates involving unusually large mean cell size due to accumulation of cell reserve material; (2) A region at intermediate specific growth rates of constant rate of specific sulfide formation per cell dry weight; (3) A region of very high specific sulfide production rates at high specific growth rates, presumably due to uncoupling of energy production (sulfide production) and biosynthesis (specific growth rate).

It was not possible to obtain a completely satisfactory and general correlation of specific growth rates and specific sulfide production rates with the system variables. However, the Luedeking-Piret type of linear correlation seems satisfactory over a sufficient range to be useful for preliminary scale-up of systems using these organisms for sulfate reduction.

Electronic sizing and counting of bacteria is particularly important to the study of bacterial growth kinetics. It was shown here that it also offers a means of studying sterilization kinetics.

An electronic sizing and counting system extending the Coulter counting technique was built and calibrated using polystyrene beads as standards. An electron microscope study of the beads had established the bead size distribution. Linearity of the system in response to particle size was demonstrated. The size distribution of beads measured electronically was considerably broader than the distribution obtained by electron microscopy.

Electronic counting was compared with the conventional bacteriological techniques of optical counting, measurement of turbidity, and colony counting. Good agreement was found with colony counts and turbidity. Reduction of electronic counts by heat killing occurred with exponential phase cultures.

Several system variables were shown to affect the electronic size of cells. A model for the electrical conductivity of the bacterial cell is proposed and compared with empirical results obtained with the counting system.

ACKNOWLEDGEMENTS

Contributions to this work have come from many persons and it is unfortunately possible to name only a few. The authors gratefully acknowledge the assistance of Mr. Ronald Charron for his many contributions to the design and construction of the continuous reactor system and Professor Alvin J. Clark and other members of the Bacteriology Department who have provided many helpful suggestions. We would also like to thank Mrs. Trudy Noller Murphy and Mr. Duane Moser for their help in various phases of the experimental work and Mr. Lloyd Spielman and Professor Simon Goren for stimulating discussions on the art of electronic sizing and counting of small particles.

This work was performed under the auspices of the U. S. Atomic Energy Commission.

REFERENCES

1. W. H. Coulter, U. S. Patent No. 2,656,508 (1953).
2. Herbert E. Kubitschek, "Electronic Counting and Sizing of Bacteria", Nature 182, 234 (1958).
3. E. C. Gregg and K. David Steidley, "Electrical Counting and Sizing of Mammalian Cells in Suspension, "Biophys. J. 5, 393 (1965).
4. R. B. Adams, W. H. Voelker, and E. C. Gregg, "Electrical Counting and Sizing of Mammalian Cells in Suspension: Part II. Electronic Circuitry and Experimental Evaluation" (in press).
5. Mattern, Brackett, and Olson, "Determination of Number and Size of Particles by Electronic Gating", J. Appl. Physiol. 10, 1 (1957).
6. R. J. Harvey and Allen G. Marr, "Measurement of Size Distributions of Bacterial Cells", J. Bacteriol. 92, 805 (1966).
7. M. Wales and J. N. Wilson, "Theory of Coincidence in Coulter Particle Counters", Rev. Sci. Instr. 32, 1132 (1961).
8. L. H. Princen and W. F. Kwolek, "Coincidence Corrections for Particle Size Determination with the Coulter Counter", Rev. Sci. Instr. 36, 646 (1965).
9. M. J. Fulwyler, "Electronic Separation of Biological Cells by Volume", Science 150, 910 (1965).
10. Robert Schleif, Dorothy Lundgren, and Mel Klein, personal communication.
11. Lloyd Spielman and Simon L. Goren, "Improving Resolution in Coulter Counting by Hydrodynamic Focussing", (to be published).
12. Ellen M. Swanton, William A. Curby, and Howard E. Lind, "Experiences with the Coulter Counter in Bacteriology", Appl. Microbiol. 10, 480 (1962).
13. W. A. Curby, Ellen M. Swanton, and H. E. Lind, "Electrical Counting Characteristics of Several Equivolume Microorganisms, J. Gen. Microbiol. 32, 33 (1963).
14. G. Toennies, L. Iszard, N. B. Rodgers, and G. D. Shockman, "Cell Multiplication Studied with an Electronic Particle Counter", J. Bacteriol. 82, 857 (1961).

15. Karl G. Lark and Cynthia Lark, "Changes During the Division Cycle in Bacterial Cell Wall Synthesis, Volume, and Ability to Concentrate Free Amino Acids", Biochem. Biophys. Acta 43, 520 (1960).

16. James L. Allison, Richard E. Hartman, Roberta S. Hartman, Alan D. Wolfe, Jennie Ciak, and Fred E. Hahn, "Mode of Action of Chloramphenicol. VII. Growth and Multiplication of Escherichia coli in the Presence of Chloramphenicol", J. Bacteriol. 83, 609 (1962).

17. R. E. Ecker and M. Schaechter, "Bacterial Growth Under Conditions of Limited Nutrition", Ann. N. Y. Acad. Sci. 102, 549 (1963).

18. Sharon J. Kniseley and Lewis J. Throop, "Electronic Particle Counting Applied to the Determination of Lytic Activity", Anal. Biochem. 13, 417 (1965).

19. E. R. Gubrieli and M. Wertheimer, "Standardization of the Electronic Counter of Blood Cells", Am. J. Clin. Path. 36, 277 (1961).

20. L. H. Princen and W. F. Kwolek, "Coincidence Corrections for Particle Size Determinations with the Coulter Counter", Rev. Sci. Inst. 36, 646 (1965).

21. R. A. Scheidt and W. J. Blake, "Use of a Suspension of Latex Particles of Known Concentration for Monitoring the Coulter Counter", Am. J. Clin. Path. 35, 293 (1961).

22. R. B. Adams, W. H. Voelker, and E. C. Gregg, "Electrical Counting and Sizing of Mammalian Cells in Suspension: Part II. Electronic Circuitry and Experimental Evaluation" unpublished report, (privately communicated) (1966).

23. K. P. Norris and E. O. Powell, "Improvements in Determining Total Counts of Bacteria", J. Roy. Microscop. Soc. 80, 107 (1961).

24. E. L. Carstensen, H. A. Cox, Jr., W. B. Mercer, and L. A. Natale, "Passive Electrical Properties of Microorganisms", Biophys. J. 5, 289 (1965).

25. Idem, "Passive Electrical Properties of Microorganisms: I. Conductivity of E. coli, S. Marcesens and M. Lysodeikticus", Electrical Engineering Technical Report No. GM09933-1, The University of Rochester, Rochester, New York (1964).

26. Georges Knaysi, James Hillier, and Catherin Fabricant, "The Cytology of an Avian Strain of Mycobacterium Tuberculosis Studied with the Electron and Light Microscopes", J. Bacteriol. 60, 423 (1950).

This report was prepared as an account of Government sponsored work. Neither the United States, nor the Commission, nor any person acting on behalf of the Commission:

A. Makes any warranty or representation, expressed or implied, with respect to the accuracy, completeness, or usefulness of the information contained in this report, or that the use of any information, apparatus, method, or process disclosed in this report may not infringe privately owned rights; or

B. Assumes any liabilities with respect to the use of, or for damages resulting from the use of any information, apparatus, method, or process disclosed in this report.

As used in the above, "person acting on behalf of the Commission" includes any employee or contractor of the Commission, or employee of such contractor, to the extent that such employee or contractor of the Commission, or employee of such contractor prepares, disseminates, or provides access to, any information pursuant to his employment or contract with the Commission, or his employment with such contractor.

0